UNIVERSITÉ DU QUÉBEC A MONTRÉAL

# GEOCHEMICAL CHARACTERIZATION AND DIRECT DATING OF ROCK ART USING RADIOCARBON AND OPTICALLY STIMULATED LUMINESCENCE: THE CASE STUDY OF SOUTHERN AFRICA AND THE CANADIAN SHIELD

THÈSE

PRÉSENTÉE

COMME EXIGENCE PARTIELLE

DU DOCTORAT EN SCIENCES DE LA TERRE ET DE L'ATMOSPHERE

PAR

BONNEAU ADELPHINE

AUGUST 2016

UNIVERSITÉ DU QUÉBEC À MONTRÉAL

# CARACTERISATION GEOCHIMIQUE ET DATATION DIRECTE DE L'ART RUPESTRE EN UTILISANT LE RADIOCARBONE ET LA LUMINESCENCE STIMULÉE OPTIQUEMENT : APPLICATION À DES SITES D'AFRIQUE AUTRALE ET DU BOUCLIER CANADIEN

THÉSE

PRÉSENTÉE

COMME EXIGENCE PARTIELLE

DU DOCTORAT EN SCIENCES DE LA TERRE ET DE L'ATMOSPHÈRE

PAR

ADELPHINE BONNEAU

AOÛT 2016

# REMERCIEMENTS

Je tiens tout d'abord à remercier mes trois directeurs de thèse, les professeurs Michel Lamothe, Daniel Arsenault et Thomas Higham. Leurs conseils, leur expertise et leurs encouragements au cours de ces quatre années ont été déterminants pour la réalisation de ce doctorat.

Le projet de caractérisation et de datation de l'art rupestre en Afrique australe a été initié en 2010 par le professeur David Pearce. Depuis mon master en archéométrie, jusqu'à l'aboutissement de cette thèse de doctorat, nous avons collaboré à la sélection des sites, à la collecte des échantillons, à l'interprétation des résultats et à leur diffusion (articles, conférences, posters). Je tiens à lui exprimer toute ma gratitude pour son inestimable aide, ses conseils et son soutien dans la réalisation de ce doctorat.

Un autre acteur important de ce doctorat fût le professeur Peter Mitchell. Il m'a permis d'accéder aux sites rupestres au Lesotho et m'a fait profiter de ces connaissances approfondies de l'archéologie de l'Afrique australe. Je le remercie chaleureusement pour ses conseils durant la rédaction des divers articles et de cette thèse de doctorat.

Mes recherches étaient basées dans le laboratoire de luminescence Lux, de l'Université du Québec à Montréal. Je tiens à remercier les membres de ce laboratoire, Magali Barré, Laurence Forget Brisson, François Hardy, et Sébastien Huot, pour m'avoir accueillie, fait découvrir la luminescence, dispensée de nombreux conseils et aidée à réaliser les analyses OSL lors de ma grossesse et des derniers mois de mon doctorat.

Mon deuxième laboratoire de recherche était le Research Laboratory for Archaeology and the History of Art, à l'Université d'Oxford, au Royaume-Uni. Je suis très reconnaissante à toute l'équipe de l'unité de datation par le radiocarbone pour m'avoir accueillie, encadrée, et conseillée. Mike Dee est particulièrement remercié pour ses encouragements, ses recommandations, et pour nos discussions dans la langue de Molière dans les pubs d'Oxford.

Je tiens également à remercier Peter Ditchfield pour son aide et sa disponibilité lors de mes passages au laboratoire.

Au sein de ce laboratoire, Fiona Brock et Richard Staff ont tenu une place à part. Ils m'ont formée et encadrée lors de mes visites au laboratoire. Leurs recommandations, leur expérience et leurs connaissances ont été des atouts importants dans la réalisation de la partie radiocarbone de mon doctorat. Je tiens également à les remercier pour les discussions « jeunes parents » autour d'un thé.

Au cours de mon doctorat, j'ai utilisé des instruments dans d'autres laboratoires que mes laboratoires d'attache. Le laboratoire de caractérisation des matériaux de l'Université de Montréal et le laboratoire de microanalyse de l'Université Laval sont remerciés pour m'avoir permis d'utiliser leurs spectromètres Raman et FTIR et leur MEB-EDS. Je tiens particulièrement à remercier Nicolas Cottenye et André Ferland qui m'ont formée à l'utilisation de leurs instruments. Enfin, je remercie Michel Préda pour son aide lors des essais d'analyses de mes échantillons avec la diffraction de rayons X, qui n'ont malheureusement pas été couronnés de succès.

L'étude du site du Lac Wapizagonke s'est déroulée en collaboration avec le laboratoire de sciences de la conservation de Parcs Canada. Je tiens à exprimer toute ma gratitude à Kenza Dufourmentelle pour m'avoir permis d'utiliser tous les instruments et ressources de son laboratoire pour la réalisation de ce projet. Je suis également extrêmement reconnaissante à Joy Moyle pour m'avoir formée et encadrée lors de cette collaboration.

Je remercie chaleureusement Laura Mallen, Charles Arthur, et Rachel King qui, lors de la collection d'échantillons au Lesotho et en Afrique du Sud, m'ont apporté leur aide, leurs connaissances des lieux, des sites et des populations locales, ainsi qu'un soutien logistique essentiel à la bonne réalisation de ces travaux sur le terrain. Je tiens également à remercier les guides et équipes d'archéologues locaux qui nous ont permis d'accéder aux sites rupestres au Lesotho et au Botswana.

J'aimerais adresser un remerciement tout particulier à Luiseach Nic Eoin. Nous avons collaboré ensemble à l'analyse des peintures et des résidus de matières colorantes retrouvées

sur des meules, ce qui a permis de reconstituer les préparations nécessaires à la réalisation des peintures. Cette étape a été déterminante dans la reproduction de peintures pour les tests OSL. Par ailleurs, Luiseach a eu la gentillesse de corriger ma thèse du point de vue de la langue anglaise, et je l'en remercie infiniment.

Au cours de ce doctorat, j'ai reçu l'aide de Laura Didier, étudiante en Master en archéométrie de l'université de Bordeaux. Elle est venue à l'Université du Québec à Montréal pour réaliser son stage de fin de master (6 mois), pour lequel elle a été encadrée par le professeur Michel Lamothe et moi-même. Ces travaux sur les peintures blanches de la vallée du Phuthiatsana au Lesotho ont été intégrés à ma thèse de doctorat. Je tiens à la remercier pour son excellent travail d'analyses et de recherche.

Les analyses U/Th présentées dans ce doctorat ont été réalisées par Bassam Ghaleb. Je tiens à lui exprimer toute ma gratitude pour ces analyses, pour son aide, ses conseils avisés, ses trucs et astuces pour préparer les échantillons, et pour le chocolat toujours disponible dans son bureau.

Je tiens à adresser un remerciement tout particulier à Raynald Lapointe et Michelle Laithier. Raynald m'a formé sur les MEB du département, m'a apporté de nombreux conseils et idées pour la préparation de mes échantillons et la réalisation de mes analyses. Michelle a réalisé la plupart des cartes de ce doctorat et a passé de nombreuses heures à m'apprendre à réaliser les figures qui ponctuent ce manuscrit. En plus de leur précieuse aide, ils ont été pour moi comme des parents tout au long de ce doctorat.

Les organismes et institutions suivants sont remerciés pour avoir subventionné mon projet de doctorat: Fond de Recherche du Québec-Société et Culture, Géotop, Fondation de l'UQAM, Conseil de Recherches en Sciences Humaines, Institut Français d'Afrique du Sud, Association France-Canada, United Kingdom's Natural Environment Research Council, South African National Research Foundation.

Le South African Heritage Resources Agency, l'Eastern Cape Provincial Heritage Resources Authority, le National Museum and Monuments du Botswana, le Department of Culture (Protection and Preservation Commission) du Lesotho et Parcs Canada sont remercés pour

avoir délivré les permis archéologiques. Je suis également reconnaissante aux propriétaires et communautés locales de m'avoir donné accés à leurs propriétés où se trouvaient les sites étudiés.

Je souhaite remercier les étudiants présents et passés du département des Sciences de la Terre et de l'atmosphère de l'UQAM, Pauline, Samuel, Clyde, Pierre-Marc, Guillaume, Jérémy, Stéphane, Noémie, Agnès, James, et Geneviève, pour les discussions, les goûters, les fou-rires et autres moments qui ont ponctué mes années de doctorat et qui ne figureront dans aucun rapport officiel.

Enfin, je voudrais remercier ma famille et mes amis pour m'avoir soutenue pendant tout mon parcours universitaire, jusqu'à l'achèvement de cette thèse de doctorat. Leur soutien a été sans faille dans les bons moments comme dans les pires. Je finirai par remercier du fond du cœur mon conjoint Samuel et mon petit garçon, Philéas, né pendant ce doctorat, pour leur patience et le réconfort qu'ils m'ont apporté tout au long de ce projet.

A Samuel et Philéas,
A mes parents

TABLE DES MATIÈRES

LISTE DES FIGURES

LISTE DES TABLEAUX

LISTE DES ACRONYMES

AMS: Accelerator Mass Spectrometry

ATR: Attenuated Total Reflection

$^{14}C$: Radiocarbon

CF-IRMS: Continuous-Flow Isotope Ratio Mass Spectrometry

EA-IRMS: Elemental Analysis Isotope Ratio Mass Spectrometry

FTIR spectroscopy: Fourier Transform InfraRed spectroscopy

GC: Gas Chromatography

HCl: Hydrochloric acid

HF: Hydrofluoric acid

ICP-MS: Inductively Coupled Plasma Mass Spectrometry

IRSL: InfraRed Stimulated Luminescence

K-feldspars: Potassium feldspars

LA-ICP-MS: Laser Ablation Inductively Coupled Plasma Mass Spectrometry

LH-SDFs: Large Headed- Significantly Differentiated Figures

MC-ICP-MS: Multi-Collector Inductively Coupled Plasma Mass Spectrometry

NaOH: Sodium hydroxide

ORAU: Oxford Accelerator Radiocarbon Unit

OSL: Optically Stimulated Luminescence

PIGE: Particle-Induced Gamma-ray Emission

PIXE: Particle-Induced X-ray Emission

RLAHA: Research Laboratory for Archaeology and the History of Art

RARI: Rock Art Research Institute

SEM-EDS: Scanning Electron Microscopy Energy Dispersive X-ray Spectrometry

SPT: Sodium Polytungstate

U-series: Uranium series

XRD: X-Ray Diffraction

XRF: X-Ray Fluorescence

## ABSTRACT

Rock art exists all around the word. It is thought to be one of the most ancient expressions of the human mind. The artist, who created these paintings, opens a window into its world and gives the viewer a unique insight into its motivation and inspiration. Over the last 20 years or so, developments in the application of chemical, physical and geological methods have made it possible to recover the recipes used by ancient painters as well as to determine the age of the art itself. The interpretation of ancient rock art from around the world has been considerably aided by the acquisition of such data. However, there is still much to do. Palaeolithic rock art in Europe and Australia were the main beneficiaries of these developments. In other parts of the world, such as southern Africa and Canada, few dates have been obtained, and little in the way of paint characterisation studies exists.

This Ph.D. project explores direct dating of rock art from sites in southern Africa and in the Canadian Shield, using radiocarbon and optically stimulated luminescence. It introduces a new preliminary detailed characterisation of the sample to be dated, which makes it possible to select the samples which are the most likely to be successfully dated. Moreover, it reduces the necessary size of the sample. Using complementary instrumentation and methods, the characterisation results bring relative dating information if linked with superpositioning information, and where no superpositioning exists, or information is not available, they can give clues as to the composition and history of a panel or a site.

Characterisation reveals the type of carbon-based paint used, which can then be radiocarbon dated, for example, charcoal, soot, or carbon-blacks. This information is essential for understanding the age obtained. At the same time, this characterisation records the presence and estimates the proportions of radiocarbon contaminants in the samples, such as calcium oxalates, calcium carbonates and humic acids. A chemical pre-treatment can then be adapted to dissolve all the contaminants detected, checked with Fourier-Transform Infra-Red (FTIR) analysis. Using these methods, 46 dates were obtained on rock art sites from southern Africa. These include the first ever dates from rock art in Lesotho and in Botswana and constitute the largest dating project on rock art ever undertaken in this part of the world.

Optically stimulated luminescence (OSL) cannot give a definitive date for rock art, but the experiments carried out for this project proved that this technique may be applied under specific conditions: where the rock support is suitable for OSL dating, given a thick paint layer and sufficient exposure of the rock face to daylight.

In the Canadian Shield, none of the dating methods was applicable. However, the precise characterisation conducted on the paints reveals different paint recipes in the same site giving new clues to reconstruct some parts of the "chaîne opératoire" of the site.

Characterisation of paint and dates obtained in this project make it possible to start developing a dialogue between the archaeological record of hunter-gatherer activity preserved in paint and that preserved in occupational deposits.

Keywords: San Rock Art, Canadian Shield rock art, paint characterization, Radiocarbon dating, OSL dating.

# RESUMÉ

L'art rupestre est présent dans le monde entier. Il est l'une des plus anciennes manifestations artistiques de l'être humain. L'artiste qui a créé ces peintures ouvre une fenêtre sur son monde et plonge son spectateur dans un aperçu sans égale de sa motivation et de son inspiration. Au cours des 20 dernières années, l'utilisation de méthodes empruntées aux sciences chimiques, physiques, et géologiques a permis de redécouvrir les recettes des artistes ainsi que de déterminer l'âge de cet art. L'interprétation de l'art rupestre de par le monde s'est considérablement enrichie grâce à l'acquisition de telles informations. Néanmoins, il y a encore beaucoup à faire. L'art pariétal paléolithique européen ou l'art rupestre d'Australie ont été les principaux bénéficiaires de ces développements. Dans d'autres parties du monde, comme en Afrique australe et au Canada, très peu de dates ont été obtenues et peu a été fait concernant la caractérisation des peintures rupestres.

Cette thèse de doctorat explore la datation directe de l'art rupestre présent sur des sites en Afrique australe et dans le Bouclier Canadien, en utilisant le radiocarbone et la luminescence stimulée optiquement (OSL). Elle introduit une nouvelle étape de caractérisation préliminaire et détaillée de l'échantillon, permettant de sélectionner ceux qui seront le plus à-même d'être datés par le radiocarbone, tout en réduisant la quantité d'échantillon nécessaire à cette datation. En utilisant des méthodes et instruments complémentaires, la caractérisation couplée à des données sur la superposition des figures, apporte tout d'abord des informations de datation relative, et quand celles-ci n'existent pas ou ne sont pas disponibles, elle donne des indices quant à la composition et à l'histoire d'un panneau ou d'un site.

La caractérisation révèle entre autre le type de pigment à base de carbone utilisé, pouvant être daté par le radiocarbone comme par exemple, le charbon, la suie ou le noir de carbone. Cette information est essentielle à la compréhension de l'âge obtenu. Dans le même temps, cette caractérisation détermine la présence et estime les proportions des pollutions pouvant compromettre la datation par le radiocarbone comme les oxalates de carbone, les carbonates de calcium ou les acides humiques. Le prétraitement chimique est par la suite adapté pour dissoudre toutes les pollutions détectées, dissolution vérifiée par des analyses en spectroscopie infrarouge à transformée de Fourier (FTIR). A partir de ces protocoles, 46 dates ont été obtenues sur des sites rupestres d'Afrique australe. Elles comportent les premières dates obtenues sur des sites au Lesotho et au Botswana et constituent le plus grand projet de datation de l'art rupestre jamais entrepris dans cette partie du monde.

La luminescence stimulée optiquement n'a pas permis de donner un âge fini pour l'art rupestre mais les expérimentations réalisées durant cette thèse ont montré que cette méthode pourrait être appliquée dans des conditions spécifiques : roche avec des minéraux sensibles à

la luminescence, recouverte d'une épaisse couche de peinture, et ayant été suffisamment exposée à la lumière du soleil.

Dans le Bouclier Canadien, aucune méthode de datation n'a pu être appliquée. Cependant, une caractérisation détaillée des peintures a montré que différentes recettes de peinture ont été utilisées sur un même site apportant de nouvelles informations pour reconstituer la chaîne opératoire de ces sites.

La caractérisation des peintures et les âges obtenus dans cette thèse permettent de commencer à développer un dialogue entre l'activité des peuples ayant réalisés ces peintures sur les sites rupestres et dans les dépôts archéologiques.

Mots clés : Art rupestre San, Art rupestre du Bouclier Canadien, caractérisation de peintures, datation par le radiocarbone, datation par OSL.

# INTRODUCTION

Rock art is thought to be one of the most ancient expressions of the human mind. It gives the viewer a unique insight into the motivation and inspiration of the artist who painted it, and opens a window into their world. The interpretation of ancient rock art from around the world has been aided considerably over the last 20 years or so by developments in the application of chemical, physical and geological methods. These developments have made it possible to recover the recipes used by ancient painters as well as to determine the age of the art itself. This being said, there is still much to do. Although Palaeolithic rock art in Europe and Australia has been extensively recorded and studied, in other parts of the world, such as southern Africa and Canada, few dates have been obtained, and little in the way of paint characterisation studies exists. However, this type of information is vital if archaeologists are to interpret these sites in proper context. This thesis asks the following questions: Is it possible to apply similar dating and characterisation methods to rock art sites in southern Africa and Canada? Do they need to be specifically adapted? What improvements are required in order to extract further information from these sites and to improve the reliability of dating and characterisation studies?

This Ph.D. project uses a well-known dating method, radiocarbon dating, and an unconventional one in the field of rock art study, optically stimulated luminescence (OSL). These techniques are mobilised to directly date rock art sites in southern Africa and the Canadian Shield. However, to apply these methods, specific compounds need to be present in the samples, namely carbon in the case of radiocarbon and quartz and feldspars in the case of OSL. But their presence is not enough to get a reliable date, their link with the event to date and to the paintings should be well understood. To assess this question, a preliminary geochemical characterization of the paint, its environment and its alterations is introduced. This preliminary step makes it possible to choose the appropriate sample to be dated and to adapt the dating method accordingly. Moreover, it proves to be efficient at providing some details how rock art was made at a site, namely, its *chaîne opératoire*.

This project is the continuation of an initial project carried out in 2010 at the Research Laboratory for Archaeology and the History of Art (RLAHA) at the University of Oxford, United Kingdom, in collaboration with the Rock Art Research Institute (RARI), at the University of the Witwatersrand, Johannesburg, South Africa. In this initial project, undertaken as part of my master's degree final internship, detached painted flakes were characterized and dated. Results were published in *Radiocarbon* and *Journal of Archaeological Science* (Bonneau *et al.*, 2011, 2012), and formed the basis of this subsequent PhD project. The aim of this thesis is to improve the previously established protocols to produce reliable results on a range of various site environments, hence the selections of sites in southern Africa and in the Canadian Shield.

The form of the thesis is as follows: firstly, a presentation of the sites, their geology and their archaeological contexts is given in chapter I. Chapter II is dedicated to the different methods and instrumentations chosen and applied. Chapter III deals with characterisation of the paintings, their environment and alteration, which is the first step prior to choosing a sample and a dating method. Chapters IV and V detail respectively radiocarbon and OSL methods with tests to adjust them to each sample. Chapter VI shows not only that dating methods can inform understanding of the processes that go into the creation of a rock painting, but that characterisation of the paints is an essential tool too. This chapter is in the form of an article submitted to the journal *Archaeometry* and in press. Two other articles were extracted of this work, submitted to *Antiquity* (Title: Direct dating reveals earliest evidence for parietal rock art in southern Africa) and *Radiocarbon* (Title: Successfully dating rock art in southern Africa using improved sampling methods and new characterization and pretreatment protocols), and are in press.

# INTRODUCTION

L'art rupestre est considéré comme l'une des expressions les plus anciennes de l'esprit humain. Il donne au spectateur un aperçu unique sur la motivation et l'inspiration de l'artiste qui l'a peint, et ouvre une fenêtre sur son monde. L'interprétation de l'art rupestre de par le monde s'est considérablement enrichie au cours des 20 dernières années grâce à l'utilisation de méthodes empruntées aux sciences chimiques, physiques, et géologiques. Celles-ci ont permis de redécouvrir les recettes des artistes ainsi que de déterminer l'âge de cet art. Néanmoins, il y a encore beaucoup à faire. Si l'art pariétal paléolithique européen ou l'art rupestre d'Australie ont été largement référencés et étudiés, dans d'autres parties du monde, comme en Afrique australe et au Canada, très peu de dates ont été obtenues et peu d'études ont été réalisées concernant la caractérisation des peintures rupestres. Cependant, ces informations sont essentielles pour permettre aux archéologues d'interpréter les sites rupestres dans un contexte approprié. Cette thèse de doctorat pose les questions suivantes: Est-il possible d'appliquer des méthodes de datation et de caractérisation similaires à celles utilisées en Europe ou en Australie, à des sites rupestres en Afrique australe et au Canada? Ont-elles besoin d'être adaptées aux spécificités rencontrées sur ces sites? Quelles améliorations sont nécessaires afin d'extraire plus d'informations à partir de ces sites et d'améliorer la fiabilité de la datation et de la caractérisation de ces sites?

Ce projet de doctorat utilise une méthode de datation bien connue, la datation par le radiocarbone, et une moins conventionnelle dans le domaine de l'étude de l'art rupestre, la luminescence stimulée optiquement (OSL). Ces techniques sont utilisées pour dater directement les sites d'art rupestre en Afrique australe et dans le Bouclier Canadien. Néanmoins, pour appliquer ces méthodes, il est nécessaire que les échantillons (ici les peintures ou la roche support) soient composés d'éléments spécifiques que sont le carbone pour la datation par le radiocarbone et les quartz et les feldspaths pour l'OSL. Mais leur présence n'est pas suffisante, il faut encore comprendre leur relation avec l'événement à dater (c'est-à-dire la date de la peinture) et avec la peinture elle-même. Pour répondre à ces

interrogations, une étape préliminaire de caractérisation géochimique de la peinture, de son environnement et de ses altérations a été introduite. Cette étape préliminaire permet de choisir l'échantillon le plus approprié pour être daté et d'adapter la méthode de datation en conséquence. En outre, cette étape de caractérisation se révèle être efficace pour fournir des détails sur la réalisation d'un site rupestre, à savoir, sa chaîne opératoire.

Ce projet se trouve dans la continuité d'une étude préliminaire réalisée en 2010 au Research Laboratory for Archaeology and the History of Art (RLAHA), Université d'Oxford, Royaume-Uni, en collaboration avec le Rock Art Research Institute (RARI), Université du Witwatersrand, Johannesburg, Afrique du Sud. Au cours de cette étude, entreprise dans le cadre de mon stage de fin d'études de master, des fragments de roche peints, détachés de la roche, ont été caractérisés et datés. Les résultats ont été publiés dans *Radiocarbon* et *Journal of Archaeological Science* (Bonneau *et al.*, 2011, 2012). Ils forment la base de ce projet de thèse. Le but de cette thèse est d'améliorer les protocoles précédemment établis pour produire des résultats fiables, sur une large variété de sites avec des environnements différents, d'où la sélection de sites en Afrique australe et dans le Bouclier Canadien.

Cette thèse de doctorat s'organise de la façon suivante. Tout d'abord, une présentation des sites, de leur géologie et de leurs contextes archéologiques est faite dans le chapitre I. Le chapitre II est consacré aux différentes méthodes et instrumentations choisies et utilisées. Le chapitre III traite de la caractérisation des peintures, de leur environnement et de leurs altérations. C'est ici l'étape préliminaire avant de choisir un échantillon et une méthode de datation. Les chapitres IV et V détaillent respectivement les tests réalisés pour la datation par le radiocarbone et pour la datation par OSL. Ces expérimentations ont permis d'ajuster chaque méthode à chaque échantillon. Le chapitre VI montre que, non seulement, les méthodes de datation peuvent apporter de l'information permettant la compréhension des processus qui entrent dans la création d'une peinture rupestre; mais également que la caractérisation des peintures est un outil essentiel à cette compréhension. Ce chapitre est sous la forme d'un article a été soumis à la revue *Archaeometry* et qui est actuellement sous presse. Deux autres articles ont été extraits de ce travail et soumis à la revue *Antiquity* (Titre : Direct dating reveals earliest evidence for parietal rock art in southern Africa) et à la revue *Radiocarbon* (Titre : Successfully dating rock art in southern Africa using improved

sampling methods and new characterization and pretreatment protocols). Ils sont actuellement sous presse.

# CHAPTER I

## DATING ROCK ART: OBJECTIVES AND CHALLENGES IN SOUTHERN AFRICA AND THE CANADIAN SHIELD

Dating has always been one of the most common questions about rock art. However, this question reveals several objectives and challenges depending on places and sites. In this chapter, differences between direct and indirect dating are explained, and objectives and challenges are detailed for the specific areas studied, southern Africa and the Canadian Shield, with rock art and specific conditions pertaining to each presented.

### 1.1 Direct or indirect dating of rock art: a terminological problem?

The aim of this PhD project is to directly date rock art. However, the definition of direct and indirect dating is different depending on the authors in question. A quick review of definitions in the literature is needed in order to be able to give the definition of direct dating which will be used for the purposes of this PhD.

In this paragraph, focus is given on absolute dating even if relative dating has its own place in comprehension of rock art too, and will be used in the interpretation to complement the absolute dates obtained.

Bednarik (1996) gave two prerequisites to directly date rock art : "first, the physical relationship of the art and the dating criterion must be direct and indisputable; and second, the propositions concerning the chronological relationship of the rock art and the dating criterion should be falsifiable and testable" (Bednarik 1996: 1). If a date is obtained without these prerequisites, it is considered indirect. Using this definition, dates obtained on calcite or calcium oxalates crusts surrounding paintings are considered to be direct dating whereas the author argues that the use of the pigment itself cannot be a direct date as, in the case of charcoal, nobody can know how old the wood used was, if the pieces of wood were of the same age (coming from different trees), and if it may have been contaminated later.

On the other hand, Pettitt and Pike (2007: 28) made a distinction between "direct dating", "indirect stratigraphic dating", "indirect associative dating" and "indirect architectural dating". In this case, direct dating is the "dating of a sample of pigment [...] that forms the art", whereas indirect stratigraphic dating is the "dating of the formation of a material [...] that stratigraphically overlies an artistic panel". Indirect associative and architectural dating are respectively defined as the association of the cave art with datable material (artefacts found in the same cave), and as the "dating of the formation of a stratigraphic layer that apparently blocks access to a decorated chamber". There is here a radical difference with Bednarik's definition.

Both points of views are arguable. However, they do not really take into account the question most interesting to archaeologists: when did the artists made these paintings? To talk about direct dating is to discuss the instance of painting. A direct date should reflect this moment in order to avoid any misunderstanding. A good way to find it is to use the paint itself or part of the paint. However, one needs to know when these parts were collected, from which vegetable/mineral species they derived, and if the dating technique used will reflect the date of collection, the date of death, or the date of use of the material. Finally, contamination due to exposure (whether to rain, sun, natural degradation, or just life at the site) should be taken into account. With this information, the date satisfies the two prerequisites of Bednarik and the definition of Pettitt and Pike. Radiocarbon and OSL dating were selected for this project. Reasons why the dates obtained with these techniques can be considered as direct dates are detailed in Chapter II.

Obtaining direct dates of rock art is of great importance, but each world region is subject to its own challenges, problems and archaeological objectives. They are now detailed for the two studied regions: southern Africa and the Canadian Shield.

## 1.2 San rock art

In southern Africa, rock art was produced by many different populations: San hunter-gatherers (also called "Bushmen), Khoekhoe pastoralists and several different agropastoralist (farmer) groups, including the South Sotho. San rock art is the most common and will be detailed here. Most of the sites selected for the project are of San rock art tradition but a few sites of Sotho tradition were also analysed (see §1.2.3.2 for justifications).

### 1.2.1 Characteristics and history of research

San peoples have lived in southern Africa for many thousands of years, as indicated by genetic studies and the evidence of physical anthropology (Lewis-Williams and Pearce, 2004). Although today they are almost entirely confined to the Kalahari Desert, they were previously much more widely distributed. They survived in the Maloti-Drakensberg Mountains of Lesotho and South Africa until the end of the nineteenth century (Vinnicombe 1976). Note that 'San' (a Khoekhoe term) is not a term they used to refer to themselves: indeed, we know of no such term, but it is commonly agreed that the groups in question were linked by common languages (called "click languages"[1], see Figure 1.1) and beliefs but each group was independent from each other (Lewis-Williams, 2003).

[1] Details about the click languages and the orthography of San names is given in appendix C.


**Figure 1.1** Locations of some San groups of languages during the colonial period (modified from Lewis-Williams, 2003)

There are still San populations in South Africa, Namibia and Botswana, mostly confined in the Kalahari Desert. Using ethnographic data and historical records, it is possible to achieve some understanding of the spirituality and myths of the San. Their main divinity is known as *//Kaggen*. He is sometimes called the Mantis, but this is only one of his avatars. He can be a human, an eland (the South African antelope), or other kind of animals. He lives with his wife and children in the spirit world. In San cosmology, the world is divided in three parts: the underground, the Earth (where people live) and the sky, with each part connected to the others. Thus spirits living in the sky or in the underground can interact with people and occasionally cause trouble (Lewis-Williams and Pearce, 2004). To "talk" to spirits, San made

rituals which were sometimes depicted in rock-shelters (details about San rock art interpretation are in §1.2.2).

San hunter-gatherers created a large number of paintings throughout southern Africa which are characterized by the use of fine lines, brush paintings, and detailed representational imagery (Lewis-Williams and Pearce, 2004). For centuries, their paintings were mysteries for which only the San themselves had keys.

When the first Europeans settlers arrived in South Africa, they considered the San to be savages, who were at best, pagans and at worst, the servants of the Devil (Lewis-Williams, 2003). Only a few people in the 18th and 19th centuries gave any attention to the San people, but their works are still invaluable sources for archaeologists trying to interpret San rock art. These chroniclers were Joseph Millerd Orpen, Wilhelm Bleek and his daughter-in-law Lucy Lloyd, George William Stow, and two French missionaries François Daumas and Thomas Arbousset. Despite their occidental vision of San habits, they recorded myths, religious behaviours, and interpretations of rock paintings from key individuals such as Qing, *//Kabbo*, *Dia!kwain* and */Han≠kasso* (Lewis-Williams, 2003). Sadly, little was recorded at this time about the painting techniques used.

In 1930, Marion How, the wife of the magistrate of Qacha's Neck, administrative district in Lesotho, invited Mapote, an old man, to paint elands with the same technique as used by San people. Mapote was not San himself, being rather MoPhuthi (as a son of the BaPhuthi chieftain, Moorosi), but had San half-brothers. He learned how to paint with them when he was young. He started by looking for a rock with little relief but sufficiently porous to absorb paints, choosing eventually a smooth sandstone. For the pigments, he asked for *qhang qhang*, a brilliant hematite coming from the basaltic part of Drakensberg. He asked then for fresh eland's blood. Hematite must, according to him, be heated at full moon by a woman, and then prepared with fresh eland's blood. The blood must be fresh in order to be able to penetrate the rock sufficiently. Mapote prepared three different pigments: a red with hematite and fresh ox's blood (as he did not have any eland's blood at his disposal), a white with clay and *Asclepia gibba* plant sap, and a black made with charcoal and water. With these colours, he painted elands on two stones and "during a few hours, the knowledge of San people revived"

(Lewis-Williams, 1995). One of these painted stones is currently conserved at the University of the Witwatersrand's Origins Center, in Johannesburg, South Africa.

Then in the 1980s, an old lady known under the pseudonym of "M" was interviewed in South Africa's Eastern Cape Province. Her father had been a San shaman and had produced many paintings which she showed and explained to her interlocutors. Her sister was also a famous shaman but had died a few years before. She confirmed Mapote's explanations in particular on the need for blood for the red but she added that the fat of eland was used as a binder to manufacture the red pigment too (Lewis-Williams, 1995). This last explanation can be linked to a San myth where *//Kaggen*, the creator of life for the San, asked his wife to mix eland blood and fat and from this mixture he created new elands (Lewis-Williams, 2003).

These two testimonies are the most detailed we have from witnesses to the last living artists. This raises an issue about the artists. Who were they? Historical records do not give any real answer to this question which is linked to the interpretation of the paintings, and which is one of the current points of research.

### 1.2.2 Current research and questions

#### 1.2.2.1 Interpretation of the art

In interpreting San rock art, there are two prevailing models or schools of thought:

- The "Shamanistic" model[2] : developed by Lewis-Williams in the 1980's using ethnographic records from extant Kalahari San, this was a real breakthrough in the interpretation of rock art in southern Africa and subsequently around the world. This model sees rock art as the representation of the "journey" of a shaman in the spirit world. Indeed to heal people, to make the rain to fall at a certain place, or to visit relatives who lived far away, shamans used dance, singing and clapping to enter trance states. In these altered states of consciousness, they were able to go through the 'veil' of rock and to travel in the three worlds (detailed in §1.2.1). Once their mission was complete, they came "back to life" and rock paintings are

[2]Term used by Jean-Loïc Le Quellec and Anne Solomon in *Afrique & histoire,* N°6(2), 2006.

seen as a way to explain what they saw (Lewis-Williams, 2003; Lewis-Williams and Pearce, 2004). At the same time, paintings are seen as "full of power" and may have been used by shamans to help them to enter trance by touching or looking at them (Lewis-Williams and Pearce, 2004). As the reference to shamanism is linked to altered states of consciousness, Lewis-Williams worked with neuroscientists to describe what people see during trance. The results show that all the people see the same kind of images at the different steps of the trance. Then their interpretation and explanation of them depend on their beliefs (Lewis-Williams and Pearce, 2004).

- The "multiple/mythological" model[3]: Against the "shamanistic" interpretation, authors such as Solomon, Pager and Le Quellec developed another model using multiple keys to interpret rock art. Representations can be seen as rituals, myth or record of historical actuality. Regarding rituals, they argue that the paintings do not all represent shamanic healing rituals but that some should be interpreted as representing female initiation, for example. Moreover, they argue that a part of social representation must be taken into account as humans are sometimes intentionality depicted as female/male, old or young or with particularities such as the female figures with exaggeratedly fat bodies (Solomon, 2006).

These two models have been intensely debated by their two main proponents: David Lewis-Williams for the "shamanic" model and Anne Solomon for the "multiple/mythological" model. Lewis-Williams asserts his model using the 19th Century Bleek and Lloyd archive of */Xam* testimonies where the word *!gi:xa* is translated as "Sorcerors", which Lewis Williams interprets as shamans. Indeed, *!gi* means "magic power" and *xa* means "full of". Thus the *!gi:xa* is a person "full of magic power". However, Solomon argue that the *!gi:ten* (plurial of *!gi:xa*) are not living people but spirits which can interfere in the living people's world. On the other hand, Solomon mentioned: "one of the foremost ethnographers [Katz] of the Kalahari San trance dance has stated that even the *Ju/'hoan* people have "no shamanistic

[3] Term used by Anne Solomon in *Afrique & histoire,* N°6(2), 2006, and Jean-Loïc Le Quellec in *Rock Art Studies : News of the World I,* 2008.

tradition"" (Solomon, 2006: 95). Thus in the "multiple/mythological" model, most of the shamanistic scenes are seen as accounts of the activities of the spirits and of spiritual possession.

Even though most researchers working on southern Africa rock art (and worldwide) agree with either one model or the other, they all recognize the necessity to date the representations to avoid lumping everything together and discuss the scenes as they were painted (Smith, 2010; for further information about this debate, the reader is invited to refer to the large amount of published articles from A. Solomon, J-L LeQuellec, D. Pearce, D. Lewis-Williams and others). Moreover, all these models focus mainly on each figure without paying attention to the visual aspect of the scene and its arrangement. As the most common method of recording southern African rock art is to trace onto white paper with black and white lines, much is lost about the relief of the rock face, the possible mineral inclusions and thus how these may have been used by the artists to emphasis some representations (Solomon 2006; Lemaitre 2013).

To move on with the interpretation debate, some choices have been deliberately made to aid both clarity and uniformity in this PhD. First, as chosen by Blundell (2004), the term "potency-owners" will be used instead of "shaman" when talking about southern African rock art tradition. Indeed, this expression reflects more appropriately the San term *!gi:xa*. The term "shaman" derives from *sama-*, which means "moving like an animal" in Altaic languages, especially in Siberia where this translation was first used by the archpriest Avvakum (1670-71) (Hamayon, 2006). Second, to avoid any misconception in interpretation, the paintings are only described: human figure, therianthrope, antelope, eland, line, etc.

To return to the question "who were the artists?", it depends on the interpretation chosen. Using the shamanistic model, the artists are the shaman themselves, who paint to explain what they saw during their "travel" in the spirit world (Lewis-Williams and Pearce, 2004). Both men and women were "potency-owners", and the testimony of "M" confirms it, at least for historic times. On the other hand, V. Ellenberger mentioned testimonies that might suggest that only men painted in the rock shelter (Mitchell, 2007). It can be postulated that depending on their gender, "potency-owners" had a specific role in the preparation and

realization of rock paintings. Mapote's testimony suggests that women were in charge of the preparation of the raw materials (heating of the hematite). And men might be in charge of the realization of the paintings.

With the "multiple/mythological" model, it is much more complicated. The artist can be the person who performed the ritual, but may have been someone else who painted in order to help with a ritual, a ceremony, or a commemoration. In this model, painting is considered as a ritual itself, thus artists would be trained people, maybe with some "magical power" (Solomon, 2006). Here we should remember the story of Mapote, who had San half-brothers and who learned to paint with them. He did not mention that he was a shaman himself, nor his half-brothers, but nevertheless he knew how to prepare paint with specific materials and recipes.

As mentioned previously, San did not recognize themselves as a single people, thus regional styles can be identified. For example, the eland is particularly represented in the Drakensberg, whereas the kudu or the springbok are more present respectively in Zimbabwe and in the Bandberg (Solomon, 2006; Le Quellec, 2008). But this distribution cannot be explained by ecology or by dietary purpose. Indeed, the eland played a negligible dietary role for the San in the Drakensberg (Solomon, 2006). Moreover, through time, San beliefs may have changed. Descendants of the San, who live nowadays in Namibia, South Africa and Botswana form the first-hand informants of archaeologists and ethnographers today, even though they do not paint anymore and lost much of their knowledge about the techniques used, having been forced to migrate into refugia, their myths and spirituality are still similar to those San beliefs recorded during colonial time. Here arises the question about the consistency between San beliefs thousands of years ago and those of today, and the incorporation of rock art into San history.

#### 1.2.2.2 Incorporating rock art into San history

Studying rock art itself is just the first step. It needs to be incorporated into general San history, that is to say, integrated with historical, archaeological and ethnographical data. Its place in San society is a research subject too as rock art is seen either as a way of explaining

what potency-owners saw in the spirits world, or as part of a specific ritual which may have different symbolic meanings (initiation, myths, etc.).

As San society changed through connections with other populations such as Bantu-speaking neighbours, moves from one place to another (from Namibia to South Africa for example), or colonization, their art changed too. Some representations are interpreted as showing the effects of creolization or hybridization due to colonialism; others, such as large-headed figures, are seen as changes in the social organisation. In the case of the latter, Dowson suggests that they are "portraiture of prominent, politically influential people" (cited in Blundell, 2004: 172). But they seem to be related to recent times (using superposition to work out relative chronologies). Other figures, known as Eldritch figures, may represent the final period of the rock art in Nomansland (Blundell and Lewis-Williams, 2001).

To corroborate these theories, rock art images are compared to historical, ethnographical and archaeological records. However, this work is extremely difficult, firstly because the historical period begins only with the colonial period from about the 17$^{th}$ century (and later in the Drakensberg, at the beginning of the 18$^{th}$ century), and secondly, because there are few archaeological records from rock art sites. Thus the importance of comparing direct dating of rock art and characterization of the raw materials used which, if they are not local, may reveal exchanges with other tribes and communities, and further confirm their possible influences.

Rock art interpretation and San history are not the primary focus of this PhD but are the keys for achieving its objectives. In collaboration with the Rock Art Research Institute of the University of the Witwatersrand and the School of Archaeology of the University of Oxford, rock art sites were selected around southern Africa for the presence of specific figures and the possibility of large sampling to develop methodologies which, if successful, will further be applied in southern Africa rock sites and elsewhere around the world.

### 1.2.3 Sites selected

#### 1.2.3.1 Archaeology

Rock art sites were selected because of the images represented and mainly according to the possibility of collecting "large" samples. Two areas served perfectly this purpose: the Thune

Valley in Botswana and the Phuthiatsana Valley in Lesotho, where two dams were under construction and thus flooded rock art sites. Sites had been entirely photographed, traced, recorded and sometimes excavated by archaeologists before any sampling and before flooding commenced. Details are given in each dedicated section.

On the other hand, the Maclear District of South Africa's Eastern Cape Province was chosen because the initial project started in 2010 with a site from this area, RSA TYN2, and this area contains figures which pose a lot of questions for archaeologists, especially the Eldritch and the large-headed figures (Blundell, 2004). Eldritch figures are most of the time painted in a white pigment, with details added in red on some paintings. "They are grotesque with scythe-like claws, ferocious teeth, emaciated bodies, and large penes" (Blundell and Lewis-Williams, 2001:3). They are thought to represent the spirit-of-the-dead and are found on top of other paintings with a translucent body. They are interpreted as being from the same scene as the figures painted underneath. However, having a date on these paintings would confirm this interpretation. Large Headed-Significantly Differentiated Figures (LH-SDFs) reported by Blundell (2004) may be linked to the "possible relationships between the San living with the Phuthi who occupied the Lundean's Nek area and those under Nqabayo and Mdwebo, who lived below the escarpment" (Blundell, 2004:141). Once again, a date from these figures would help to confirm this interpretation.

Moreover, the sites in the Maclear District are very similar to those from the Phuthiatsana Valley and form excellent candidates for the testing of protocols and methods.

#### 1.2.3.2 Geology

In southern Africa, most of the sites are found on geological formations which are part of the Karoo Supergroup (360 - 145 Ma). In this project, all the sites studied in southern Africa conform to this. Thus, a general introduction to this Supergroup will be made first and then the specific formation will be detailed for each area.

The Karoo Supergroup is dominated by sedimentary rocks which were deposited just on top of the sedimentary rocks of the Cape Supergroup, in the inland Karoo Sea. It is constituted of alternating shales, mudstones and fine-grained sandstones. They accumulated slowly in the

Karoo basin and attain a thickness of about 8000 m in the south of the basin. During the depositional sequence, the Clarens, Elliot and Molteno sediments are widespread in the basin. This deposition ended about 190 Ma ago by the extrusion of the volcanic basalt lavas of the Drakensberg group (Table 1.1; Maud, 2008).

In the Late Jurassic, just after the end of the sedimentation, the southern hemisphere of Gondwana began to break up and created the south part of the African continent. Then during the Cretaceous period, which seems to have been warm and humid, both physical and chemical erosions took place forming the Drakensberg Mountains and the Maloti plateau (Lesotho) (Maud, 2008). At the same time, weathering altered the sandstones to clay. Erosion of this megalith (by water and wind) left a large number of rock shelters in which San rock art can now be found. Because of these shelters, the first geologists surveying the area, such as du Toit (1939), called this sandstone "Cave sandstone". Nowadays, its common occurrence is the Clarens, Elliot and Molteno Formations (Maud, 2008).

**Table 1.1** Abridged geological succession of the Cape and Karoo Supergroups (modified from Maud, 2008)

| Era | Geological epoch/period (ages in Ma) | | | Geological group, formation, etc. | Dominant rock or material type |
|---|---|---|---|---|---|
| MESOZOIC | Cretaceous | 145 | Uitenhage Group | Mzamba Formation | Marine siltstone |
| | | | | Sundays River Formation | Marine mudstone, siltstone |
| | | | | Kirkwood Formation | Fluvial sandstone, mudstone |
| | | | | Enon Formation | Conglomerate |
| | | | | Mngazana Formation | Conglomerate |
| | Jurassic | 200 | Karoo Supergroup | Drakensberg Group | Basalt, dolerite |
| | Triassic | 250 | | Clarens, Elliot and Molteno Formations | Sandstone, siltstone, mudstone |
| | | | | Beaufort Group | Shale, mudstone |
| PALAEOZOIC | Permian | 300 | | Ecca Group | Shale |
| | Carboniferous | 360 | | Dwyka Group | Tillite (diamictite), shale |
| | Devonian | 416 | Cape Supergroup | Witteberg Group | Sandstone, shale |
| | | | | Bokkeveld Group | Shale, sandstone |
| | Silurian | 444 | | Table Mountain Group | Sandstone |
| | Ordovician | 495 | | | |
| | Cambrian | 545 | | Cape Granite Suite | Granite |
| | Late Precambrian | 800 | | Kaaimans and Gamtoos Groups | Quartzite, quartz-schist, phyllite, limestone |

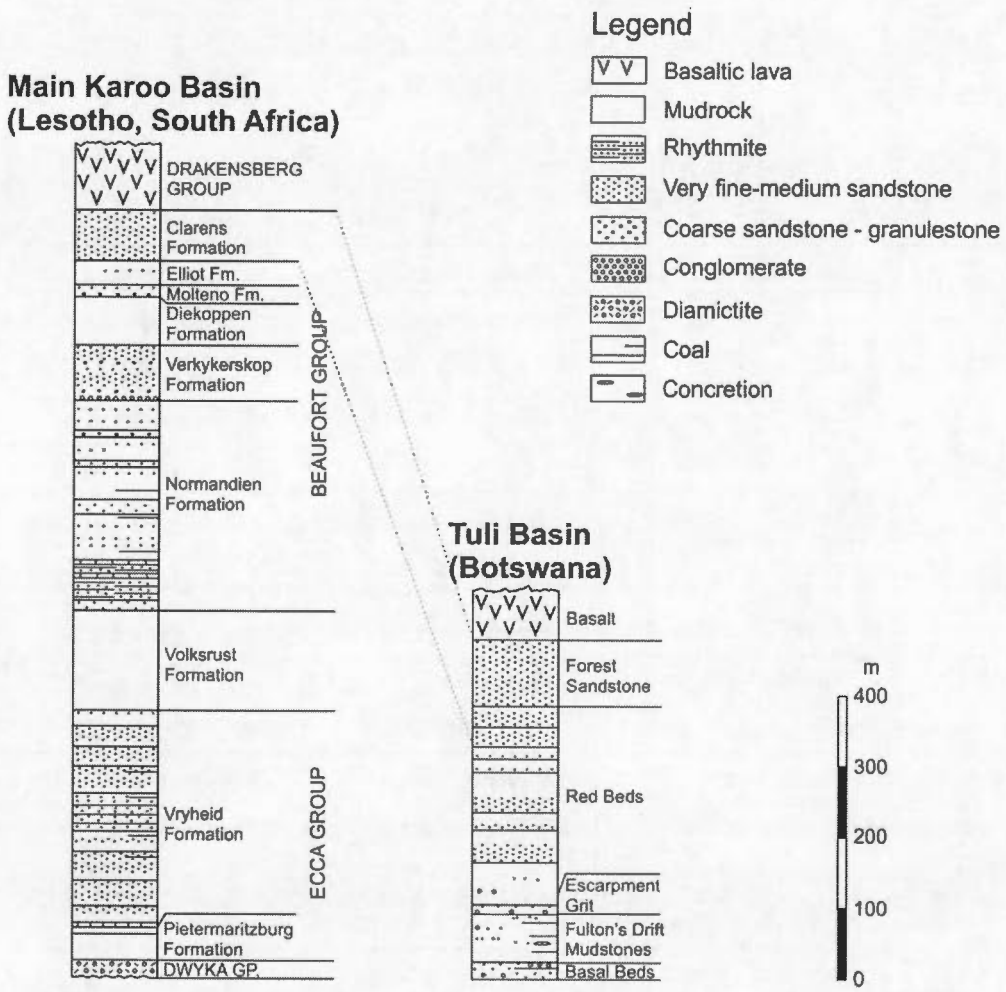


**Figure 1.2** Stratigraphic correlations of Clarens Formation in the Main Karoo Basin (South Africa and Lesotho) and the Tuli Basin (Botswana)

1.2.3.3 Maclear District, South Africa

The Maclear District is located around the town of Maclear, in the Eastern Cape Province, South Africa. About 300 rock art sites have been recorded in this area and the adjacent districts.

*Local geology*

Most of the sites are found in Clarens Formation sandstone rock shelters, but a few others are in Elliot Formation sandstone rock shelters. The Clarens Formation is overlain by the Drakensberg Group, composed of volcanic rocks, and underlain by the Elliot Formation. It is 145 m in thickness (in average) and results of eolian depositions in a semi-arid desert during the Late Triassic/Early Jurassic (Johnson *et al.*, 2006). It consists of fine-grained sandstones, sandy siltstones and mudstones. The cement of the rocks is mainly calcitic and chloric (Eriksson, 1979).

The Elliot Formation is a fluvial deposit which has an average thickness of 300 m, locally reaching 500 m. Deposited during the Late Triassic, it was previously called the "Red Beds" because of its colours from yellowish grey to pale red. It consists of mudrocks, and fine-to medium-grained sandstones (Johnson *et al.*, 2006).

*Local history and archaeology*

This area is part of a larger region known as "Nomansland" by the colonial administration (Blundell, 2004). Three major historical records are available for this area: Henry Francis Fynn's (mid-19$^{th}$) and Walter Stanford's (end-19$^{th}$) journals and the testimony of an old woman called "M" in the 1980's (cf. §1.2.1). Geoff Blundell (2004) did his PhD project on sites including those in the Maclear district. Most of the following sites information is from his work.

Although very few dates from archaeological deposits are available for Nomansland, they give the evidence of an occupation by hunter-gatherers from at least 22 000 years ago to the colonial period (Opperman and Heydenrych, 1990). In this area, San were in interaction with

different neighbours such as Bantu-speaking pastoralists and English and Dutch colonials (Blundell, 2004).

*Selected sites*

Fourteen rock art sites were selected, mostly because of the presence of particular representations and because of the presence of black paints: RSA BUX1 (on Elliot formation sandstone), RSA CHA1, RSA FRE1, RSA FRE4, RSA LAB1 (also called Storm Shelter), RSA LAB3, RSA LAB6, RSA LAB10, RSA MEL6, RSA MEL8, RSA MEL9, RSA PRH1, RSA TYN2 (Figure 1.3). Paintings are all of the San Later Stone Age (from 50 000 BP to historical times) tradition with fine-lined paintings and colours gradients.

None of these sites have been excavated, thus no archaeological material is available for comparison with the paintings or to give idea of possible periods of occupations. The two most important sites of these fourteen are RSA LAB1, or Storm Shelter, and RSA TYN2. Only these will be fully presented here.

*Storm Shelter, RSA LAB1*

This shelter was discovered in 1992 by Sven Ouzman and Geoff Blundell, as they were looking for a place to shelter from a storm, hence its name of Storm Shelter (Le Quellec, 2008). It is approximately 30 m in length. Most of the paintings are "classic" images of San rock art with elands, antelopes, human figures, therianthropes and a detailed representation of a "rain animal" (Pearce, 2010). However, other images caught Blundell's attention: large-headed human figures and Eldritch figures (Figure 1.4, Figure 1.5). As mentioned previously, these figures are of importance for understanding societal changes in San history (Blundell and Lewis-Williams, 2001).

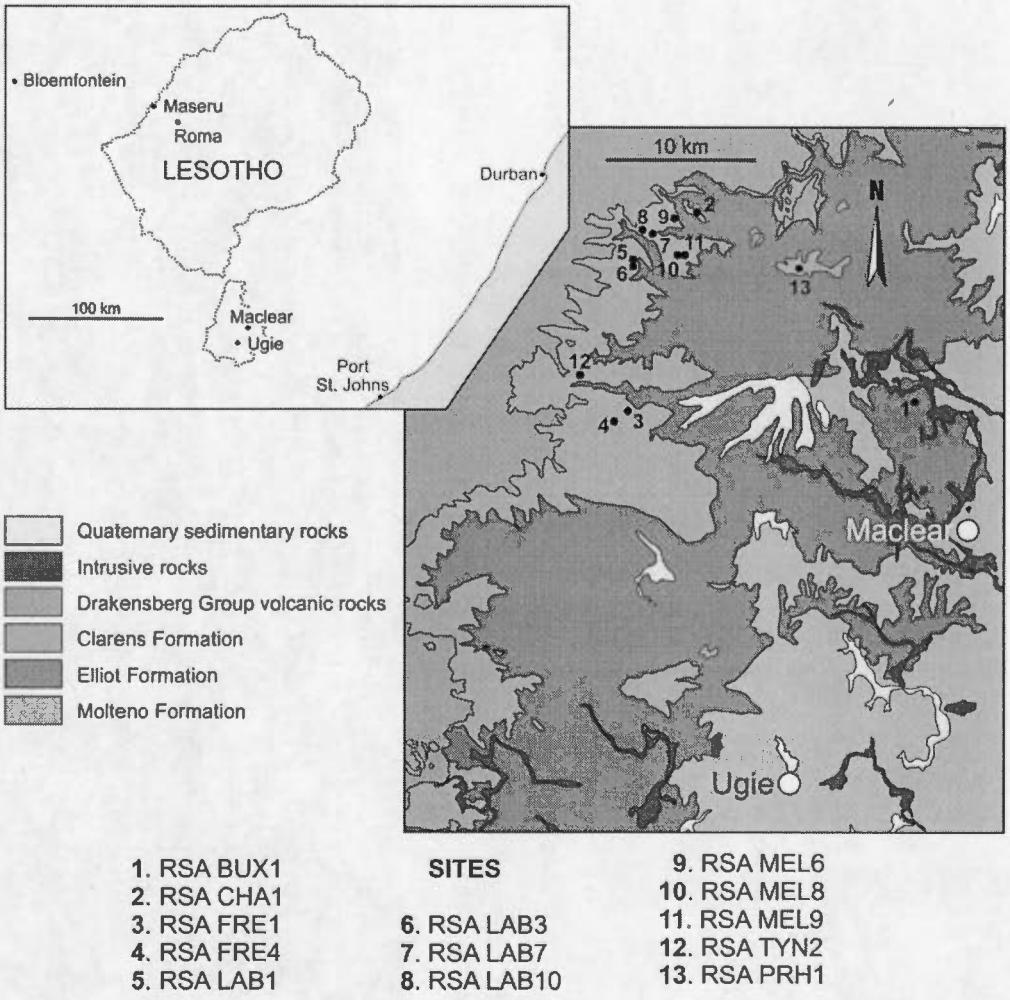


**Figure 1.3** Geological map (from Thomas, 2002) and location of sites of the Maclear district

**Figure 1.4** Black-and-white drawing of the primary panel at Storm Shelter (from Blundell, 2004)

**Figure 1.5** Photo of the primary panel at Storm Shelter (© D.G. Pearce)

"Type 3" figures have also been identified in this shelter by Mallen (2008) (Figure 1.6). They are characterized by their subject (monochrome human beings, felines and quadruped images) and were made with a coarse pinkish red pigment. These figures are argued to be related to autonomous multi-ethnic raiding groups, who lived during the historical period (Mallen, 2008; Pearce 2010).

**Figure 1.6** Photo of "Type 3" images at Storm Shelter (© D.G. Pearce)

*RSA TYN2*

This shelter is approximately 25 m long, 3 m high and 6 m deep. As with Storm Shelter, paintings are mainly of San fine-line tradition with "classic" representations (Figure 1.7). "Type 3" figures are present too (Mallen, 2008; Pearce 2010). Whereas paintings are mostly concentrated on one single panel at Storm Shelter, at RSA TYN2 paintings are scattered throughout the shelter. Its shape is like an L, dividing it into two main panels. The second panel, on the small part of the L, suffers from major rock flaking. These flakes detach from the rock face and bring with them part of the paintings (Pearce, 2010). Collected in 2008 and 2009, they were analysed during the initial project in 2010 at the Research Laboratory for Archaeology and the History of Art, University of Oxford, United Kingdom.

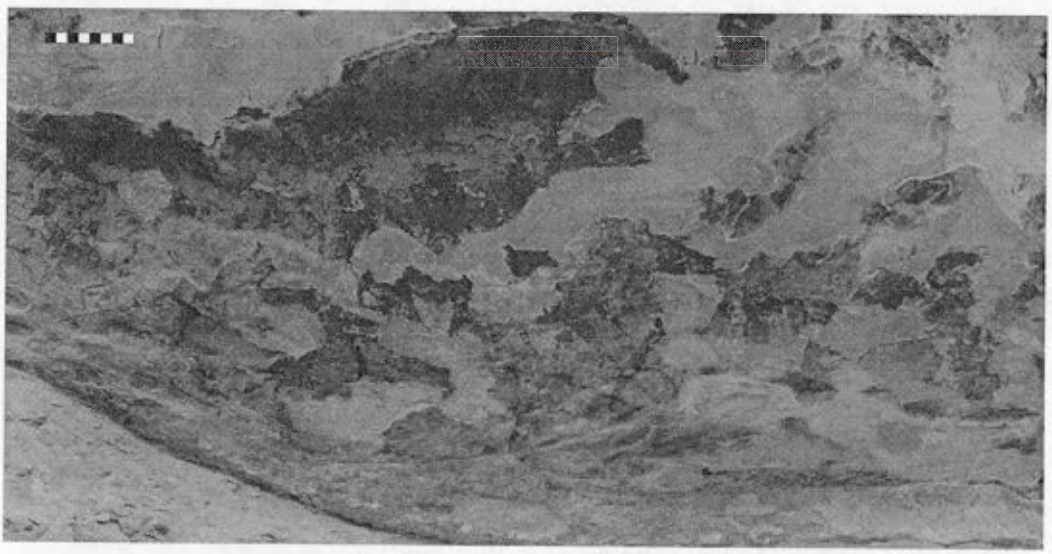

**Figure 1.7** Photo of TYN2 shelter (© A. Bonneau)

1.2.3.4 The Phuthiatsana River Valley, Lesotho

The Phuthiatsana River valley is located approximately 30 km east of Maseru, the capital city of Lesotho.

*Local geology*

Sites are found on the Clarens Formation and the Lesotho Formation. This area is part of the same geological area as the Maclear District. The Clarens Formation in Lesotho is the same as in the Maclear District, but its deposition was made in a more arid environment. The Lesotho Formation is part of the Drakensberg Group of volcanic rocks. It is thought that the Phuthiatsana River has eroded through basalts and sedimentary rocks to produce the valley (FM Associates and Southern Waters, 2008).

*Local history and archaeology*

From 1979 to 1982, this valley (and three other areas) was examined by Smits and his team in order to record rock art sites as part of the Analysis of Rock Art of Lesotho project. Thus the sites recorded were called "ARALXXX" (Smits, 1983). 493 sites were recorded, of which 259 sites from the Phuthiatsana valley. In this area, San rock art is thought to have been made by *//Ku//e* San, nowadays extinct (Smits, 1983). However, the Metolong catchment where the dam has been built is only a very small section of the Phuthiatsana Valley, comprising 28 rock arts sites.

Between 1989 and 1990, excavations and survey were conducted in the Phuthiatsana Valley by Prof. Peter Mitchell. These were resumed in 2008 as a dam was planned to be built in this valley and thus flood archaeological and rock art sites. Amongst them, following previous data recorded in 1989 and 1990 and archaeological survey, the most important sites were excavated. Excavations gave evidence of Middle Stone Age occupations in several rock shelters and then of different occupations by hunter-gatherers, possibly San communities, through time to Sotho-speakers people living here during colonial time (Mitchell, 1994; Mitchell and Arthur, 2014; Mitchell and Whitelaw, 2005). Among the artefacts, some grindstones show red, white and black stains which may represent pigments in preparation (Arthur and Mitchell, 2010). They are being analysed by Luiseach Nic Eoin, as part of her Ph.D. project at the University of Oxford, United Kingdom. Comparisons between our researches have been made and results are presented in Chapter III. Paleoenvironmental analyses were conducted at two excavated sites (Ntloana Tsoana and Ha Makotoko) showing a considerable temperature fluctuation across the Pleistocene/Holocene boundary (Roberts *et al.*, 2013).

In parallel with the excavations, records of the 28 rock art sites, which are to be flooded (Figure 1.8), were done by Lara Mallen and some panels were removed from the rock to be conserved in museums. Five separate painted traditions have been identified in the Metolong Dam area. The two greatest traditions in number are San fine-line tradition (Figure 1.9) and Basotho tradition (Figure 1.10). Ochre smears, finger-painted figures and figures of unknown traditions complete the list (Arthur *et al.*, 2010).

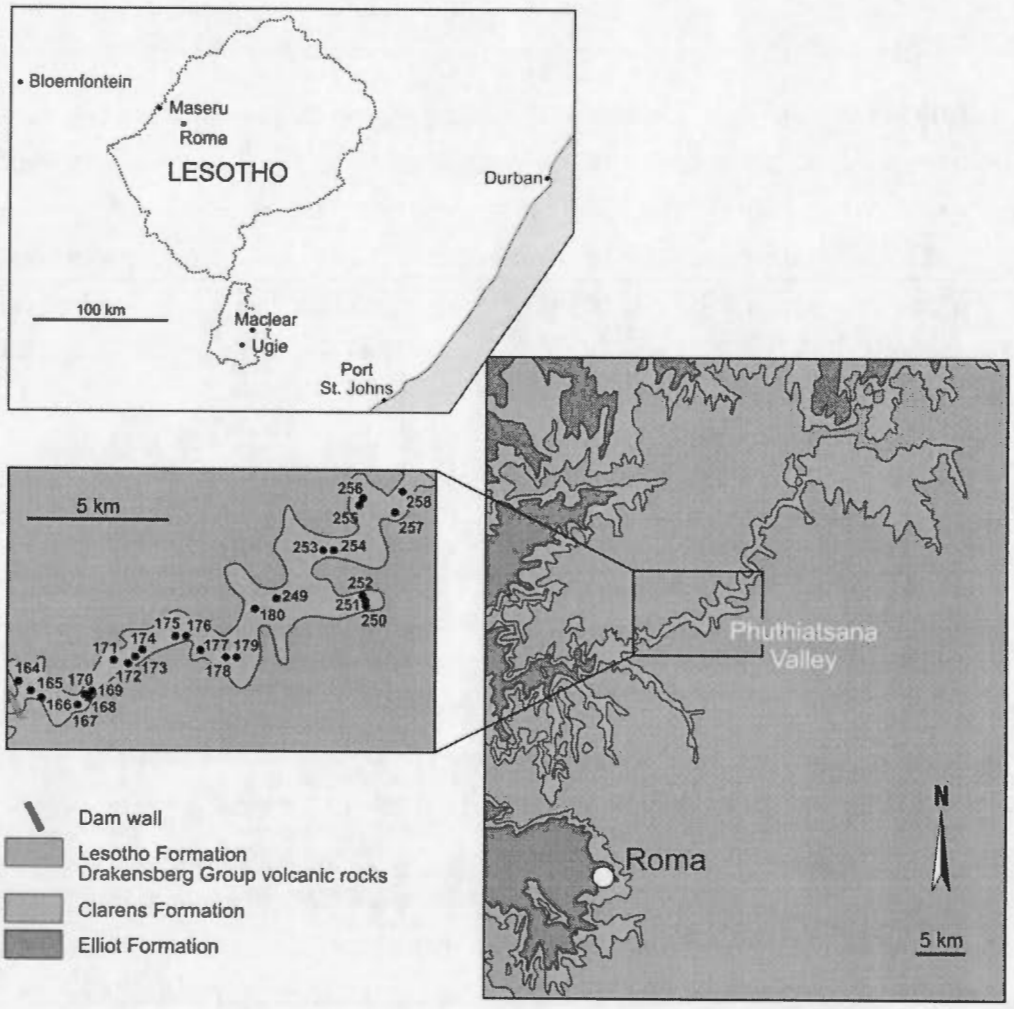


**Figure 1.8** Geological map (from Directorate of Overseas Surveys, 1982) and location of sites in the Metolong Dam area (sites are noted without the "ARAL" prefixes)

**Figure 1.9** San fine-line tradition rock art at ARAL 258 (© D.G. Pearce)

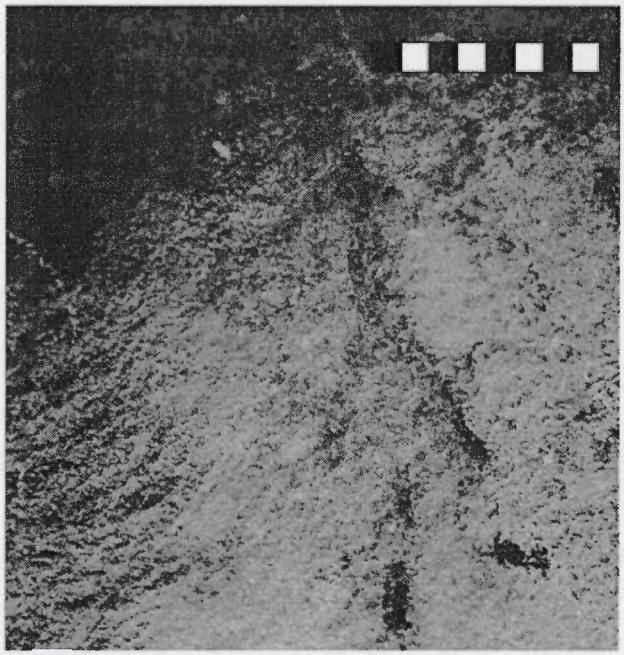

**Figure 1.10** Basotho tradition rock art at ARAL 254 (© D.G. Pearce)

*Selected sites*

For this Ph.D. project, only San and Basotho paintings were analysed (few figures of unknown tradition are incorporated too). Basotho paintings were added to the corpus as they were of known age and thus gave a chronological point to test dating protocols.

However, as the sites were destroyed, all sites and identified figures were sampled for further analyses.

The Phuthiatsana Valley is close in distance and in culture to the Maclear district area. Thus most of the figures are similar and representations thought to be linked to creolization are present (Arthur *et al.*, 2010). Moreover, as excavations were conducted in some shelters, establishing the dates of rock art is very important to correlate them with archaeological deposits. Comparisons with Luiseach Nic Eoin's work are aimed at achieving the same result. Finally, this area was selected for the possibility to collect large samples to try different protocols and thus apply the best one to paintings in the Maclear district.

1.2.3.5 The Thune River Valley, Botswana

The Thune River Valley is located in the Kalahari Desert, near the town of Mathathane, at approximately 20 km west of the South African border and 500 km north-east of Gaborone, the capital city of Botswana.

*Local geology*

Curiously, rock art sites in this valley are found only on sandstones, whereas basalt and granite shelters are also present along the river bank. This may reflect the better suitability of sandstones to create paintings as they are more porous and absorb paintings. These sandstones are part of the lower Stormberg series, nowadays called Lebung series (Johnson *et al.*, 1996). They are part of the Tuli basin, one of the several contemporaneous Karoo basins (Figure 1.11). Such as the Main (Great) Karoo basin, the sedimentation ended by the extrusion of the volcanic basalt lavas. The Lebung series is similar in stratigraphy to the series comprising the Molteno, Elliot and Clarens Formations. However, in the Tuli basin, sandstones are present in Mosolotsane Formation and Ntane Formation, forming the Lebung

series. They are called "forest sandstones" in specific places and correlate well with the Clarens and Elliot Formations (Johnson *et al.*, 1996). Interestingly, sandstones from Lebung series were called "cave sandstones" by geologists of Botswana, the same designation as for the Clarens Formation in South Africa and Lesotho (Geological Survey Department, 1966).

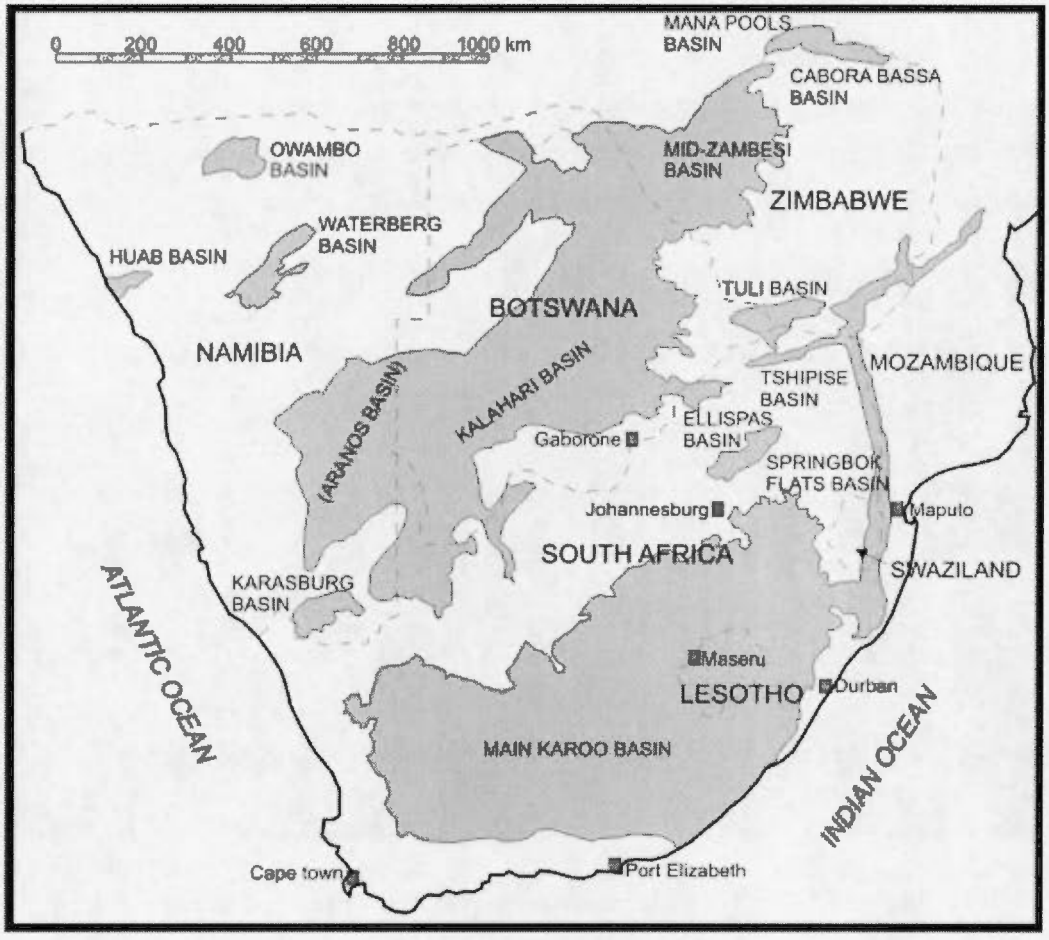


**Figure 1.11** Karoo Supergroup basins in southern Africa (modified from Johnson *et al.*, 1996)

*Local history and archaeology*

Even though rock art sites around this valley seemed to have been recorded before, it is unclear when and by whom in Walker's report (2009). As a dam was planned to be built such

as was the case in Lesotho, an archaeological survey of potentially impacted archaeological sites was required. 40 archaeological sites are present in the narrow band of about 35 km long and 5 km wide, of the Thune River Valley. Among them, six rock art sites will be flooded and 18 others may be impacted in case of exceptional floods. All 24 sites were recorded and some excavated (Walker, 2009).

As part as the Thune Dam project, rock art sites were recorded (traced, photographed and copied), and some Later Stone Age artefacts have been found by survey. Excavations were conducted by local archaeologists but the results have not been reported yet. The Thune Dam has now been impounded and the sites sampled are underwater (Figure 1.12).


**Figure 1.12** The Thune Dam (photo provided by local archaeologists)

*Selected sites*

As only 6 of the 24 sites were to be flooded, they were the only ones sampled (Figure 1.13): TD2, TD3, TD12, TD20, TD21. Their graphics include fingers paintings and San fine-line tradition paintings, but interestingly, few superimpositions appear. Distinctive San regional representations are recorded such as giraffes and fishes (Figure 1.14). The most important

representation in these sites is sheep paintings (Figure 1.14) as these constitute the only example at this time in Botswana. In archaeological contexts, sheep remains have not been recorded before 2200 BP, giving a useful chronological starting point for these paintings (Walker, 2009). On the other hand, fat-tailed sheep may have been considered by San as full of "power" because of the large quantity of fat they contained (Le Quellec, 2008).

The finger paintings are peripheral to, or superimposed upon, San paintings and thus appear to have been made at a later period.

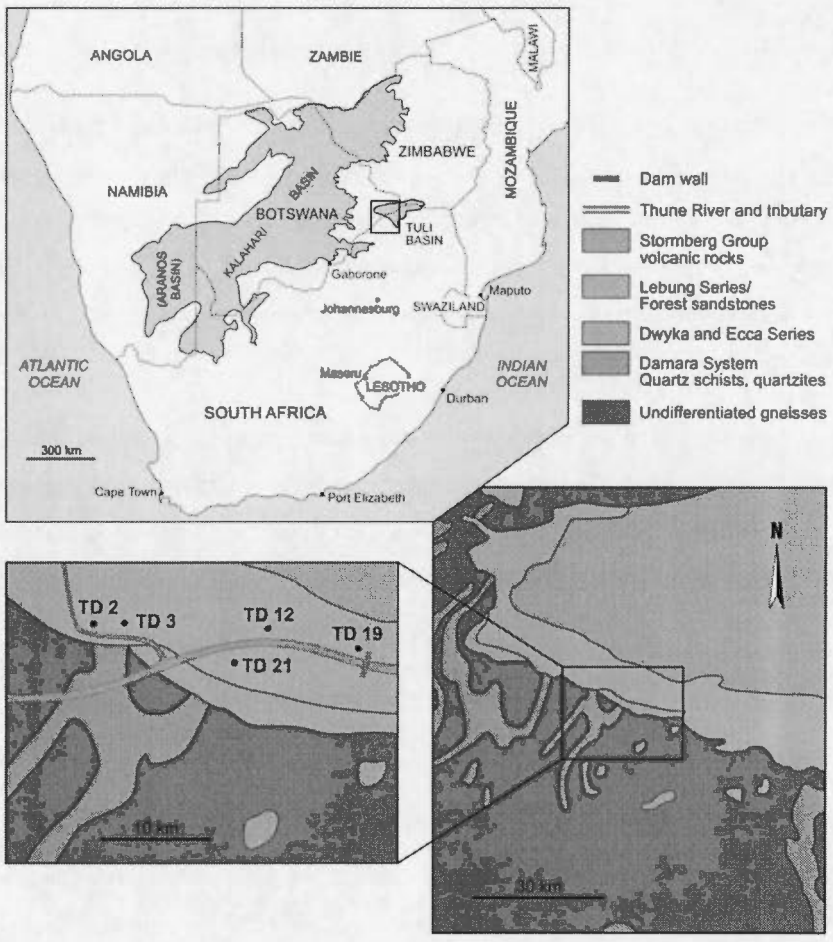


**Figure 1.13** Geological map (from Geological Survey and Mines Department, 1973) and location of the Thune Dam area sites

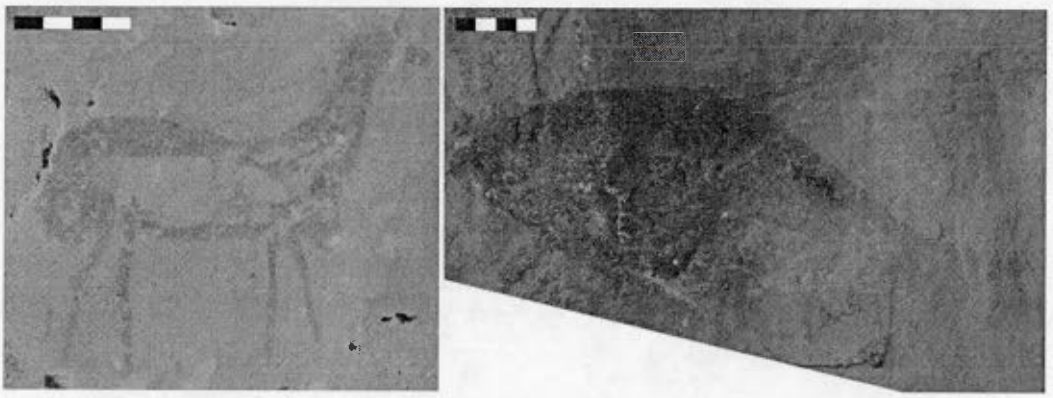

**Figure 1.14** Sheep and fish paintings in the Thune Dam area (© A. Bonneau)

As with the Metolong dam, sites in the Thune dam area were selected due to the possibility of collecting large samples on figures which sometimes have chronological attributions. Moreover, they are San paintings of another distinctive regional tradition than the Maclear district and the Metolong Dam area. Comparing pigments used and dates will reveal similarities and differences in San rock art in southern Africa, regardless the style of representations.

Southern African sites give the possibility to make and test protocols able to obtain absolute and direct dates on rock art. Once these protocols are efficient, it will be interesting to apply them to sites in another part of the world. Rock art of the Canadian Shield has been chosen for this purpose and for their situation as open-air sites (details about the choice of both southern Africa and Canadian Shield rock art are given in §1.4).

## 1.3 Rock art in the Canadian Shield

### 1.3.1 Characteristics and history of research

More than 750 rock art sites are recorded in the Canadian Shield, mainly on rock formations along riverbanks and lakeshores. Made by hunter/fisher-gatherers speaking Algonquian languages, the art is thought by archaeologists to date from the Woodland period (from 1000 BC to the beginning of European colonization) or from the Late Archaic (from 4000 to 1000 BC; Arsenault, 2004). However, some sites with horses and guns representations attest that rock art continued to be made during colonial time (Lemaitre, 2013).

Rock art is present in two main areas in Canada: the Canadian Shield and in the cordillera along the Pacific west-coast, although there is some more appearing in the Prairies and in the Maritimes provinces. Access to sites was possible only for the ones present in the former area. The denomination "Canadian Shield" refers to the geological core of the North American craton. It covers a large part of Canada around and underneath the Hudson's bay. It is composed of mostly metamorphic, igneous and sedimentary rocks of Precambrian age. As rock art from Algonquian tradition is mostly concentrated in this geological formation, it has been used to name this art.

Algonquians lived in small "families" of about 20 to 40 members during winter in very large hunting areas, and then in summer, they aggregated with other families around fish-rich lakes and rivers. These groups counted about 200 people. Marriages, ceremonies, and vision quests took place during summer time (Wright, 1995).

The Great Lakes used to be the core area of the Algonquians tribes living in the boreal forest, but even after the arrivals of the first Europeans they used to live extensively far from the Great Lakes regions too. They were divided in two linguistic areas:

- The Cree language spoken by the Cris, the Montagnais, the Innus and the Naskapis

- The Ojibwa language spoken by the Odjibwas, the Algonquins, the Nipissings and the Ottawas

The Algonquians share a series of common cultural traits through the Canadian Shield with some regional differences. Their spirituality is no exception to this rule. Their world is divided into four "layers": the cosmos, the Earth where people live, the underworld and the subaquatic world. These layers are interconnected and powerful spirits living in the cosmos and the underworld, the Manitou, can interfere in people's lives in good or bad ways. Rocks and cliffs are thought to be passages from one world to another and place where supernatural entities lived as the Thunderbird. Thus, the rock is seen as a living thing (Lemaitre, 2013).

To talk with the Manitou, to cure people, to visit long distance relatives or to see in the future, four categories of "potency-owners" exist in the Algonquian tribes: the *nanandawi*,

the *wabeno*, the *tcisaki*, and the *mide*. The three first categories of "potency-owners" use songs, dances and possibly drugs to enter a kind of trance. The *mide* can be seen more as medicine-men, with initiation rituals and transmission of knowledge from master to apprentice. Part of their apprenticeship was carried out using engraved tree barks (Lemaitre, 2013; for more information about the four types of "shaman", refer to Lemaitre, 2013: 102-105).

Rock art in the Canadian Shield may have been executed by these potency-owners, as ethnographic and historic testimonies suggest. For example, the site GfKu-1, in the Oxford House area, was described by local people to be the work of a "shaman" during the first half of the 18th century. Other rock art sites near Sault Ste Marie were executed by Myeengun, a great chief and *mide*, to commemorate a war at the beginning of the 18th century. Other testimonies mentioned that teenagers painted their visions on rocks after their vision quests. On the other hand, some sites are thought to appear suddenly, as if by magic. The *Maymaygwashiuk*, little fairies living in the rock, are believed to have been the creators of such sites. They live in the same world as humans and thus can be seen sometimes. They can help humans to communicate with the Manitous and in the context of a rock art site, can act as an interface between the various interconnected worlds of the Algonquians (Arsenault and Zawadzka, 2013).

In the Canadian Shield, rock paintings were most of the time, made during the summer season, from within canoes. But it is possible that some sites might have been produced during the winter season, the artist standing on the hard frozen water. The artists used their fingers to paint and in some cases brushes, long-thin bones, hematite sticks or feathers were employed to draw fine details. Red is the most commonly used colour. Although, orange, yellow, white and black colours were also part of the artist's palette. The rock surface and the rock itself seem to have been selected following different criteria. The surface to be painted should be smooth and preferably covered with a white mineral deposit in order to accentuate the paintings. The rocks are selected because of their good acoustics (Waller and Arsenault, 2008), the place in the landscape, their shapes (sometimes a face can be seen in the rock) or of the presence of a spirit in or close to the rock (Arsenault, 2004). Paintings are made on

cliffs with a little edge, which help to preserve them. A few paintings were found on small boulders. But it may be due to the state of the research (Lemaitre and Arsenault, 2011).

Around sites, offerings, mostly tobacco, were found but coins, guns, clothes, and arrowheads, could have been also deposited. The offerings used to be, and still are in certain places, a common practice in Algonquian society and sometimes offerings are left on some rock outcrops with no rock art. On top of some rock formations with paintings, archaeologists have found circles of rocks, which are interpreted as thunderbird's nests. These places were used to communicate with the manitous after days of privation. Moreover, quartz veins are thought to be due to the impact of thunderbirds lightning, whereas the white mineral deposits are thunderbird droppings (Arsenault and Zawadzka, 2013).

As many rock art sites and their natural support are closely associated with thunderbirds, their representations are to be expected in Canadian Shield rock art. Other representations include anthropomorphic and zoomorphic figures, illustration of material culture objects (canoes, weapons, pipes), but also handprints and a large array of geometric motifs more or less complex in appearance. Only positive hand prints have been recorded to date. Very few anthropomorphic figures have sexual attributes. The zoomorphic figures are the most common with about 30% of the representations. They are linked to the Algonquians cosmology as few of the animals that they ate are painted. These could be the clan animals but in that case, some animals are missing (Lemaitre and Arsenault, 2011).

The artists used the natural features appearing on the rock surface such as the relief, crack, holes, mineral veins, etc., to structure and organize their compositions. Even though a certain freedom is given to the artists, it seems that they usually followed a common organization, including register and association of figures. Some paintings are very high compared to current water levels. It is possible the artists had to climb to paint on this specific spot, or that this apparent distance is due only to climatic water level changes (Lemaitre, 2013).

Rock art sites are landmarks. This art is made to be seen by people using the rivers and lakes networks to travel. So why paint at a specific place? Different interpretations are proposed by Lemaitre and Arsenault (2011): to accentuate the sacrality of a place, to make an offering, to contact the manitous, to commemorate an historical event, to warn about a danger (waterfall

or vortex, which indicates the presence of a malicious spirit), to indicate the way. On the other hand, some sites are difficult to see and may have been created to be kept secret and known from only a few people.

The first mention of rock art in the Canadian Shield was in 1669 in the journal of two Sulpician priests, along with maps made during the French Regime (17$^{th}$ century). Then in the second half of the 19$^{th}$ century, Newton Flanagan, employee of the Hudson's Bay Trading Company, and G. Mallery, member of the Bureau of American Ethnology, investigated Canadian rock art by prospecting and by local population survey.

The first systematic researches, however, began only in the 1950's. Whereas rock art sites in the United States of America (USA) are well known, mainly because of the facility to access the sites, Canadian Shield ones are poorly known and recorded. Selwyn Dewdney, Thor Conway, Kenneth Kidd, Tim Jones, Jack Steinbring and Grace Rajnovich surveyed and recorded rock art sites in the Canadian Shield from the 1960's, and gave the first interpretation about its meaning and site choice. Most of these surveys were mitigatory, in order to collect the maximum of data before dam construction flooded the sites.

In Quebec, at the end of the 1960's and during the 1970's, Gilles Tassé recorded rock art sites, and analysed with chemical techniques the components of the paints, especially the mineral crusts surrounding the paint layer.

In the 1990's, research was severely curtailed by lack of funding and retirement of most of the researchers. However, this was revived by the discovery of a rock painting site on Lake Cassette, in Quebec, the so-called Nisula-Pepeshapissinikan, followed by an intensive analysis of its components starting in 1992. Thanks to this first research project at Nisula-Pepeshapissinikan and from 1996 onward, Daniel Arsenault and his team pursued a project named PETRARQ, and then other ones focusing on rock art recording and interpretation in the Canadian Shield.

### 1.3.2 Current research and questions

In the last 20 years, the rock art of the Canadian Shield has been mainly studied by Daniel Arsenault and his students, as well as Serge Lemaitre. They have interpreted this art by combining archaeological, historical and ethnological records. However, as most of the sites are made on cliffs, archaeological remains are very few and in the case of archaeological excavations in the vicinity of the sites (for example, on riverbanks or lakeshores), the occupations are often too numerous to be able to attribute the site to one or other of these occupations. Sometimes however, information may be found on top of the cliffs, in the so-called 'thunderbirds nests'. In order to mitigate this lack of archaeological records, Serge Lemaitre (2013) proposed to investigate sites in their archaeological context, giving different context levels: context of the rock face, context of the cave/cliff/boulder, context of the tribe/society of the painter.

Applying this methodology, Lemaitre was able to propose two hypotheses about rock art in the Canadian Shield. Firstly, the distribution of the representations can be divided in two areas, one to the east of the Canadian Shield, and one other on the west, Lake Nipigon being the border between the two areas. This division seems to correlate with divisions made in ceramic analysis, even if the division can be debated. Secondly, the distribution of sites follows the summer/winter dynamic of the Algonquian tribes. Indeed, rock art sites seem to be well distributed around the Great Lakes where the summer camps for Algonquian families were located. However, sites do not fit in this model and it is perhaps only a bias in the actual state of the research (Lemaitre and Arsenault, 2011; Lemaitre, 2013). Following this model, it is possible that rock paintings were seasonal or annual rituals/activities, and thus that some sites may have been produced over a long time. But on the other hand, panels have a unity in their organization and figures are often of the same size. If almost no superimposition exists in Canadian Shield rock art, a few attestations of refreshed paintings are found, such as the representation of a *Mishupishu* at Agawa rock on Lake Superior (Lemaitre, 2013).

Discussing the interpretation of rock art, Canadian rock art does not escape the debate about "shamanic model". As with southern African rock art, archaeologists may agree or not with this theory. Steinbring, for example, is against this theory and argues that no deep trances existed in the Ojibwa tradition (Lemaitre, 2013).

As mentioned in the previous section, different kinds of potency-owners existed in the Algonquian society. Even though testimonies confirm that potency-owners, more precisely *mide*, were the authors of some sites, they do not say that they commemorate something seen during trance. Moreover, we know that on one site from the 18th century, near Sault Sainte-Marie, Myeengun painted a rock outcrop to commemorate a war.

If one takes into account the homogeneity of the iconographic selection, it does not seem parsimonious to attribute the art only to visions obtained during trances. In this case, the selection of representations would have been more complex (Lemaitre, 2013). Lemaitre mentioned too that people could paint or engrave on different supports without being a potency-owner in the Algonquian society. However, some potency-owners draw representations which can be understood only by them; they are idiosyncratic figures.

Another research point, developed by Arsenault, is the use of the *chaîne opératoire* of a site, from the selection of a site until its abandonment, through raw material collection and preparation, conceptualization of the motifs or scenes to be represented and paintings, and use and reuse of the site. In this model, data about pigment characterization and dating points are of great importance. They then can be correlated with landscapes and rock surface descriptions to reconstitute the *chaîne opératoire*.

As with southern African rock art, Canadian Shield rock art still lacks the dated chronologies necessary to confirm the hypotheses addressed by Lemaitre and Arsenault, in order to compare sites and representations with time and not only in space, and to better understand the organisation of a site (one or more periods of painting).

### 1.3.3 Sites selected

Following the current research and work of Serge Lemaitre and Daniel Arsenault (co-supervisor of this Ph.D.), two areas were selected in the Canadian Shield: the Cliff Lake in Ontario, with eight rock art sites, and the *Mikinak* site at Lake Wapizagonke in Quebec. They are located respectively in the Superior Province and the Grenville Province, the two central geological provinces of the Canadian Shield.

The Canadian Shield is a Precambrian craton covering five provinces (Alberta, Saskatchewan, Manitoba, Ontario, Quebec) and two territories (Northwest and Nunavut). It consists of crystalline igneous, metamorphic and sedimentary rocks. From 4.0 billion to 570 million years ago, these rocks were submitted to numerous geological events such as volcanic eruptions, deformation, faulting, uplift, erosion, weathering, etc. (Fensome *et al.*, 2014).

#### 1.3.3.1 Cliff Lake, Ontario

Cliff Lake is located in south-western Ontario, about 40 km southwest of Lac Seul, and 200 km west of Lake Nipigon (Figure 1.15).

*Local geology*

Sites in the Superior province are found on Precambrian rocks, more precisely granite and granodiorites. One site (262) is found on a white and crystalline rock, maybe quartz or feldspar-rich.

*Local history and archaeology*

Around this lake, six rock art sites were recorded by Selwyn Dewdney in the mid-1960's (Dewdney and Kidd, 1967). Visited in 2012 by Daniel Arsenault and Serge Lemaitre, a detailed look at the sites and Dewdney's records showed that some "figures" were omitted and two new sites were found. A new recording will be made soon.

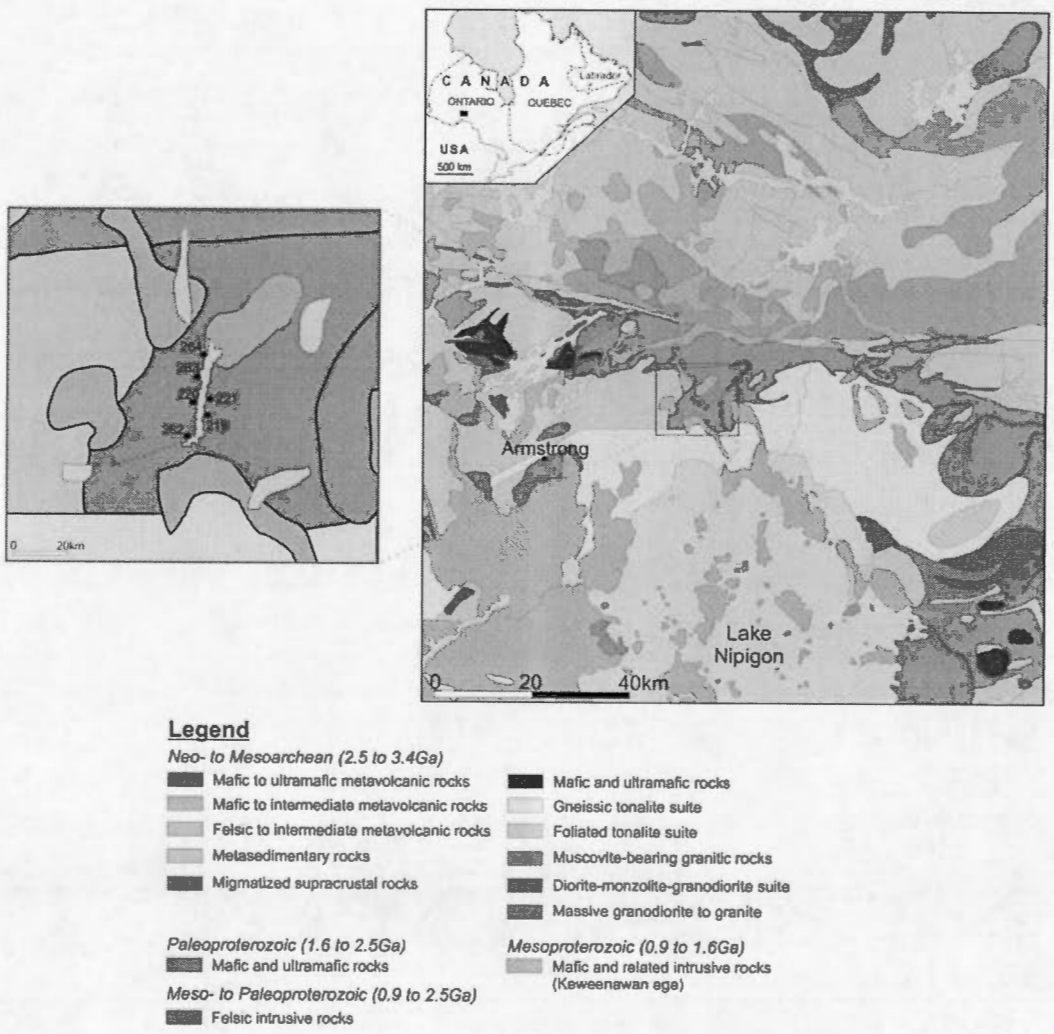


**Figure 1.15** Geological map (from Ontario Geological Survey, 1991) and location of the Cliff Lake sites

Rock art was made with fingers except one figure at site 262 whose fingers were finely painted, perhaps with a brush. The figures are mainly geometric but human and animal figures such as moose, otters and canoes with their stylized crew also occur. They are painted mainly in red and in site 262, orange and dark red paints were used (Figure 1.16).

**Figure 1.16** Paintings at site 262 (© A.Bonneau)

No archaeological excavations have been made on the banks of this lake.

These sites were selected because of the different colours used and their proximity with the Lake Nipigon, which seems to form a virtual border in Serge Lemaitre's model. However, only rocks and weathering crusts were collected for OSL tests, as no paint collection was allowed.

1.3.3.2 Lake Wapizagonke, Quebec

The Lake Wapizagonke is located in the Parc National de la Mauricie, about 100 km North of Trois-Rivières. The site has the following Borden code: CdFg-05 (Figure 1.17).

*Local Geology*

The Lake Wapizagonke is situated in the Grenville Province, the youngest Precambrian terrain to be accreted to the Canadian Shield. Its geological history is complex and the regional metamorphism is very high. The rocks are mainly dating from the Early Proterozoic (1,5 - 1Ga). The site is made on pyroxene-rich gneiss, a metamorphic rock composed mainly of pyroxene, plagioclases, alkaline-feldspars, quartz, amphiboles and magnetite (Desrochers, 2011).

*Local history and archaeology*

Jacques Béland, in 1951, was the first to describe this site. In the 1960's, excavations were conducted on the lakeshores and elsewhere in the Park, showing several occupations dating from the Woodland period (Woodland period: 200 BC-1200 AD). In the 1960's, René Ribes made the first records of the rock paintings but mentioned that some of them had disappeared. In 1966, Selwyn Dewdney made another record of the site and noted that vandals had taken pieces of rock paintings. In 1976, Gilles Tassé recorded the site another time and tried to reconstitute the site using Béland's photos (Tassé and Dewdney, 1977; Lemaitre, 2013).

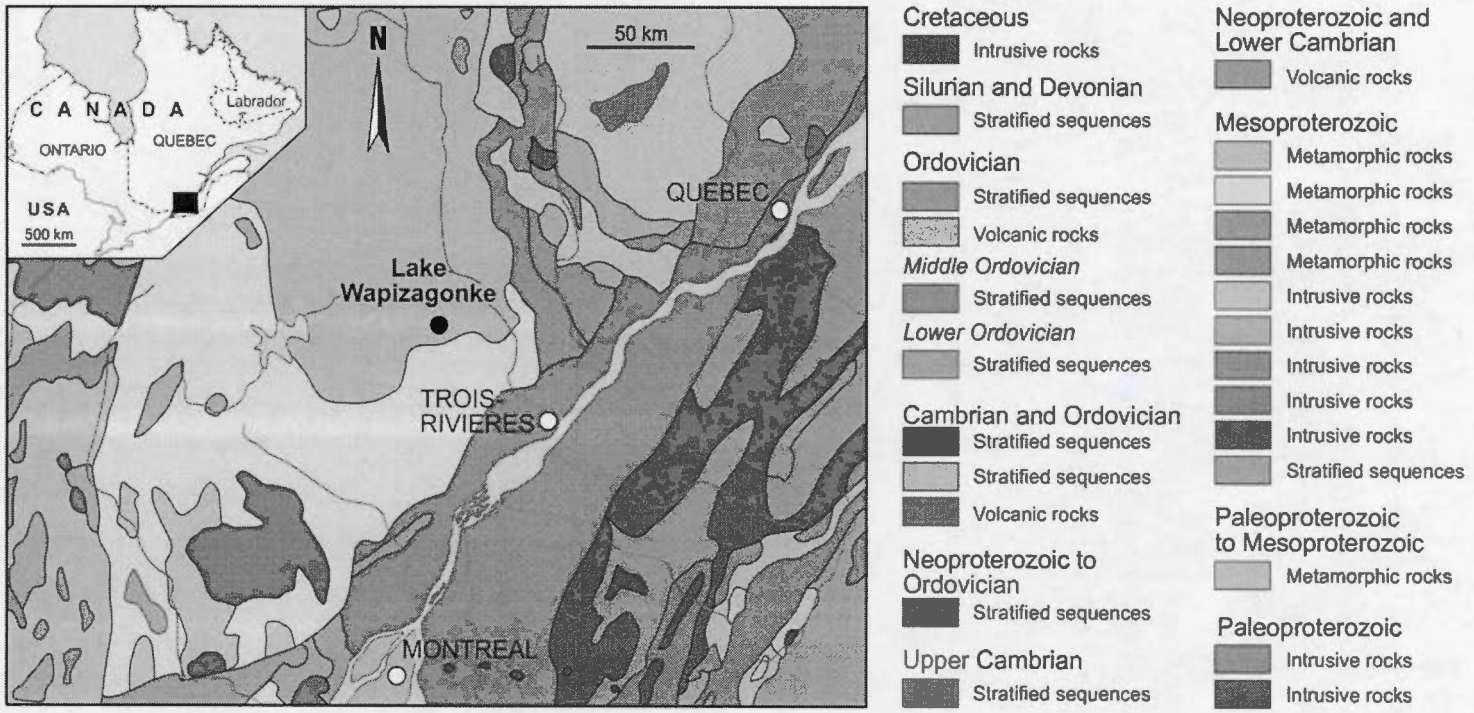


**Figure 1.17** Geological map (from Wheeler *et al.*, 1996) and location of the Lake Wapizagonke

During fieldwork, flakes of rocks with paint which had fallen into the lake were collected and stored for analysis. They were analysed by the Canadian Conservation Institute in the 1970's by Taylor *et al.* (1974) and more recently by Helwig (2011). Results showed that paintings were made with hematite-based material surrounded by amorphous silica crusts resulting from weathering.

Other excavations were conducted revealing occupations by hunter-gatherer tribes from the Archaic Period to the second half of the 19$^{th}$ century (Dagneau, 2010).

In 2011, subaquatic excavations were conducted by Parks Canada. Flakes with paint were collected in the sediments of the lake and stored in Parks Canada buildings, at Ottawa, Ontario (Dagneau, 2010). Analyses were conducted on these flakes.

Rock paintings were made with red pigments and using fingertips. Zoomorphic, anthropomorphic and geometric figures form the graphic of the site (Figure 1.18).


**Figure 1.18** Rock art paintings at Lake Wapizagonke

In this PhD Project, Lake Wapizagonke was selected because of the presence of fallen painted flakes which can be used to conduct analysis. Indeed, this site has a long history of recording and analysis but the question of its age is still unresolved. It is used in this Ph.D.

project as a typical Canadian rock art site where pigment characterization and dating protocols can be applied in order to resolve dating issue.

As detailed in this section, sites were selected in southern Africa and in the Canadian Shield to answer regional questions. However, one can discuss this choice of both Canadian and southern Africa rock art. The following paragraph addresses this question.

### 1.4 Discussion: southern African and Canadian rock arts dating: similarities and differences

This Ph.D. project follows an initial pilot project realized in 2010 at the Research Laboratory for Archaeology and the History of Art (RLAHA), Oxford University, United Kingdom. First results were obtained on San rock paintings from site RSA TYN2, in the Maclear district, South Africa. The methodology developed needed to be improved by testing on large samples. An opportunity for such sampling was raised by the planned construction of two dams in Lesotho and Botswana. Thus methodologies and protocols could be tested and the size of samples reduced when applying them to other San rock paintings sites.

As good results were obtained on these sites, the necessity of testing them at rock art sites elsewhere in the world appeared. Therefore, Canadian Shield rock art was chosen due to ease of access as one of my supervisors, Daniel Arsenault, works on these sites, and because of its lack of chronological data. Moreover, Canadian Shield rock art is similar in some points to San paintings, e.g. the pigments used and the weathering crusts surrounding the paintings. On the other hand, only a few black paints are reported from the Canadian Shield and those would not be accessible.

The choice of these two areas very distant from each other was motivated by the possibility of applying the protocols developed for the rock art of one region to another. The two areas were geographically far afield, but easily accessible to me due to the supervision of this project, and would benefit from the application of such techniques.

# CHAPTER II

# METHODOLOGY AND DATING TECHNIQUES APPLIED

In this chapter, the methodology and techniques used in this Ph.D. are explained, justified and detailed. Previous researches are first listed and discussed to lead to the methodology used. Each step is detailed with the protocols used and the respective objectives, results and issues (unless otherwise stated, all the following preparations and measurements were carried out by the author).

## 2.1 Dating rock art: a quick review of dating techniques, advantages and issues

'How old is it?' is the question most frequently asked about rock art, but the question which is maybe the most complicated to answer. Many techniques have been tested in order to try to provide answers, from historical records, oral testimonies, and stylistic characteristics to physical and chemical techniques such as radiocarbon and Uranium-series dating.

Firstly, different techniques used to date rock art around the world are reviewed. Then focus turns to those applied in southern Africa and in the Canadian Shield and the results they have provided.

### 2.1.1 How to date rock art? Review of techniques applied around the world

One of the first attempts to date rock art was through use of historical records or testimonies of the living descendants of the artists. This was possible during colonial times when Europeans arrived in southern Africa or in North America and where artists were still painting. However, these records (journals and letters) were usually made by missionaries, explorers or soldiers, giving a Eurocentric angle to the description, and the location and date of the sites are not well detailed, if mentioned at all. Examples of these include Father Jacques Marquette, along the Mississippi River, and Lieutenant W.H. Emory for North America (Grant, 1984), Joseph Millerd Orpen, Georges William Stow, Wilhelm Bleek and

Lucy Lloyd for southern Africa (Lewis-Williams, 2003), or Basedow (1914) for South Australia. Sometimes, these visitors left graffiti on top of the paintings with their name and the date, giving a terminus *ante quem* for the original paintings (Figure 2.1).


**Figure 2.1** Graffiti in the Maclear district, South Africa (© A. Bonneau)

Direct testimonies from descendants are extremely rare but the story of an old woman, known as 'M', in the 1980's, is one of them. She showed and described paintings made by her father in South Africa (Lewis-Williams, 2003).

Historical records are invaluable but only for recent times, and cannot be used, for instance, to date Franco-Cantabrian Palaeolithic rock art. Archaeologists thus started to excavate sites where possible. Material culture remains and rock fragments with paintings in archaeological layers made it possible to correlate rock art to an occupation. When excavations were not possible on site (due to the location of rock art on a cliff or a rock shelter with rocky floor, etc.), they were conducted in the vicinity of the sites and were sometimes able to provide indications of the paintings' authorship.

Stylistic studies were of great importance in providing age estimations, but for a long time it was assumed that the simplest figures were the oldest and the most sophisticated ones the youngest. This was challenged when the first radiocarbon dates were provided in the 1960's (discussed below). Previously, stylistic studies were conducted in order to correlate sites and to try to date an undated site by correlation with a site of known age. Linked to stylistic research, iconography could be used when a representation was found on both rock art and archaeological objects such as ceramics. It was thus assumed that the same people painted and made the objects. The same approach was used in comparing the techniques of paintings between sites and on objects (Bednarik, 2002). The representations painted can be good dating elements, especially for more recent times as one can find guns, horses or Victorian dresses drawn in rock shelters which are doubtless influenced by the arrival and contact with European colonists (Figure 2.2).

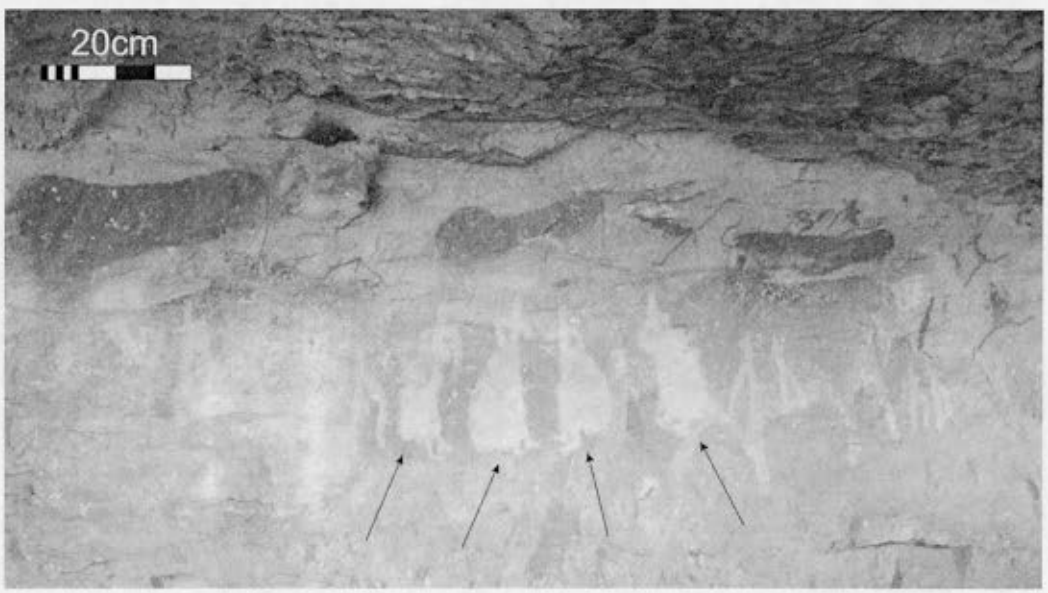


**Figure 2.2** Representation of women wearing Victorian dresses, at RSA BUX1, South Africa (© A. Bonneau)

At some sites, paintings are made on top of others giving a very complicated chronology of superimpositions, but which can also give relative dates for paintings. The Harris matrix has been applied to interpret such paintings at different sites in South Africa (see in §2.1.2).

However, these attempts give few absolute dates. Thus, physical and chemical techniques, mostly borrowed from Earth sciences, have been used to try to provide ages for rock paintings.

One of the most (if not the most) used technique nowadays is radiocarbon dating. From its beginning in the 1940's, this technique has been used to date a great number of archaeological remains from bones to parchments through ceramics, charcoal, textiles, etc. Because of the sacred nature (both religious and scientific) of rock art, it was extremely difficult to collect enough samples to provide a date before the 1980's and the development of AMS (Accelerator Mass Spectrometry), which can provide dates from samples weighing only a few milligrams. The first radiocarbon date obtained on rock art with $^{14}C$ AMS was at the Oxford Radiocarbon Accelerator Unit, at the University of Oxford, on South African rock art (see in §2.1.2). While most of the paintings dated with this technique were made of charcoal or carbon-based pigments (e.g. Valladas *et al.*, 2001; White *et al.*, 2012), attempts have been made with other kinds of carbon-based paint components. In Australia, paintings made of beeswax have given a radiocarbon age of about 4000 BP (Nelson *et al.*, 1995).

Oxygen-plasma oxidation has been used to extract binders from pigments for radiocarbon dating (Armitage *et al.*, 2001; Chaffee *et al.*, 1994; Russ *et al.*, 1990, 1991). This technique has the advantage of oxidizing only organic and not inorganic carbon contained in calcium oxalates and calcium carbonates, which are the most common weathering products found on rock art and the most common contaminants for radiocarbon dating. Its disadvantage is that it oxidizes all organic compounds present in the sample, the sources of which can be different from the original binder, including microbiological organisms, pigment and binder decompositions, human use (due to application of fat, blood, or other substances during rituals, touching the paints, etc.), etc. Thus, this technique requires careful characterization of the paintings to know what is being extracted, but has given good results on rock art of known ages (Armitage *et al.*, 2001). Attempts have been made to directly extract binders through chromatography and then date them using radiocarbon by Mori's team in Libya (Mori *et al.*, 2006). It is the first and only successful attempt thus far to date directly extracted binders. They used the proteinaceous material content in the sample. However, as mentioned earlier for oxygen-plasma oxidation, it is difficult to know if this material is really correlated

to the painting, although the date obtained of about 6000 BP is consistent with archaeological evidence found in the area.

Radiocarbon dating has been applied to weathering crusts containing carbon which surround layers of paintings. Calcium carbonates (Tacon *et al.*, 2013), calcium oxalates (Gillespie, 1997; Mazel and Watchman, 1997; Mazel and Watchman, 2003) and diatoms in silica crusts (Aubert *et al.*, 2004) have been dated with varying degrees of success. The main issues of using weathering product layers are the delay between the paint and the formation of the layer, and the source of the carbon metabolized. In any case, the dates obtained have to be considered as a *terminus ante quem* or *post quem* depending on the place of the layer dated.

Calcium carbonate crusts surrounding rock art, especially in caves, have recently been dated using Uranium-series dating. This dating technique, usually devoted to stalagmite dating in caves, needs only few milligrams of calcite which gives the opportunity to sample above and below rock paintings (Pike *et al.*, 2012). The main constraint for the application of this technique is the possibility of leaching of uranium through groundwater runoff. Ages obtained are again *termini ante quos* and *post quos*.

Binders have also been investigated with amino acids racemization in order to try to date them. The first study by Denninger (1971) using paper chromatography on South African rock art, did not give exploitable results such as the second by McCarty *et al.* (1994) on American rock art. In the two cases, they were not able to recover the ratio between the different amino-acids because of the insufficient sample size.

Optically stimulated luminescence (OSL) proved to be a useful tool in dating rock art where it has been covered by sediments (Huyge *et al.*, 2007), mud-wasp nests (Roberts *et al.*, 1997), or when a boulder detached from the rock face has taken paintings with it (Chapot *et al.*, 2012). In that last case, sediments under the falling bolder and the rock surface in contact with sediments were dated to give a minimum age to the paintings. It requires that the sediments and rocks were well exposed to sunlight before being buried.

Another dating technique borrowed from Earth sciences is cosmogenic dating, but it is rarely used because it dates the time a stone was exposed to cosmogenic rays, exposure following

the retreat of an ice-sheet for example. Cosmogenic rays are highly penetrative and thus a thick layer of ice, rock or sediments is required to block them. Two studies using this method gave disputable results, especially one of the Côa Valley sites (Bednarik, 1995; Phillips *et al.*, 1997; Pillans and Fifield, 2013).

Finally, lichenometry, the study of the growth of lichens on top of paintings, was investigated by Bednarik (2002). It requires a study of the different species of lichens and their growth through time and exposure to daylight/weather. This technique may be able to date material as far back as 9000 BP, but is difficult to apply because of the lichen growing references needed.

In conclusion, in the past, many different techniques and attempts have been made to provide ages for rock art, but few were successful. Focus is now shifted to the researches in the two world regions selected: southern Africa and the Canadian Shield.

### 2.1.2 In southern Africa

In southern Africa, representations of horses, guns, and other European objects and people made it possible to attribute a narrow time period to some recent panels. The case of the "white camel" of Makgabeng is one of them. Painted in the Northern Sotho style, it was photographed in 1916. Recently, it has been linked with the region history: around 1908, some officers of the British South African police patrolled the region of the Limpopo River on two of these animals. It has been possible to date this painting and to replace it in its historical context (Smith and van Schalkwyk, 2002).

In the 1960's and 1970's, much effort was put into the construction of relative chronologies based on stylistic differences (e.g. Pager, 1971; Vinnicombe, 1976; the most recent reviews of the dating evidence are those by Mazel (2009a, 2009b)). Unfortunately, none of these stylistic sequences seem to have been real, and have long been abandoned. More recently, attempts have been made to construct chronological sequences from observable superimpositions in various sites of the Drakensberg (e.g. Russell, 2000; Swart, 2004), essentially through the application of Harris matrices (initially conceived for analysing archaeological stratigraphies) to rock art (Harris, 1975). Thembi Russell (Russell, 2000)

showed that, where art is concerned, a necessary prerequisite to the use of this method is the identification of well differentiated artistic schools, traditions or styles (Le Quellec, 2008). This technique gave interesting results at the site of Main Caves North. It was possible to identify seven sequences, which partially corroborate the old chronologies established by Patricia Vinnicombe and Harald Pager in the same large region. One new point is that, while monochrome paintings are found in all the sequences, the presence of shaded polychromes is more significant, as these only emerge after the third phase identified using the Harris matrix (Le Quellec, 2008). Despite these encouraging results, according to Pearce (2010b) this technique does not translate well to painted contexts, and tends to produce fallacious sequences. If it is constrained to one site, the Harris matrix is a great asset, however attempts to use it at multiple sites simultaneously to try to date them yielded controversial interpretations.

Where possible, excavations should be conducted in the rock-shelters with art in order to correlate occupation sequences with the paintings themselves. However, in most cases where this has been achieved, numerous occupations have been found. There is still an unresolved problem of relating mural paintings to dated living floors (Solomon, 2006). Attempts to correlate colouring materials between grindstones and rock paintings, in Lesotho, were made during this Ph.D., in partnership with Luiseach Nic Eoin, a Ph.D. candidate at the University of Oxford, United Kingdom (see Chapter III).

More recently, radiocarbon dates were obtained for San rock paintings, but there are only a few of them. Indeed, it has long been assumed that the black paints were based on mineral pigments rather than carbon, and so a few attempts had been made to radiocarbon date the paintings.

The majority of dated San rock art is on collapsed wall paintings or loose painted stones dated by association from the layers of deposit in which they were found. The oldest dates for southern African paintings obtained in this manner are from the Apollo 11 shelter in southwestern Namibia. Three $^{14}C$ dates on material found in close proximity to 7 fragments of painted stones gave dates of between 27,500 and 25,500 BP (Wendt, 1976: it is not entirely clear how these dates were interpolated from the adjacent $^{14}C$ dates, nor would they

have been calibrated), leading to the claim that these represented the oldest African "art mobilier" known at that time. The oldest date so far obtained in South Africa in this manner for collapsed wall paintings is ~3600 BP (uncalibrated) at Steenbokfontein Cave (Jerardino and Swanepoel, 1999). A few other, more recent examples have also been found. These are, of course, dates for the burial of the painted pieces rather than dates of the painting itself.

The earliest attempt to directly date paintings was made by Denninger (1971) in which, using paper chromatography, he examined amino acids apparently derived from binders in paint. He contended that the rate of decomposition of amino acids differed, and by examining the amino acids present, ages could be assigned to paintings. The technique was not further pursued.

The most concerted work on $^{14}C$ dating of South African paintings has been undertaken in the Kwa-Zulu Natal Drakensberg by Mazel and Watchman. They succeeded in obtaining one accelerator mass spectrometry (AMS) date on plant fibres found mixed into paint (Mazel and Watchman, 1997). They argued that the fibre derived from plant sap used as a binder in the paint. This date calibrated to AD 1443–1653. They also $^{14}C$ dated layers of calcium oxalates found lying both over and under paintings (Mazel and Watchman, 2003): two dates on overlying layers calibrated to between approximately 1000 and 2000 BP; six dates on underlying layers came to between approximately 2000 and 4000 BP (Mazel and Watchman, 2003: Table 2). These are minimum and maximum ages, respectively.

The earliest direct dating of paint, as defined in Chapter I, was from Sonia's Cave Upper, Boontjieskloof, obtained by AMS at the Oxford Radiocarbon Accelerator Unit in 1981 (OxA-515). It gave a $^{14}C$ determination of 500 ± 140 BP (Van der Merwe *et al.*, 1987). The imprecision of the result lends itself to a wide calibrated age range of AD 1323–1625 (68.2% probability) and AD 1234–1802 (95.4% probability). Of the nine samples of different colours from various sites in South Africa subjected to dating, only one black sample (of two studied) contained sufficient carbon after preparation for dating. The X-ray fluorescence (XRF) analyses of most of the samples showed a high concentration of calcium attributable to either the presence of calcium carbonates or to contamination from the Sellotape used to mount the samples for XRF, but which could have included calcium oxalates.

Radiocarbon has succeeded in giving absolute dates for southern African rock art on charcoal paintings, calcium oxalates layers and plant fibres found in paintings. This technique will be further developed in this Ph.D. project (see §2.2).

### 2.1.3 In the Canadian Shield

In the Canadian Shield, attempts at dating have been very few in number. Most of them were based on superimpositions, on comparisons of representations on rock art with those on ceramics, on comparisons of paintings with real objects found during excavations, on oral traditions or on studies of historical journals and letters (Dewdney and Kidd, 1967; Rajnovich, 2002). The results suggest that the oldest sites should be about 2000, or even 5000 years old.

As with southern Africa, representations of historical events, European objects or animals have been used to date sites back to colonial times. A horse was painted at the Agawa site, Lake Superior, for example. Stylistic studies comparing rock art and representations on ceramics and birch bark were tried as well but the results were conclusive only for recent times (Lemaitre, 2013; Rajnovich, 1994).

Historical journals and maps give a *terminus ante quem* for some sites. The *Voyages from Montreal through the Continent of North America to the Frozen and Pacific Oceans in 1789 and 1793* by Alexander Mackenzie, journals of the priests Dollier de Casson and De Brehant de Gallinée, or maps drawn by the Jesuit priest Laure are some examples of records of rock art sites, which were used to locate and date them. Sometimes, they recorded testimonies of local people, which mentioned who was/were the artists of a site, for example, the great chief and *mide*, Myeengue, who is said to be the artist of rock art sites near Sault Ste Marie. He painted to commemorate a war at the beginning of the 18$^{th}$ century (Lemaitre, 2013).

Few superimpositions are present in the Canadian Shield, thus complex relative chronologies, such as those developed in South Africa, were not possible. On the other hand, purely stylistic analysis leads to regional distinctions rather than to chronological ones (Lemaitre, 2013).

Steinbring and Elias tried to correlate the level of water to the flooding of rock art sites which degraded the paintings (Lemaitre, 2013). Their study of the Moose Pictograph Site in Manitoba is the basis of their technique. They argue that the paws of the moose are only faintly visible today because of water immersion due to a warming in the region at about AD1350-1400. Thus, the pictograph would be about 800 to 1000 years old. This theory has been disputed by Dewdney, who argues that it is just a common degradation of the pigment due to cycles of freezing and defrosting in the lake. Colour intensity of the pigment has been used too to date rock art relatively, but as it is impossible to know the exact shade of the paint at the beginning, this technique was not further pursued (Lemaitre, 2013).

At the Lake of the Painted Cave, painted fragments of rock were found in archaeological layers. Radiocarbon dates were obtained from related materials but no results have been yet published (Lemaitre, 2013).

A silica crust is present on top of most of the rock paintings in the Canadian Shield. Attempts have been made to correlate their thickness and their opacity. But the mechanism of their formation is still unclear and highly dependent on climatic changes (Aubert *et al.*, 2004). Thus, no date was confirmed (Lemaitre, 2013).

Lichenometry was used by Dewdney at Cuttle Lake, giving a date of at least 100 years old for the paintings. It is the only example of the use of this technique in the Canadian Shield (Dewdney and Kidd, 1967).

Radiocarbon dates were obtained on organic compounds inside silica crusts at the Nisula site: 2500 ± 275 BP (N1; uncalibrated; OZA–403, $\delta^{13}C$ assumed = –25 ‰) and 2440± 610 BP (N2; uncalibrated; OZB–350, $\delta^{13}C$ assumed = –25 ‰) (Aubert *et al.*, 2004). As in the case of radiocarbon dating on calcium oxalate crusts, and because the samples were taken under the paint layer, these dates are maximum ages, that is to say that the paintings cannot be older than the dates but can be much younger.

A wide range of techniques were used to date rock art in the Canadian Shield and as with southern African rock art, radiocarbon dating seems to be the most promising technique.

However, one needs to know exactly what is to be dated. This remains unclear for some dates obtained.

Radiocarbon and optically stimulated luminescence have been selected for this Ph.D. project. The following paragraph details this choice.

## 2.2 Dating techniques applied: description and working hypothesis

In Chapter I, the description of the sites selected for this Ph.D. shows that they are thought to be from 8000 to 100 years old in southern Africa and from 5000 to 100 years old over the Canadian Shield. These estimations give a range of possibilities to select the best dating technique(s).

From Figure 2.3, radiocarbon, lead 210, caesium 137, uranium-series (U-series) and optically stimulated luminescence (OSL) dating seem to be the best candidates to date the sites. However, the samples need to contain specific components to be suitable for these techniques. In the case of lead 210 and caesium 137, used mostly to date sediments, they require large samples (several grams) which cannot be obtained from rock art sites, even in the case of the sites which will be destroyed, e.g. by dams. U-series dating requires the presence of uranium and thorium in crusts which need to be thick enough to get a few milligrams of sample. None of these requirements were present at selected sites.

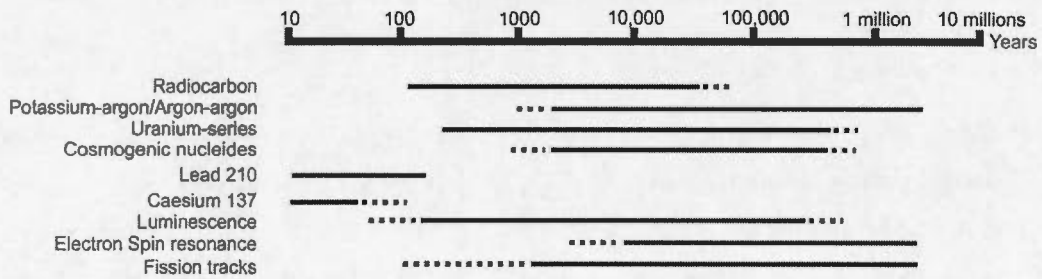


**Figure 2.3** The effective dating ranges of some dating techniques, modified from Walker (2005)

Radiocarbon has been successfully applied in southern Africa and in the Canadian Shield. However, dates obtained can be arguable as the origin of the carbon used is often not well

defined, such as the plant fibre in a paint layer (Mazel and Watchman, 1997). Indeed, it has been proved by Hall *et al.* (2007) that plants can grow on rock faces even after paintings were made. It is thus difficult to prove that the plant fibre originates from the paint or the binder and not from previous or later growing phase. This technique has been selected as black paintings were recorded in southern Africa and in the Canadian Shield and may contain carbon-based pigments. However, only a few sites in the Canadian Shield present black paints and most of them are now underwater (Lemaitre, 2013). Only one fragment from the Lake Wapizagonke has a black layer. However, it is unclear if it is paint or rock degradation. For the other fragments with red paintings, investigations on weathering crusts will be carried out to try to apply radiocarbon dating.

Optically stimulated luminescence (OSL) dating is mostly applied on quartz and feldspars, the most common minerals on Earth continents. Sites in southern Africa are on Clarens Formation sandstone and Lebung series sandstone, composed of quartz and feldspars with a calcitic/chloric matrix (Eriksson, 1979; Johnson *et al.*, 1996). Sites in the Canadian Shield are found on granodiorite and gneiss which contain quartz and less abundant feldspars (Desrochers, 2011; Percival and Easton, 2007).

Radiocarbon and OSL dating were thus selected for their range of application and the presence of components in paints or in the rock support, which are suitable to apply them. Each method is here detailed with the methodology and instrumentation used.

### 2.2.1 Radiocarbon dating

Developed by Libby in the 1940's, radiocarbon dating is based on the decay of the radioactive isotope of carbon, carbon 14 ($^{14}C$), or 'radiocarbon'. Produced in the upper layer of the atmosphere by the capture of a neutron and the release of a proton by the nitrogen atom ($^{14}N$), $^{14}C$ then combines with oxygen to form $^{14}CO_2$ and follows the cycle of carbon, being absorbed by plants through photosynthesis and by animals through the ingestion of plants. As the absorbed $^{14}C$ decays, it is constantly renewed through atmospheric exchanges, which makes its activity constant during life. Once an organism dies, the exchange with atmospheric $^{14}C$ stops and $^{14}C$ starts to decay following a well-known radioactive decay equation (Figure 2.4).

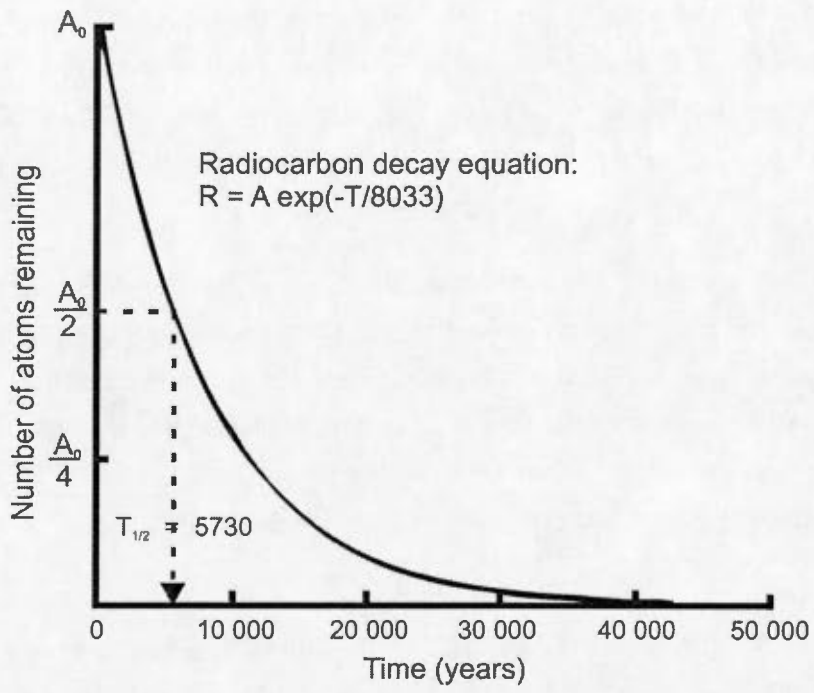


**Figure 2.4** The decay curve of radiocarbon (Equation details: R is $^{14}C/^{12}C$ ratio in the sample, A is the original $^{14}C/^{12}C$ ratio of the living organism and T is the amount of time that has passed since the death of the organism)

Radiocarbon can be measured on any biogenic material such as wood, peat, plant remains, shell, coral, bone, textile, etc. In this study, carbon-based pigments are thought to be made of charcoal, soot, or carbon black, that is to say an incomplete combustion of an organic compound such as fat, resin, wax, etc. On the other hand, binders or organic residues in silica crusts may be dated for example fat, wax, resin, or sap (Rudner, 1983; for more details about binders, see §2.3.1.2) in the case of binders, and diatoms in the case of silica crusts (Aubert *et al.*, 2004).

It is thus necessary to comprehensively characterize what is being dated, to understand what can influence the date (see §2.3). Indeed, contaminants may change the date by adding recent or old carbon components. The main contaminants identified in the previous studies were calcium carbonates, humic acids, calcium oxalates, and organic compounds in silica crusts surrounding painting layers (Aubert *et al.*, 2004; Bonneau *et al.*, 2011; Valladas *et al.*, 2001;

Watchman, 1990). Interestingly, what is considered as contaminant in one study can be the dated material used in other studies. However, as their mechanisms of formation and the source of carbon metabolised are not clear, they were removed for the dates obtained in this Ph.D. A methodology for their identification and removal is part of the unique contribution of this Ph.D.

Calcium oxalates and calcium carbonates have been the subject of pre-treatment improvements for radiocarbon dating. Hedges *et al.* (1998) mentioned that HCl (hydrochloric acid) does not always succeed at dissolving calcium oxalates. During the preliminary project in 2010, an improvement of the Acid-Base-Acid pre-treatment proved to be successful at dissolving calcium oxalates in South-African samples (Bonneau *et al.*, 2011). This pre-treatment has been improved as part of this Ph.D. project (see Chapter IV).

In 2010, the first dates concerning this project were obtained at the Oxford Radiocarbon Accelerator Unit (ORAU), University of Oxford, United Kingdom; the same laboratory where the first AMS age on rock art was obtained in 1981 (Van der Merwe *et al.*, 1987). Thus, a natural co-supervision of this project was established and I visited this laboratory on three occasions during this project (September 2011, June 2012, and September to December 2013) to prepare and date the samples.

Samples for radiocarbon dating were collected *in-situ* by myself in 2011 and 2012, and by Prof. David Pearce in 2013, after selection dependent on the results of the preliminary characterization study (see §2.3 and Chapters III and IV). They were collected using a sterile scalpel blade which was changed between each sample, by an operator wearing nitrile gloves, changed between each sample. They were collected in glass vials previously cleaned with methanol in an ultrasonic bath, and then baked at 500°C overnight to evaporate any organic residue, and sealed with aluminium foil cover with paraffin film.

After pre-treatment (see Chapter IV), samples were treated following the routine protocols at ORAU (Brock *et al.*, 2010). Samples were subsequently frozen and dried using a VaCo 5 freezer-dryer for a minimum of 12 hours. Once dried, they were weighed, and, if large enough, an aliquot was collected for FTIR spectroscopic analysis in order to assess if any contaminant remained. Only one sample presented calcium oxalates after pre-treatment and

was accordingly rejected. Samples were weighed into clean tin capsules prior to combustion at 1000°C in an elemental analyser (EA) coupled to a gas source isotope ratio mass spectrometer (IRMS). The combusted samples yielded $N_2$ and $CO_2$, with a chemical trap used to remove water and any other contaminant gases present. The $N_2$ and $CO_2$ were separated in a GC column, using helium as a carrier gas (stream = 100 mL/min). $1/50^{th}$ of the gas produced was directed into the IRMS for stable isotope measurements ($\delta^{13}C$ and $\delta^{15}N$) using a CF-IRMS system. The remaining $CO_2$ was transferred to a reactor rig and collected cryogenically. The reactor rigs contained 2.0-2.5 mg of iron catalyst (<10 μm 99.9+% Fe powder, Sigma Aldrich) that had previously been out-gassed in the presence of 500 mbar $H_2$ at 450°C for 1 hour.

Most of the samples selected for radiocarbon dating produced low carbon yields of between 0.05 and ~0.6mg, and were dated as non-routine "very small graphite" AMS targets. Three other samples were large enough to be treated as routine "small graphite" targets (~0.8 mg C), and a further three gave "large graphite" (~1.6 mg C) targets. For "very small graphite" samples, a desiccant, magnesium perchlorate ($Mg(ClO_4)_2$), was added to the water trap of the reactor rigs, following a previously established protocol (Motuzaite-Matuzeviciute *et al.*, 2013).

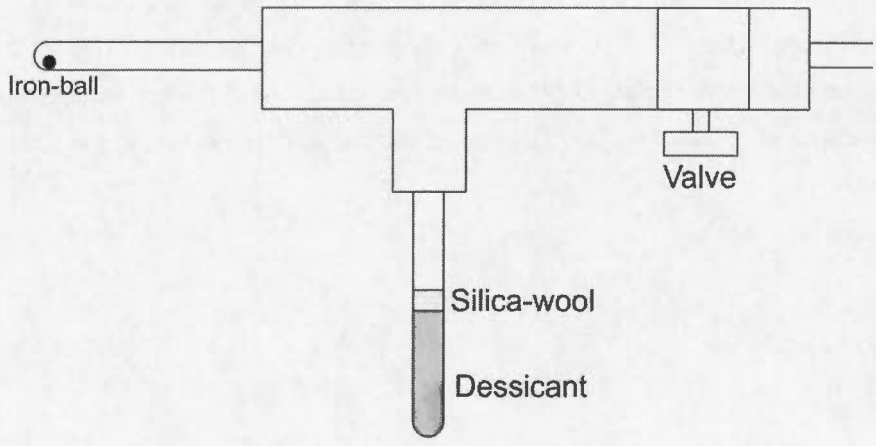


**Figure 2.5** Schema of a "very small graphite" reactor rig

Graphitization followed, with the reduction of $CO_2$ in the presence of excess hydrogen (in the ratio of ~2.2 $H_2$:$CO_2$) and the iron powder, and heated at 560°C for 6 hours to yield pure C (graphite) and water by cooling and condensing (Equation 2.1 is the net result of different competing equilibria (Dee and Bronk Ramsey, 2000)).

$$CO_{2(g)} + 2H_{2(g)} \rightarrow C_{(s)} + 2H_2O_{(g)} \quad (2.1)$$

The presence of the desiccant helped to draw out $H_2O$, and therefore optimized the conversion of $CO_2$ to graphite for the very small samples, where any trace of water would affect the small samples. This addition has previously been found to be necessary for the lowest yielding samples (i.e. those ≤0.5 mg C) (Motuzaite-Matuzeviciute *et al.*, 2013).

The resulting graphite produced is pressed into aluminium targets and then sent to the AMS for radiocarbon dating. In the AMS, the sample is ionized in the ion source by bombardment with caesium. Particles formed are negatively charged which eliminates $^{14}N$, the main isobar, as it does not form a negative ion. Electromagnetic fields are used to select ions having a mass equal to 14. However, this mass covers several chemical species including molecular hydrocarbons. These particles are then attracted by a high-voltage (2.5 MVolts) source and molecular ions reduced using a stripper gas. Electrons are stripped during this process and the atoms are then accelerated and only atoms of $^{14}C$ are selected based on their velocity and collected by ion detector for $^{14}C$ and Faraday collectors for $^{13}C$ and $^{12}C$ (Figure 2.6). The result is not an absolute number of $^{14}C$ atoms but an isotopic ratio of $^{14}C$ relative to that of the stable isotopes of carbon ($^{13}C$ or $^{12}C$). Hence, another $\delta^{13}C$ is calculated and used for age calculation.

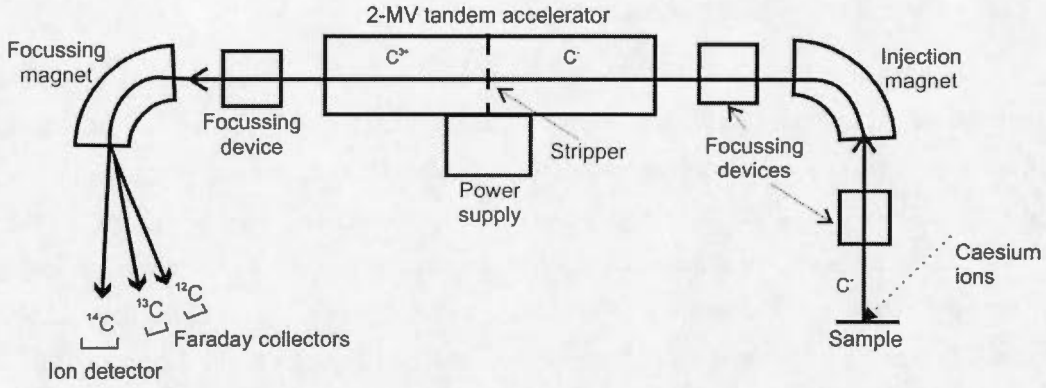


**Figure 2.6** Schematic diagram of an AMS, modified from Walker (2005)

At ORAU, the AMS used for "very small graphite" targets is the ORAU 3 MV HVEE (High Voltage Engineering Europa) AMS system (Bronk Ramsey *et al.*, 2004; Staff *et al.*, 2014). Using this system, uncertainties of ±25 to ±30 $^{14}C$ years can be reliably reported on single target measurements (Bronk Ramsey *et al.*, 2004). However, this implies that each stage of the dating process is well known and excludes any contamination. In this project, uncertainties were added to the calculation of the ages as the pre-treatment protocol was in development. On the other hand, where possible, samples were sub-sampled and two measurements were carried out. Because the samples in this study are very small, they may be very vulnerable to contamination. To combat this, tiny sub-samples of as many samples as possible were analysed with FTIR spectroscopy following pre-treatment to identify potential contaminants. Where contamination was visible, samples were withdrawn.

Conventional radiocarbon ages before present (BP) were calculated relative to the oxalic acid (HOXII) standard and normalized for isotopic fractionation (Stuiver and Polach, 1977).

Dates obtained were calibrated using OxCal and the ShCal13 calibration curve (Hogg *et al.*, 2013).

### 2.2.2 Optically stimulated luminescence dating

The principle of optically stimulated luminescence dating is based on the emission of light, luminescence, by some minerals, such as quartz and feldspars. They act as natural dosimeters, recording surrounding radioactivity to which they are exposed. Radioactive decay produces emissions (α, β and γ-rays) that eject electrons from peripheral orbitals. Minerals store a small population of those free electrons in defects in their crystal structure. These can be released and produce luminescence by heating or exposure to daylight. Thus it is possible to date the last time a sediment or a rock was exposed to the Sun before being buried.

The intensity of the luminescence is used to assess the radiation to which the sample was exposed during the burial period. By comparison with the signal emitted after exposure to laboratory doses, a "paleodose" (the total absorbed dose from the time of burial), is calculated. It is expressed in Gray (Gy). In parallel, the radioactivity surrounding the sample is calculated. It is expressed in Gray per year (Gy/yr) and known as the "dose rate". Using these two results, the age can be calculated using Equation 2.2 (Aitken, 1985, 1998).

$$Age = \frac{\text{Paleodose (Gy)}}{\text{Dose rate (Gy/yr)}} \qquad (2.2)$$

Luminescence can be released following: i) heating which results in "thermoluminescence" (Aitken, 1985), or ii) shining a beam of light (preferably monochromatic) onto the sample, which results in "optically stimulated luminescence" (Huntley *et al.*, 1985).

At the sub-atomic level, electrons become trapped at sites within the crystal structure of minerals after being ionized by radioactive decay emissions. These sites are due to defects in the crystal structure and attract electrons. Depending on the kind of trapping centres, electrons can remain stored from a few seconds to several thousands of years. When an electron is released, it emits part of the energy stored as photons of light (Figure 2.7). These photons are recorded for luminescence dating (Duller, 2008).

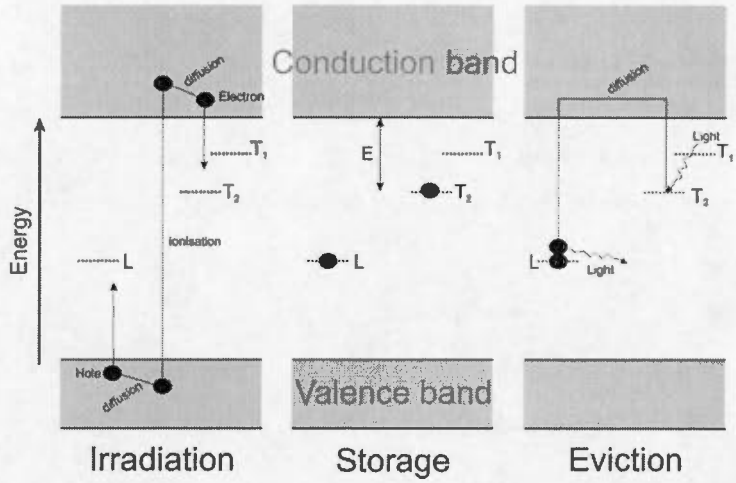


**Figure 2.7** Illustration of the luminescence process, modified from Duller (2008)

In most luminescence studies, the samples in question (e.g. sediments, rocks, ceramics) were buried after heating or exposure to sunlight, protecting them from daylight exposure. Figure 2.8 summarizes the most common cycle undertaken by a sample before luminescence dating.

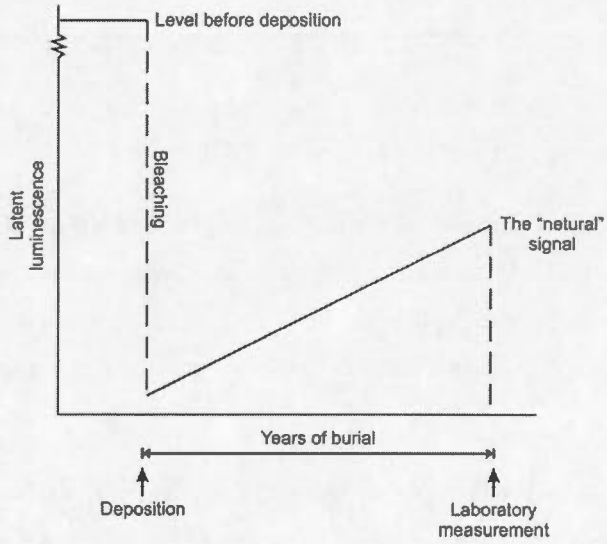


**Figure 2.8** Evolution of the luminescence signal in a sample, modified from Aitken (1998)

In this Ph.D. project, the working hypothesis is different. The paintings studied have existed on rock-shelters or on cliffs which are otherwise exposed to daylight for several hours per day. Thus one can assume that the rock surface is bleached and does not have remnant OSL signal. However, when a painting is made on the surface of the rock, it should protect the rock face from the sun and an OSL signal will emerge (Figure 2.9).

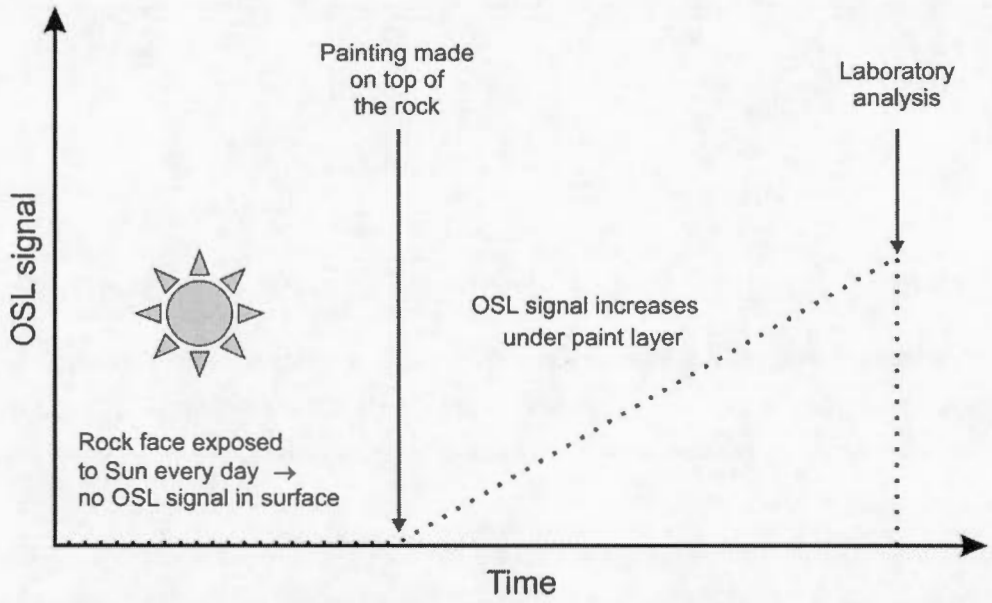


**Figure 2.9** Working hypothesis

Thermoluminescence is associated with electrons trapped in "hard-to-bleach" traps, whereas OSL is associated with "easy to bleach" ones. The working hypothesis, which supposes that rock faces have been exposed to the sun for a long time, resulting in empty traps of the minerals at the surface is to be tested in this thesis. To limit residual geological luminescence, OSL was selected.

The working hypothesis meets at some points the one used for surface OSL dating. This application of OSL is still in development but ages were obtained on both rock faces and historical buildings (Chapot *et al.*, 2012; Freiesleben *et al.*, 2015; Galli *et al.*, 2014; Rhodius *et al.*, 2015; Sohbati *et al.*, 2012; Sohbati *et al.*, 2015). The main limit of such analysis is the bleaching of minerals at the surface of the sample to be dated, as they were not always well

exposed to daylight. This issue should be avoided in this project as rock surfaces are exposed to daylight several hours per day. On the other hand, Freiesleben (2014) in her master thesis raises the problem of thermal transfer (due to the necessity of pre-heating the sample) in K-feldspars at the surface of rocks which artificially increase the OSL signal.

In the case of southern Africa and the Canadian Shield, the rock supports are sandstone, gneiss and granodiorite. Southern African rocks contain mostly potassium feldspars (K-feldspars) and quartz in proportions ranging from 80/20% to 20/80% quartz/K-feldspars (Eriksson, 1979). Their grain sizes range from 125 to 60 μm. After sieving tests, the fraction between 150-90 μm was selected.

Gneissic Canadian Shield rocks contain a large proportion of quartz and plagioclase feldspars. Very few K-feldspars have been found in mineralogical studies (Desrochers, 2011; Percival and Easton, 2007). The use of luminescence emitted by plagioclases has not been explored in this PhD project, to keep a focus on K-feldspars and quartz. Quartz, from the 150-250 μm fraction, which is most abundant, was selected and investigated.

Samples were collected in two forms by myself in 2011 and 2012 and by Prof. David Pearce in 2013:

- Raw rocks and detached rock face fragments found *in-situ*, stored in aluminium foil and plastic bags.
- Cores of rocks drilled at night, using red light with a coring drill (8 mm in diameter for cores with paint on surface; and 1.2 cm in diameter for cores with no paint on surface), cooled with distilled water. The coring drills were cleaned between each sample through immersion for 5 minutes in an ultrasonic bath filled with distilled water. Cores were stored in aluminium foil, plastic bags and two black plastic bags dedicated to the storage of OSL samples.

OSL analysis was carried out at the Laboratoire Lux, Département des Sciences de la Terre et de l'atmosphère, Université du Québec à Montréal, Montreal, Canada.

Samples were prepared in a dark room in different ways dependent on the aim of the experiment in questions. For tests on the rock itself (checking the suitability of the minerals for OSL dating), about 2-3mm was removed from the outside part of the rock with a drill. This sample was then size reduced with a hammer and then grounded with a pestle and mortar in order to reduce it to powder. The help of a mechanical press was required in the case of the Canadian rocks as they were too hard to be grounded only with a pestle and mortar. For painting reproductions, a rock (about 15-20 cm in diameter) was cut into two pieces using a mechanical press in a dark room. This should ensure that the OSL signal at the cut surface is saturated. Cores were then made using the same coring drills and the same cleaning protocol as used in *in-situ* collection. To investigate the evolution of the OSL signal in the rock, cores were cut every millimetre using a 0.2 mm thick diamond saw connected to a drill and mounted on a millimetre bench (Figure 2.10).

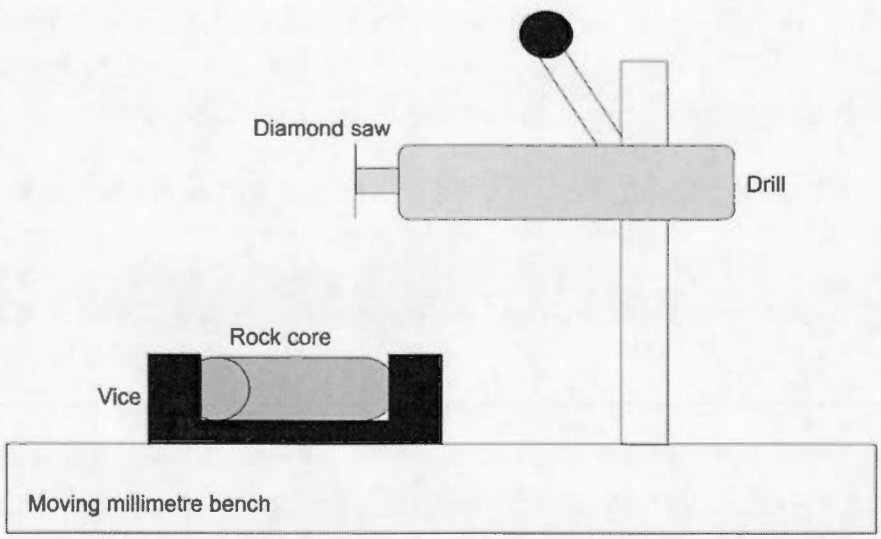


**Figure 2.10** Scheme of the mounting for rock cores preparation (the sizes of the rock core and vice were deliberately amplified)

Once cut, each slice was immersed in a 10% Hydrochloric acid (HCl) solution overnight to dissolve calcium carbonates and assist the grinding process. In the case of the Canadian samples, this step was not done as the rocks do not have a calcitic matrix. Slices were directly crushed in an agate mortar. An acidification with HCl 10% for 1 hour is then made, followed

by three distilled water cleanings and one methanol cleaning. They were then left to dry at room temperature overnight. Sieving was subsequently undertaken and the fractions between 90-150 μm were selected for southern African rocks, and the fractions between 150-250 μm for the Canadian ones. K-feldspars were separated from quartz using density separation with sodium polytungstate (SPT) at a specific density of 2.58. The floating fraction, containing K-feldspars, was cleaned three times with distilled water and once with methanol. They were left to dry at room temperature overnight. They were then mounted on aluminium discs for OSL recording. The fraction which sinks at the bottom of the tube after SPT separation contains mostly quartz but needed to be "purified". After cleaning as described above, they were acidified with Hydrofluoric acid (HF) 10% for 15 minutes, cleaned three times with distilled water, acidified again with HF 45% for 45 minutes, cleaned three times with distilled water, acidified with HCl 10% for 30 minutes to remove calcium and fluorine ions liberated by the HF acidification, cleaned three times with distilled water and finally cleaned once with methanol. The first step with HF at 10% is added to avoid intense chemical reaction between HF and plagioclases. Indeed, this reaction is exothermic and should be avoided as it may release luminescence. Once dried, they were mounted on aluminium discs for OSL recording. This entire protocol is summarized in Figure 2.11.

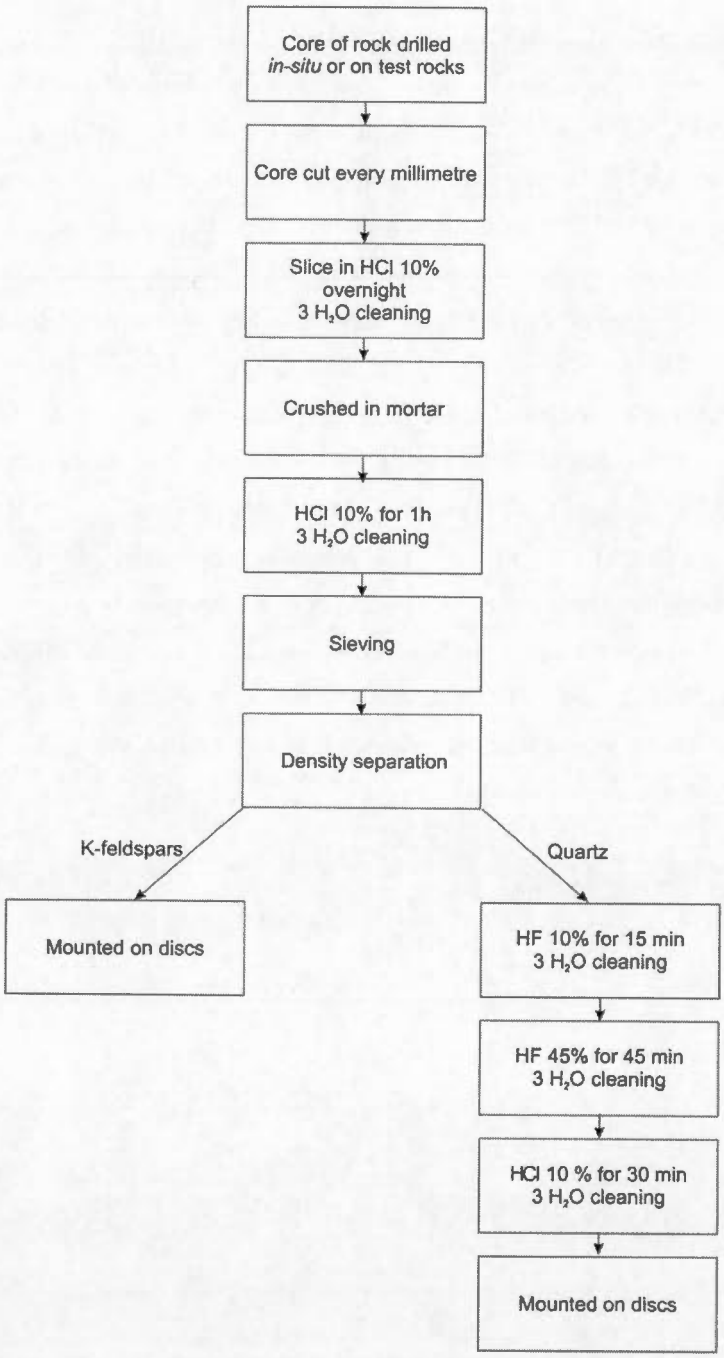


**Figure 2.11** OSL samples preparation protocol

Samples were analysed using a Lexsyg system (Richter *et al.*, 2013). Infrared LEDs were used to stimulate K-feldspars, and blue ones for quartz. The luminescence was filtered with a combination of two filters and detected with photomultiplier tubes from Hamamatsu (H7360-02) and EMI (9235QB) range 300-650 nm and 160-630, with quantum efficiencies of approximately 27% at 400 nm and 30% at 200 and 340 nm, respectively (Richter *et al.*, 2013). Due to instrument break, analyses were finished using a Risø TL-DA-15 automated reader, fitted with an EMI9235QA photomultiplier tube. Infrared diode excitation were used (1.4 eV, 875 nm) and luminescence was filtered through a Corning 7-59 and Schott BG39 filter combination allowing detection of the 3.1 eV emission. Recording were done under nitrogen atmosphere. The transfer to another instrument required tests to adjust preheat temperatures as the filling gas was different in the two instruments. Results and adjustments can be found in Appendix B. Data were treated using Analyst and Excel. Details of the sequences used are given in Chapter V.

Dose rate was calculated using the concentration of radioactive elements in rocks and paintings: uranium, thorium and potassium. Their concentration was obtained using a gamma spectrometer, at the Laboratoire Lux. Samples were ground to powder with a mechanical grinder. They were then transferred in plastic tubes, weighted, and sealed with paraffin. Samples are stored for 21 days, to achieve equilibrium between uranium and its gaseous decay product, radon. Samples were then left in the gamma spectrometer for 5 to 7 days of counting. Using the conversion rates in Adamiec and Aitken (1998), dose rates were calculated for rocks supporting paintings.

However, in this project, the dose rate could not be calculated as a homogeneous 50cm-sphere around the sample. A 50 cm-sphere around the sample is considered, where half of it is seen as coming from the rock, and the second half from atmospheric cosmic rays. Cosmic rays are constituted of "slow" and "hard" components, mostly electrons, neutrons and muons which are highly energetic. Their intensity is dependent on altitude, latitude and longitude (Gosse and Phillips 2001). As the cosmic rays interact directly with the rock, their rate may be calculated applying the equation in Prescott and Hutton (1988, 1994), with no attenuation.

At the junction of the two half-spheres is a 100 μm to 1 mm thick paint layer (Figure 2.12). To calculate its contribution to the dose rate, one red pigment from Lesotho was sealed in a plastic tube and its potassium content measured in the gamma spectrometer. Then its uranium and thorium contents were analysed with ICP-MS. In parallel, white and red earths collected close to the Lesotho sites and which were thought to be possible sources for the red and white pigments were prepared as rocks and measured in the gamma spectrometer. Calculation of their dose rate used the same protocol as for rocks.

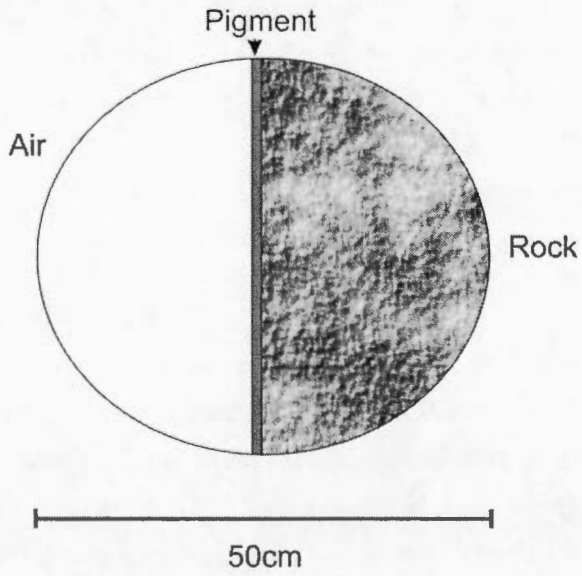


**Figure 2.12** Schema of the dose rate sphere estimation (the pigment layer has been deliberately amplified)

Chemistry for the uranium and thorium analysis on the paint layer was carried out by Bassam Ghaleb, Geotop, Université du Québec à Montréal. First, a triplet of spikes of known concentrations, $U^{236}$, $U^{233}$ and $Th^{229}$, were introduced in a Teflon beaker, weighed and left to dry on an heating plate at 95°C. Then, the sample was introduced and weighted. It was acidified with 1 ml of nitric acid 15M and 1 ml of HCl 6M, and then dried on an heating plate at 95°C. The remaining grains were dissolved in *ca.* 0.5 ml of HF 29M (hydrofluoric acid, equivalent 48%), then dried as previously and finally 1 ml of boric acid was added to remove fluorine and calcium ions. Then, uranium and thorium were separated using an ion exchange

resin, AG1X8 200-400 mesh. Firstly the resin was conditioned with HCl 6M. The sample dissolved in HCl 6M was introduced, and the resin retained uranium and iron. The remainder was collected in a Teflon beaker (B1). Then, uranium and iron were released from the resin using $H_2O$ and collected in a second Teflon beaker (B2). This part (B2) was then dried and dissolved in nitric acid 3M in order to separate uranium from iron. The resin UTEVA 100-150 µm was conditioned with nitric acid 3M and the sample introduced. Uranium was captured by the resin and the rest went to a "bin" beaker. Uranium was released using nitric acid 0.02M and collected for MC-ICP-MS (Multiple collector - inductively coupled plasma - mass spectrometry) analysis. The part of the sample in beaker B1 was dried and dissolved in nitric acid 7M. To separate thorium from the rest of the elements, the resin AG1X8 200-400 mesh was used, conditioned with nitric acid 7M. The sample was introduced and thorium captured by the resin. The rest was collected in a "bin" beaker. To release thorium, HCl 6M was added and thorium collected for MC-ICP-MS analysis. The instrument used was a MC-ICP-MC Nu-Instrument II, with a WARP filter and three ion detectors. The dose rate of the paint has been calculated using conversion rates in Adamiec and Aitken (1998).

Finally, the dose rate calculation needs an evaluation of the humidity inside the rock (Duller, 2008). In South Africa, on Clarens Formation sandstones, humidity has been recorded during a study of rock art site conservation, showing that the amount of water is between 0.5 and 1.3% depending on the time of the year (Hall *et al.*, 2007). No data is available for the Canadian Shield. However, rock cannot retain a large quantity of water, in contrast to sediments. Hence, the same evaluation of the water content has been used for Canadian rocks.

The two dating techniques presented above and their related methodologies show the great importance of properly characterizing the material to be dated; firstly to know if the technique is applicable, secondly to apply it with the correct parameters, thirdly to interpret correctly the dates obtained from use of these techniques. That is why, before the selection of one of these techniques to date a sample, a detailed characterization of its compounds was carried out.

## 2.3 Characterizing paintings before dating: a necessary step

Characterizing paint before obtaining a radiocarbon date is not a new procedure, but one which, prior to this project, tended to be reduced to a quick analysis of the paint. Where X-ray fluorescence (XRF) was used, the absence of iron or manganese in the paint was considered to be due to the presence of a carbon-based pigment without subsequent investigation. Where scanning electron microscopy coupled to energy dispersive X-ray spectrometry (SEM-EDS) was used, observations and elemental analysis might have tentatively pointed to charcoal or carbon-black pigments. However, no molecular analysis was carried out, nor investigation into the degradation of the pigment or the weathering products which could form radiocarbon contaminants. The initial study in 2010 and the subsequent publication (Bonneau *et al.*, 2011) showed the importance of paint characterization in order to adapt the pre-treatment protocol for radiocarbon dating.

This section investigates previous studies on rock painting characterization around the world and more specifically in southern Africa and the Canadian Shield, to propose a characterization methodology which will meet requirements for dating selection and which, at the same time, will give the required results to interpret how the paints were made, one of the archaeological problems for the selected sites.

### 2.3.1 Previous studies on rock art pigments: archaeology, ethnography and chemical characterization

Research into rock art pigments is linked to the study of colouring materials used for different purposes: dying, body painting, rituals, rock paintings, etc. The same material can have several uses, e.g. "ochre" has been used to dye clothes and hair, for body and rock painting, for burial rituals, etc. (Watts, 2002).

The term "ochre" originates from the Greek "okhros", denoting an instable and undetermined colour. It has several definitions depending on the field of science in question: archaeology, geology, material chemistry, industrial chemistry, etc. In archaeology, Watts (2002: 1) defines "ochre" as "a general term for any ferruginous earth, clay, mineral or rock containing sufficient haematite (an iron oxide) or iron hydroxide (e.g. goethite) to produce, respectively, either a red or a yellow streak". For Henshilwood *et al.* (2009: 29), "Ochre is typically a

product of chemical weathering which has been sufficiently enriched in iron oxide (generally haematite) or iron hydroxide (typically goethite) to produce (respectively) a reddish or yellowish mark when drawn over a surface". On the other hand, from a geological point of view, "ochre (...) applies to earthy and pulverulent forms of the minerals hematite and limonite which are almost invariably more or less impure through the presence of other metallic oxides, silica and argillaceous matter" (Visser, 1937: 7). Eastaugh (2008: 285) gives another definition of ochre as pigment which is quite similar to those previously mentioned : "Ochres are secondary deposits occurring either as soils or 'gossans' (the weathered, highly oxidised surface outcrops of ore deposits) which have become enriched in the colour-bearing constituent, usually iron oxides or iron hydroxides."

Common to these definitions is that ochre is a secondary material (due to degradation/weathering of rocks) composed of clayish minerals, the colour of which is due to iron oxides or hydroxides. However, these are mostly applied to pieces of ochre found in archaeological layers or to ochre deposits which are to be exploited for industrial purpose. In this project, the ochre is a component of the paint and may have been processed (through sieving, grinding, etc.). In Bonneau *et al.* (2012), a definition has been given as "a rock or a coloured earth, whose colour comes from an iron oxide compound (either hydrated or not), such as limonite, goethite or haematite. An ochre pigment therefore contains mainly silicon, aluminium, and iron. The presence of other minor elements such as potassium, sodium, chlorine or calcium can 'classify' ochres: potassium ochre, sodium ochre, chlorine ochre, calcium and potassium ochre, etc.", which meets previous definitions and which will be used in this project. For further information about the debate around the definition of "ochre", the reader is invited to refer to Dayet (2012: 35-106).

When characterizing rock art, one investigates the paint and its components: the pigments which give the colour, the charges which make the pigment attach to its support, and binders which dilutes the pigments and charges to make a liquid paint. The notion of charge has been defined in Menu *et al.* (1993). It is however often difficult to know if charges were introduced on purpose or not. For example, in the case of red ochre, the pigment is iron oxides and the clayish materials are the charges, but they are all part of the original raw material used. In other cases, such as for charcoal, there is no need for charges. When well-

mixed with water, charcoal is a perfect paint. Although deliberately introduced quartz and feldspars were identified in French Palaeolithic caves (Clottes *et al.*, 1990; Menu and Walter, 1992; Menu *et al.*, 1993; Vignaud *et al.*, 2006), their introduction is much less clear for southern African and Canadian rock art. Hence, when the term "pigment" is used, it covers both the colouring material and the possible charges. If an obvious mixture is identified, the pigment will be defined as an anthropic mixture of several raw materials.

Following these preliminary definitions, studies of the characterization of rock paintings are detailed in the next paragraphs, beginning with international studies (a brief review) and then moving to focus on southern African and Canadian studies.

2.3.1.1 Around the world

Even though ethnographic researches were conducted during the 18$^{th}$ and 19$^{th}$ centuries, the first chemical studies of Palaeolithic rock art were carried out by H. Moissan at the beginning of the 20$^{th}$ century (Clottes *et al.*, 1990). Most characterization of rock paintings was carried out during the 1970's and the 1980's using techniques borrowed from Earth sciences: polarized microscopy, thin section analysis, X-ray fluorescence (XRF) and X-ray diffraction (XRD) (Huwiler, 1972; Taylor *et al.*, 1974; Van der Merwe *et al.*, 1987; Wainwright, 1985).

In the 1990's, research into rock painting became more and more intensive thanks to the reduction in the size of samples needed and a keen interest in prehistoric art. This work was contemporaneous with the availability of a large number of radiocarbon ages from the same sites and the development of ion-beam techniques such as PIGE (particle induced γ-ray emission) and PIXE (particle induced X-ray emission). Most of the articles focus on European Palaeolithic rock paintings (e.g. Clottes *et al.*, 1990; Menu and Walter, 1992; Menu *et al.*, 1993; Pomies *et al.*, 1999) but Australian (Ford *et al.*, 1994) and South African rock art received growing interest (Peisach *et al.*, 1991; Van Rijssen, 1990; Wilson *et al.*, 1990).

Finally, the beginning of the 21$^{st}$ century saw the use of spectroscopic (Raman and FTIR spectroscopies) and portable techniques to characterize rock art. These have the advantage of being non-destructive and in the case of portable techniques such as Raman spectroscopy (e.g. Lahlil *et al.*, 2012; Tournié *et al.*, 2011), XRF (e.g. Huntley *et al.*, 2015; Koenig *et al.*,

2014) and XRD (e.g. Beck *et al.*, 2014), analysis can be carried out directly *in-situ* without removing any paint.

Other methods such as LA-ICP-MS and synchrotron rays opened new fields of research making it possible to track provenance of the raw materials (Resano *et al.*, 2007; Zipkin *et al.*, 2014) and to get more and more information about pigment process, pigment degradation, weathering products and their influence on rock art conservation (Hoerlé, 2005).

All of these new methods had their limits, however, especially portable ones, which give preliminary results but cannot replace laboratory machines which are much more precise. Moreover, even though these instruments may seem to be user-friendly they are not at all, and can give totally nonsensical results (e.g. lead interpreted as arsenic) or even degrade sites when used by untrained hands. Roman and rock art sites were burnt by use of a portable Raman spectrometer for example (Janet Ambers, personal communication, 2010).

Characterization of paint was more often the study of pigments rather than binders. Even though a mysterious reputation arose, following ethnographic studies which mentioned the use of blood (e.g. Rudner, 1983), very few analyses were carried out to identify binders used to make rock art and most of them were not able to give definitive results (Livingston *et al.*, 2009; Spades and Russ, 2005; Vázquez *et al.*, 2008).

After this quick review of rock paintings analysis around the world, focus is now given to southern Africa and the Canadian Shield.

#### 2.3.1.2 In southern Africa

Prior to chemical characterization of southern African rock art, there was some early interest in the painting talents of San people during colonial times. One example of this was Marion How, the wife of the magistrate of Qacha's Neck district, Lesotho, who invited, in 1930, Mapote, an old man, to paint eland with the same technique as used by San people (details given in Chapter I, §1.2.1).

In the 1980's, an old lady known under the name of "M" was interviewed. Her father was a San shaman and had carried out many paintings which she showed and explained to her

interlocutors. She confirmed Mapote's explanations, in particular on the need to use blood for the red but she added that the eland fat was used as binder to make red paint (Lewis-Williams, 1995).

Confirming these accounts, Ione Rudner (1987) compiled literary sources and observations of people in southern Africa. Her study references animal and vegetable fats, egg, dung, blood, plant sap, gum and honey as possible binders for body-painting pigments. For pigments, she noted that San may have used ash, charcoal, soot, iron oxides (i.e. red ochre, yellow ochre, hematite, goethite) and perhaps pigments coming from plants and roots.

Rudner's research is a very important base for chemical characterization as it gives some clues to possible pigments and binders. However, it references only recent practices for rock paintings. It is very likely that process changed through time, in different areas, and due to differential availability of some raw materials. It is only since the 1990's that a renewed interest in San rock art allowed analyses but these are still very sparse.

Various techniques are used to analyse rock paintings. Most frequently used is Scanning Electron Microscopy coupled with X-Ray Energy Dispersive Spectrometry (SEM-EDS) (Arocena *et al.*, 2008; Hall *et al.*, 2007; Hoerlé, 2005; Hughes and Solomon, 2000; Mazel and Watchman, 1997; Wilson *et al.*, 1990). Studies using this technique have identified the presence of iron oxides as red and yellow pigments, manganese oxide or carbon for the black, calcium carbonates and calcium sulphates for the white, and for all colours, the presence of quartz and aluminosilicates. Minor elements such as potassium, chlorine and titanium have also been detected with SEM-EDS, in very different proportions depending on the site in question. These analyses of minor and trace elements were continued thanks to the PIXE technique (Peisach *et al.*, 1991). The first elementary analyses on San pigments were carried out with X-Ray Fluorescence, and produced results similar to those previously mentioned (Van Rijssen, 1990).

These elemental analyses were often combined with structural analysis techniques such as Raman spectroscopy (Prinsloo *et al.*, 2008; Prinsloo *et al.*, 2013; Tournié *et al.*, 2011), X-Ray Diffraction (XRD) (Arocena *et al.*, 2008; Hughes and Solomon, 2000) and Fourier Transform Infrared (FTIR) spectroscopy (Prinsloo *et al.*, 2008). Use of these techniques made it possible

to determine the nature of the components of the pigments by showing the presence of hematite, goethite, red and yellow ochres, amorphous carbon, calcite, gypsum and other more or less hydrated calcium carbonates and calcium sulphates. Anatase, quartz and calcium oxalates (whewellite and weddellite) were also detected.

Analyses with *in-situ* Raman spectrometer (Tournié *et al.*, 2011) give some results but these are not as comprehensive as the results obtained by combination of various techniques on *ex-situ* material in the laboratory. The most important problems are the feasibility of bringing instruments on site and their ability to record good spectra on the paintings. Spectra obtained in this way show strong fluorescence and only few peaks were recorded giving us just an idea of the main components of pigments.

As regards the binders, very few analyses have been carried out. The first, by Denninger (1971), used paper chromatography. His primary aim was to recover amino acids and to try to date them due to their decomposition. Characterization and dating were unfortunately not successful. Thereafter, Arocena *et al.* (2008) postulated that the presence of calcium oxalates and in particular of whewellite, showing a specific habit, was related to the use of plant sap, *Aloe Vera* according to them, as a binder or whitener. However, calcium oxalates can have various sources: lichens, bacteria (Watchman, 1990), reaction between the binder, the rock and the rain, etc.; and it seems difficult, even impossible, to differentiate them by their morphology.

Williamson (2000) detected haemoglobin in paintings at Rose Cottage Cave using "Haemastix", clinical strips used usually to detect blood in the urine. Even though tests suggested the presence of blood, and that tests were conducted to identify and reduce contamination, especially with the use of EDTA to confirm the presence of contaminants, this test remains controversial and it can be seen only as a preliminary test before further investigations (Matheson and Veall, 2014).

Analyses using Raman spectroscopy (Prinsloo *et al.*, 2008; Tournié *et al.*, 2011) showed the possible presence of fat in the pigments and on the rock, as well as a carotenoid pigment, called bacterioruberin, which is a pigment secreted by halophiles and aeraulic archaebacteria, bacteria needing at the same time oxygen and salts to develop. This red pigment would

enable them to be protected from the sun. More recently, Prinsloo *et al.* (2013) investigated Raman and FTIR signatures of fresh and artificially aged paints made by Stephen Townley-Bassett, with known raw materials. Townley-Bassett produced paintings with pigments found on the sites or in their immediate vicinity, with techniques that are probably very close to those used by the San painters. A few experiments showed most notably that the paints which best resist erosion are those using egg or gall as a binder (Le Quellec, 2008). The Prinsloo *et al.* (2013) study is an excellent step in developing methodologies to track binder signatures using Raman and FTIR analysis.

Previous research on southern African rock paintings are few in comparison with other regions of the world but point to the same results using several techniques to get the information. Thus, they are important bases with which to establish the methodology of this Ph.D. project.

#### 2.3.1.3 In the Canadian Shield

In the Canadian Shield, the main colour for the paint is red. For a long time, archaeologists called this pigment "hematite" even though very few chemical analyses were carried out to confirm this attribution.

Hematite, iron oxide, is called *onummun* or *wanaman* by Amerindian people. It symbolises life, health and strength. Myths tell that hematite is the blood of the Giant Beaver following its attack on the Thunderbird, or that it is the blood of the Horned Snake after a battle against the Thunderbird (Lemaitre, 2013).

Archaeological investigations revealed hematite mines exploited by Amerindian people. One of them is at the Hell's Door, along the Mattawa River. Dewdney and Kidd (1967) mentioned ethnographic sources that attest to the heating of yellow ochre to turn it into red ochre. This was then mixed with fish glue, fish fat, bear fat, or sturgeon oil to make paintings.

Very little chemical characterization of rock paintings have been undertaken on rock paintings from the Canadian Shield (Taylor *et al.*, 1974; Wainwright, 1985, 1990), even though they were among the first in the world to be carried out. Parks Canada and the

Canadian Conservation Institute made a few cursory analyses for conservation purposes which were not published.

These chemical studies made use of microscopy, polarized microscopy, SEM-EDS, XRD and more recently, Raman spectroscopy, revealing that the red pigments were made of iron oxides with an amorphous component which had not been identified (Taylor *et al.*, 1974). A thin layer, transparent or white depending on sites, can be found under and on-top of the paint layer and has been identified as amorphous silica with a bit of gypsum. Analysis of this layer at the Nisula site, Quebec, showed the presence of diatoms in it (Aubert *et al.*, 2004). Three sites were studied in the Canadian Shield: Lake Wapizagonke, Lake Agawa and Peterborough.

All these previous studies show that characterization of rock paintings requires an objective in order to select analytical techniques which must compromise between the samples needed and the collection possible on-site. Furthermore, in most of the recent studies, only one or two analytical techniques were used to characterize rock paints, leaving a lot of questions. In fact, almost all the time, studies were developed more to test new methods or instruments rather than to answer archaeological problems.

In this project, the methodology applied was developed as a compromise between methodological development needs and archaeological problems. It is detailed in the following section.

## 2.4 Detailed methodology and instrumentation applied

Archaeological problems in rock art analysis centre on the *chaîne opératoire* of production and use from raw material acquisition to the application of the paint to the rock. The concept of *chaîne opératoire* for a rock art site is much larger than mentioned here. The reader is invited to refer to Chapter I for more information.

In conversation with archaeologists in charge of the sites for this study, focus was applied to the preparation of the raw material (grounding, sieving, leaching), possible mixtures made to obtain the hues needed by the artists, the possible preparation of the rock (which includes the characterization of the rock itself), and the degradations that occur following painting.

Acquiring this information accords with what is needed for radiocarbon dating and OSL dating. Indeed, for radiocarbon dating, one looks for organic compounds in the paint: organic pigment such as soot, charcoal, burnt bones, or carbon-blacks, and binders such as egg, fat, blood, etc. On the other hand, contaminants (degradation of pigments, lichens and bacteria actions, weathering products, etc.) need to be identified in order to remove them prior to dating.

Concerning OSL dating, it is important to understand how the paint was made in order to be able to reproduce it for artificial tests to validate working hypotheses. Knowledge of the rock is required, along with its possible preparation, and the type of pigments used (focus is given to red paints which are the thickest and seem to be the best at covering rocks). In order to reproduce rock paints, red and white soils were collected in the vicinity of the Lesotho sites (see §2.4.3).

This section details the steps of the protocol used for characterization. The instrumentations, their locations and a brief presentation of their principle are explained.

### 2.4.1 General characterization methodology

A multi-instrumentation protocol was selected to acquire all the information needed to characterize the pigment and its alterations through time. Following the preliminary research carried out at the RLAHA, University of Oxford, United-Kingdom in 2010, a first protocol was published in the *Journal of Archaeological Sciences* (Bonneau *et al.*, 2012). It formed the basis of the protocol used in this PhD.

Samples, collected *in-situ*, were analysed unprepared and in cross-section. They were first observed with binocular microscopy, and then under the SEM. Analyses were carried out with SEM-EDS, Raman spectrometry and FTIR spectrometry. All these steps have been carried out on both unprepared samples and samples in cross-section, except FTIR spectroscopy analysis which was carried out only on unprepared samples (Figure 2.13).

Each step of this protocol is justified and detailed below with a brief presentation of its principle.

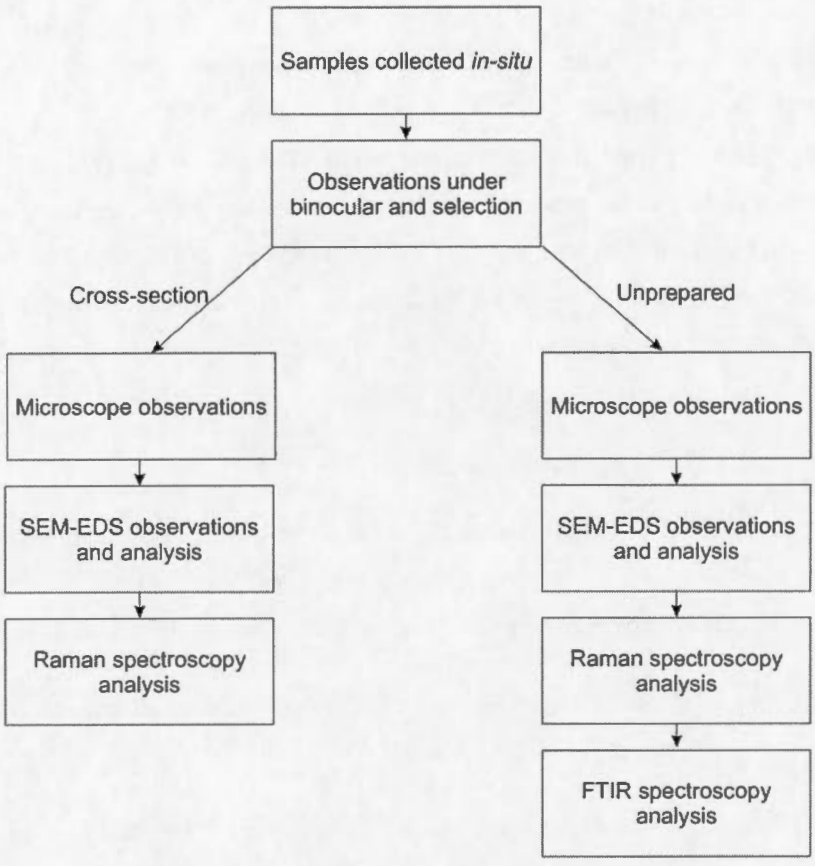


**Figure 2.13** Characterization methodology

### 2.4.2 Information about the schedule of this project

At the beginning of this PhD project, samples for radiocarbon dating had to be collected in less than two weeks in the Maclear district of South Africa. Thus, a week of intensive characterization was carried out at the University of the Witwatersrand, Johannesburg, and the University of Pretoria, Pretoria, South Africa. Samples collected first for characterization had to be analysed in order to select good candidates for radiocarbon dating. Microscopy, SEM-EDS, Raman spectroscopy and FTIR spectroscopy were carried out on unprepared samples. Then, selected representations were sampled for radiocarbon dating.

In the middle part of this project, following preliminary results I had obtained on white paints, an internship focusing on white paint characterization from sites in Lesotho was

proposed to students of the Master program in archaeometry, at the Université Michel de Montaigne, Bordeaux III, France. Laura Didier was the candidate selected for this six-month internship at the Laboratoire Lux, Université du Québec à Montréal. She carried out microscopy, SEM-EDS and Raman analysis on 2/3 of the white samples collected in the Lesotho sites. Her study was supervised by Prof. Michel Lamothe and myself. She followed the methodology detailed below and was trained in its use by myself. Her results were complimented by my own analyses on the other samples previously characterized and by FTIR spectroscopy. They were integrated to the sample database, available in the Appendix, and used in the results and discussion of this Ph.D.

### 2.4.3 Sample collection and preparations

Samples were collected *in-situ* in southern Africa and at the Cliff Lake, by myself during the summers of 2011 and 2012 (Table 2.1). Samples from Lake Wapizagonke were collected by Gilles Tassé and the underwater excavation team of Parks Canada (Dagneau, 2010).

Samples for pigment characterization were taken with sterile scalpel and gloves, and stored in gelatine capsules.

Photos were taken before and after each sample collection for records. In the case of the Lesotho and Botswana sites, samples collected were as large as possible with the aim of "saving" them for further analysis. Only identifiable representations were sampled. In the Maclear district, the focus was given to dating by Prof. David Pearce, the archaeologist in charge. Collection of samples was made in two steps in that case. First, a sample of about 1 $mm^2$ was collected for pigment characterization. Where results showed the presence of carbon-based pigments, a second collection was made for radiocarbon dating. In that case, the sample required was about 3 $cm^2$. To get it, existing cracks and holes in the figures were exploited, in agreement with Prof. Pearce and conservation requirements. Some figures were not sampled because of their importance and/or the quantity of sample required. The estimation of the quantity of sample required to get a radiocarbon date was improved through the project. It was one of the objectives of this Ph.D.

| | South Africa | | Lesotho | | Botswana | | Cliff Lake, Canada | | Lake Wapizagonke, Canada | |
|---|---|---|---|---|---|---|---|---|---|---|
| | Collected | Studied | Collected | Studied | Collected | Studied | Collected | Studied | Collected | Studied |
| Red paint | 2 | 2 | 98 | 29 | 43 | 0 | 0 | 0 | 16 | 16 |
| White paint | 3 | 3 | 48 | 48 | 1 | 0 | 0 | 0 | 0 | 0 |
| Black paint | 70 | 70 | 18 | 18 | 11 | 11 | 0 | 0 | 0 | 0 |
| Pink paint | 0 | 0 | 3 | 0 | 0 | 0 | 0 | 0 | 0 | 0 |
| Orange paint | 0 | 0 | 11 | 0 | 0 | 0 | 0 | 0 | 0 | 0 |
| Rock surface | 14 | 14 | 28 | 28 | 5 | 5 | 3 | 3 | 3 | 3 |

**Table 2.1** List of paint samples collected and studied in this thesis

Red and white soils were collected in the immediate vicinity of rock art sites studied in the Phuthiatsana Valley, Lesotho. Three samples were collected from each source to evaluate the homogeneity of the material and stored in plastic bags. GPS points were recorded for each source (Figure 2.14).

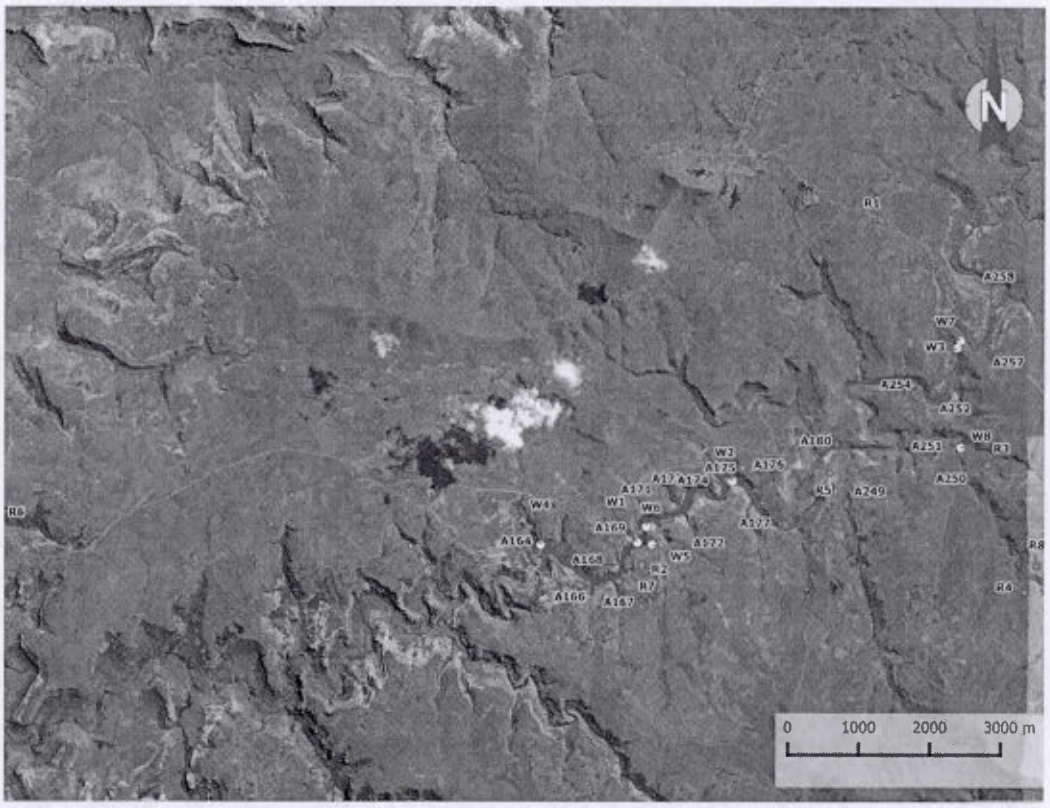


**Figure 2.14** Location of soils collected in the Phuthiatsana Valley, Lesotho (Map drawn by François Hardy, R: red soils, W: white soils, A: Aral sites)

Samples were analysed unprepared and in cross-section. As unprepared samples, they were observed by binocular glass directly put on a glass slide, and selected pieces were put on a carbon-stub. Pictures and maps of them were made. Another piece was selected to be embedded in epoxy resin to make a cross-section. The sample was positioned on a piece of double-sided tape in the mould under binocular glass. Then the epoxy resin (EpoFix, Struers) was poured gently in the mould with a pipette to avoid bubbles and to avoid moving the

sample during this step. The resin was left to dry at room temperature under a fume cupboard for at least 24 hours. Then, the sample embedded in resin was polished by hand with polishing cloths (Bruhler Fibrmet discs).

Finally, for Lake Wapizagonke, rock paintings on flakes collected on-site and in the lake, were analysed at Parks Canada, Ottawa, Canada, as the fragments are prohibited from leaving the storage facility. Samples for pigment characterization (FTIR spectroscopy and SEM-EDS) were collected under a binocular glass with a scalpel, cleaned between each sample with methanol, and put on a carbon-stub or directly in the machine. Manufacture of cross-sections was not permitted. Samples on the carbon-stub were allowed to be transported to Montreal, for Raman spectroscopy.

### 2.4.4 Microscopy

Often omitted in characterization studies, microscopic observations are of crucial interest. They are used to assess the homogeneity of the sample: whether it is a mixture or one material, whether crystals are on top of or under the paint layer, etc. With cross-sections, it is possible to see the "stratigraphy" of the sample (that is to say the different layers composing the paint) and thus to evaluate possible repaint or superposition of paints. This reveals the painting techniques and preparations of the artists.

These observations were made with a Leica DMLP microscope, equipped with a Leica DFC450 camera and objectives at x10, x20 and x50, using reflected light, at the Département des Sciences de la Terre et de l'atmospère, Université du Québec à Montréal, Canada. Photos were taken with the LEICA software.

At Parks Canada, observations were made under a LEICA binocular glass equipped with a LEICA camera.

### 2.4.5 Scanning electron microscopy coupled with Energy-dispersive X-ray Spectrometry (SEM-EDS)

To be able to recognize pigments made of charcoal or to differentiate iron oxides by their shape, precise observation is needed. This is conventionally carried out by SEM observations. However, the first way used to characterize paint layer was through elemental analysis. SEM-EDS was one of the first techniques to do this with XRF. XRF analysis is well efficient to detect chemical elements from potassium, whereas SEM-EDS starts detecting chemical elements from boron (Pollard and Heron, 1996). In this study, elements such as carbon, sodium, magnesium or silicon were needed for a first identification of the paint. Moreover, SEM-EDS requires smaller samples than conventional XRF, and gives spatial repartition for elemental analysis. On the other hand, XRF is much more sensitive to heavy chemical elements which can be of great interest in tracking raw material provenance. However, this question was not an objective of this project.

LA-ICP-MS and ion-beams analyses were considered as well, but they were rejected for this project due to the inaccessibility of instruments and their elevated costs.

SEM-EDS analyses have two objectives: observation of the shape of the particles and analysis of the chemical elements (qualitative and semi-quantitative) making up the sample. As it is possible to focus on very small points (about 10 µm diameter) and to make maps of the partitioning of the chemical elements, a first identification of the sample layers can be achieved. Moreover, the shape of the particles discriminates several of them with the same chemical composition, such as iron oxides and hydroxides (Arias *et al.*, 2011), calcium carbonates, calcium sulphates, carbon-based pigments (Tomasini *et al.*, 2012).

In this project, different SEM-EDS were used through time depending on the place the analyses had to be done and on the availability of instruments.

At the University of the Witwatersrand, Johannesburg, South Africa, a JEOL 6300 SEM-EDS was used with an electron beam of 30 kV and 44 pA. The chamber was under a pressure of 9 mPa. Samples on carbon-stub were not coated before analysis. Observations were made with secondary electrons.

The Laboratoire Lux owns a Hitachi TM-3000 SEM equipped with a Quantax 70 Bruker EDS, cooled with Peltier effect. Analyses were carried out on variable pressure with a 15 kV electron beam. Observations were made with backscattered electrons. Samples on carbon-stubs were not coated before analysis. For some cross-sections, a carbon-coating was required. All samples studied were analysed with this method. However, this SEM is a table one and is thus subject to some limits, especially in terms of magnification. Therefore when more intensive observations were needed, samples selected were observed and analysed with the SEM-EDS at Université Laval, Quebec City, Canada, and the SEM-EDS at Géotop, Université du Québec à Montréal, Montreal, Canada.

The Earth Sciences department at Laval University owns a JEOL 840-A SEM equipped with a PGT Avalon EDS. An electron beam of 15 kV was used and observations were done with secondary electrons. Samples were observed on carbon-stubs with a gold-palladium coating.

At Géotop, a SEM-EDS was available during summer 2014. It was used mainly at the end of the project, to complement analyses and to realize elemental maps on cross-sections. The SEM-EDS is a Hitachi S3400N equipped with an Oxford Instrument EDS, cooled by Pelletier effect. An electron beam of 15 kV was used and observations were done with secondary electrons under high vacuum, or with backscattered electrons at a pressure of 60 Pa. Only red paint were observed unprepared on a carbon-stub with a carbon coating. Elemental maps were conducted at a pressure of 60 Pa, with an electron beam of 15 kV and a probe of 60. 10 frames of 512x384 pixels were acquired per map, with an accumulation of 2000 µs per point.

At Parks Canada, the SEM-EDS used was a VEGA equipped with an Oxford Instruments EDS. An electron beam of 15 kV was used and observations were done with secondary electrons. Samples were observed on carbon-stubs with a carbon coating.

EDS analyses were all done with 180 seconds acquisition time.

### 2.4.6 Raman spectroscopy

Raman and FTIR spectroscopic analysis allows investigation of the molecular composition of the sample. This second step is important as it makes it possible to know how chemical

elements are arranged together. Indeed, when calcium is detected alone with the SEM, it can come from calcite, aragonite or calcium oxalates. Only molecular analysis can reveal their mineralogical forms.

Historically, XRD was used to perform crystallographic analysis. However, micro-XRDs are very rare and if only powder XRD is available, it requires several milligrams of sample. For this study, no micro-XRD was available. Given this, Raman spectroscopy seemed to be a better choice, considering the type of pigments expected.

Invented in the 1910's, Raman spectroscopy was applied to pigment analysis only in the 1990's. Coupled to a microscope, a Raman spectrometer can analyse spots as small as a few microns, is totally non-invasive and no sample preparation is required. Moreover, it is able to analyse both amorphous and crystallized compounds. This is a considerably advantageous compared against the XRD, which is not able to characterized amorphous compounds. Previous studies in South Africa (Prinsloo *et al.*, 2008; Prinsloo *et al.*, 2013; Tournié *et al.*, 2011) and around the world (e.g. Lahlil *et al.*, 2012) gave important results on both pigment and binder characterization.

Following previous research, green (514 nm or 539 nm) and near-infrared (785 nm) lasers are the best choices to characterize our samples. Depending on laser and Raman instrument availability, where possible, samples were analysed with both lasers.

At the University of the Witwatersrand, South Africa, a Horiba Jobin-Yvon Raman Spectrometer with a 514 nm laser, and x50 long-focal objective has been used.

The Université du Québec à Montréal does not own a micro-Raman spectrometer. Thus, analyses were carried out at the Laboratoire de caractérisation des matériaux, Université de Montréal, Canada. An InVia microspectrometer Raman was used with 514 and 785 nm lasers and x50 long-focal objectives.

Interpretations of spectra were made using Grams and CrystalSleuth as software, and RRUFF database, IRUG database and a personal database made by myself with reference minerals

from the geological collection of the département des Sciences de la Terre et de l'atmosphère, Université du Québec à Montréal.

Raman spectroscopy is a useful tool for molecular characterization of pigments. However, in the case of some kinds of minerals such as calcium oxalates, it is limited due to the difficulty of exciting these molecules with visible wavelengths. Thus to complement Raman analysis, FTIR spectroscopy analysis was carried out.

### 2.4.7 FTIR spectroscopy

FTIR spectroscopy was very rarely used as a tool for mineral characterization. Most of the studies using it for pigment analysis focus on organic bonds and not on inorganic ones at the beginning of the spectrum, that is to say from 400 to 1000 $cm^{-1}$. Indeed, some spectra do not show at all this part (Stuart, 2007).

In Bonneau *et al.* (2012), FTIR was of great use in identifying minerals such as feldspars, which were not distinguishable with Raman analysis alone. Moreover, it proved to be very sensitive to calcium oxalates, humic acids, and calcium carbonates which are contaminants for radiocarbon and which need to be identified and quantified. Indeed, one of the advantages of FTIR spectroscopy is in quantitative analysis.

For this Ph.D. project, because of the small size of samples, a micro-FTIR was used. Samples were crushed into two diamond cells, provided by the Rock Art Research Institute, University of the Witwatersrand, Johannesburg, South Africa. Most of the analyses were carried out at the Laboratoire de caractérisation des matériaux, Université de Montréal, Canada.

The Stingray system combines a FTIR spectrometer Digilab FTS7000e and a microscope IR UMA600. Analysis is carried out over a spectral range of 4000-750 $cm^{-1}$, with 128 scans at 2 $cm^{-1}$ resolution.

At the University of Pretoria, Pretoria, South Africa, analyses were conducted with the diamond ATR of a Vertex 70v (Bruker Optics) spectrometer, under the supervision of Linda Prinsloo, Chief Researcher, Department of Physics, University of Pretoria. Spectra were acquired with 32 scans at 4 $cm^{-1}$ resolution over a spectral range of 4000-400 $cm^{-1}$.

At Parks Canada, a Bruker micro-FTIR was used. Analysis is carried out over a spectral range of 4000-400 $cm^{-1}$, with 128 scans at 2 $cm^{-1}$ resolution.

Interpretations of spectra were made using Grams and CrystalSleuth as software, and RRUFF database, IRUG database and a personal database made by myself using reference minerals from the geological collection of the département des Sciences de la Terre et de l'atmosphère, Université du Québec à Montréal.

Results predominantly gave information on inorganic compounds of the paints but were invaluable in quantifying radiocarbon contaminants.

## 2.5 Conclusion on the general methodology

Using the precise characterization protocol detailed above, it was possible to select samples for radiocarbon and OSL dating. However, more than 300 samples were collected during collection field trips and it was not possible to characterize all of them because of time and money constraints. Focus was given to black pigments which would most likely form candidates suitable for radiocarbon dating. Then, red and white pigments from Lesotho were characterized for reproduction of paints for OSL tests. In the Canadian Shield, only one black sample was available on the selected sites, thus, mostly red pigments were characterized.

The general methodology applied in this Ph.D. has been improved through time and tests to conduct to the final figure (Figure 2.15). More details about specific data processing or sample preparation are given in the related chapters.

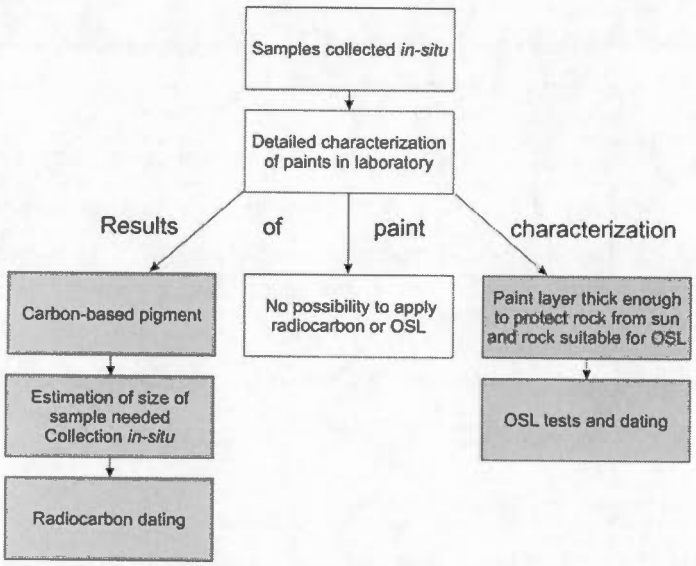


**Figure 2.15** General methodology applied in this PhD

# CHAPTER III

## THE ARTISTS' PALETTE: HOW PAINTS WERE MADE

From raw materials to paint, the artist may prepare his colours in different steps to obtain the hues and textures required. Very little is known today about this preparation. However, this part is one of the most important to evaluate dating potential and to understand changes in pigments uses.

The preparation steps can be summarized under the term of *chaîne opératoire*. It comprises the acquisition of the raw material (mining, trading, gathering, etc.), its preparation (grinding, sieving, heating, mixture, etc.), the selection, and eventually preparation, of the surface for painting, the selection of the tools to paint (brush, fingers, etc.), the choice of the representation and the application to the surface (one or more layers, thickness, uses of the natural defaults of the surface, preliminary draft before final image, etc.). After their realization, paintings will degrade because of weather, human, animal and bacterial activities, etc. Furthermore, modifications and alterations may have occurred depending on populations using the sites. All of these steps need to be investigated as they can modify the paint and thus give another picture than the real pigment used at the first time.

In this chapter, results for each colour will be detailed by regions of southern Africa (Maclear district in South Africa, the Phuthiatsana valley in Lesotho and the Thune valley in Botswana). This objective is to reconstruct the *chaîne opératoire* for each colour and each area/site and to make comparison between sites and geographic areas. Characterization of paints at Lake Wapizagonke is presented under the form of an article, being Chapter VI.

Black paints in southern Africa were the most intensively studied for this PhD (101 samples) as some of them were found, in a previous study, to be made of carbon-based pigments and thus having a great potential for radiocarbon dating (Bonneau *et al.*, 2011 ; Bonneau *et al.*,

2012). In parallel, 51 white paint samples and 29 red and dark red paint samples were characterized. Most of them are from Lesotho sites.

Each sample was analysed using the characterization protocol detailed in Chapter II. All the results for each sample can be found in appendix at the section containing the catalogue of samples. Moreover, to avoid unnecessary repetitions of peaks observed during Raman spectroscopy and FTIR spectroscopy analyses, tables 3.1 and 3.2 summarise peaks recorded and link them to their interpretation. Where unconventional peaks are found or where a detailed explanation of the position of peaks is required, further developments will be provided. Finally, the rock supporting paintings from the three studied areas was analysing using the same characterization protocol as for the paintings. Results are summarized in this chapter and detailed characterization can be found in Appendix A. They are used as background for paint characterization and to distinguish alteration naturally occurring on the rock and those specific to paint.

**Table 3.1** FTIR spectroscopy peaks and their interpretations (n/a is used for chemical formula when the name of the compound reflects different molecular or mineralogical shapes)

| **Mineral** | **Chemical formula** | **FTIR peaks ($cm^{-1}$)** |
|---|---|---|
| Albite | $NaAlSi_3O_8$ | 738, 755, 775, 794, 981, 1007, 1079, 1108 |
| Anorthoclase | $(Na,K)AlSi_3O_8$ | 1162, 1001 |
| Apatite | $Ca_5(PO_4)_3(OH,F,Cl)$ | 964, 1024, 1417, 1454 |
| Calcium carbonates | $CaCO_3 \cdot n(H_2O)$ | 1434, 1460 |
| Calcium oxalates | $Ca(C_2O_4) \cdot n(H_2O)$ | 778, 884, 950, 1314, 1382, 1463, 1489, 1621, 3058, 3255, 3335, 3423, 3486 |
| Calcium sulphates | $nCaSO_4 \cdot n(H_2O)$ | 1109, 3400, 3545 |
| Hectorite | $Na_{0,3}(Mg,Li)_3Si_4O_{10}(OH)_2$ | 813, 835, 853, 950, 1057, 1067, 1120, 3627, 3675 |
| Humic acids | n/a | 816, 1620, 1637, 1686, 1721/ Broad peak 2600-2650 $cm^{-1}$ and enlargement of the 3000$cm^{-1}$ massif |
| Illite/ Montmorillonite | $(K,H_3O)(Al,Mg,Fe)_2(Si,Al)_4O_{10}[(OH)_2,(H_2O)]$/ $(Na,Ca)_{0,3}(Al,Mg)_2Si_4O_{10}(OH)_2 \cdot n(H_2O)$ | 724, 742, 760, 786, 1005, 1032, 1092, 1106, 1148, 1324, 1646, 3619 |
| Kaolinite | $Al_2Si_2O_5(OH)_4$ | 778, 799, 862, 884, 948, 1003, 1033, 1113, 1144, 3619, 3698 |
| Microcline | $KAlSi_3O_8$ | 728, 779, 1020, 1036, 1058, 1084, 1104, 1129 |
| Quartz | $SiO_2$ | 778, 799, 909, 1004, 1043, 1135 |

**Table 3.2** Raman spectroscopy peaks and their interpretations (n/a is used for chemical formula when the name of the compound reflects different molecular or mineralogical shapes)

| Mineral | Chemical formula | Raman peaks ($cm^{-1}$) |
|---|---|---|
| Albite | $NaAlSi_3O_8$ | 190, 208, 290, 416, 480, 509, 763, 815 |
| Anatase | $TiO_2$ | 396, 518, 638 |
| Anhydrite | $CaSO_4$ | 1016 |
| Apatite | $Ca_5(PO_4)_3(OH,F,Cl)$ | 429, 964 |
| Barite | $BaSO_4$ | 985 |
| Bassanite | $2CaSO_4 \cdot (H_2O)$ | 1010 |
| Calcite | $CaCO_3$ | 281, 1088 |
| Carotenoid | n/a | 1002 |
| Clay | n/a | 1245, 1327, 1442, 1550, 1700/ 1152, 1256, 1320, 1574, 1745 |
| Feroxyhyte | $\delta$-$Fe^{3+}O(OH)$ | 390, 664, 1327 |
| Goethite | FeO(OH) | 300, 395 |
| Gypsum | $CaSO_4 \cdot 2(H_2O)$ | 415, 492, 1008, 1135 |
| Hectorite | $Na_{0,3}(Mg,Li)_3Si_4O_{10}(OH)_2$ | 263, 445, 606, 707 |
| Hematite | $\alpha$-$Fe_2O_3$ | 225, 247, 293, 412, 498, 613, ~1300 |
| Hydromagnesite | $Mg_5(CO_3)_4(OH)_2 \cdot 4(H_2O)$ | 1114 |
| K/Ca nitrate | $KNO_3$ / $Ca(NO_3)_2$ | 1051 |
| K-feldspars | $KAlSi_3O_8$ | 261, 465, 512 |
| Kaolinite | $Al_2Si_2O_5(OH)_4$ | 268, 284, 444, 476, 514 |
| Quartz | $SiO_2$ | 206, 265, 292, 356, 395, 466, 1163 |
| Magnetite | $Fe_3O_4$ | 233, 286, 658 |
| Manganese oxides | n/a | 653 |
| Rutile | $TiO_2$ | 445, 611 |
| Weddellite | $Ca(C_2O_4) \cdot 2H_2O$ | 906, 1475 |
| Whewellite | $Ca(C_2O_4) \cdot (H_2O)$ | 498, 897, 1466, 1490 |

## 3.1 Maclear district, South Africa

In the Maclear district, 75 samples were collected. 72 were black paint samples (but after microscope observations, two turned out to be dark red) and 3 white paint samples. They were all characterized as part of this project.

### 3.1.1 Rock and surface preparation

Paintings in the Maclear district are found on the Clarens Formation sandstone, composed of quartz and feldspars in a calcitic/chloric matrix (Eriksson, 1979; Tournié *et al.*, 2011). Commonly occurring alterations at the surface of this rock are calcium sulphates and clay (Johnson *et al.*, 2006; Tournié *et al.*, 2011).

Characterization of the rock support from two sites and from samples of paint collected as detached flakes of rocks confirms these characteristics. A white to orange layer is found at the surface of the rock at almost all sites studied in the Maclear district. It is composed of calcium sulphates, clay and calcium oxalates. Eolian deposits under the form of quartz and feldspars (about 10-20 µm diam.) were observed too.

Underneath this layer, a highly crystallised layer of rock (about 100 µm thick) with no matrix is observed. It has been previously reported by Bonneau *et al.* (2012) and Hoerlé *et al.* (2016).

The rock itself is composed of quartz, microcline, albite and anorthoclase, in a matrix composed of calcium and chlorine. Their size is between 50 and 200 µm diam. with the majority about 100 µm diam.

No preparation of the rock surface is visible. However, all the paintings were realized on the white weathering crust visible at the surface of the rock and which may act as a preparation layer for the artists.

### 3.1.2 Black paints

#### 3.1.2.1 Microscope

Samples were first observed unprepared under the microscope with a magnification of between x100 and x500. Four textures were observed: pleated-paper texture (1), coarse-grained texture (5), smooth texture (17) and fine-grained texture (47) (Figure 3.1).

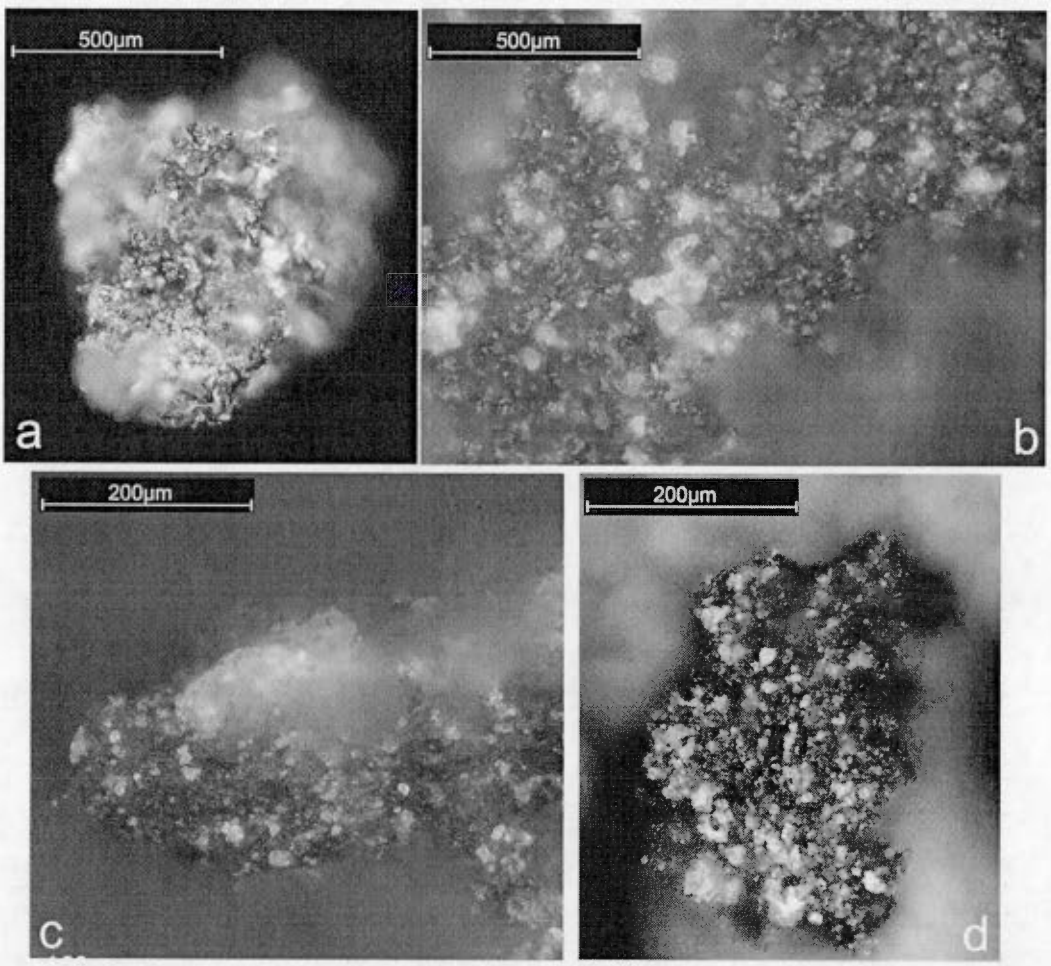


**Figure 3.1** Textures observed with the microscope on black paint from the Maclear District (a: pleated-paper texture, b: coarse-grained texture, c: smooth texture, d: fine-grained texture)

The pleated-paper texture was found only on one sample from an antelope at RSA BUX. It looks like waves of black fine layers of papers. The coarse-grained texture is a layer of black paint composed of "large" crystals (about 100 μm). It has been observed in sites RSA BUX1, RSA CHA1, RSA FRE1, and RSA PRH1, and on both human and animal figures. The smooth texture can be seen in sites RSA BUX1, RSA CHA1, RSA LAB1, RSA LAB3, RSA LAB10, RSA MEL6, RSA MEL9 and RSA TYN2, on both human and animal figures. It is characterized by a uniform layer of paint (no grain can be seen even at x500 magnification). Finally the fine-grained texture, composed of small crystals (about 10-20 μm), has been observed in sites RSA CHA1, RSA FRE1, RSA FRE4, RSA LAB1, RSA LAB3, RSA LAB7, RSA LAB10, RSA MEL8, RSA PRH1 and RSA TYN2, on human, animal and geometric figures.

The black layer is usually uniform with some red, yellow, orange, white and/or transparent grains on top which can be seen as aerosol particles (Figure 3.2). They can be correlated with yellow/orange layers observed on top of the black paint layer and which are similar to those found on top of the rock face. These layers are not homogenous either on a single figure, or on a site or area. Samples taken from two figures closed together may have weathering layers or not, and if present, their colours and thickness may be different. These layers and particles can be interpreted as weathering products. These yellow/orange layers can be observed under the paint too but with a larger thickness. They are likely to be rock alteration, present before the paint was made.

On four samples, the black paint layer shows more scattered black grains in a white matrix, resulting in a greyish paint (Figure 3.3).

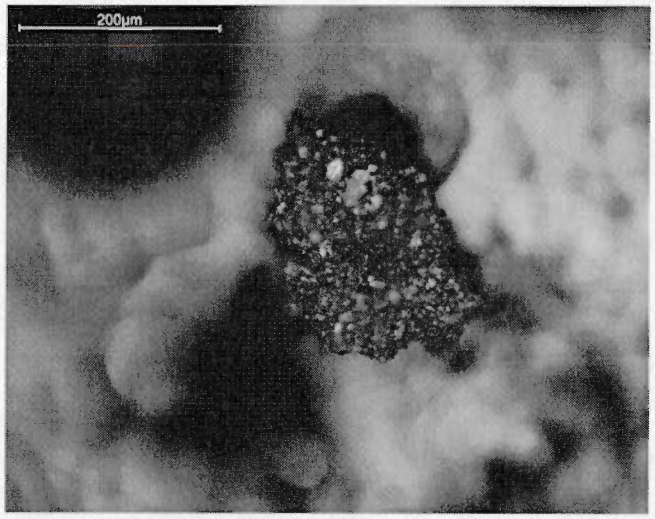


**Figure 3.2** Uniform black paint layer with few grains on top

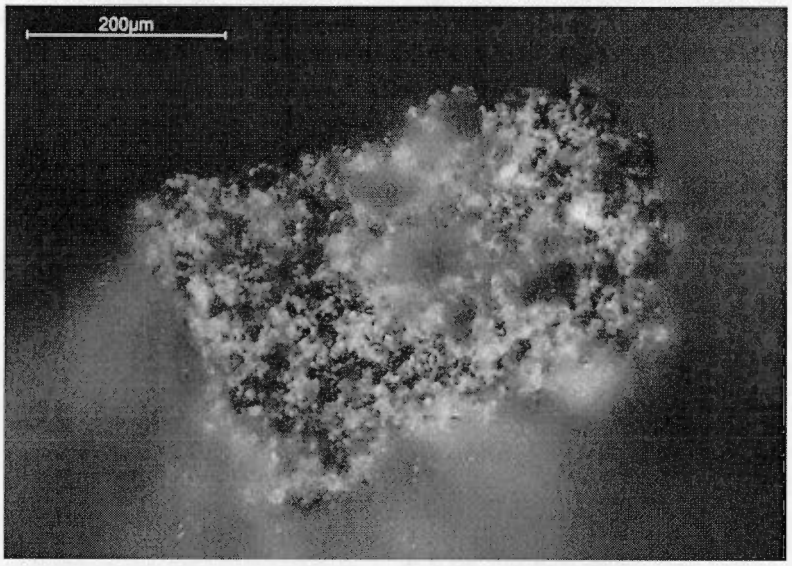


**Figure 3.3** Black paint layer made of scattered black grains.

On some samples, red and white layers can be seen under the black paints. They appear only on multi-coloured figures and are doubtless the continuation of the paint layer made next to

the black paint. It is interesting to note that black paint was always on top of these other colours, which indicates that it was used at the end of the realization of the figure.

After microscope observations, it turned out that two samples, which looked like black on-site, were in fact red paints: MEL6P2 and MEL9P3. They are detailed in a specific section below (see §3.1.4).

44 samples out of 70 were mounted in cross-sections.

All samples in cross-section presented a fine-grained texture except BUX1P3 which has got a smooth texture (Figure 3.4). This sample is a reference sample taken from black stains, naturally occurring on rock face in the site RSA BUX1 to be compared to black paints in case such material was used to make paint.

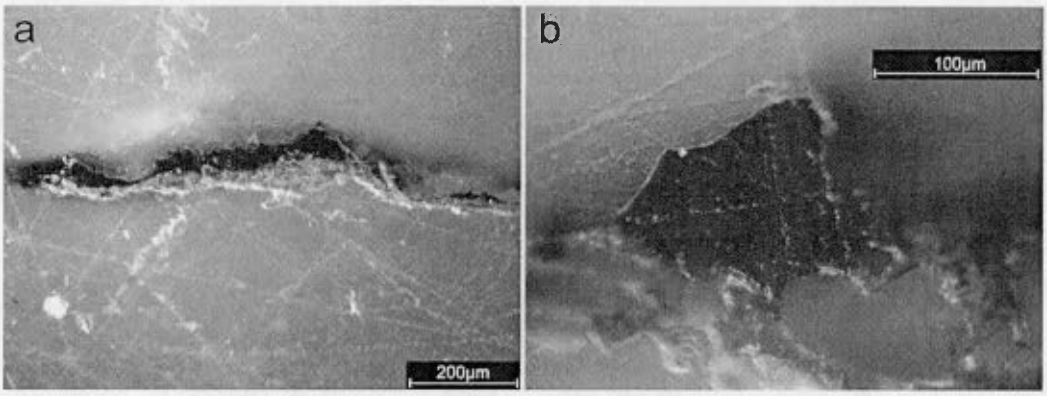


**Figure 3.4** Textures observed with the microscope on black in cross-section: a) fine-grained texture, b) smooth texture

The black layer of paint is from 10 µm to 300 µm thick. 11 samples show transparent and/or white grains in the black layer. It may be intentional mixture by the artists to make a special colour or to make the paint to adhere easier to rock. It may be natural weathering too. Most of the samples are from sites RSA FRE1 and RSA LAB1. The other samples present a black layer uniform in colour.

On top of the paint layer, a transparent to white layer of weathering products has been observed on 6 samples and is about 5 to 10 µm thick. Underneath the paint layer, another weathering layer is observed on all the samples. Its colour goes from transparent-white to orange. It is mostly fine-grained. This weathering layer has been previously observed on the rock face and thus is interpreted as a natural weathering crust of the rock. It is between 50 and 150 µm thick.

A grey layer with a smooth texture has been observed just under the black paint layer on 4 samples from RSA LAB1 and RSA TYN2. It is followed by a fine-grained white layer attributed to rock weathering. It is from 30 to 100 µm thick depending on the samples. It may be a weathering product layer, but can be seen as a paint layer too. Indeed, in some other samples, from the same site, transparent and white grains have been observed in the black layer. It is possible that artists used the same material to mix with the black pigment and to make a first paint layer. It may help in the painting process or give a special colour. However, it is difficult to judge about the initial colour of the paint as weathering products are visible on top of the paint.

Sample LAB1-2012-2 is the only one where two layers of black paints were observed. This paint thus was made on top of another one, black too (Figure 3.5).

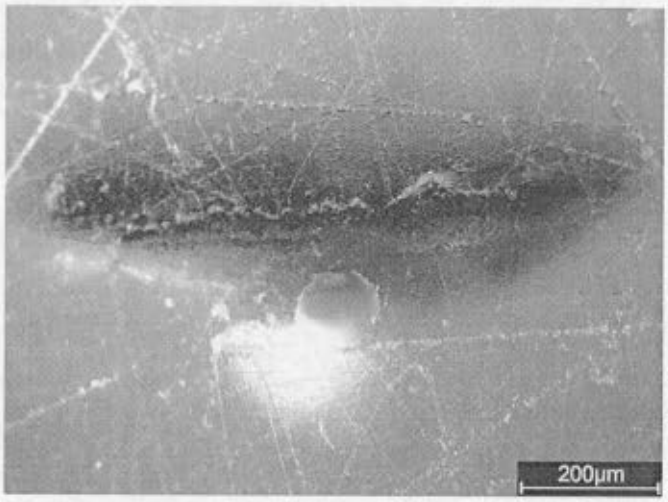


**Figure 3.5** Cross-section of samples LAB1-2012-2

3.1.2.2 SEM-EDS

Four different textures were recorded for particles composed of carbon during SEM observations: the morphology of charcoal (1), a smooth texture (18), a fine-flaky texture (38) and a flaky texture (12) (Figure 3.6).

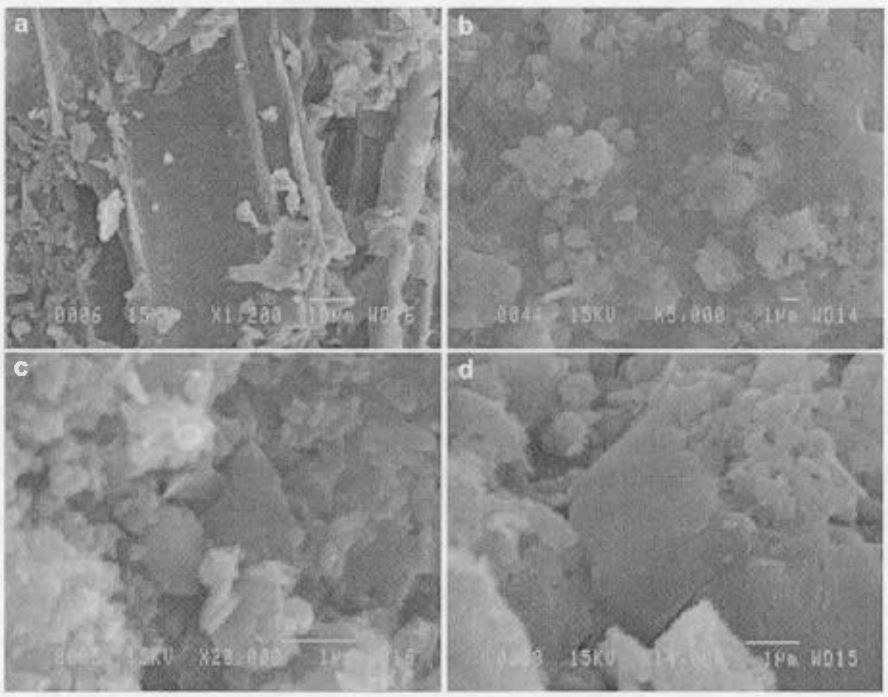


**Figure 3.6** Textures recorded on black samples (secondary electron images): a) charcoal, b) smooth texture, c) fine-flaky texture, d) flaky texture

The smooth texture was recorded on sites RSA BUX1, RSA FRE1, RSA FRE4, RSA LAB1, RSA LAB7, RSA LAB10, and RSA MEL9, and on both human and animal figures. However, this category is not uniform. For 14 of them, it is impossible to see the shape of the carbon particles. The layer seems to be like a thin film on top of the rock grains. For 1 of them, the layer presents some cracks. For 3 of them, the smooth layer crumbles to large (5 μm) or small (1-2 μm) flakes.

The fine-flaky texture was recorded on all the sites studied except RSA BUX1 and RSA MEL6. It is made of small flakes from 0.5 to 2 µm diameter.

The flaky texture was found on sites RSA FRE1, RSA LAB1, RSA LAB3, RSA MEL8, RSA TYN2, and RSA PRH1. The black layer is here made of flakes about 5 µm diameter.

On half of the samples analysed, the quantity of sulphur combined with calcium is high. It is doubtless due to the presence of calcium sulphates which are well-known weathering products of rock art around the world and in South Africa. Moreover, calcium sulphates are common Clarens formation sandstone alterations, resulting of the reaction between calcium in the rock and acidic rains (Johnson *et al.*, 2006). Other elements, as magnesium, phosphorus and chlorine are attributed to weathering products.

Sodium, aluminium, silicon, titanium and iron were recorded on almost all the samples and can come from small aerosol particles or from the rock support.

On sample LAB7-2012-4, barium was found. This element may come from the rock support, but has not been recorded on the two rocks studied, from RSA LAB1 and RSA BUX1. It is unclear at this stage how to interpret it.

On samples MEL8P1 and MEL8P2, iron was recorded under the form of flakes of about 1 µm diam. They are doubtless from the adjacent red paint layers.

Only cross-sections on samples to be dated and on samples from site RSA LAB1 were analysed by SEM-EDS.

The black layer is made of carbon and calcium for all the 17 samples studied. Silicon and aluminium were recorded under the form of grains, mostly at the surface of the paint layer. However, for three samples at RSA LAB1 (LAB1-2012-3, LAB1-2012-6 and LAB1-2012-7), silicon and aluminium seem to be part of the paint layer, as a mixture. Sulphur was recorded as clusters inside the paint layer, found predominantly at the top of the paint layer. Sodium, magnesium, phosphorus and iron were recorded in the paint layer but are attributed to weathering products as is sulphur.

Surrounding the paint layers, two layers appear. The first one, on top of the paint layer, is thin, about 5 to 10 µm thick, and is made of silicon and aluminium. It was observed only on one sample at RSA LAB1. It is a weathering crust, already observed on the natural rock surface.

The second weathering layer is found under the paint layer. It is composed of calcium, sulphur, grains of silicon, grains of silicon and aluminium, and sometimes silicon and aluminium as a matrix. Sulphur is found as layers correlated with calcium, or as clusters as observed in the paint layer. At RSA LAB1 and RSA TYN2, EDS maps correlate sulphur and calcium layers to grey layers observed under the paint layers with microscope. Grains of silicon and grains of silicon and aluminium are mostly at the bottom of the weathering crust, and are seen as the joint between the weathering crust and the rock.

#### 3.1.2.3 Raman spectroscopy

Samples were analysed with both green (514 nm) and near-infrared (785 nm) lasers. Peaks of carbonaceous matter were recorded on all samples with both lasers. Peaks around 1300 $cm^{-1}$ are called the "d-band", whereas peaks around 1500 $cm^{-1}$ are called the "g-band". The g-band corresponds to C-C stretching vibrational mode of the crystallized, i.e. ordered, carbon part of the sample. The d-band represents C-C stretching vibrational mode of the disordered, i.e amorphous, carbon part of the sample (Coccato *et al.*, 2015).

The shapes of these peaks were classified in three types:

- Type 1: the g-band is more intense than the d-band.
- Type 2: the g-band and d-band have got the same intensity.
- Type 3: the g-band is less intense than the d-band.

First, spectra recorded on unprepared samples are presented. With the green laser, 37 samples show type 1 spectra, 11 samples type 2 spectra, and 7 samples type 3 spectra (Figure 3.7). For 15 samples, carbonaceous peaks were too weak to make a proper categorization of them. With near-IR laser, 48 samples show type 3 spectra, and 6 type 2 spectra. The 16 samples left are the ones analysed in 2011 at the University of the Witwatersrand, where 785 nm laser was not available.

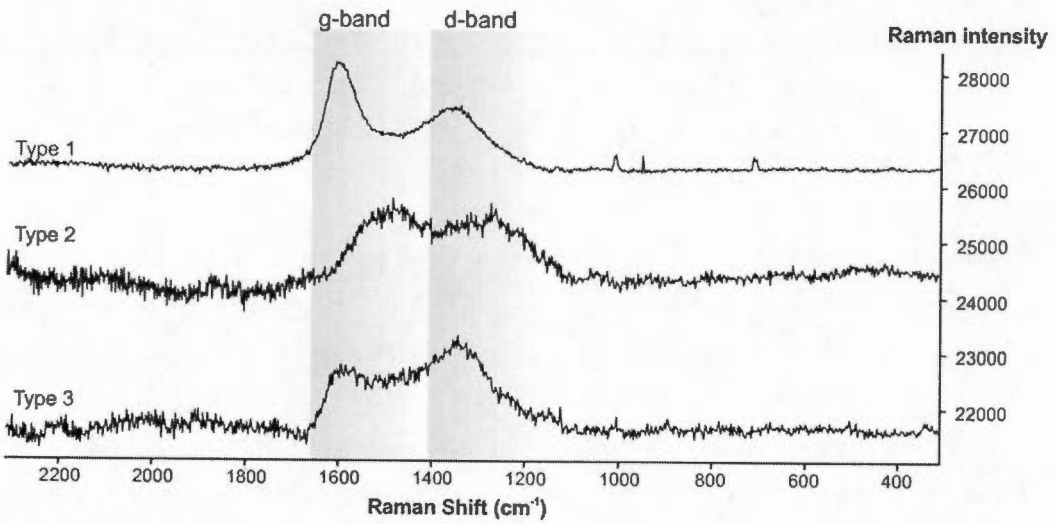


**Figure 3.7** Raman spectra recorded on Maclear black paints (green laser)

This difference in the shape of spectra is due to the type of excitation used and thus to the type of bonds excited. Indeed, C-C bonds depending on impurities surrounding and degrees of order will react to different excitation wavelengths (Stuart, 2007). This is valid for the type of minerals analysed too. Some will react to the green laser, whereas others not, but will not react to near-IR laser, thus the necessity to use both lasers to have complementary results.

With the green laser, calcium oxalates under the form of whewellite or weddellite were recorded on 37 samples, and in the case of 10 samples, the two mineralogical forms were observed on the same sample. Calcite was identified in 11 samples, and hydromagnesite in 10 samples.

Calcium sulphates more or less hydrated were found on 36 samples. Doublets with peaks at 1007 and 1015 $cm^{-1}$ were often recorded on the samples, pointing to a natural mixture of calcium sulphates more or less hydrated.

On three samples, quartz and feldspars were identified, but the peaks of feldspars were too weak to make a detailed identification.

With the near-IR laser, 33 samples contain calcium oxalates (both whewellite and weddellite) and 22 samples contain calcium sulphates more or less hydrated. In 8 samples, peaks of both gypsum and bassanite were recorded on the same sample. Calcite was identified in 11 samples.

In LAB1-2012-3, peaks were associated to hematite type 3, coming from a red paint layer underneath the black paint layer.

Four samples (LAB1-2012-5, LAB1-2012-6, LAB1-2012-7, and TYN2P7) show the peaks of Si-O amorphous bond at 1148, 1249, and 1321 $cm^{-1}$. These peaks are associated to clay minerals. In the case of samples, LAB1-2012-5 and TYN2P7, presence of white and red paint layer underneath the black layer points to a contamination from adjacent pigments. However, the possibility of a deliberated adjunction by the artist is not to be excluded. LAB1-2012-6 and LAB1-2012-7 do not seem to have any other kind of pigment around it, and here an artist deliberate admixture is possible. Elemental maps made with SEM-EDS confirm the presence of silicon and aluminium in the paint layers of these samples.

As for SEM-EDS analysis, only samples to be dated were analysed with Raman spectroscopy.

With the green laser, all samples show amorphous carbon type 1 spectra. Comparing with data obtained on unprepared samples, the spectra were the same except for TYN2P9 which had a type 2 spectrum on unprepared sample. With the near-IR laser, all samples show amorphous carbon type 3 spectra. Comparing with data obtained on unprepared samples, the spectra were the same except for FRE4-2012-2 and FRE4-2012-7 which had a type 2 spectrum on unprepared sample. This change may be due to the weakness of the peaks recorded on unprepared samples which makes the distinction difficult.

With the green laser, whewellite and weddellite were recorded in the black paint layer. However, whewellite is present in the surrounding layers of the paint layer but not weddellite. In these surrounding layers, calcium sulphates more or less hydrated and calcite were recorded too.

With the near-IR laser, whewellite and weddellite were observed for calcium oxalates in the paint layer and in the surrounding layers. Moreover, clay minerals and hematite were recorded in the weathering layer underneath the paint layer.

D and g-bands of carbon were deconvoluted using Grams. These two bands were included in the parameters as Lorentzian shaped curves. Other possible bands, D2, D3 and D4, were included as Gaussian but were not taking into account in the study as they do not appear on each spectrum/sample.

With laser 785 nm, the d-band varies from 1318 and 1342 $cm^{-1}$ on unprepared samples and from 1319 to 1334 $cm^{-1}$ on cross-section. The g-band oscillates from 1552 to 1598 $cm^{-1}$ on unprepared samples, and from 1575 to 1606 $cm^{-1}$ on cross-section.

With laser 514 nm, the d-band varies from 1340 and 1378 $cm^{-1}$ on unprepared samples and from 1340 to 1362 $cm^{-1}$ on cross-section. The g-band oscillates from 1563 to 1608 $cm^{-1}$ on unprepared samples, and from 1595 to 1605 $cm^{-1}$ on cross-section.

These results show a high variation in the positions of the peaks in each category. Interestingly, the variations between unprepared and cross-sections are relatively small if compared in each sample, except for one sample, BUX1P3, which is a reference sample from natural black stains occurring at the surface of the rock. It points to a single type of pigment used to make the paint and the absence of posterior pollution, by fires for example. Using data from positions, area and intensity of each peak, principal components analysis was carried out with JMP to see if any sub-group was distinguishable, with no successful results. The spectra recorded on the Maclear samples are homogeneous.

Compared to the study of carbonaceous matter by Coccato *et al.* (2015), the spectra recorded are attributed to charcoal and other flame carbons of different origins.

3.1.2.4 FTIR spectroscopy

All samples were analysed with FTIR except LAB1-2012-10 which was too small.

Calcium oxalates were recorded on all samples except those from RSA BUX1 (Figure 3.8). The peak at 1621 $cm^{-1}$ is enlarged in most of the spectra due to OH deformation of water at 1640-1680 $cm^{-1}$, already observed at the surface of the rock support, and present in clay minerals. Calcium oxalates were found on all samples. Feldspars and quartz were identified in 50 samples. Most of the time, it was not possible to give a detailed interpretation of the peaks but quartz was formally identified in four samples and albite in one sample. Calcium carbonates were observed in five samples. Finally, humic acids were found only on samples from RSA BUX1.

Peaks at 2769, 2855, and 2929 $cm^{-1}$ were observed on all samples. They are associated to C-H stretching modes in organic compounds such as egg, resin or fat which might have been used as binder, and in methanol, solvent used to clean the diamond cells. These peaks are most probably due to methanol rather than binders as the other peaks of these potential binders are not present in the spectra.

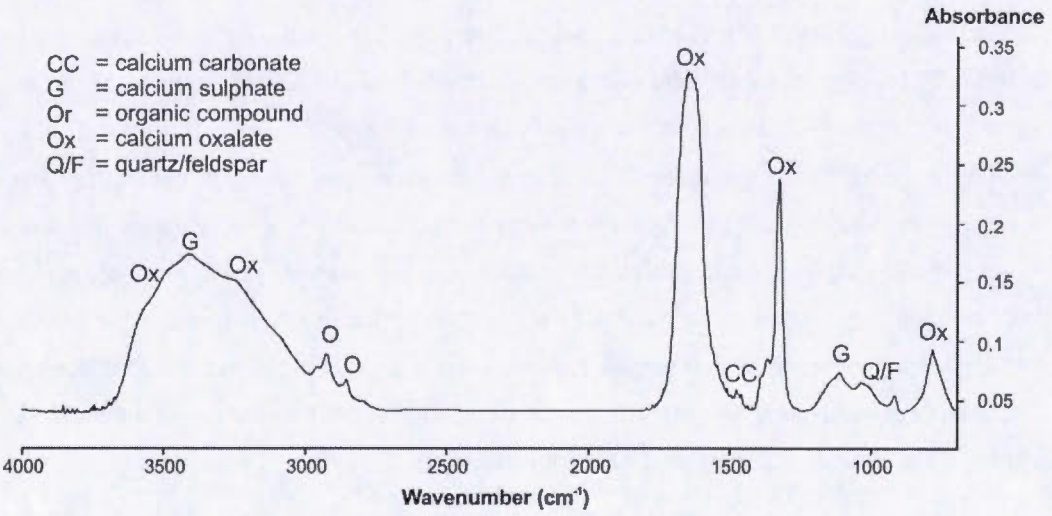


**Figure 3.8** FTIR spectrum recorded on black paints from the Maclear district

3.1.2.5 Conclusion

All the black paints collected from 13 different sites in the Maclear district are all carbon-based paints. Their morphology under SEM proves that they are all carbon blacks, that is to say an incomplete combustion of organic compound, except for one which is charcoal. Three different morphologies were observed for these carbon blacks, pointing to at least four different recipes including the charcoal recipe found only on one sample. Nevertheless, deconvolution of Raman peaks did not bring more information about the type of organic compounds burnt, but it confirms the identification as carbon blacks and charcoal pigments. Interestingly, all samples presenting a type 3 Raman spectrum with the green laser, have a flaky texture under SEM.

Clay minerals were found to be mixed with carbon blacks in at least two samples at RSA LAB1 and maybe two others at RSA LAB1 and RSA TYN2.

If compared to the representations, no distinction is found between the pigment used and the figures realized. However, comparing panels to panels and sites by sites, some distinctions can be made. At site RSA FRE4, all the samples from the first panel and three figures from the second are carbon-blacks with a fine-flaky texture, whereas two other figures from the second panel are carbon-blacks with a smooth texture. This distinction is found in others sites as RSA TYN2 or RSA LAB1 where interestingly the representation of a possible mushroom, on top of the other figures present the specific recipe with type 3 Raman spectrum and flaky texture, whereas the other carbon-blacks samples from this sites have got a smooth or fine-flaky texture. Moreover, figures made with carbon-blacks with a fine-flaky texture are found on top of the figures made with carbon-blacks with a smooth texture. It is here the confirmation of a change in the paint preparation through time (with sometimes the addition of clay to carbon-blacks with a smooth texture) even if no clue about the delay between the two recipes is available at this point. It can be interpreted as well, as the use of the shelter by different populations, painting with different recipes.

In the black paint layer, weddellite and whewellite were recorded in all samples. It is interesting to note that only whewellite was found in the weathering layers surrounding the paint ones. It may be due to the presence of a specific binder in the paint layer which

attracted bacteria or lichens which produce only weddellite. However, it is difficult to conclude at this step as no binder analysis was conducted. On the other hand, this difference in the presence of calcium oxalates between paint and weathering layers was recently reported in Hoerlé *et al.* (2016).

The weathering crusts surrounding the paint layer are of two types. The first one, found on top of the paint layer, is thin, about 5-10 µm thick, and composed of clay minerals and calcium oxalates. The second one, found underneath the paint layer, is thicker, about 50 to 150 µm thick, and made of calcium oxalates, calcium sulphates more or less hydrated, clay minerals, calcite, hydromagnesite and grains of quartz and feldspars. Interestingly, calcium sulphates are found as layers at the junction between the paint layer and the weathering layer underneath or as clusters at the top of the bottom weathering layer.

The black samples are all possible candidates for radiocarbon dating. However, contaminants as calcium oxalates, calcite and humic acids were recorded. Their proportion will be estimated to evaluate the amount of sample needed for radiocarbon dating (see Chapter IV).

### 3.1.3 White paints

These three white paint samples were collected next to black ones which may be suitable for radiocarbon dating. They are characterized to take into account the radiocarbon contaminants they may add to the black paints samples.

#### 3.1.3.1 Microscope

Only a fine-grained texture was observed on the three white paint samples (Figure 3.9). The white paint layer is yellow/orange at his top, maybe due to weathering process. Orange, red, black and transparent crystals are seen on top of the white paint layer, which are identified as weathering deposit.

Samples from RSA PRH1 show a bright white when the one from RSA LAB9 has got a yellowish hue.

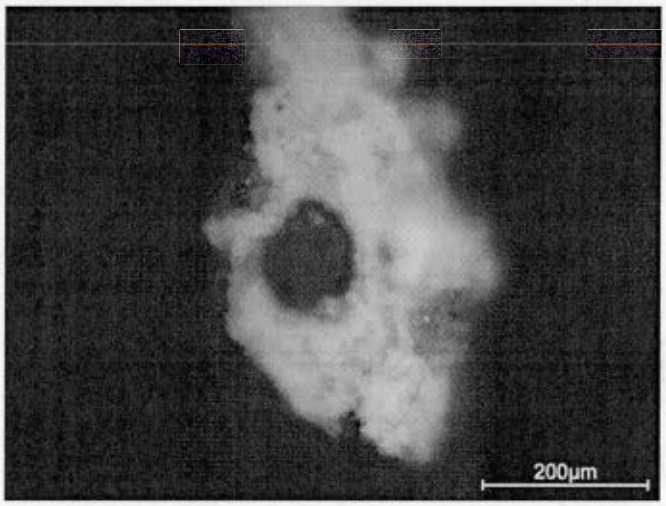


**Figure 3.9** Microscopic image of a white sample from Maclear District sites

All samples were mounted in cross-sections. They all exhibit a thick white layer, homogeneous in colour and between 100 and 200 µm thick (Figure 3.10). They are all fine-grained and a few brown grains are occasionally visible at the bottom of the layer.

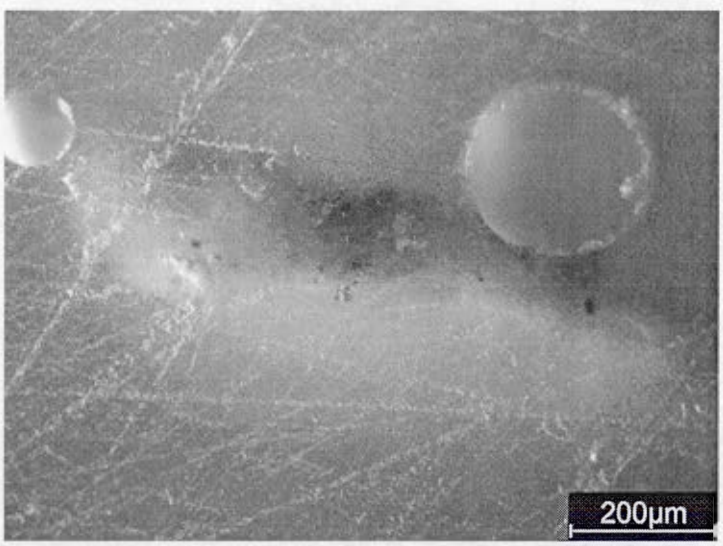


**Figure 3.10** Microscopic image of a white sample from Maclear District sites, in cross-section

3.1.3.2 SEM-EDS

Two textures were observed during SEM analysis: a fine flaky texture with flakes between 1 and 2 µm (1) and a flaky texture with flakes of various sizes from 1 to 5 µm (2). These two textures correspond to two different elemental compositions: the former being composed of sulphur and calcium, whereas the latter is composed of aluminium, silicon and potassium (Figure 3.11).

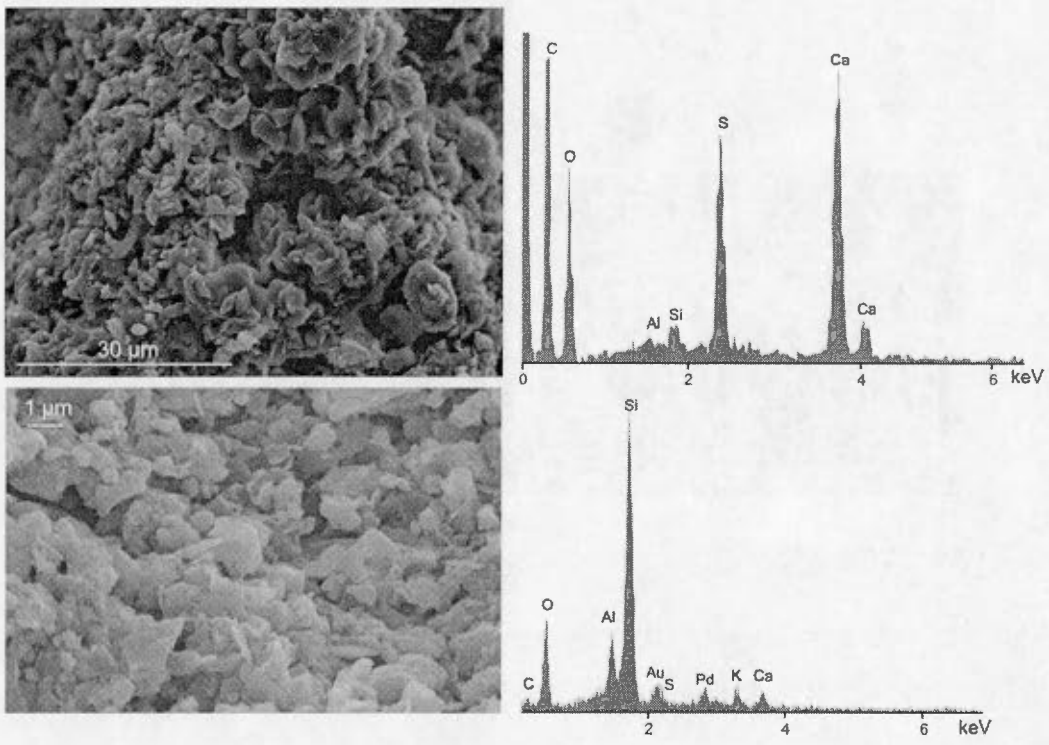


**Figure 3.11** Textures and EDS spectra recorded on white samples from Maclear District sites (Au, Pd, and C peaks are from coating)

Magnesium, sulphur and calcium may be attributed to weathering products, but they may be part of the pigment too. Raman and FTIR analysis will help the attribution.

In cross-section, the same elemental distinction was found between the sample from RSA LAB1 being composed of sulphur and calcium, whereas the two samples from RSA PRH1 are composed of aluminium, silicon, sodium and potassium.

In the case of the sample from RSA LAB1, the layer made of sulphur and calcium is found on top of a layer made only of calcium. Small grains of silicon and aluminium are found in the sulphur and calcium layer too (Figure 3.12).

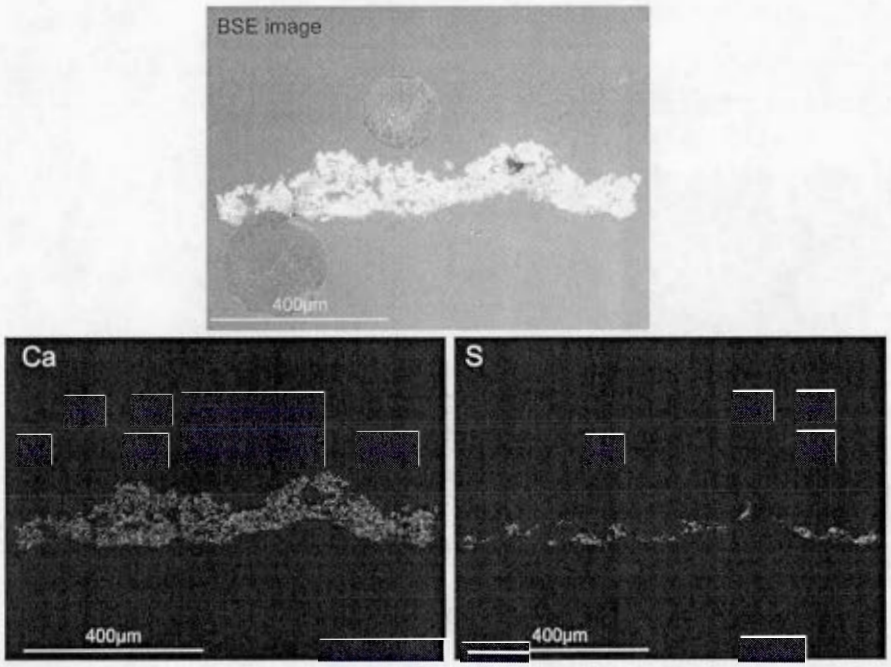


**Figure 3.12** Elemental maps recorded on sample LAB1-2012-9 in cross-section

The two samples from RSA PRH1 show clusters of calcium at their surfaces. They are attributed to weathering products, maybe calcium oxalates.

Minor elements recorded on all samples are magnesium, phosphorus, chlorine and iron. Sulphur is to be added for samples from RSA PRH1, and sodium for sample LAB1-2012-9. They are interpreted as weathering products.

3.1.3.3 Raman spectroscopy

Spectra recorded on the three samples showed two different series of peaks. LAB1-2012-9 contains both calcium oxalates and gypsum, whereas the RSA PRH1 samples exhibit only clay peaks (440, 463, 896, 1155, 1255, 1313, 1440, 1467, 1576, 1689, 1751, 1803, 1857cm$^{-1}$)

(Figure 3.13). These peaks can be correlated to kaolinite or montmorillonite (Košařová *et al.*, 2013). The two samples from RSA PRH1 were taken from the two tusks of the same elephant and show the same peaks confirming that the same paint was used for both of them.

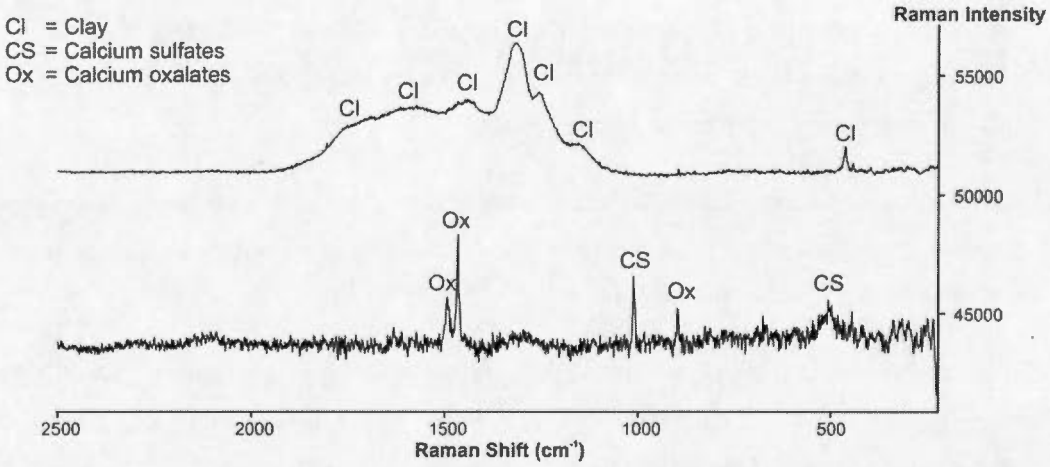


**Figure 3.13** Raman spectra recorded on white paints from Maclear District

Spectra recorded on samples mounted in cross-sections gave the same results as previously described on unprepared samples. Calcium oxalates were recorded on RSA PRH1 samples at the surface of the paints layers. The presence of epoxy resin peaks makes it difficult to observe all clay minerals peaks for samples from RSA PRH1, but they were the same as previously described.

3.1.3.4 FTIR spectroscopy

Spectra recorded on the three samples showed two different series of peaks (Figure 3.14). LAB1-2012-9 contains gypsum and calcium oxalates. A massif centred around 3300 $cm^{-1}$ comprised peaks linked to O-H bonds from water components of gypsum and calcium oxalates. Peaks at 1036 and 1165 $cm^{-1}$ are linked to Si-O bonds from quartz and/or feldspars. They may come from the rock.

The two other samples from RSA PRH1 show peaks of attributed to kaolinite. Peaks in the 700 to 1200 $cm^{-1}$ region are associated to Si-O and Al-O stretching modes, peaks in the 3400 to 3750 $cm^{-1}$ region are associated to OH stretching modes (Madejova and Komadel, 2001).

However, looking closer to the FTIR spectra, the 1000-1100 $cm^{-1}$ massif is larger than expected for pure kaolinite. Moreover, the quartz doublet at 779 and 799 $cm^{-1}$ is more intense too. These observations point to a mixture composed of kaolinite, quartz, K-feldspars and Na-feldspars. This kind of mixture is similar to the composition of natural white soils collected in Lesotho (see §3.2.6), indicating a natural and maybe local provenance of this clay. Peaks of clay are the same for both of the samples from RSA PRH1 which is to be expected as they come from the same representation.

Calcium oxalates were recorded on both samples too. Finally, a weak peak of calcium carbonates was observed. It is impossible to determine their origin (rock, pigment, weathering product) with FTIR analysis.

On all the three spectra, the peak at 1626 $cm^{-1}$ is larger than expected or show a peak at 1684 $cm^{-1}$ in the case of RSA LAB1 sample. This peak can be attributed to OH deformation of water, already recorded at the surface of the rock, and present in gypsum too.

Peaks at 2769, 2855, and 2929 $cm^{-1}$ were observed on all samples. They were detailed previously and are thought to be linked to methanol used to clean diamond micro-compression cells.

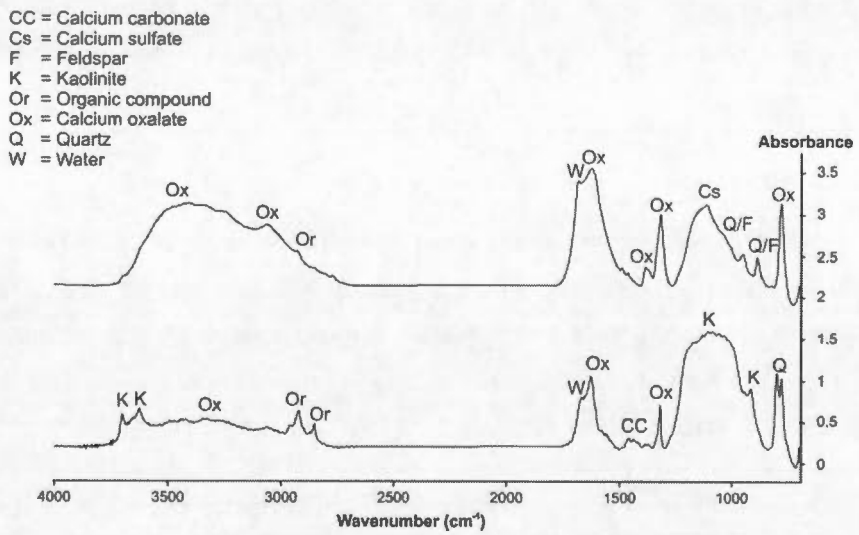


**Figure 3.14** FTIR spectra recorded on white paints from Maclear District sites

3.1.3.5 Conclusion

Results show that LAB1-2012-9 is composed of gypsum, whereas the two samples from RSA PRH1 are composed of clay, and more precisely kaolinite, maybe locally found. These two pigments do not contain carbon and thus cannot be used for radiocarbon dating and on the other hand, cannot influence radiocarbon dating on the adjacent black paint layer.

As previously recorded on black paints, calcium oxalates (only whewellite), calcium sulphates and calcium carbonates were recorded as weathering products in and underneath the paint layers.

3.1.4 Red paints

3.1.4.1 Microscope

Only a smooth texture was observed on both samples (Figure 3.15). On sample MEL9P3, little black paint with a fine-grained texture was recorded, maybe as a superposition of colour. The figure of an eland where it has been taken has got a homogeneous colour and thus it is possible that this superposition was intentional.

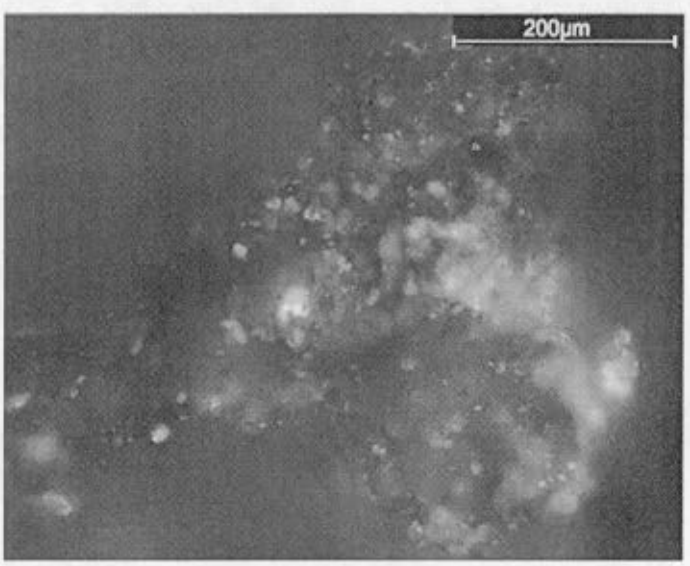


**Figure 3.15** Microscopic images of a red sample from Maclear District sites

At the junction between the rock and the red paint layer, an orange layer is present. It is a commonly found process of alteration of the red pigment, especially when composed of hematite. Indeed, using the water present is the rock or the support, hematite can turn into goethite and thus become orange (Cornell and Schwertmann, 2003).

Few white and transparent crystals were observed on top of the red layer. They are seen as weathering deposit.

All samples were mounted in cross-sections.

The two red layers have got a fine-grained texture but their colour is not homogeneous. Different shades can be observed from orange/red to dark red (Figure 3.16). They are from 100 to 200 µm thick.

An orange layer is found under the red layer of MEL9P3 interpreted as weathering products.

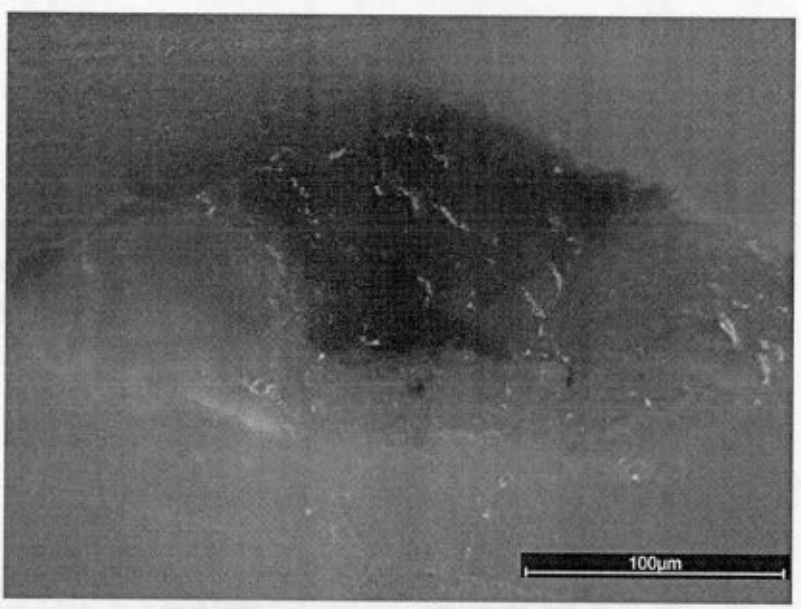


**Figure 3.16** Microscopic images of a red sample from Maclear District sites, in cross-section

3.1.4.2 SEM-EDS

The two samples present a fine-flaky texture under SEM observations. However, sample MEL6P2 is finer with flakes not larger than 0.5 µm and often much smaller, whereas MEL9P3 exhibits flakes about 0.5 to 1 µm diam. (Figure 3.17). Their difference is visible in their EDS spectra too as MEL9P3 shows the presence of manganese coupled with iron. Both of them are composed of iron oxides.

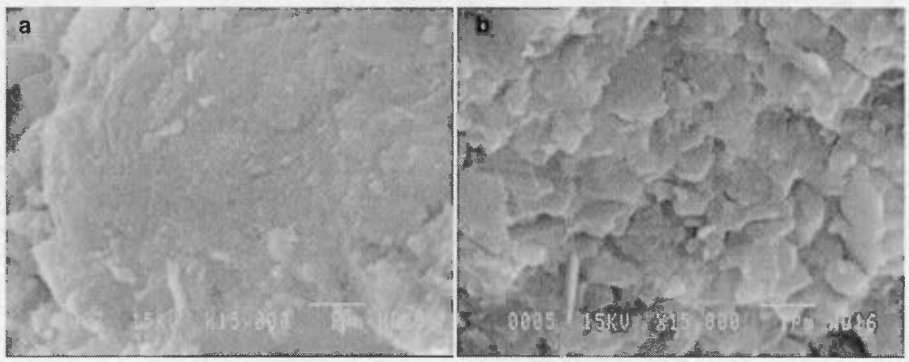


**Figure 3.17** SEM images of the texture of red samples from the Maclear District (secondary electrons): a) MEL6P2, b) MEL9P3

The presence of sodium, aluminium, silicon, and potassium can be linked to different parts of the sample: to the pigment as iron oxides are often used as "ochre" which are mainly clay (Eastaugh, 2008), to aerosol deposits on top of the sample (white and transparent grains observed under the microscope), to the rock support.

MEL6P2 shows few elements to be linked to weathering products: phosphorus and calcium; whereas MEL9P3 has a high proportion of sulphur linked to calcium and his EDS spectrum exhibits phosphorus and magnesium too.

In cross-sections, the red layers show different textures (Figure 3.18). MEL6P2 is composed of a silicon and aluminium matrix with grains of iron from 5 to 10 µm diameter. MEL9P3 shows coarser grains, from 10 to 50 µm diameter, composed of iron and manganese, in a silicon and aluminium matrix. In the matrix of both samples, titanium was recorded as minor element. In the surrounding weathering layers, calcium is the main component with silicon

and aluminium. Sulphur is found as clusters in these layers but always linked to calcium. Minor elements recorded for these weathering layers are sodium, magnesium, phosphorus, chlorine and potassium.

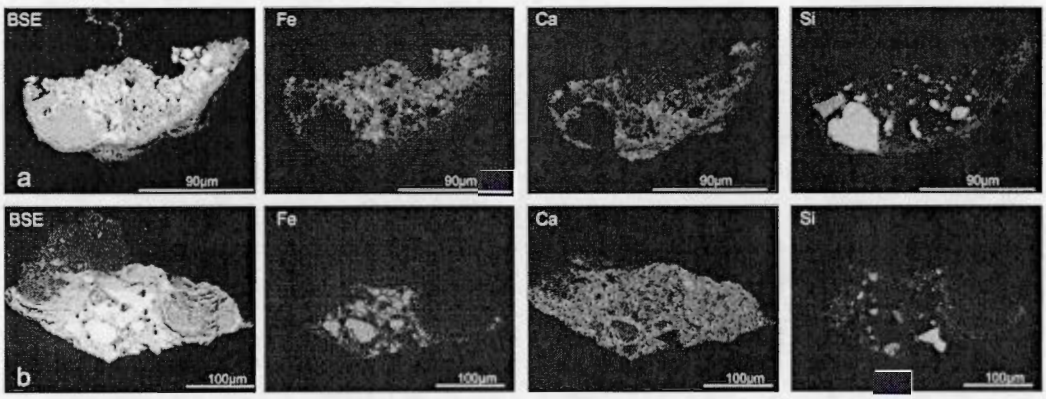


**Figure 3.18** Elemental maps recorded on red samples from Maclear sites: a) MEL6P2, b) MEL9P3

3.1.4.3 Raman spectroscopy

On unprepared samples, the two samples gave two different series of peaks. Firstly, MEL6P2 was found to be made of hematite type 2 (Figure 3.19). Peaks commonly assigned to hematite are 225 (Fe-O stretching), 247, 293, 412 (Fe-O bending), 498 (Fe-O stretching), and 613 $cm^{-1}$ (Fe-O bending) (de Faria and Lopes, 2007).

However, depending on samples, these peaks have different intensities. These served to categorize hematite in types:

- Type 1: Peak at 412 $cm^{-1}$ is the most intense.
- Type 2: Peak at 293 $cm^{-1}$ is the most intense.
- Type 3: Peak at 225$cm^{-1}$ is the most intense.

MEL6P2 exhibits more peaks than the ones commonly attributed to hematite. Peaks at 1251 and 1336 $cm^{-1}$ are linked to the presence of amorphous Si-O bonds, attributed to clay minerals. Peak at 665$cm^{-1}$ can be attributed to both manganese bonds present in the structure of hematite, to Fe-O symmetric stretching commonly found in magnetite, or the decrease in

the crystallinity of the sample, sometimes attributed to the heating process of hematite, even if it can be introduced by grinding or weathering too (de Faria and Lopes, 2007).

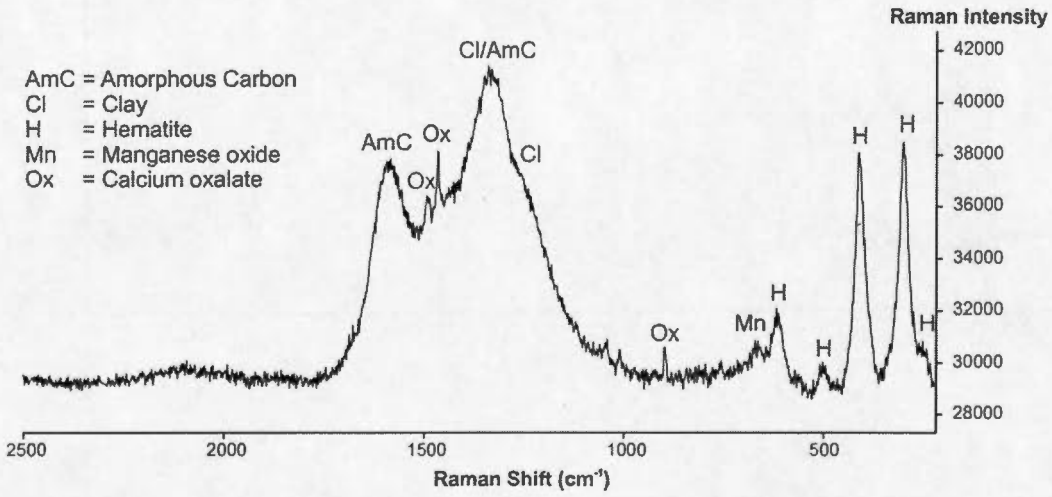


**Figure 3.19** Raman spectrum recorded on MEL6P2

MEL9P3 shows peaks at 503, 596 and 633 $cm^{-1}$ (Figure 3.20). They are attributed to iron and manganese oxides (more precisely respectively to Fe-O bonds for the first, and to Mn-O bonds for the two others), but it is impossible to give a final mineralogical determination. It may be a natural mixture of manganese and iron oxides found in soils. The presence of peaks of clay supports this hypothesis.

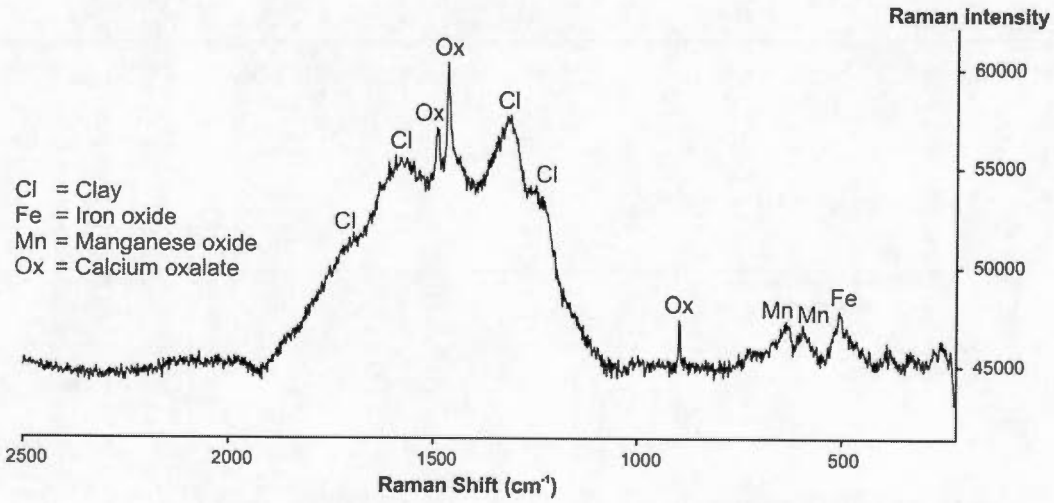


**Figure 3.20** Raman spectrum recorded on MEL9P3

Calcium oxalates (whewellite) and calcium sulphates more or less hydrated were recorded on both samples.

Analysis conducted on cross-section confirms previous peaks recorded on the two samples. Calcium oxalates were observed in the paint layer and in the weathering ones surrounding it. However, calcium sulphates are located only in the weathering layers.

3.1.4.4 FTIR spectroscopy

Spectra recorded on the two samples show almost the same peaks. They are composed of calcium oxalates, calcium sulphates, and clay (Figure 3.21). Calcium oxalates and calcium sulphates are weathering products, whereas the clay is a natural component of the pigment. Indeed, as recorded in previous analyses and defined in chapter II, the red pigments are made of red ochre, which is composed of clay minerals and iron oxides. The clay mineral can be either natural compound of the red pigment, or intentionally added by the artists.

A closer look at the 1620 $cm^{-1}$ calcium oxalate peak shows that it is larger than expected. This enlargement can be attributed to OH deformation of water, already recorded at the surface of the rock.

Peaks at 2769, 2855, and 2929 $cm^{-1}$ were observed on both samples. They were detailed previously and are thought to be linked to methanol used to clean diamond micro-compression cells.

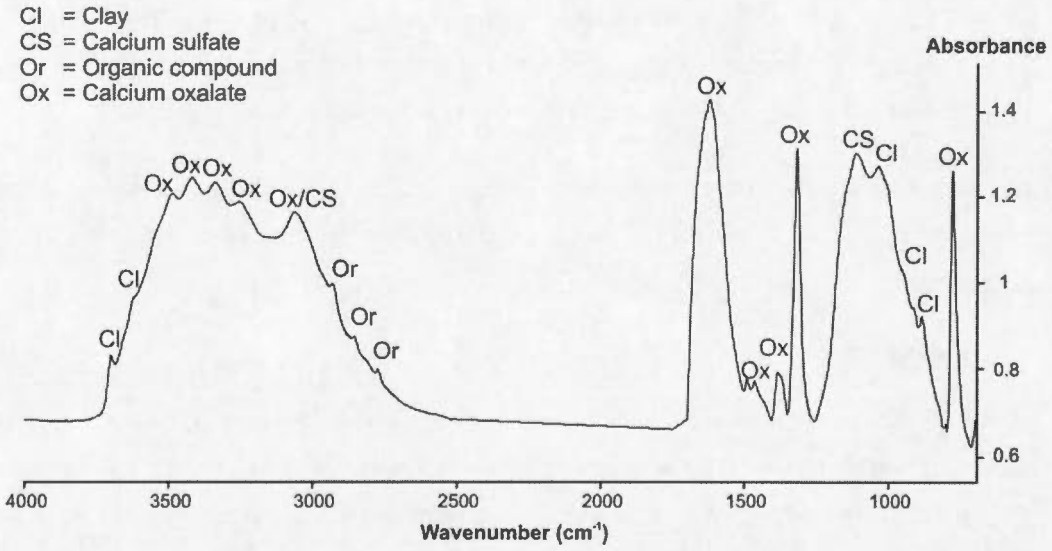


**Figure 3.21** FTIR spectrum recorded on a red sample from Maclear sites

3.1.4.5 Conclusion

The two red paints analysed here were first collected as they appear to be black on-site. One is composed of hematite, whereas the second is composed of iron and manganese oxides. They are both comprised in a clay matrix. MEL6P2 is composed of iron oxides grains from 5 to 10 µm diameter, and which seems to be homogeneously distributed in the clay matrix. MEL9P3, at the opposite, is composed of fine and large grains, from 10 to 50 µm diameter, mostly concentrated in mounds in the clay matrix. The first sample looks like a processed paint which may have been grinded and/or settled, whereas the other appears as a raw material or as a coarse artificial mixture.

Calcium oxalates and calcium sulphates were identified as weathering products in and surrounding the red paint layer.

### 3.1.5 Weathering products and alterations

#### 3.1.5.1 Microscope

Microscopic observations reveal that two layers of weathering products are present. One on top of the paint layer is composed either of scattered yellow, orange, white, transparent and red grains which are interpreted as aerosol particles, or a thin crust, about 5-10 μm thick with a fine texture and a white to orange colour. This layer is not found on each sample.

The second layer is found underneath the paint layer. It is similar in texture and colour to the layer observed on top of the rock support, and is doubtless the same layer. It is from 50 to 150 μm thick.

#### 3.1.5.2 SEM-EDS

SEM-EDS analysis shows that calcium was present in each paint sample studied. It is associated with minor elements in the paint layer such as magnesium, sulphur, chlorine and phosphorus. Their proportion is very weak in the paint layer. They are mostly identified in the surrounding weathering crusts.

Elemental mapping was very useful at determining the elemental compositions of the weathering layers as well as finding weathering layers which were not observed by microscope (Figure 3.22). Indeed, elemental maps of silicon and aluminium show that these elements were present with calcium as a thin layer, about 5 to 10 μm thick, on top of the paint layer. The second layer underneath the paint layer proves to be composed mainly of calcium, silicon and aluminium. Sulphur appears as clusters in this layer or as a proper layer, coupled with calcium, making a junction between the paint layer and the weathering layer. It is about 20-30 μm thick. Minor elements recorded are sodium, magnesium, chlorine, phosphorus, potassium and iron, as previously found in the weathering crust on top of the rock.

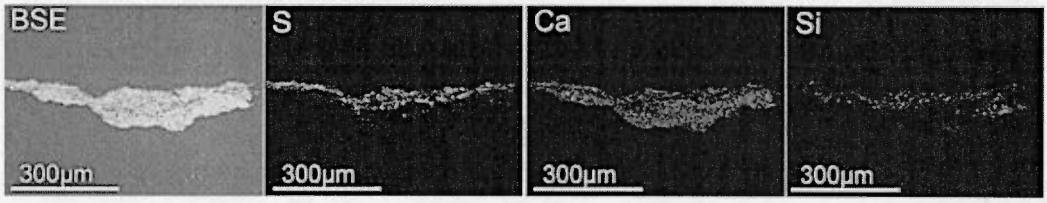


**Figure 3.22** Elemental maps recorded on cross-section, revealing weathering crusts layers

3.1.5.3 Raman spectroscopy

In the paint layers, calcium oxalates under the forms of whewellite and weddellite were observed. Only whewellite was recorded in the weathering layers.

Calcium sulphates more or less hydrated were found with calcite, clay and hydromagnesite in the weathering crust underneath the paint layer (Figure 3.23).

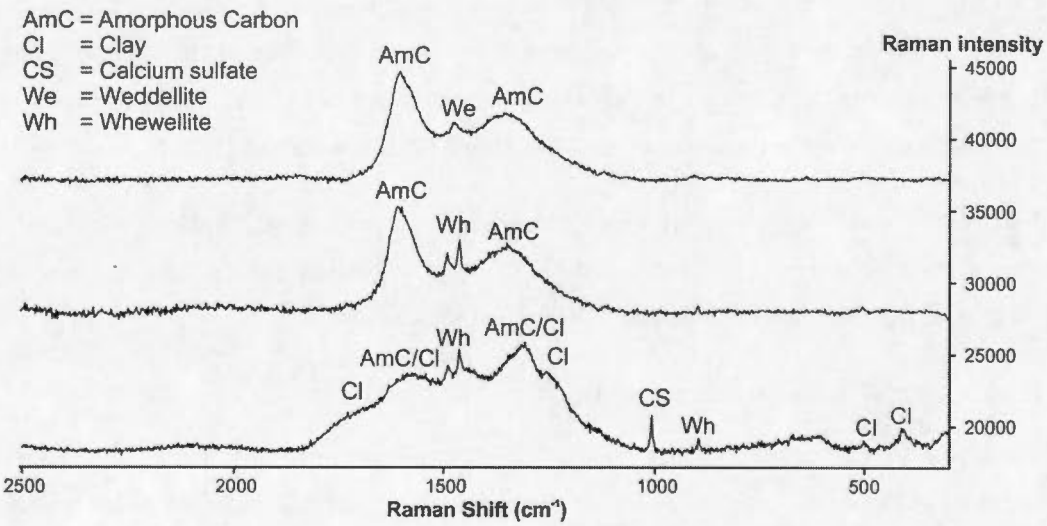


**Figure 3.23** Raman spectra of weathering products recorded on paintings from Maclear District sites

#### 3.1.5.4 FTIR spectroscopy

Calcium oxalates, calcium sulphates, and calcite were recorded on samples from Maclear sites. Humic acids were observed only on black samples from site RSA BUX1.

#### 3.1.5.5 Conclusion

The main weathering product observed on each sample whatever their colour is calcium oxalate. Interestingly, both whewellite and weddellite are present in the black paint layer, whereas only whewellite is present in the surrounding weathering layers. It has been previously reported by Hoerlé *et al.* (2016) and may be due to the presence of specific binders in the paint. This observation was made only on black paints, which point to the use of a specific binder. However, Hoerlé *et al.* (2016) reported this distinction for each colour studied (white and red). Thus it is possible that this observation only on black paints is a bias in the samples studied.

Calcium sulphates more or less hydrated were found as clusters in the weathering layer or as a layer at the junction between the sample and the weathering layer. It may be a reaction between the calcium contained in this weathering layer and acidic rain. This reaction was found to make cracks in the paint layers at site RSA TYN2 (Bonneau *et al.*, 2012).

Finally, the weathering crusts are composed of calcite, hydromagnesite and clay minerals. SEM-EDS analysis recorded chlorine and phosphorus too but their exact mineralogy was not identified. They are thought to be under the form of ions or salts.

### 3.1.6 General discussion and conclusion

Black paints analysed were found to be made of carbon-based pigments, and more precisely of carbon-blacks and charcoal. Their morphology under SEM shows that at least three different kinds of carbon-blacks, linked to the organic compound burnt, were used. Moreover, an intentional admixture with clay was found in at least two samples at RSA LAB1.

Carbon-blacks and charcoal were previously reported in South African sites (Bonneau *et al.*, 2012; Prinsloo *et al.*, 2008; Tournié *et al.*, 2011). Mapote, the old man who visited Marion

How (see chapter I) used charcoal to make black paint and Rudner (1982, 1983) mentioned the possibility of the use of such pigment in San paintings as it was used for body paintings. Furthermore, it is the first time that an intentional mixture with clay is reported. It results in a greyish colour. This intentional admixture proves that San processed their pigments to make the hues desired.

White paintings are composed of gypsum for one sample and kaolinite for the two others. Gypsum has been previously identified in previous studies (Prinsloo *et al.*, 2008; Tournié *et al.*, 2011), whereas clay have been only suggested by testimonies (Mapote) and by Rudner (1982, 1983). The composition of the clay used at RSA PRH1 is similar to white soils collected in Lesotho, in the immediate vicinity of sites in the Phuthiatsana valley. It is impossible to correlate the pigment to a specific source of clay; however, the white soils collected, according to results presented in §3.2.3, are doubtless degradation of the Clarens Formation sandstone. As Maclear sites were made on Clarens Formation sandstone too, the white clays available in the vicinity of the Maclear sites should have the same composition. Thus the kaolinite used to make this paint may be locally found.

Dark red paints, which were black on sites, are composed of hematite mixed with clay for one sample and of iron and manganese oxides mixed with clay for the other one. If the first type of pigment has been previously reported for San paintings (Hughes and Solomon, 2000; Prinsloo *et al.*, 2008; Tournié *et al.*, 2011), the second one was for the first time observed, even if manganese oxides were thought to be used by San artists (Rudner, 1982, 1983). Interestingly, the hematite-based paint is fine-grained and seems to have been composed of ochres, processed by grinding and maybe separation by settling, whereas the other one is coarser and may result of an intentional mixture of mineral grains and clay.

Weathering products identified in this study were previously largely reported for San paintings (Arocena *et al.*, 2008; Bonneau *et al.*, 2012; Hoerlé, 2005; Hughes et Solomon, 2000; Mazel and Watchman, 1997; Prinsloo *et al.*, 2008; Tournié *et al.*, 2011). Humic acids were however observed for the first time. They were found only on one site, RSA BUX1, in charcoal and carbon-black paintings. This site is the only one on the Elliot formation sandstone. It is at a lower elevation than the other sites which would be enough to permit the

development of other bacteria or lichens (Chen *et al.*, 2000). Moreover, humic acids are common degradation for charcoal (Trompowsky *et al.*, 2005).

Using these results, it is possible to propose some steps of the *chaîne opératoire* of these sites. First, the rock does not seem to have been prepared but the thick white weathering crust at its surface may act as a preparation layer, and artists may had searched for such crust. Then, raw material are acquired and prepared. In the case of black paints, charcoal may have been found after wild fires or manufactured; carbon-blacks should have been made from at least three different organic compounds, not identified. At RSA LAB1 (and maybe at RSA TYN2), carbon-black was mixed with clay. This addition can help the adhesion of the paint to the rock (Garate *et al.*, 2004; Menu *et al.*, 1993), but gives a grey hue to the paint too. In the case of white paints, kaolinite may have been found locally and processed by grinding and cleaning, whereas the source of gypsum is more difficult to deduce. In Lesotho, it crystallizes at the surface of Clarens Formation sandstone and forms large and thick concretions (Figure 3.24). It is possible that the same occurs in the Maclear district and was used as pigments. On the other hand, gypsum is present almost everywhere in the main Karoo basin (Johnson *et al.*, 2006). The red paints seem to be a mixture between pure hematite (or iron and manganese oxides) and clay but they may have been found as ochre too.

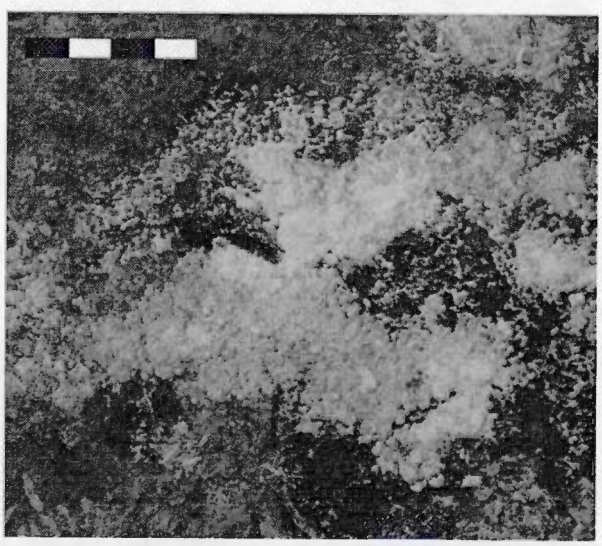

**Figure 3.24** Gypsum found at the surface of Clarens Formation sandstone in Lesotho

Paintings are then mixed with a liquid binder and applied with a brush or another similar tool which makes it possible to paint fine lines and details. Black paint is the last colour to be applied. Once paint is created, weathering starts with rain, wind, bacteria and lichens leaving calcium oxalates in and surrounding the paint layer.

Are those paintings suitable for radiocarbon or OSL dating? The presence of carbon-based samples points to the use of radiocarbon dating on them, even the presence of humic acids, calcium oxalates and calcium carbonates. However, a sample composed of charcoal is going to give only a maximum age for the paint whereas the carbon-black paints will reflect the age of the paint.

The two dark-red paintings are thick, 100 to 200 µm, and their dark colour may protect the rock from daylight. However, it was not possible to collect samples from them as it would require too large samples at this stage of the project.

## 3.2 The Phuthiatsana Valley, Lesotho

In the Phuthiatsana Valley, 178 paint samples were collected. 18 were black paint samples, 11 orange paint samples, 48 white paint samples, 3 pink paint samples and 98 red/dark red paint samples. Out of these samples, all the black and white paint samples were characterized with 29 red/dark red paint samples. These red samples were the first collected in the region in 2011.

In complements of these paint samples, 8 white soils and 8 red soils were collected for comparison and preparation of artificial paintings for OSL tests. They were all characterized following the same protocol as for the paint samples, without preparation of cross-section.

### 3.2.1 Rock and surface preparation

As it was the case for paintings in the Maclear district, in the Phuthiatsana Valley, paintings are found on the Clarens Formation sandstone, composed of quartz and feldspars in a calcitic/chloric matrix (Eriksson, 1979; Tournié *et al.*, 2011). Commonly occurring alterations at the surface of this rock are calcium sulphates and clay (Johnson *et al.*, 2006; Tournié *et al.*, 2011).

Characterization of the rock support from one site and from samples of paint collected as detached flakes of rocks confirms these characteristics. A white layer is found at the surface of the rock at almost all sites studied in the Phuthiatsana Valley. It is composed of calcium sulphates, clay and calcium oxalates. Eolian deposits under the form of quartz and feldspars (about 10-20 µm diam.) were observed too.

Underneath this layer, a highly crystallised layer of rock (about 100 µm thick) with no matrix is observed. It has been previously reported by Bonneau *et al.* (2012) and Hoerlé *et al.* (2016).

The rock itself is composed of quartz, microcline, albite and anorthoclase, in a matrix composed of calcium and chlorine. Quartz is about 50% of grains composing the rock. In the other 50% composed mainly of feldspars, 1/3 is microcline and anorthoclase and 2/3 is albite. The grain size is between 50 and 200 µm diam. with the majority about 100 µm diam.

No preparation of the rock surface is visible. However, all the paintings were realized on the white weathering crust visible at the surface of the rock and which may act as a preparation layer for the artists.

### 3.2.2 Black paints

#### 3.2.2.1 Microscope

Samples were first observed unprepared under the microscope with a magnification of between x100 and x500. Four textures were observed: coarse-grained texture (2), smooth texture (3), fine-flaky texture (2), which consists of small flakes rather than crystals, and fine-grained texture (11). The coarse-grained texture was recorded on human figures at ARAL 171 and ARAL 252. The smooth texture was observed on both human and animal figures at ARAL 172, ARAL 175 and ARAL 252. The fine-flaky texture was recorded only on horses, at ARAL 254. The fine-grained texture was found on horses, human and animal figures at ARAL 166, ARAL 175, ARAL 249 and ARAL 252.

Orange, yellow, red, white and transparent crystals were observed on top of the black paint and sometimes a white to yellow layer which can be seen as weathering deposits and layers.

On top of sample ARAL166-2012-2, small black crystals with a round shape were observed on top of the weathering crust. They may be interpreted as soot deposited by fire. If it is the case, this sample could not be dated as this soot is not different in composition from charcoal or carbon-blacks and thus may influence the date obtained.

16 samples out of 18 were mounted in cross-sections.

In cross-section, black layers show two different textures: one made of fine grains (14) and one other made of coarse grains (2) (Figure 3.25). The paint layers are from 20 to 300 µm thick. 11 samples exhibit a paint layer 50 µm thick or less, and in most of the cases this layer presents grains which are very sparse. Their colour is homogenous except ARAL171C1 which is a mixture of black, orange and yellow grains.

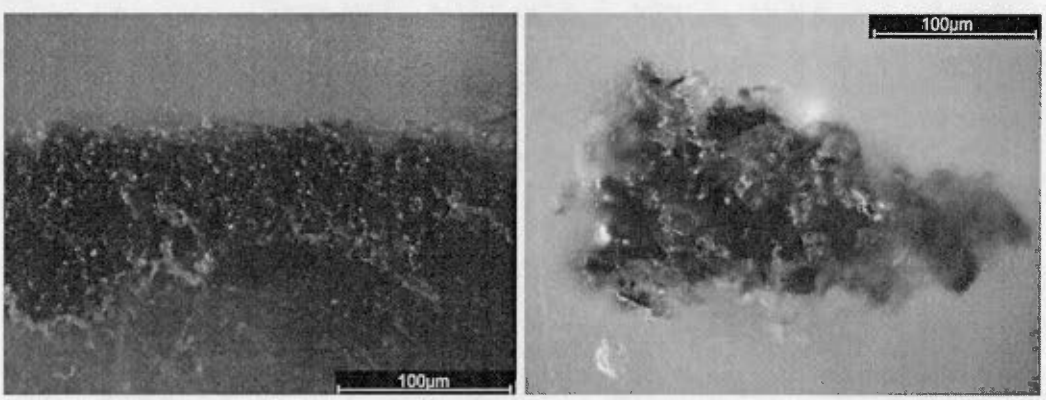


**Figure 3.25** Textures observed on cross-sections on samples from the Phuthiatsana Valley: left) fine-grained texture, right) coarse-grained texture

On top of the black layer, a transparent layer has been observed on 4 samples. Sometimes, orange and yellow grains are present in this layer. It is between 10 and 30 µm thick and is seen as a weathering crust.

Under the black layer of paint, a transparent, yellow, white or orange layer is often observed and is seen as a weathering crust. The colour of this layer is constant within the same panel but its thickness is highly variable, from 20 to 200 µm. Underneath the paint layer, rock is sometimes observed with large transparent grains (about 100 to 200 µm) in a white matrix.

At ARAL 175, three samples, from the same panel, were found of having the black paint layer directly on top of the rock. It may be a place where no weathering crust was on top of the rock face, or the artists prepared the surface to remove it.

3.2.2.2 SEM-EDS

Five different textures were recorded during SEM observations: the morphology of charcoal (5), a smooth texture (5), a fine-flaky texture (2), a flaky texture (2), and a texture composed of small balls and flakes (4) (Figure 3.26).

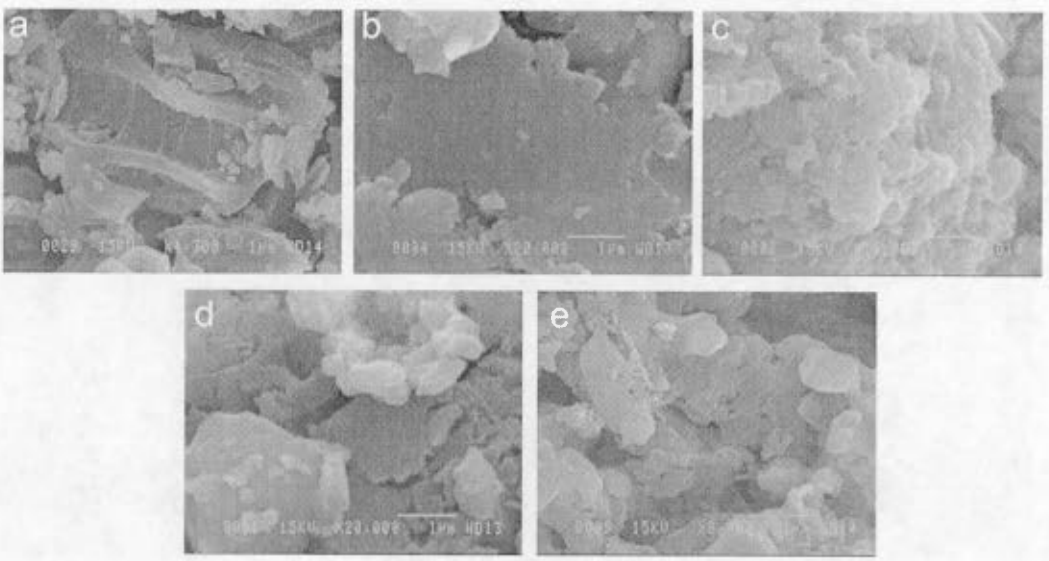


**Figure 3.26** Textures recorded on black samples from the Phuthiatsana Valley (secondary electron images): a) charcoal, b) smooth texture, c) fine-flaky texture, d) flaky texture, e) small balls and flakes

The category with a smooth texture is not homogeneous. For one of them, it is impossible to see the shape of the particles composing it. It looks like a film on top of the grains of the rock. On the other hand, the smooth layer crumbles into flakes of about 5 µm large, for two samples, and small flakes of about 1-2 µm large, for two others.

The texture composed of small balls and flakes of about 0.5-1 µm diam. is similar to the shape of the soot particles recorded on a reference sample and as shown in Tomasini *et al.* (2012).

Carbon was recorded as the main chemical element composing the black layer. It is found with sulphur and calcium in all the samples. However, it is interesting to note that for samples made of charcoal, the proportion of both of these elements are very low. These figures are mostly attributed to Basotho and this difference may be due to the time elapsed between the paint realization and the analysis. Other elements, magnesium, phosphorus and chlorine, were recorded and attributed to weathering products as sulphur and calcium.

Sodium, aluminium, silicon, potassium, iron, and titanium were recorded on the samples and are attributed to the rock support or to aerosol particles.

Analysis in cross-sections made it possible to see the repartition of the chemical elements between the different layers: paint, weathering crusts, and rock support (Figure 3.27).

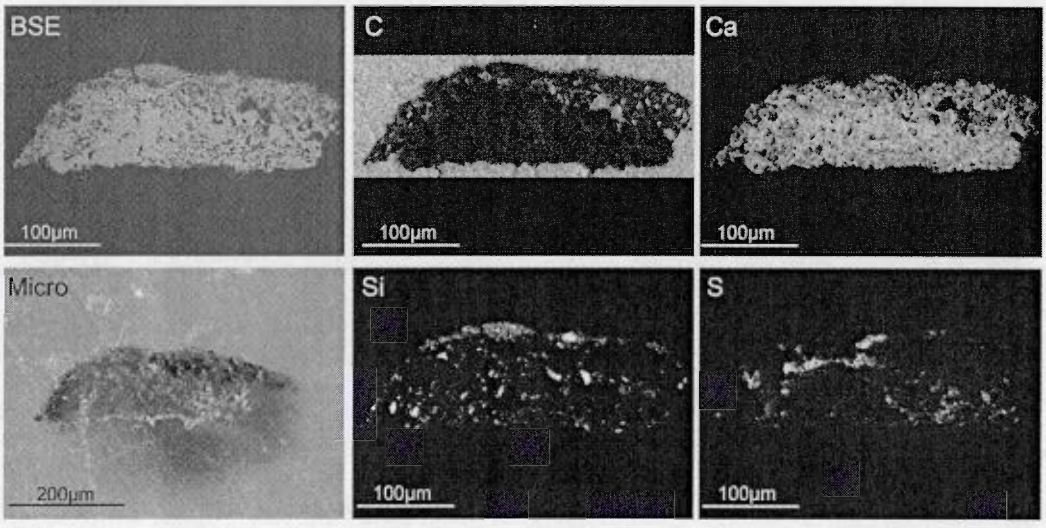


**Figure 3.27** Elemental maps recorded on a black sample mounted in cross-section from the Phuthiatsana Valley

It confirms that carbon is the main chemical element composing the black paint layer, with a high proportion of calcium inside, except samples previously identified as charcoal and attributed to the Basotho paint tradition. Phosphorus and chlorine were recorded too as minor elements in the black layer and are considered as weathering products. Silicon and aluminium were recorded in the black layer in 4 samples, with minor elements as sodium, potassium, and/or iron. They are under the form of grains from 10 to 50 µm diameter (2) or as a kind of matrix (2). They may be intentional addition made by the artists to give a better texture to the paint. For one sample, Aral171C1, large grains were observed in the paint layer during microscope observations.

A weathering crust composed of silicon and aluminium (with minor elements as sodium, potassium and iron) has been observed on top of the black layer in three samples. Whereas, a weathering crust composed of calcium with silicon and magnesium as minor elements was recorded on top of the black layer in one sample.

A weathering crust is visible under all the black paint layers studied. It is mainly composed of calcium along with silicon and aluminium. Sulphur is present as minor element and is concentrated at the top of this layer, right under the black paint. Magnesium, phosphorus, chlorine, sodium, potassium, iron and titanium were also recorded in this layer as minor elements.

Under this weathering crust, a layer of rock made of grains of silicon and of grains of silicon, aluminium, potassium or sodium is observed with a matrix of calcium, sulphur and sometimes silicon and aluminium. These observations are in agreement with the ones done on the pieces of rock support.

#### 3.2.2.3 Raman spectroscopy

Samples were analysed with both green (514 nm) and near-infrared (785 nm) lasers. Peaks of carbonaceous matter composed of amorphous and crystallized carbon were recorded on all samples with both lasers. Spectra were categorized as detailed previously in §3.1.2.3.

With the green laser, all samples show type 1 spectra, whereas with near-IR laser, all samples show type 3 spectra, except ARAL252C4, which exhibits a type 2 spectrum. This difference

in the shape of spectra is due to the type of excitation used and thus to the type of bonds excited. Indeed, C-C bonds depending on their degrees of order and the impurities surrounding them will react to different excitation wavelengths (Stuart, 2007).

With the green laser, calcium oxalates (whewellite and weddellite) were recorded on samples ARAL166-2012-2, ARAL166-2012-3, ARAL172C1, ARAL175-2012-1, ARAL175-2012-3, ARAL175-2012-12. Calcium sulphates more or less hydrated were found on samples ARAL166-2012-2, ARAL166-2012-3, ARAL175C2, ARAL175-2012-3, ARAL249-2012-1, ARAL252C1, ARAL252C2, and ARAL252C4. Along with calcium oxalates, they are seen as weathering products. Finally, calcite and quartz are present respectively in samples ARAL175C2 and ARAL175-2012-12, and are attributed to the rock support.

With the near-IR laser, whewellite was recorded on samples ARAL166-2012-3 and ARAL172C1, and calcium sulphates more or less hydrated on samples ARAL166-2012-2, ARAL166-2012-3, ARAL172C1, ARAL175C2, ARAL249-2012-1, and ARAL252C4. Calcite was observed on ARAL175-2012-1 and, quartz on ARAL175C2. In sample ARAL252C1, hematite (type 2[4]) was recorded from the red paint layer present under the black paint.

In cross-section, laser 514 nm and 785 nm were used too. With the green laser (Figure 3.28), amorphous carbon type 1 was recorded on all samples except for three of them where no amorphous carbon spectrum was obtained (Aral166-2012-3, Aral175-2012-11, and Aral175-2012-12). In the black layer, weddellite was recorded; whereas in the surrounding layers and in the paint layer, whewellite is observed. Calcium sulphates more or less hydrated and calcite were identified in the surrounding layers too. Feldspars (458, 476, 512 $cm^{-1}$; and 469, 497 $cm^{-1}$) were recorded in the black layer for Aral252C2 and under the black layer in Aral166-2012-2. Feldspars have been identified in Aral252C2 during EDS mapping analysis too. For the latter, feldspars are from the rock support underneath the black layer.

With the near-IR laser (Figure 3.28), amorphous carbon type 3 has been recorded on all samples except for Aral166-2012-3 where clay peaks prevent for any identification of the

[4] For precision about the type of hematite, see § 3.1.4.3

type of amorphous carbon, and for Aral175-2012-12 which exhibits a type 2 amorphous carbon. However, in that last case, peaks of amorphous carbon were extremely weak which maybe introduce a bias in this identification. As with the green laser, weddellite was identified in the black layer, whereas whewellite is present in the surrounding layers and in the black paint layer. In these surrounding layers, calcium sulphates and calcite peaks appear occasionally. Clay was recorded only on sample Aral166-2012-3.

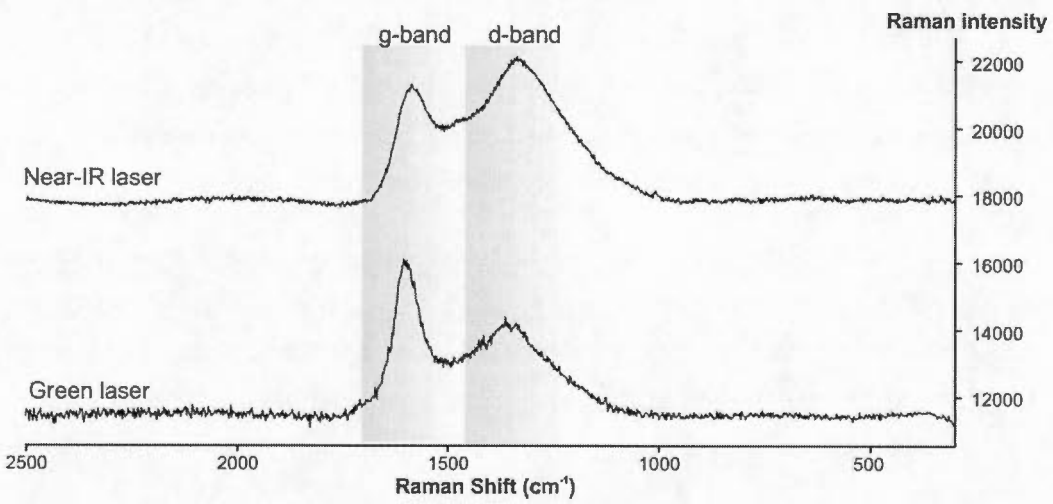


**Figure 3.28** Example of spectra recorded on black paints from the Phuthiatsana Valley (green and near-IR lasers)

D and g-bands of carbon were deconvoluted using Grams with the same parameters as mentioned in §3.1.2.3. Sample Aral166-2012-3 was not included as clay minerals peaks partially hide amorphous carbon peaks making the deconvolution impossible.

With laser 785 nm, the d-band varies from 1318 and 1341cm$^{-1}$ on unprepared samples and from 1319 to 1361 cm$^{-1}$ on cross-section. The g-band oscillates from 1565 to 1587 cm$^{-1}$ on unprepared samples, and from 1568 to 1587 cm$^{-1}$ on cross-section.

With laser 514 nm, the d-band varies from 1348 and 1372 cm$^{-1}$ on unprepared samples and from 1331 to 1373 cm$^{-1}$ on cross-section. The g-band oscillates from 1576 to 1602 cm$^{-1}$ on unprepared samples, and from 1590 to 1607 cm$^{-1}$ on cross-section.

These results show a high variation in the positions of the peaks in each category using the green laser. Interestingly, the variations between unprepared and cross-sections are little if compared in each sample. Variations with the 785 nm laser are smaller than with the 514 nm laser. It may be explained by the weakness of peaks recorded on most of the samples with the green laser, which introduces large errors in the deconvolution process. Furthermore, the two lasers do not excite the same chemical bonds. Moreover, humic acids were identified during FTIR analysis (see below) and they are more sensitive to green laser than near-IR one (Corrado *et al.*, 2008). Two of their peaks are at the same place as the peaks of amorphous carbon, 1315 and 1600 $cm^{-1}$, and may have influenced the deconvolution.

Compared to the morphology observed under the SEM, the small-ball texture makes a separate group (Figure 3.29), with both lasers. If compare to the study of carbonaceous matter by Coccato *et al.* (2015), the spectra recorded are attributed to charcoal and other flame carbons of different origins.

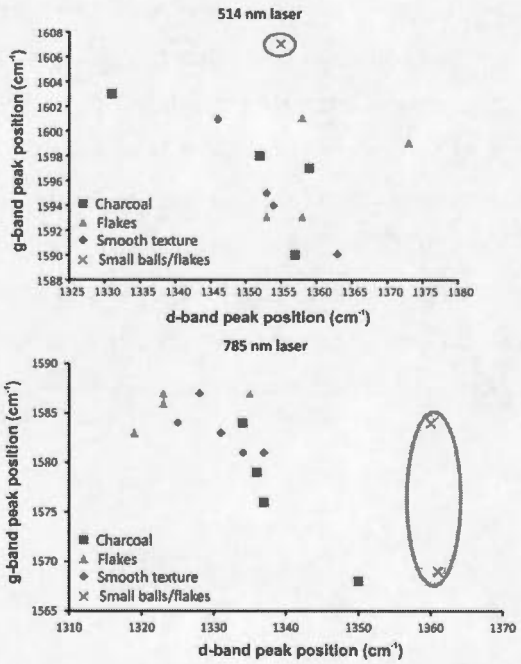


**Figure 3.29** D-band position against g-band position

3.2.2.4 FTIR spectroscopy

Three samples out of 18 were not analysed by FTIR because of the small quantity of sample available.

Calcium oxalates were observed on all the samples. They were in equal proportion as gypsum and quartz/feldspars except for two samples. Aral175-2012-11 presents very weak calcium oxalates peaks, less than 10% of the spectrum, whereas Aral252C2 shows a pre-eminence of calcium oxalates peaks (about 75%).

On all spectra recorded, the 1620 $cm^{-1}$ calcium oxalate peak is larger than expected. This is due the presence of peaks at 1630-1640 $cm^{-1}$, associated with OH deformation of water, already encountered at the surface of the rock and in soils collected in the vicinity of the sites.

On seven samples (Aral 166-2012-2, Aral 166-2012-3, Aral175-2012-1, Aral 175-2012-2, Aral 249-2012-1, Aral 254-2012-2, Aral 254-2012-3), the massif at 3000 $cm^{-1}$ is larger with a peak around 2600-2650 $cm^{-1}$ (Figure 3.30). This large massif has been previously reported on coal (Guo and Bustin, 1998) and humic acids studies (Baes and Bloom, 1989; Trompowsky *et al.*, 2005), attributing this peak and enlargement to the OH stretch of H-bonded –COOH of humic and fulvic acids. In our project, it is attributed to humic acids present in the samples. Moreover, it is interesting to note that all the samples presenting these characteristics were identified as charcoal, except Aral175-2012-1, Aral175-2012-2, and Aral249-2012-1. On the other hand, Aral171C1 which has been identified as charcoal, does not present these characteristics, maybe due to charcoal age and/or exposition to weather and bacteria. Indeed, humic acids are degradation of charcoal but are themselves sensitive to rain and bacteria which degrade them.

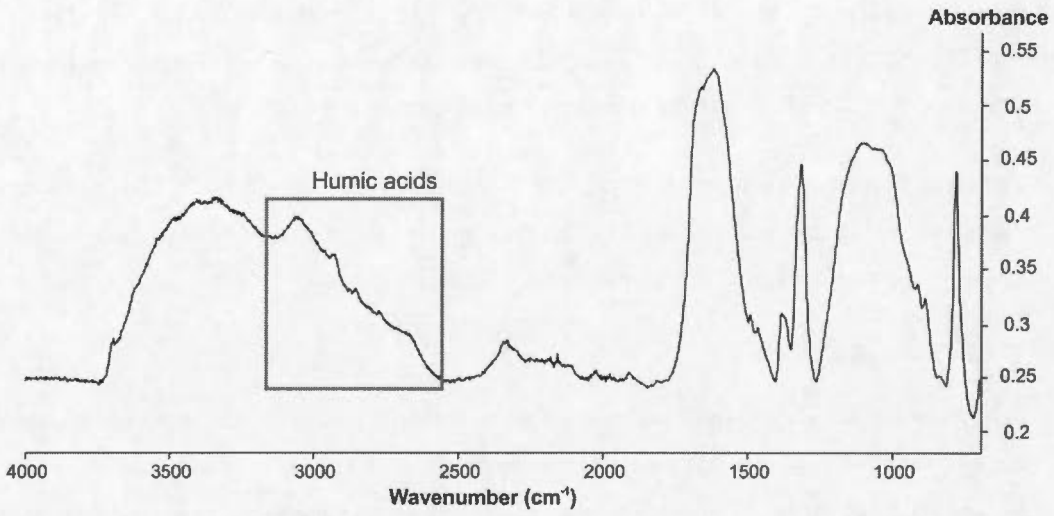


**Figure 3.30** FTIR spectrum of a black sample containing humic acids

On the opposite of previously mentioned samples, Aral175-2012-11 shows a weak massif at 3000 $cm^{-1}$, indicating a small proportion of water, and organic bond stretching modes in this sample. Indeed, it is dominated by peaks of albite (see below).

Calcium sulphates were observed in all samples except Aral175C1. Calcium sulphates are a common weathering product of Clarens Formation sandstone, and has been recorded in previous studies (e.g. Bonneau *et al.*, 2012; Hall *et al.*, 2007; Hoerlé, 2005; Prinsloo *et al.*, 2008; Tournié *et al.*, 2011).

Aral 166-2012-3 and Aral 175-2012-11 are composed of albite, feldspar composing Clarens Formation sandstones (Eriksson, 1979), and observed on SEM-EDS and Raman analysis of the rock (see appendix A). All the other spectra exhibit peaks at 913, 1005, 1039, 1151, 3692 $cm^{-1}$, but they were not all recorded on the same spectrum. It was not possible to give a final mineral attribution to these peaks but they are doubtless associated to Si-O, Al-O bonds and OH stretching modes from clayish minerals, quartz and/or feldspars. For four of the samples (Aral 172C1, Aral 175-2012-12, Aral 254-2012-2, Aral 254-2012-3), peaks can be attributed to clay and maybe more precisely to kaolinite (Madejova and Komadel, 2001). These minerals can come from the rock, such as kaolinite has been observed in degraded Clarens Formation sandstone (Johnson *et al.*, 2006), or may be intentional addition from the artists.

On all samples except five (Aral 166-2012-2, Aral 172C1, Aral 175C2, Aral 175-2012-1, Aral 175-2012-11), peaks at 2770, 2853, 2925, 2960 $cm^{-1}$ were observed. They are attributed to residues of methanol used to clean diamond micro-compression cells.

Calcium carbonates were found in two samples: Aral175C2 and Aral 254-2012-3. They can be seen as weathering products or as a contribution from the matrix of the rock. Indeed, Clarens Formation sandstone is composed of a calcitic matrix.

3.2.2.5 Conclusion

The eighteen black samples were all identified as carbon-based pigments. Five of them are charcoal, four are composed of soot and nine others are carbon-blacks. Within the carbon-black group, three different morphologies were observed under the SEM, revealing that three different recipes were used. Nevertheless, deconvolution of Raman peaks did not bring more information about the type of organic compounds burnt, but it confirms the identification as carbon blacks and charcoal pigments.

Carbon-blacks and charcoal were previously reported in other San rock art sites but soot is for the first time identified, even if its use was suggested by Rudner (1982).

A possible admixture with clay is observed on sample Aral166-2012-3 but it is possible that this clay comes from the surface of the rock support too. Another possible intentional admixture is found in Aral171C1 with large grains of quartz, feldspars and anatase found in the paint layer. As Aral166-2012-3, this paint is composed of charcoal.

Weddellite was found with whewellite in the paint layer whereas whewellite is alone in the surrounding weathering crusts. Other weathering products were identified as calcium sulphates more or less hydrated and calcium carbonates. On the other hand, magnesium, phosphorus and chlorine were recorded under SEM-EDS analysis but their exact molecular form was not found. They are thought to be under the form of ions or salt, or in the case of magnesium as hydromagnesite.

A thin weathering crust was found on top of the paint layer and is composed of clay minerals with occasionally calcium oxalates. It is similar to the weathering crust found at the surface

of the rock in Maclear and in Lesotho, and is interpreted as a natural weathering. Aerosol particles were found too as quartz and feldspars on top of the paint layer.

### 3.2.3 White paints

#### 3.2.3.1 Microscope

Two textures were observed: smooth texture (1), and fine-grained texture (47) (Figure 3.31). The smooth texture was found only on an eland, at site ARAL 169. The fine-grained texture was recorded on all the other samples.

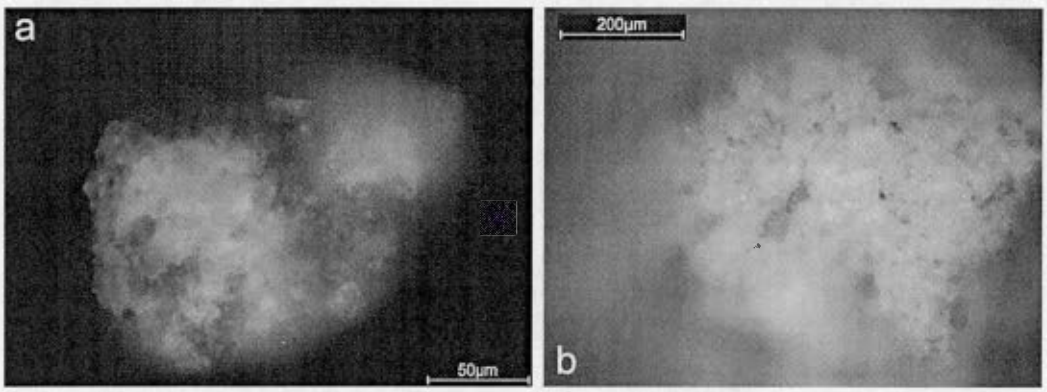


**Figure 3.31** Microscope images of white paints from the Phuthiatsana Valley: a) smooth texture, b) fine-grained texture

On top of the white layer, orange, red, black and transparent crystals were observed. They formed on some samples a yellow to orange layer, identified as a weathering crust.

The white layer has different hues from bright white to brownish white through yellowish white. It is possible that these hues are influenced by the weathering products around and in the paint layer.

In three cases, the white paint layer is on top of a red paint layer which is the colour used next to it. On the other hand, one case (ARAL 258-2012-5) seems different with a thin red layer underneath the white paint layer which gives a pinkish hue to the white paint. This superposition seems to have been made on purpose by the artist.

42 out of 48 samples were mounted in cross-sections.

Three different textures were observed: a coarse-grained texture (2), a smooth texture (1) and a fine-grained texture (39) (Figure 3.32). The white layer is mainly between 100 and 200 µm thick, even if the thickness scatters between 10-20 µm and 300 µm thick. The white layer is homogeneous in colour and few red or brown grains appear time to time at its surface.

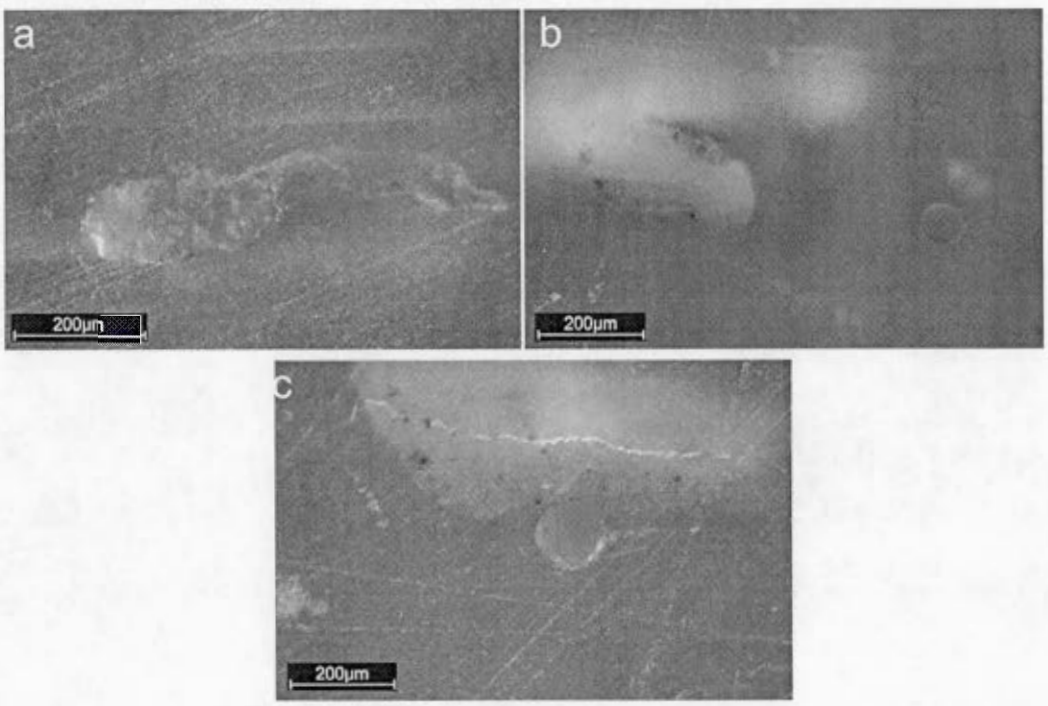


**Figure 3.32** Microscope images of white paints mounted in cross-sections from the Phuthiatsana Valley: a) coarse-grained texture, b) smooth texture, c) fine-grained texture

A white, yellow or orange layer is found on top of the white layer. It is about 10 to 50 µm thick and mostly fine-grained. It contains red, orange and transparent grains, about 2-5 µm in diameter. It is attributed to weathering products and aerosol particles.

Underneath the white paint layer, a white to yellow layer is observer. It is thicker than the one on top of the paint layer, about 50 to 200 µm thick. It contents red, orange and transparent grains, about 2-5 µm in diameter.

In three samples, a red paint layer was found underneath the paint layer and on top of the white weathering crust. They are from adjacent red paint except for ARAL 258-2012-5, which does not have a red colour close to the sample taken and which is interpreted as an intentional superposition by the artists to give a pink colour.

The rock is found directly underneath the paint layer for 7 samples, or under the weathering crust.

3.2.3.2 SEM-EDS

SEM observations show five different textures: a coarse-grained texture (3), a fine-grained texture (22), a smooth texture (10), a flaky texture (7), and a fine-flaky texture (6) (Figure 3.33).

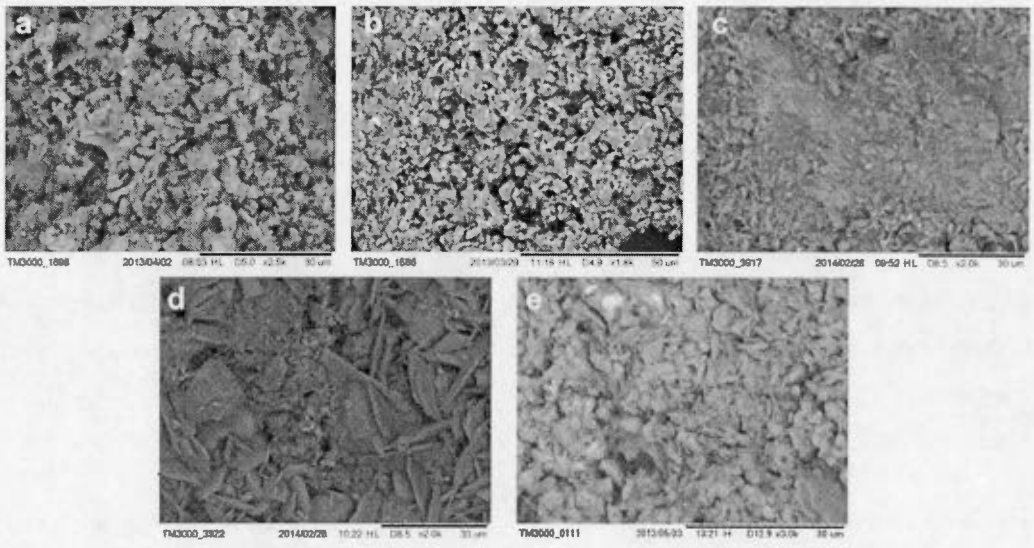


**Figure 3.33** SEM secondary electron images of the different textures observed on white paints from the Phuthiatsana Valley: a) coarse-grained texture, b) fine-grained texture, c) smooth texture, d) flaky texture, e) fine-flaky texture

The coarse-grained texture is composed of cubic grains about 10 µm for one sample, and of long grains (10-20 µm long) for another one. The last sample composing this group is the reference sample ARAL169-2012-RW1, which exhibits both long and cubic grains. Long

grains are composed of sulphur and calcium, whereas cubic grains contain only calcium in all samples.

The fine-grained texture is composed of grains from 1 to 5 μm. However, for ten of them, larger grains are present in the texture, with cubic or long shapes, and are about 10 μm. Five samples are composed of sulphur and calcium, two of sodium, aluminium, silicon, potassium, titanium and iron, whereas the other 14 samples are composed either of sulphur and calcium, or sodium, aluminium, silicon, potassium, titanium and iron. It is unclear which part is the pigment, and which part is the weathering product or the rock. Cross-sections will help to distinguish the layers. Finally, one sample, ARAL164-2012-1 shows peaks of phosphorus, fluorine, chlorine, and calcium. These elements may be correlated to bones. His texture is different of the others with a mixture of grains of different sizes.

The smooth texture is homogeneous for almost all samples. On two samples, the layer seems to crumble to small flakes, about 1-2 μm. The presence of small grains (1-2 μm) and long grains (5 μm) on top of the smooth textured layer was recorded on 5 samples. One sample is composed of calcium, two of sodium, aluminium and silicon, one of sodium, aluminium, silicon, potassium, titanium and iron, one of either calcium or sodium, aluminium, silicon, potassium, titanium and iron, and five of either sulphur and calcium or sodium, aluminium, silicon, potassium, titanium and iron. It is unclear which part is the pigment, and which part is the weathering product or the rock. Cross-sections will help to distinguish the layers. Two samples, ARAL175-2012-8 and ARAL175-2012-9 exhibit a high proportion of phosphorus which seems to be linked to sulphur and calcium.

The flaky texture is composed of flakes from 5 to 20 μm. On sample ARAl254I3, the texture is a mixture between small grains/balls, less than 1 μm in diameter, and long flakes about 10 μm long. The composition of samples being part of this type is very different, from calcium, to sulphur and calcium, through clay elements such as sodium, aluminium, silicon, titanium, etc. Two samples, ARAL175I2 and ARAL254I3, show a high proportion of phosphorus linked to calcium and sulphur in the case of the former, and only calcium for the latter.

The fine-flaky texture is composed of flakes from 1 to 5 μm. They are composed of calcium for two of them, sodium, aluminium, silicon, potassium, titanium and iron for two of them, of

sodium, aluminium, and silicon for one, and of either calcium, or sodium, aluminium, silicon, potassium, manganese, and iron for the last one. ARAL254I4 and ARAL254I13 exhibit a high proportion of phosphorus linked to calcium.

On three samples, ARAL 169-2012-7, ARAL175-2012-6 and ARAL180-2012-13, red paint was observed underneath or close to the white paint layer. Thus, iron, and in the case of ARAL 169-2012-7, titanium were recorded. This red layer is composed of small flakes, about 2 µm.

Magnesium, phosphorus, chlorine, sulphur and calcium were recorded on almost all the samples and are attributed to weathering products such as calcium oxalates, calcium sulphates, or hydromagnesite.

Sodium, aluminium, silicon, potassium, titanium, and iron can be attributed to both rock and clayish minerals. However, clayish minerals can be found on top and in the Clarens Formation sandstone (Johnson *et al.*, 2006). So it is here impossible to attribute these elements to one or another.

28 cross-sections out of 42 were analysed with SEM-EDS.

Observing textures, it was not possible to distinguish specific morphologies, except for some layers composed of sulphur and calcium which exhibits a flaky texture, as expected for a paint composed of gypsum.

Different elemental compositions were observed on paint layer:

- Sulphur and calcium were found in 5 samples.
- Silicon, aluminium and sodium and/or potassium were found in 16 samples.
- Calcium was found alone in 4 samples.
- Calcium and phosphorus were found in 4 samples.

One sample, Aral180-2012-13, is in the second composition group with a high proportion of iron. Under microscopic observations, it is yellow rather than white. It is possible that this sample is composed of iron oxides which make its yellow colour.

On top of the sample, a thin layer composed of either calcium and sulphur, or silicon and aluminium was recorded on some samples. It is a weathering layer.

Under the paint layer, a weathering layer was observed too. A thin layer of sulphur and calcium is occasionally recorded at the junction between the paint layer and this weathering crust. This layer comprises minor elements as magnesium, chlorine, and phosphorus which are attributed to weathering products. They were previously recorded at the surface of the rock face.

Finally, rock is found under the weathering layer and is composed of grains of silicon, and grains of silicon and aluminium, about 100 μm in diameter, in a matrix of calcium, silicon and aluminium with magnesium in some samples.

3.2.3.3 Raman spectroscopy

23 samples exhibit peaks of clay, 16 samples peaks of gypsum, 4 samples peaks of calcite, 4 samples peaks of apatite, and one sample peaks of goethite (Figure 3.34).

Samples with clay peaks show different series. Most of the time, clay is found as a broad peak composed of shoulders at 1152, 1256, 1320, 1574, 1745 $cm^{-1}$. However, hectorite was identified on samples from site Aral180, and kaolinite was recorded on sample Aral169-2012-9. This second set of peaks was observed on soils collected in the vicinity of the sites too.

Anatase and rutile were recorded in two samples composed of clay.

The sample where goethite has been recorded is Aral180-2012-13 which has been previously reported as having a yellow hue, rather than being white.

When apatite was recorded, it appears always with calcium sulphates.

Calcium oxalates as whewellite were recorded on all the samples. Other weathering products occur as calcium sulphates more or less hydrated, hydromagnesite, barite, or potassium nitrates/hydrated calcium nitrates.

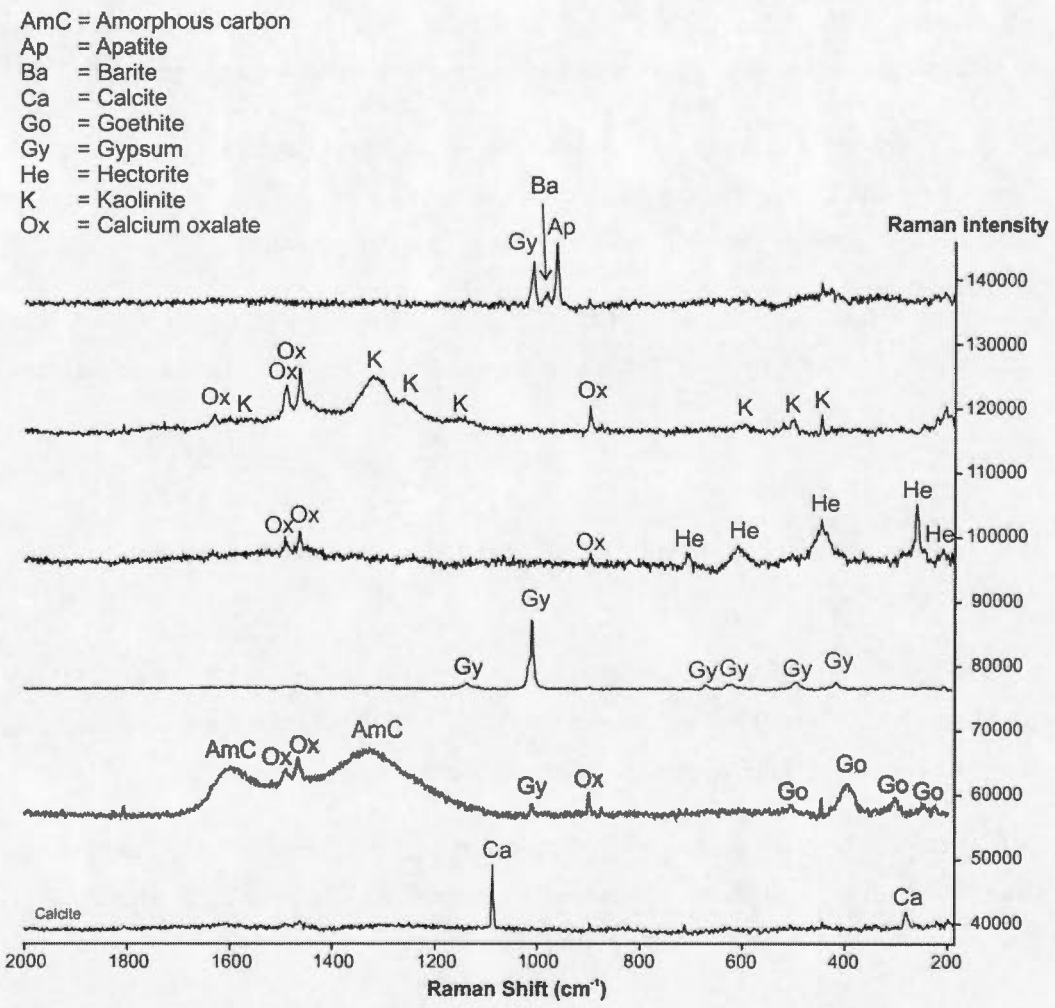


**Figure 3.34** Raman spectra recorded on white paints

Barite and potassium nitrates/ hydrated calcium nitrates were found only at site ARAL175. The latter has been previously reported by Tournié *et al.* (2010) at the surface of the rock face at Main Caves Giant's Castle, uKhahlamba-Drakensberg Park, South Africa, as soluble salts that precipitated on the rock face.

In cross-sections, spectra were extremely difficult to interpret due to the presence of resin peaks which hide most of the other peaks except those from calcium sulphates and calcium oxalates.

The presence of clay was confirmed for most of the samples identified as it follows analysis on unprepared samples, but no more information about its mineralogy was exploitable.

Samples composed of apatite were found mixed with calcium sulphates in cross-sections too. Comparison with EDS maps show that indeed sulphur is present in the paint layer along with phosphorus. It is possible that both were mixed to get a suitable paint.

As on unprepared samples, only whewellite peaks were recorded in samples in cross-sections. It is interesting as weddellite was reported on black samples found in the same sites as the white samples.

3.2.3.4 FTIR spectroscopy

Out of 48 samples, only one sample, ARAL 254I10, was too small to be analysed by FTIR spectroscopy.

Calcium oxalates were recorded on all samples except ARAL164-2012-1, ARAL175I2 and ARAL169-2012-RW1. The two first samples were identified as apatite, whereas the last one is a white concretion collected on top of the rock as a reference sample.

Peak of calcium oxalates at 1620 $cm^{-1}$ is larger than expected. This can be attributed to OH-deformation of water, already encountered on Lesotho and Maclear rocks as well as on Lesotho soils collected in the vicinity of the sites.

Apatite was identified on two samples ARAL164-2012-1 and ARAL175I2. It is not possible with these peaks to make the difference between fluoroapatite and hydroxylapatite. Combining with results from the other analyses, it is possible to conclude that the pigment used here is cremated bones. In both samples, a high proportion of calcium sulphates was recorded, and peaks of gypsum were inverted: peak at 1140 $cm^{-1}$ is higher than peak at 1110 $cm^{-1}$. This inversion is commonly found in naturally formed calcium sulphates (Prasad *et al.*, 2005), and indicates here a different crystallization history. It is possible that a mixture was intentionally made by the artists (see discussion paragraph below). The two samples were collected on representations of animals, one monochrome (ARAL164-2012-1) and one polychrome (ARAL175I2).

Calcium sulphates are present in all samples, except ARAL172-2012-7. Calcium sulphates peaks observed shift from 1100 to 1120 $cm^{-1}$ for the first peak ($\nu_3$, $SO_4$: stretching mode) and from 1140 to 1170 $cm^{-1}$ for the second ($\nu_3$, $SO_4$: stretching mode). These peaks point to the presence of a mixture of more or less hydrated calcium sulphates such as gypsum, bassanite, and anhydrite, and thus to their presence as weathering products more than pigments. At site ARAL175, all samples except ARAL175-2012-8 show inverted peaks of calcium sulphates: peak at 1140 $cm^{-1}$ is higher than peak at 1110 $cm^{-1}$. This inversion is found on samples ARAL254I4 and ARAL164-2012-1 too. As mentioned above, this characteristic can be linked to the history of crystallization of calcium sulphates (Prasad *et al.*, 2005). Unlike the other samples presenting calcium sulphate peaks, the ones recorded on these samples do not shift in a range of more than 4 $cm^{-1}$ (1117, 1147, 1621, 1684, 3399, 3523 $cm^{-1}$), which indicates a purer crystallized material, and which are associated to gypsum. ARAL164-2012-1, ARAL175-2012-8 and ARAL175-2012-9 were collected on white monochrome representations, similar in style, but of unknown tradition. On the other hand, ARAL175I2 and ARAL175P1bis, from the same site, are clearly San fine line tradition and are made of the same pigment. Moreover, ARAL254I4 is composed of the same pigment and is attributed to San fine line tradition, in another site. It is thus possible, that these representations were in fact to be categorized as San painting tradition (see discussion paragraph below).

ARAL169-2012-RW1, reference sample collected on rock, exhibits peaks at 1124, 1140, 1620, 1684, 3401, 3542 $cm^{-1}$, but which are shifted in the range of order than previously recorded on samples. They correspond to peaks of calcium sulphates more or less hydrated. It arises the question of the use of this concretion to make paintings. As it is a natural weathering product, it is almost impossible to distinguish from natural calcium sulphates which will develop after painting realization. In this reference sample, the presence of calcium carbonates, and Si-O and Al-O bonds was observed. Calcium carbonates are seen as weathering products which formed at the same time as calcium sulphates, and Si-O and Al-O bonds as small aerosol particles deposited during crystallization. Sample was taken with care of not collecting any part of the rock, so these peaks cannot be attributed to the rock. The concretion is about 1 cm and more thick, and was observed as stains about 10 cm diam.

Clay was identified in 29 samples, on sites ARAL 172, ARAL175, ARAL176, ARAL180, ARAL250, ARAL254 and ARAL258 (Figure 3.35). Two types of clay were observed. One is found only on site ARAL180 and can be identified as hectorite associated to calcium carbonates, common admixture in hectorite, which seems to confirm this attribution (Madejova and Komadel, 2001). Moreover, hectorite contains magnesium which has been recorded in cross-sections during SEM-EDS analysis. The second type of clay is kaolinite. It has been identified on sites ARAL172, ARAL175, ARAL250, ARAL254 and ARAL258. Interestingly, all images of ostrich and ostrich footprints at site ARAL258 presented the same peaks of kaolinite, with the particularity of weak peaks at 3620 and 3698 $cm^{-1}$. On samples from site ARAL176, and on ARAL25413 and ARAL25414, it is unclear if the clay comes from the pigment or from minerals from the rock as peaks are very weak and few in numbers.

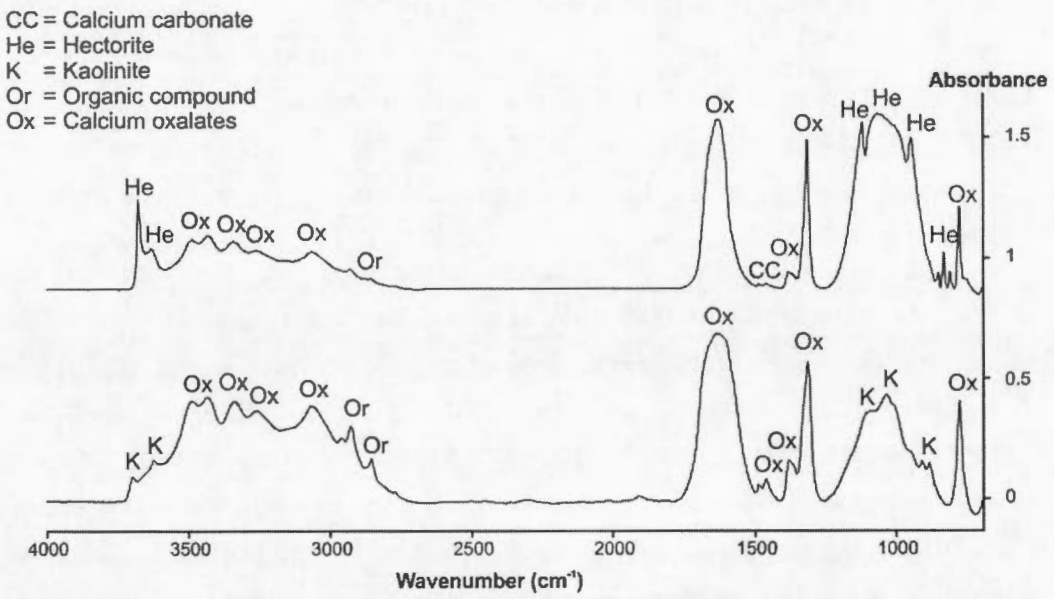


**Figure 3.35** FTIR spectra of white paints made of clay from the Phuthiatsana Valley

Hectorite was not found in the white soils found in the vicinity of the sites, whereas kaolinite was. It is hence possible that some of the raw materials used to make these paintings were found locally.

The presence of Si-O and Al-O stretching bonds attributed to quartz and feldspars was recorded on 11 samples on sites ARAL169, ARAL172, ARAL175, ARAL180, and ARAL258. In most of the samples, there were not enough peaks to have a proper identification. However, albite was identified in ARAL180-2012-13 and ARAL258-2012-8, and microcline in ARAL258-2012-8. They are minerals constituting the rock support of the paintings.

Calcium carbonates peaks were observed in 11 samples from sites ARAL169, ARAL172, ARAL175, ARAL180 and ARAL254. For 6 samples (ARAL169-2012-2, ARAL169-2012-4, ARAL169-2012-7, ARAL169-2012-9, ARAL172P3, ARAL175-2012-6), they are seen as the pigment used, because of their high quantity in the paint. It has been compared with Raman analysis and EDS mapping on cross-sections to conclude that, for only four of them (ARAL169-2012-2, ARAL169-2012-4, ARAL172P3, ARAL175-2012-6), calcium carbonates were associated to the pigment used. In the case of ARAL175-2012-6, kaolinite was identified too. This painting seems to be a mixture between calcium carbonates and clay. It naturally occurs as what is called "white earth", in which the white colour is mainly given by calcium carbonates (Eastaugh, 2008), but it may be an artist mixture too. In the other samples mentioned, peaks are weaker and calcium carbonates are seen as weathering products coming from the rock, and in the case of samples from ARAL180, as a contribution from the hectorite used as pigment (see above).

Peaks of organic compounds (2770, 2853, 2925, 2956 $cm^{-1}$), were recorded in all samples except ARAL169-2012-RW1, ARAL175-2012-6, and ARAL258-2012-5. They are associated to the use of methanol to clean diamond micro-compression cells.

#### 3.2.3.5 Conclusion

Following these results, it appears that 22 samples are composed of kaolinite, 1 sample of white earth, that is to say a natural mixture of clay and calcium carbonates, 7 samples of hectorite, 4 samples of calcite, 4 samples of gypsum, 4 samples of cremated bones mixed with calcium sulphates, and finally for 4 samples, it is impossible to conclude between gypsum and clay.

The samples composed of kaolinite are the most numerous and it might be explained by the availability of this raw material in the vicinity of the sites. Moreover, as detailed in §3.2.5, they are easy to process to make a suitable paint. On the other hand, hectorite and white earth were not observed in the soils collected.

All of these minerals were already found in previous studies (Arocena *et al.*, 2008; Bonneau *et al.*, 2013; Hoerlé, 2005; Hughes et Solomon, 2000; Mazel, A. D. et Watchman, 1997; Prinsloo *et al.*, 2008; Tournié *et al.*, 2011) but for the first time, cremated bones are identified. Apatite and calcium carbonates present in the paint point to the use of bones. To make them white, they need to be heated close to fire for several (7 to 12) hours turning first black and then white. Interestingly, calcium sulphates were found mixed with them. It is possible that cremated bones once crushed, did not made a proper paint and had to be mixed with calcium sulphates. On the other hand, apatite can occur naturally in calcium sulphates sources (Nathan and Lucas, 1972). The proportion of phosphorus and the presence of calcium carbonates points to cremated bones rather than naturally occurring apatite. This paint was used to make three white paints of unknown tradition and a polychrome eland from San painting tradition (Arthur *et al.*, 2010). As the same paint was used to make all of these representations, it may be possible to conclude that the white figures are of San paintings traditions. However, the possibility of a transmission of recipes through populations cannot be excluded.

Weathering products identified are the same as in the black paints, except that only whewellite was recorded. Samples from the same sites and close to each other exhibit this difference. It may be explained by the type of binder used to manufacture the paint. It is possible that binders, as plant sap, contain weddellite when used and then they stayed in the paint layer, or that the binder used was more attractive to specific types of lichens and bacteria which produced weddellite rather than whewellite.

### 3.2.4 Red paints

#### 3.2.4.1 Microscope

Two textures were recorded on the red and dark red paint layers: a smooth texture (5) and a fine-grained texture (24). The smooth texture was observed at sites ARAL 180, ARAL 252 and ARAL 254 on eland and human figures.

Sample ARAL175P1 presents a pinkish hue under the microscope and sample ARAL 252P2 a brownish one. The former was not characterized (and left for a further project) whereas the latter was treated in this section.

The red/dark red paint layers are homogenous with few black grains inside in the case of dark red. The red paint layers show more orange/yellow grains inside.

On top of the paint layer, transparent, white, yellow and grey crystals are found and are thought to be weathering deposits. In few cases (2), they formed a thin crust on top of the paint layer.

At the junction between the red/dark red paint layers, an orange hue can be observed. As previously noted for the red paints in the Maclear area, this may be due to an alteration of the pigment by hydration of the iron oxides.

Samples were not mounted in cross-section.

#### 3.2.4.2 SEM-EDS

SEM observations reveal four morphologies: small balls about 1 μm in diameter (3), a fine-flaky texture composed of small flakes from 1 to 3 μm in diameter (8), a flaky texture with flakes from 5 to 10 μm in diameter (4), and a smooth texture (8) (Figure 3.36). For five samples, the morphology was not identified.

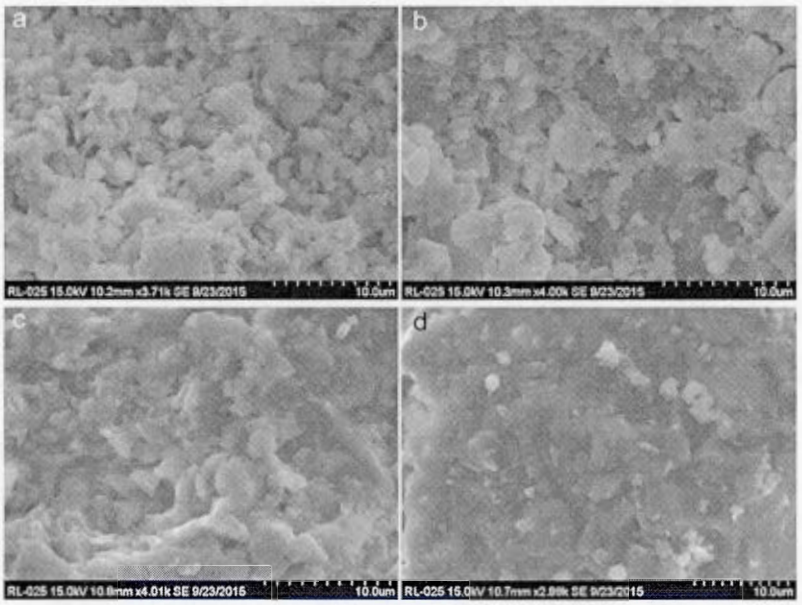


**Figure 3.36** Secondary electron SEM images of red paints: a) small balls, b) fine-flaky texture, c) flaky texture, d) smooth texture

The small ball texture is composed of iron and manganese with aluminium, silicon and sodium as minor elements. It is found only at site Aral171 on human figures with a large rectangle body.

The other samples whatever the morphology they exhibit, are composed of aluminium, silicon and iron, which are attributed to clay minerals and iron oxides. Minor elements as titanium, manganese and copper, linked to the geological history of the iron oxides, make it possible to separate 6 groups:

- Group 1: no other chemical element than iron was recorded: 6 samples.
- Group 2: titanium was recorded with iron: 5 samples.
- Group 3: titanium and manganese were recorded with iron: 2 samples.
- Group 4: titanium and copper were recorded with iron: 1 sample.
- Group 5: copper and manganese were recorded with iron: 2 samples.
- Group 6: titanium, copper, and manganese were recorded with iron: 1 sample.

Looking at these groups, none of them can be correlated to only one texture. Cross-sections analysis would have been of great help to make a better determination, but because of time constraints they were not realized.

Along with silicon and aluminium, magnesium appears in high proportion in four samples. It may be correlated with weathering products or to its natural presence in the clay used.

The presence of aluminium and silicon with iron points to the use of "ochres" as raw material. The elemental composition recorded is similar to those found on the red soils collected in the vicinity of the sites.

Three samples in the fine-flaky texture group are composed mainly of iron with aluminium and silicon as minor elements. Here, iron oxides seem to have been directly used from their mineral form and crushed. This would require to find a vein of hematite and to mine it. This process is longer than just collecting soils from the floor and the transformation of the sample by grinding would require hard grindstones.

Magnesium, phosphorus, sulphur, chlorine and calcium were recorded in all samples and are attributed to weathering products. No specific crystal shape was identified to help about determining their mineralogy.

3.2.4.3 Raman spectroscopy

Four minerals were found to be the main component of red paints in the Phuthiatsana Valley: hematite, magnetite, manganese oxides, and iron hydroxides (Figure 3.37). They are detailed one by one in the following paragraphs.

Hematite type 1 has been recorded in seven samples, and hematite type 2 in thirteen samples (Hematite was categorized according to types described in § 3.1.4.3). For four samples, the peaks of hematite were too weak to categorize them. In the group of hematite type 1, four samples exhibit a peak at 660 $cm^{-1}$ attributed to the presence of magnetite or to the decrease in the crystallinity of the sample, sometimes attributed to the heating process of hematite, even if it can be introduced by grinding or weathering too (de Faria and Lopes, 2007). The same peak is present in four samples in the hematite type 2 group. In this group, another peak

is often encountered, a broad peak at 655 $cm^{-1}$, attributed to Mn-O bonds and due to the presence of manganese in the structure of hematite. It has been found in eight samples of the hematite type 2 group. None of these peaks were recorded on the samples with weak hematite peaks. However, in Aral176P1, peaks of hematite and manganese oxides (653 $cm^{-1}$) were recorded on the same sample but independently. It can be interpreted as a mixture, even if it is difficult to know if it is intentional or natural.

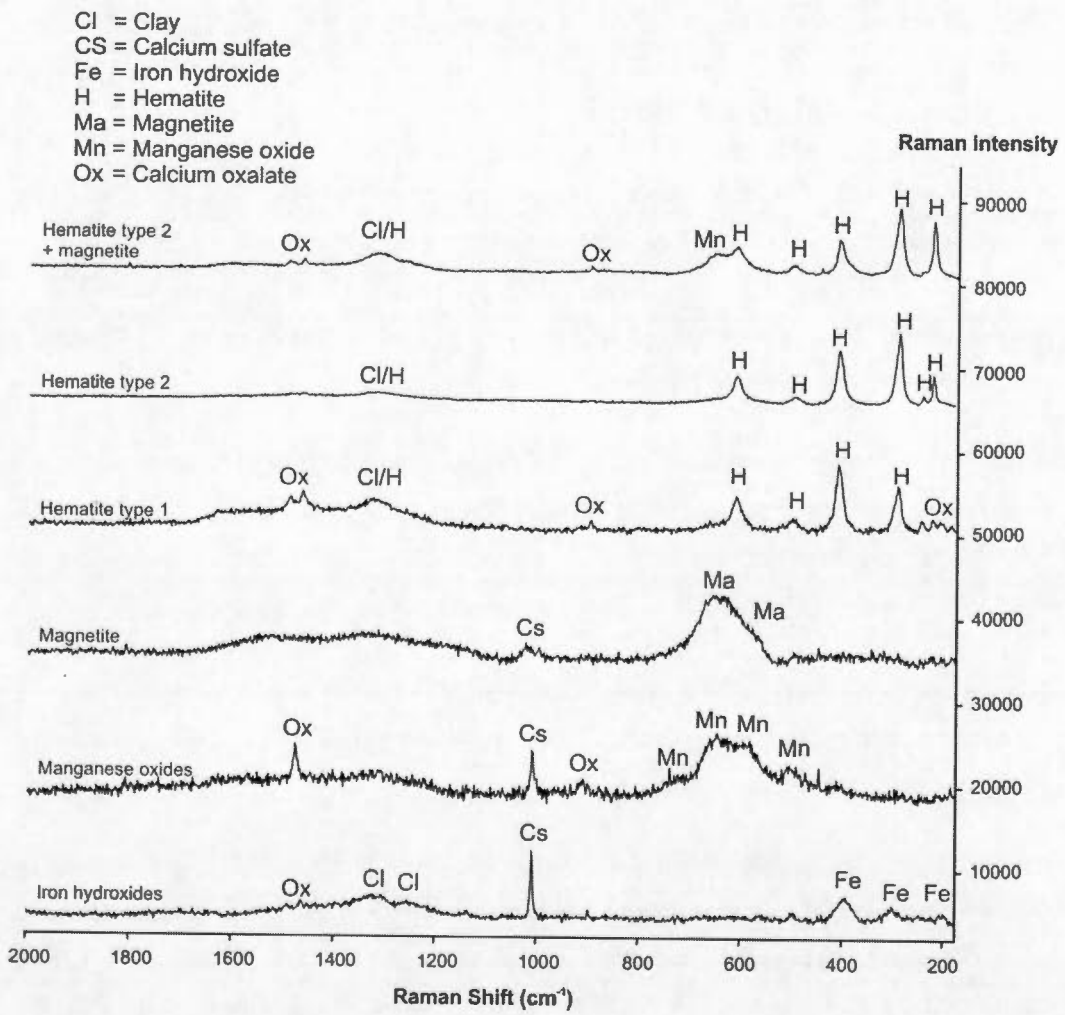


**Figure 3.37** Raman spectra recorded on red paints in the Phuthiatsana Valley, Lesotho

Magnetite alone with peaks at 660 $cm^{-1}$ was found on sample Aral252P1. Manganese oxides were recorded on sample Aral252P2. Finally, iron hydroxides composed the paint of Aral180P1.

Clay was encountered in 11 samples. For the other samples composed of hematite, a peak at 1320 $cm^{-1}$ is recorded almost of the time, but is attributed to Fe-OH asymmetric stretching from hematite. The presence of clay points to the use of "ochres" to make the paints in at least 11 samples. It complements the SEM-EDS analysis where aluminium and silicon were main compounds of the same samples.

Comparing Raman results, morphology and chemical results with SEM-EDS, samples from Aral 171 detached by their shape as small balls and their specific composition of hematite type 2 with a large proportion of manganese. It gives a brownish colour rather than a proper dark red one.

Samples from Aral 252 are specific as they exhibit the same morphology, the same EDS spectra with a high proportion of iron, but their Raman spectra show either magnetite, or hematite or manganese oxides. They are all part of the same panel with the same colour. This bias in the analysis is introduced by the use of unprepared samples. It is interpreted as the use of natural ochre, composed of different iron and manganese oxides.

Weathering products were recorded as calcium sulphates more or less hydrated, calcium oxalates under the form of weddellite and whewellite, and barite. The presence of a carotenoid has been recorded only on one sample at site Aral175.

Barite and the carotenoid were found only on site Aral 175. The same peaks were recorded on white samples at this site.

Quartz and feldspars were recorded on some samples and are attributed to the rock support or to aerosol particles.

Finally, carbonaceous matter appears on some samples. They are attributed to organic compounds present in the sample such as fatty acids or bacteria for example.

3.2.4.4 FTIR spectroscopy

Calcium oxalates were recorded on each sample. The peak at 1620 $cm^{-1}$ is enlarger in most of the spectra due to the presence of a peak at 1650-1680 $cm^{-1}$ attributed to OH deformation of water. This peak has been previously reported in other colours and areas studied here, and is a component of clay minerals. Calcium sulphates were observed on 24 samples. Calcium carbonates were recorded in two samples. There are thought to come from the calcitic matrix present in the rock support.

Clay often mixed with quartz and feldspars were found in all samples. Montmorillonite or illite with albite has been identified in two samples. The other samples are mostly composed of kaolinite and quartz (Figure 3.38).

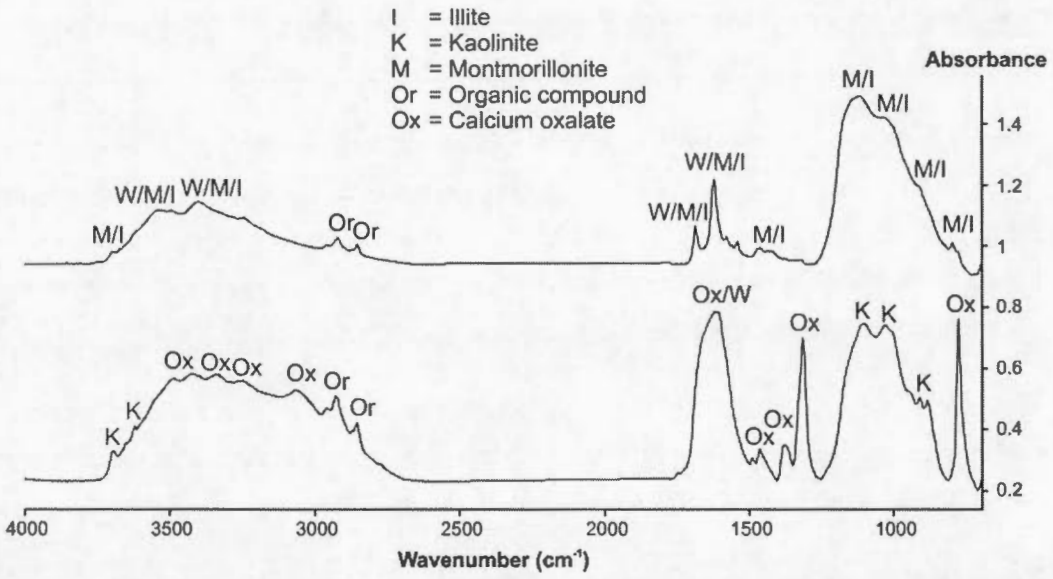


**Figure 3.38** FTIR spectra recorded on red paints in the Phuthiatsana Valley, Lesotho

3.2.4.5 Conclusion

Red paints in the Phuthiatsana Valley are composed either of hematite, or magnetite, or manganese oxides, or iron hydroxides. Sub-groups are visible in the hematite-based paint, firstly by the presence of manganese oxides, secondly by the presence of magnetite, and thirdly by the use of both ochre and what seems to be pure hematite.

The type of pigment used is constant within one panel and specificities were observed in two sites. Hematite type 2 mixed with manganese oxides and as small balls is found only at Aral 171 on human figures depicted wearing skin cloaks (*karosses*). At Aral 254, all the red figures attributed to San rock art tradition were made with hematite type 1 whereas a stain, which is attributed to colonial time, is made of hematite type 2.

If peaks of calcium sulphates were found in almost all the samples, calcium oxalates are much fewer. Whewellite is the main form found, weddellite being present only on samples from sites Aral 172, Aral 252 and Aral 254. Moreover, another kind of weathering product, barite, was found only on samples from site Aral 175.

### 3.2.5 Weathering products and alterations

#### 3.2.5.1 Microscope

Under microscope observations, transparent, white, orange and red grains are found on top of the paint layer, whatever the colour. They are attributed to aerosol particles. Black grains were observed occasionally and are correlated to fires made in the rock shelter, and thus are interpreted as soot.

In cross-section, a thin white to orange layer is observed on top of the paint layer, in 8 samples. It is thin, about 5-10 µm thick. Underneath the paint layer, a thicker white to orange layer is observed in almost all the samples, from 50 to 200 µm thick. It is found on top of the rock support when observed on the cross-section (Figure 3.39).

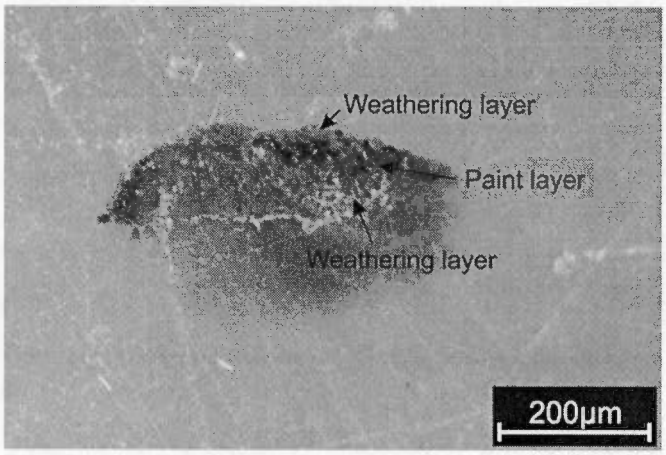


**Figure 3.39** Sample mounted in cross-section showing weathering layers

3.2.5.2 SEM-EDS

Small rounded grains (about 1 µm diam.) and long grains (about 10 µm long) were observed on top of the paint layers. The former are composed of calcium, whereas the latters are composed of sulphur and calcium. They are thought to be calcium oxalates and calcium sulphates.

Magnesium, phosphorus, and chlorine were recorded too and are attributed to hydromagnesite and soluble salts that crystallized at the surface of the rock.

With cross-sections, the two layers observed under the microscope were found too. The layer on top of the paint layer is composed either of calcium and sulphur with a few silicon and aluminium, or of silicon and aluminium with a few calcium. Elemental maps made it possible to "see" this layer whereas it had not been observed during microscopic observations (Figure 3.40).

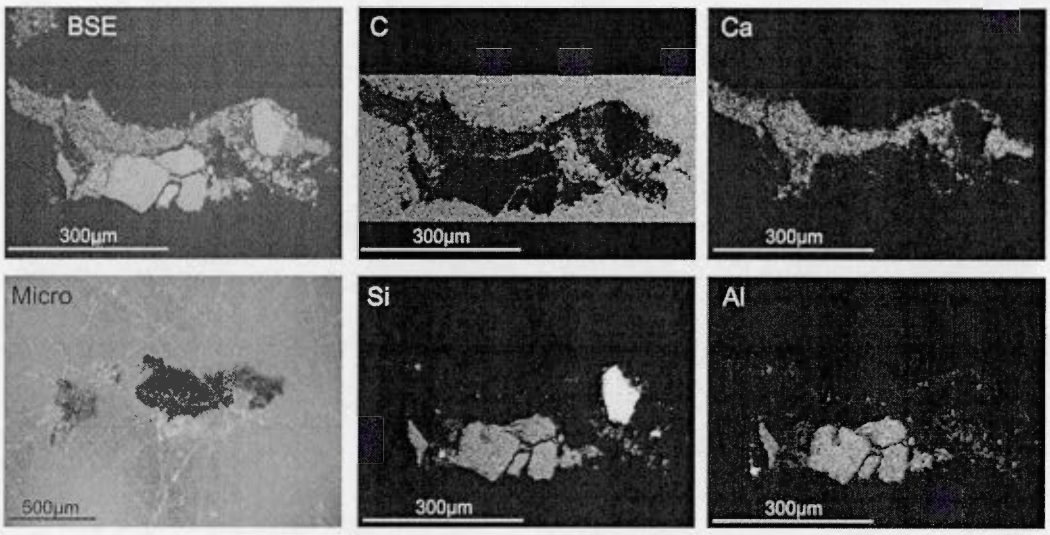


**Figure 3.40** Elemental maps on a cross-section showing weathering layers (Black paint from the Phuthiatsana Valley)

The second layer underneath the paint layer is thicker and its composition is highly variable. It is mainly composed of calcium, silicon and aluminium. Sulphur occurs as islands in this layer or forms a homogeneous layer at the junction between the sample and the weathering layer. It is always linked to calcium. Phosphorus is found as islands in this layer too and linked to calcium. Magnesium and chlorine are spread through this layer without accumulating at a specific point.

3.2.5.3 Raman spectroscopy

Calcium oxalates are found in all the paint layers but its proportion is weaker in red paints than in the other colours. Whewellite and weddellite were recorded in black and red paint layers whereas only whewellite was found in the white paint layers. This may be due to the use of different binders which do not attract the same lichens or bacteria.

Calcium sulphates more or less hydrated were recorded on all paint colours. However, in the case of the white paints, it was difficult to distinguish between the paint made with gypsum and calcium sulphates originating from weathering. The pigment was mostly gypsum

whereas the weathering products were calcium sulphates more or less hydrated. Inversion of the conventional intensity of their FTIR peaks was another clue.

Clay was recorded too and is attributed to the natural degradation of the rock. It is found on the two weathering layers surrounding the paint one. Hydromagnesite was recorded on each colour.

Barite, potassium nitrates/hydrated calcium nitrates, and a carotenoid were observed only at Aral 175. If barite and nitrates are common weathering products on rock surfaces, the carotenoid is thought to have been produced by a bacterioruberins (Tournié *et al.*, 2010). Samples presenting these weathering products are confined in one single panel of this site, exposed to rain and sun and highly flaking.

#### 3.2.5.4 FTIR spectroscopy

Calcium oxalates are the main components characterized in the samples. However, as seen during Raman analysis, the red paints exhibit very few calcium oxalates comparing to white and black paints.

Calcium sulphates, calcium carbonates, and clay are found in each colour but they are difficult to distinguish from paint layer in the case of white paints. Elemental maps and Raman analysis were taking into account to achieve this distinction.

#### 3.2.5.5 Conclusion

The main weathering product found both in and surrounding the paint layer is calcium oxalates. Both forms were observed in the paint layers, but only whewellite is present in the surrounding layers. This distinction is visible only for red and black paints, whereas for white paints, only whewellite was recorded.

Calcium sulphates more or less hydrated occur mostly in the bottom weathering layer as islands or as a uniform layer at the junction between the paint layer and the weathering layer.

Barite, a carotenoid from bacterioruberins, and potassium nitrates/hydrated calcium nitrates were observed on white and red paints on a single panel at Aral 175. This specificity may be

attributed to a specific orientation of the panel, to binder used to make the paint, or to posterior human actions. Barite and nitrates are common weathering products found at the surface of rock (Tournié *et al.*, 2010).

Clay has been previously reported as a weathering product of Clarens Formation sandstone (Johnson *et al.*, 2006) and has been observed during characterization of the rock.

### 3.2.6 White soils

Eight white soils were collected in the immediate vicinity of sites in the Phuthiatsana Valley. They were fine-grained soils for 5 of them, two were coarse-grained soils and one was a piece of rock which crumbles when being touched. They are thought to be potential raw materials used by the San artists to make their paintings. They were analysed unprepared, after crushing in mortar and after separation by settling, following the same protocol as for paint.

#### 3.2.6.1 Preparations

As mentioned in Chapter II, some sites in the Phuthiatsana valley were excavated and grindstones with traces of red, white and black pigments were found (Arthur and Mitchell, 2010) and studied by Luiseach Nic Eoin, as part of her Ph.D. project. One can conclude that colouring materials may have been grounded before being used as paint. Thus, the raw materials were crushed in a ceramic mortar.

In the literature, mentions can be found of red stains on ostrich eggs or on shells (Barham, 2002; Marean *et al.*, 2007) found on South African sites. It is possible that these recipients were used to prepare the paint for painting, or to prepare the soil by cleaning in water or for separation by settling.

To confirm the use of separation by settling, a quick experience was conducted on 6 out of the 8 samples of soils collected. They were crushed first in mortar and then separated by settling by adding distilled water to them in a beaker. They were mixed and left for one minute. Then the supernatant was transferred in a new beaker and left drying at room temperature for 24h. The result is shown in Figure 3.41. The supernatant was separated by

settling another time using the same protocol once in the case of 5 samples and twice for one sample. They were called separations 1, 2 and 3. This soil separation resulted in a fine-grained powder which was characterized.

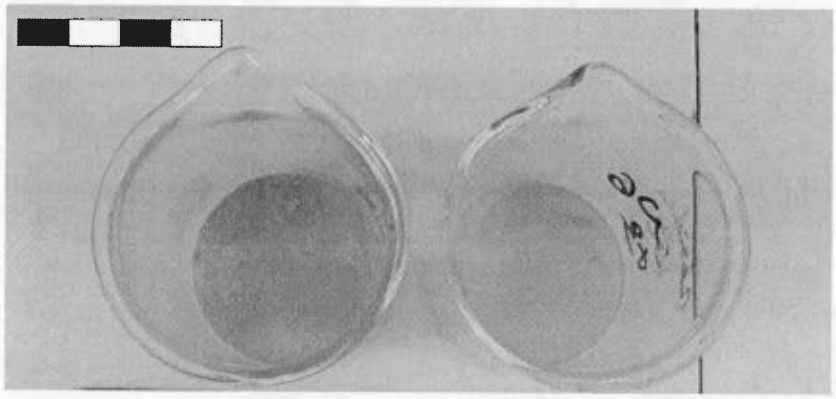

**Figure 3.41** Results of one separation by settling on a white soil

3.2.6.2 Microscope

The soils unprepared are all similar. They are composed of white and transparent crystals in a proportion which varies with soils but which can be evaluated as between 30-70% to 70-30%. Few red, brown, yellow and orange crystals are present (Figure 3.42).

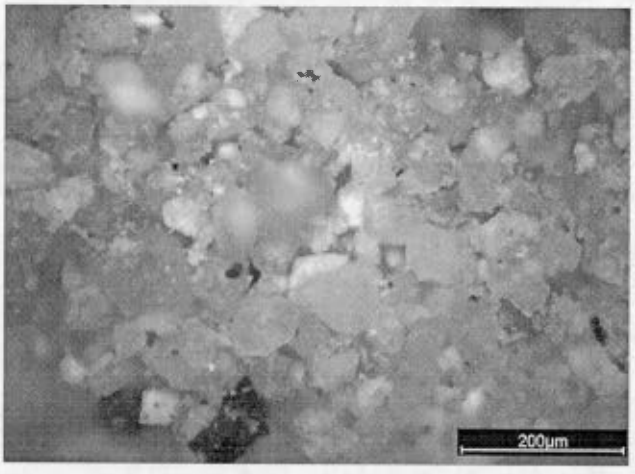


**Figure 3.42** Microscope photo of a white soil unprepared

After crushing in mortar, soils are finer but they show the same kind of crystals. After one separation, soils are finer and whiter. Transparent grains and grains with other colours are fewer. After a second separation, transparent crystals are less in number and the soils seem whiter. The grains with other colours are still present in the same proportion. For one sample, a third separation has been done but the resulting supernatant was similar to the one after two settlings (Figure 3.43).

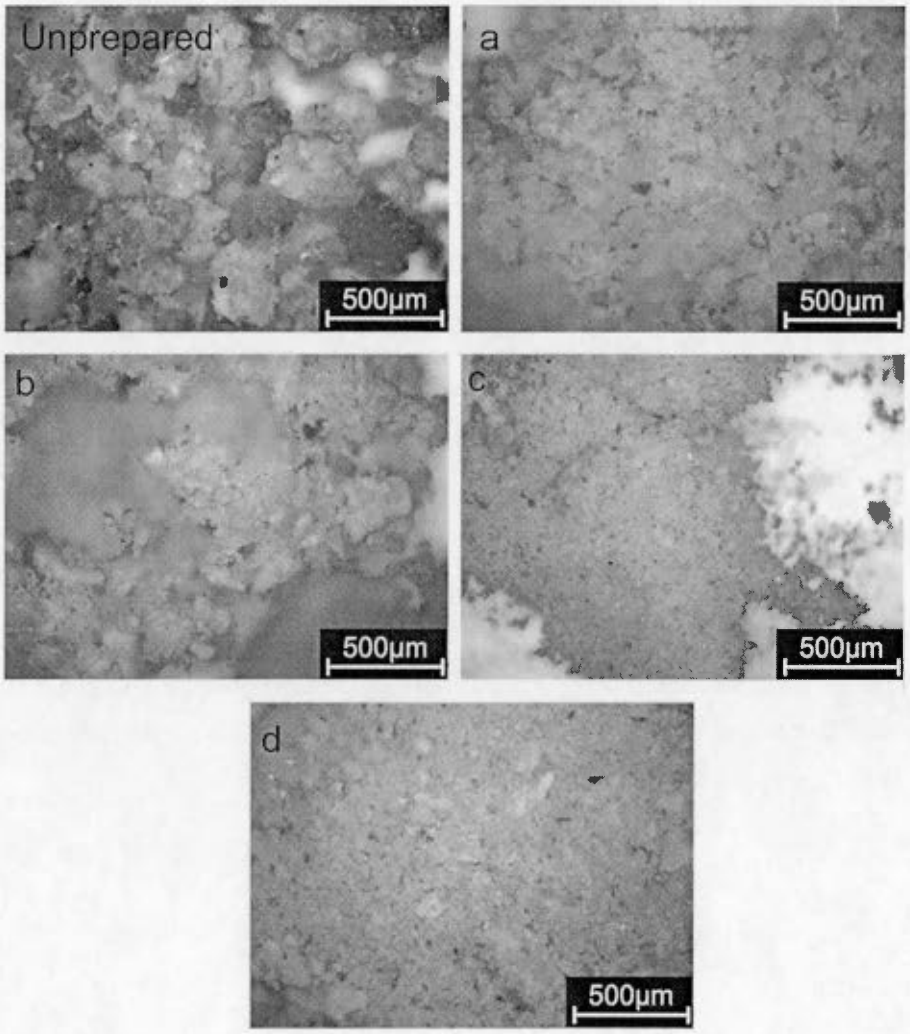


**Figure 3.43** Microscope observations of a white soil after crushing in mortar (a), after one separation (b), after two separations (c) and after three separations (d)

3.2.6.3 SEM-EDS

Observations of soils under SEM show two textures on soils with no preparation (Figure 3.44):

- A soil composed of coarse grains about 100 µm diameter mixed with round fine grains about 2-5 µm in diameter (6 samples).
- A soil with a smooth texture with fine grains and flakes on top of it, about 2-5 µm in diameter (2 samples).

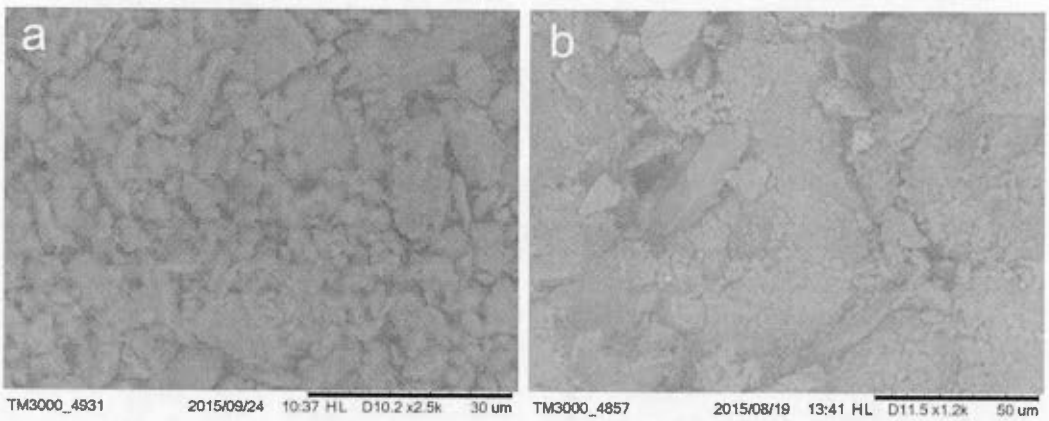


**Figure 3.44** Backscattered electron images of white soils: a) coarse-grained texture, b) smooth texture

Once crushed and separated by settling, soils show all the same morphology: grains about 10 µm in diameter mixed with fine rounded grains about 2-5 µm. The repetition of cycles of separation does not change the morphology (Figure 3.45).

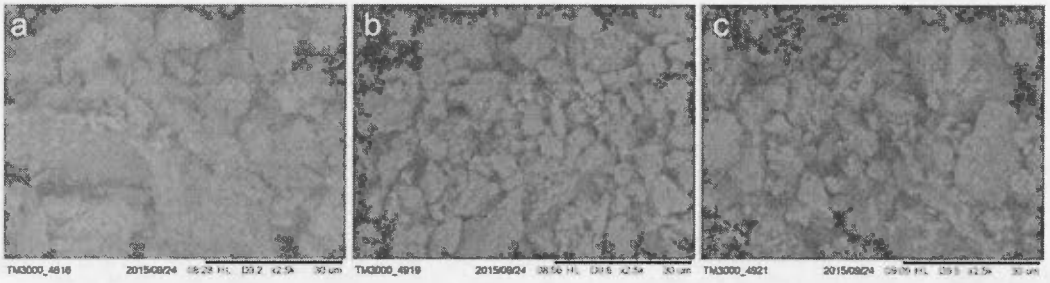


**Figure 3.45** Backscattered electron images of white soils after 1 (a), 2 (b) and 3 (c) separation by settling

All the samples are composed of sodium, magnesium, aluminium, silicon, potassium, titanium and iron. In four samples, calcium was recorded too, and in one other sample, sulphur and calcium. The elemental composition of the soils is constant whatever the separation made.

3.2.6.4 Raman spectroscopy

Amongst the 8 soils analysed, one of them, Lesotho-2012-W5, cannot give interpretable Raman spectra because of a high fluorescence. Spectra recorded on both unprepared and prepared soils give the same results (Figure 3.46). A broad peak centred at 1500 $cm^{-1}$ appears after separation by settling. It is attributed to clay minerals in the sample. The separation by settling promotes fine particles composing the sample, especially clay minerals, and thus results in a higher proportion on them in the sample, which is recorded in the Raman spectra.

White soils all exhibits peaks of albite coupled to clay minerals identified with peaks at 253, 289, 314, 330, 355, 410, 463, 480, 507, 580, 603, 708, 763, 813, 1173, 1245, 1293, 1478, 1519, 1613 $cm^{-1}$. Only Lesotho-2012-W8 does not show these peaks but those of illite/montmorillonite at 263, 291, 410, 464, 508, 664, 708, 757, 1103, 1158, 1294, 1366, 1490, 1616, 1744 $cm^{-1}$ (Košařová *et al.*, 2013). In this illite, albite is present too as minor components, referring to the intensity of the peaks.

Anatase was found at part of three white soils: Lesotho-2012-W3, Lesotho-2012-W4, and Lesotho-2012-W6.

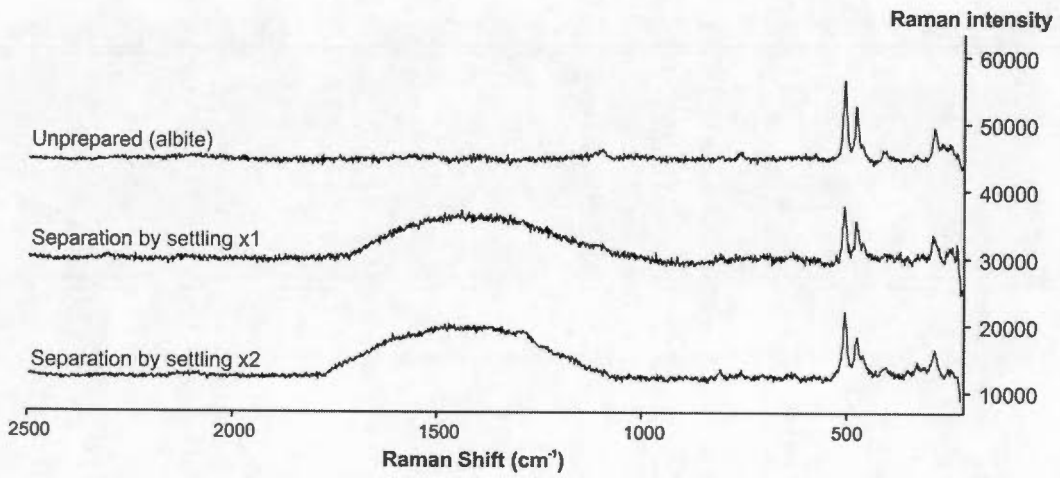


**Figure 3.46** Example of Raman spectra recorded on unprepared and prepared white soils

3.2.6.5 FTIR spectroscopy

As for Raman analysis, FTIR spectra recorded on both unprepared and prepared soils give the same results (Figure 3.47).

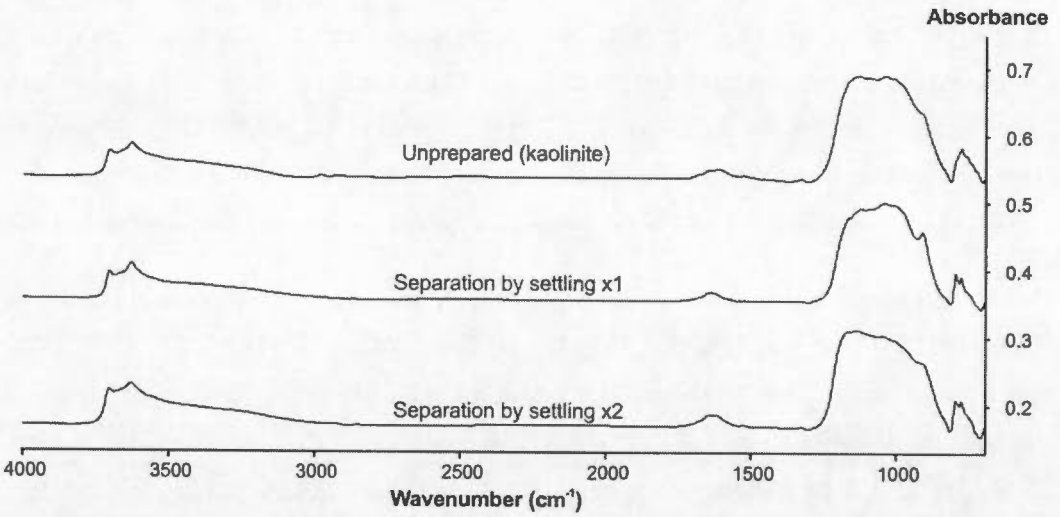


**Figure 3.47** Example of FTIR spectra recorded on unprepared and prepared white soils

Kaolinite was found to be the main component of six soils, whereas the two others are made of illite/montmorillonite.

Kaolinite is found mixed with albite and sometimes quartz which enlarges the broad peak centred at 1050 $cm^{-1}$ and gives a long set of peaks: 725, 744, 761, 787, 777, 797, 914, 1004, 1033, 1081, 1115, 1648, 3381, 3623, 3698 $cm^{-1}$.

In one sample, the white soil is composed of kaolinite with albite, but another kind of clay, illite or montmorillonite, is also present.

Illite or montmorillonite were recorded on two samples. As for kaolinite, peaks of albite are observed. Peaks of illite and montmorillonite are the same under FTIR analysis (Madejova and Komadel, 2001) which makes it impossible to determine which of these two minerals is composing the soils.

Calcium carbonates were found in four samples: Lesotho-2012-W3, Lesotho-2012-W4, Lesotho-2012-W6, and Lesotho-2012-W8.

#### 3.2.6.6 Conclusion

White soils collected in the vicinity of sites in the Phuthiatsana Valley are either kaolinite, or montmorillonite/illite, or a mixture of them. Albite and quartz are present in the clays. Clay are products of degradation of the surrounding sandstones but maybe at different formation stages.

If only crushed in mortar, they are still coarse grained and to get a smooth and fine powder to paint and to observe a fine-grained texture as found in the paintings, it requires a separation by settling. It is highly possible that this step was in fact more a cleaning step of the soils. Mixing ground soils in water makes it possible to retrieve plants particles and to select only the finer part of clay which gives a whiter colour.

### 3.2.7 Red soils

Eight red soils were collected in the immediate vicinity of sites in the Phuthiatsana Valley. They were fine-grained soils. They are thought to be potential raw materials used by the San artists to make their paintings. They were analysed unprepared, after crushing in mortar and after separation by settling, following the same protocol as for paint.

3.2.7.1 Preparations

As for the white soils, 4 of the red soils were crushed in a ceramic mortar and separated by settling twice for three of them and three times for one of them (Figure 3.48).

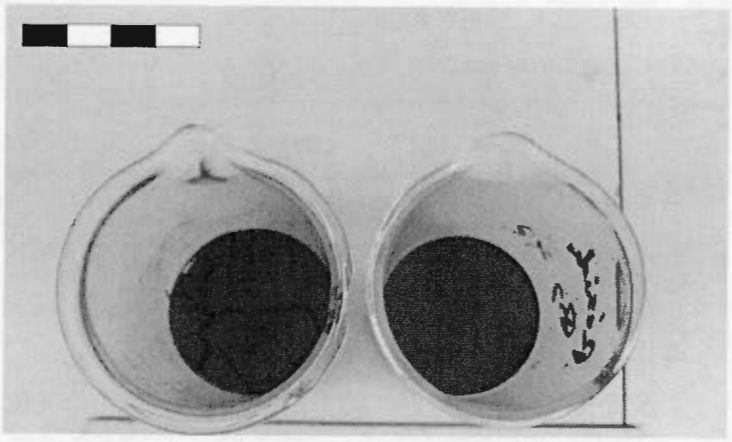

**Figure 3.48** Results of one separation by settling on a red soil

3.2.7.2 Microscope

Three kinds of unprepared soils were observed: a fine-grained soil (grains less than 20 µm diam.) (2), a fine-grained soil with grains stuck together as balls (4), and a coarse-grained soil (grains from 30 to 100 µm diam.).

Interestingly, out of the 8 soils collected and which seemed to be red with naked eyes, 3 were in fact orange under the microscope, the two fine-grained soils and on fine-grained with grains stuck together as balls.

All the soils present large transparent or white crystals and some black crystals. In the case of red soils, orange crystals are found; and in orange soils, red crystals are recorded. It is probable that the red and orange crystals are iron oxides more or less hydrated. And thus their presence in the other colour is expected. In one sample, white grains are included in the red matrix.

After crushing in mortar, the soils are finer but they stay similar to the unprepared ones. After one separation by settling, red and orange soils are finer. In the case of orange soils, they became darker. Sparse transparent, white and black grains are present. The second settling amplified these observations and the soil is finer. On one sample, a third settling was conducted but as for the white soils, the resulting soil was similar to the one from the second settling (Figure 3.49).

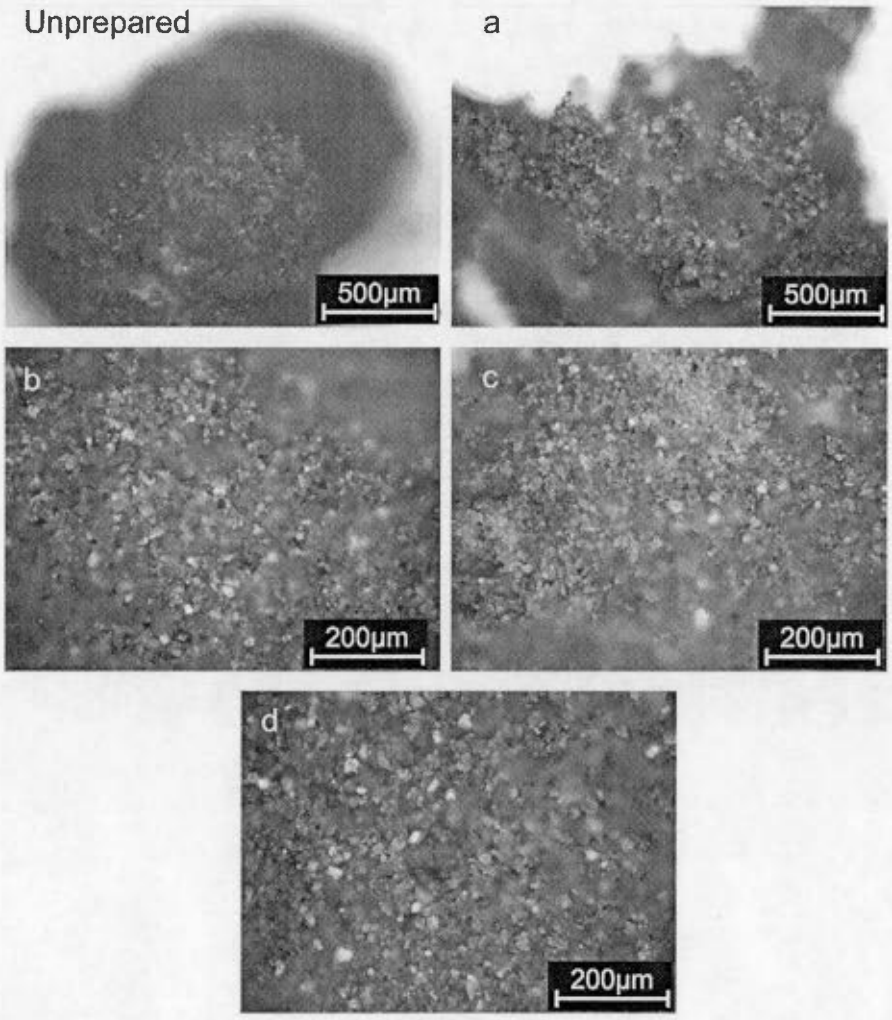


**Figure 3.49** Microscope observations of a red soil unprepared, after crushing in mortar (a), after one separation (b), after two separations (c) and after three separations (d)

3.2.7.3 SEM-EDS

SEM observations show almost the same texture on each unprepared soil: a smooth texture with at its surface, coarse and fine grains rounded or as flakes. Coarse grains are about 10 to 30 µm diameter and fine grains about 2 to 10 µm diameter. Lesotho-2012-R2, Lesotho-2012-R6 and Lesotho-2012-R7 exhibit the coarser grains.

Once separated by settling, whatever the number of cycles, the soils are finer grained with grains about 10 µm diameter mixed with fine rounded grains about 2-5 µm (Figure 3.50).

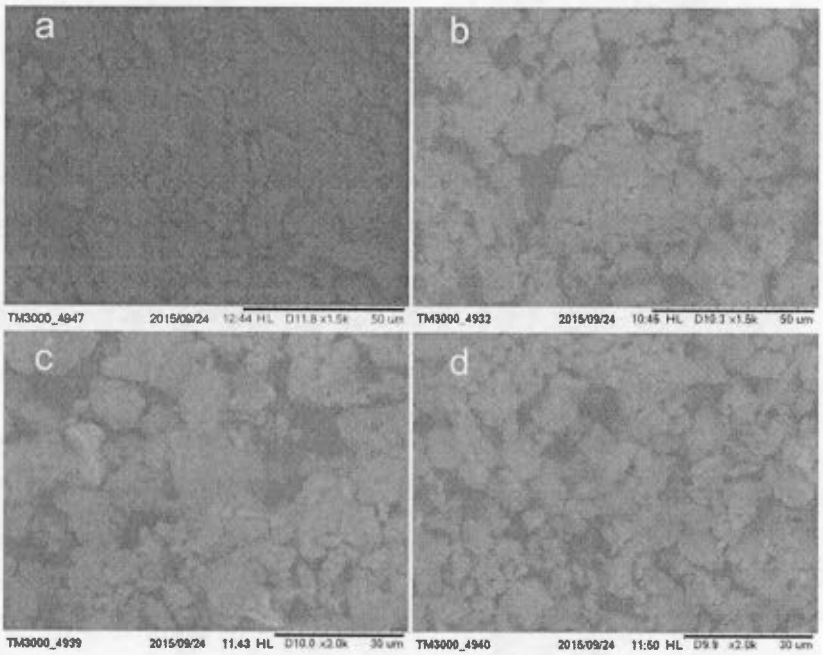


**Figure 3.50** Backscattered electron images of red soil: a) unprepared, b) after 1 separation, c) after 2 separations, d) after 3 separations.

Elemental composition is the same whatever the preparation of the soil. Two main types were recorded:

- Six soils composed of sodium, magnesium, aluminium, silicon, potassium, calcium, titanium and iron.

- Two soils composed of magnesium, aluminium, silicon, titanium and iron.

The proportion of iron is higher than recorded on white soils and is interpreted as the origin of the red colour of the soils.

3.2.7.4 Raman spectroscopy

Unfortunately, red soils suffer for very high fluorescence even using the near-IR laser. Attempts at using very low laser power and at accumulating for few seconds (5-10s) about 100 times did not help at acquiring a proper exploitable spectrum. Hence, mineralogical identification was conducted only with FTIR spectroscopy.

3.2.7.5 FTIR spectroscopy

Kaolinite was identified with quartz and feldspars in all the samples, except Lesotho-2012-R6, with peaks at 750, 780, 797, 911, 1003, 1033, 1090, 1118, 1162, 1635, 3621, 3649, 3696 $cm^{-1}$ (Figure 3.51). Lesotho-2012-R6 exhibits peaks of illite/montmorillonite at 778, 1007, 1050, 1125, 1162, 1632, 3629 $cm^{-1}$ (Madejova and Komadel, 2001).

Calcium carbonates were found only on sample Lesotho-2012-R8.

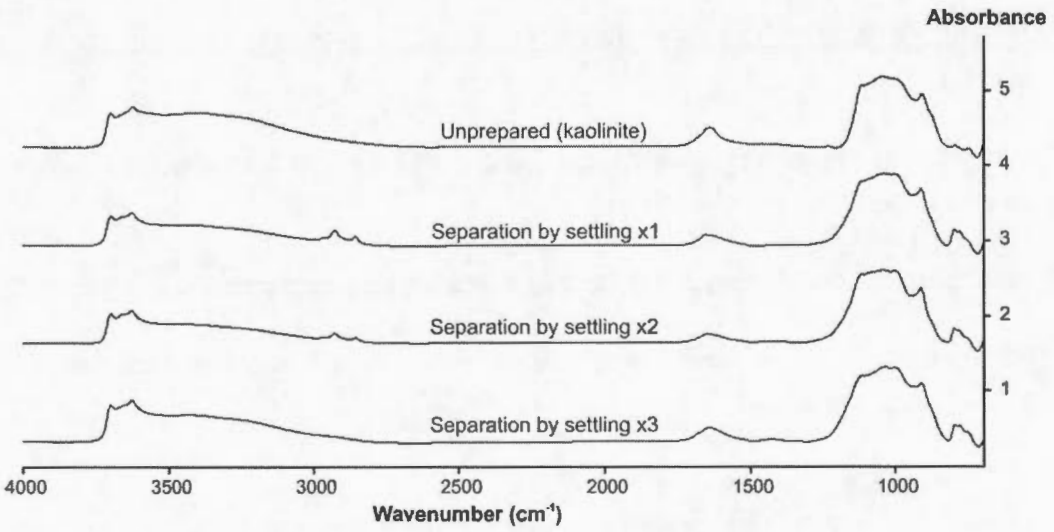


**Figure 3.51** FTIR spectra recorded on red soils from Lesotho

3.2.7.6 Conclusion

The red soils are composed of kaolinite with quartz and feldspars for seven samples, and of illite/montmorillonite for one sample. The colour is given by iron oxides or hydroxides but it was not possible to determine their exact mineralogy.

As for white soils, grinding is not enough to produce a fine-grained paint as found on rock art sites. Separation by settling proves to produce comparable raw material. Moreover, this step, which is thought to be more a cleaning step in the process of the pigment, gives the soil a brighter red colour.

3.2.8 Discussion on paints in the Phuthiatsana Valley, Lesotho

Red, black and white paints were studied from rock art in the Phuthiatsana Valley, Lesotho. The black paints are all carbon-based paints, made with charcoal, soot and three different carbon-blacks. The red paints were made with red ochres (whose colour is given by hematite associated to manganese oxides in some samples), pure hematite mixed with clay, magnetite, manganese oxides, and iron hydroxides. In the case of paints made with the three last components, they exhibit a dark red, even brown colon. Finally, white paints are composed of cremated bones, calcite, gypsum, and two types of clay: hectorite and kaolinite.

This large variety of raw materials used shows the diversity in the paint techniques and in the procurement of pigments. They may be correlated to the presence of different populations who painted at the same time in this valley, or reflect changes in paint techniques through time. The raw materials identified were for some of them previously reported for San rock art in South Africa (Arocena *et al.*, 2008; Bonneau *et al.*, 2012; Prinsloo *et al.*, 2008; Tournié *et al.*, 2011) but it is the first time that a characterization study is conducted on San rock art in Lesotho and which comprises as numerous sites. Preliminary results obtained on a selection of white paints in this valley were published during this PhD (Bonneau *et al.*, 2014). Moreover, it is the first time that cremated bones for white paints, magnetite and manganese oxides for dark red paints and soot for black paints were identified, even if they were thought to be possible pigments according to Rudner (1982).

About red paint, Mapote reported that hematite was burnt before being used for painting. No attempt has been conducted in this PhD to examine the changes in burnt soils but would be investigated in a future project.

Cremated bone-based paints were found only on monochromes white human and antelope figures of unknown tradition and on a polychrome eland attributed to San fine-line tradition (Arthur *et al.*, 2010). As the same recipe, comprising cremated bones and gypsum, was used to paint them, it is possible that they were made by the same population. However, as the style of representations is different, a recipe transmission can be proposed too.

Weathering products encountered are similar to those previously recorded in this Ph.D. on Maclear District sites and from previous studies (Arocena *et al.*, 2008; Bonneau *et al.*, 2012; Prinsloo *et al.*, 2008; Tournié *et al.*, 2011). Interestingly, calcium oxalates do not exhibit the same mineralogy if they are in the paint layer or in the weathering crusts. However, this difference is visible only for black and red paints. The same difference has been reported recently from a site in the Maclear District by Hoerlé *et al.* (2016). It may be related to the binders used to make the paints, but it is impossible to conclude without binder analysis. On the other hand, it is highly possible that this binder has been entirely metabolized by lichens and bacteria to produce calcium oxalates.

Comparison with soils collected in the vicinity of the sites makes it possible to conclude that some raw materials may have been found locally. They were prepared by grinding and cleaning (and separated by settling) to acquire the texture needed to paint. On the other hand, grindstones with red and white stains were found during excavations conducted in the rock shelters. They were analysed by Luiseach Nic Eoin, as part of her Ph.D. at the University of Oxford (Ph.D. completed in September 2015; Nic Eoin, 2015).

Characterization of red stains on grindstones from Aral 175 (also called Ha Makotoko) was conducted by Luiseach Nic Eoin following the same protocol as used in this study for rock paintings (detailed in chapter II). It makes it possible to detach similarities in composition between red stains on one grindstone (L194) and three elands painted in the rock-shelter. They all presented a flaky texture with titanium as minor element linked to iron and a hematite type 2 Raman spectrum. This study shows that it is possible to discuss and correlate rock art with painted remains excavated. It needs more methodological development and extension to more objects and sites, but discussion about the process of raw materials before using them for paintings can now be further developed.

Following these characterization results, some steps of the *chaîne opératoire* of the sites can be detailed. First, the rock surface does not seem to have been prepared, even if a few white paints were found directly on the rock surface which may be due to removal of the white natural crust of the rock. The rock naturally exhibits a white thick layer at its surface, which acts as a preparation layer. This layer is not homogeneous through one single site, and a selection of specific places to paint is likely to have been done. About black paints, charcoal can be found in nature or can be easily collected from fires. Soot and carbon-blacks are more complicated to find in nature, even if it is always possible to collect them after fire woods. However, it is more likely that they were manufactured. Soot can be obtained by maintaining a rock, ceramic, or shell above fire. Soot will accumulate at its surface and it can be easily removed with a sharped tool. Carbon-blacks are the results of incomplete combustion of an organic compound, and can be made by burning fat, resin or sap in a recipient on a fire. About white paints, kaolinite can be found in the vicinity of the sites as showed by the analysis on soils collected a few kilometres around the sites. Hectorite, another type of clay, was recorded and not found during analysis. However, only eight samples were collected and

an extensive collection would be required to better estimate the local clay resources. Gypsum is a common mineral in the Main Karoo Basin (Johnson *et al.*, 2006) but is found at the surface of the rock too. Calcite can be found from shells and eggs, but is, as gypsum, a common mineral in the Main Karoo Basin (Johnson *et al.*, 2006). Finally cremated bones are made by burning bones close to fire for several hours. They were all found mixed with gypsum. Red paints are made either with red ochres, or with pure hematite mixed with clay. The red ochres observed are similar to the red soils collected in the vicinity of the sites and may be the sources of raw materials. Concerning "pure" hematite, it was not possible to find distinctive minerals as augite, found previously at RSA TYN2, and indicating provenance of the mineral (Bonneau *et al.*, 2011). As for magnetite and manganese oxides, their origin is not established, even if these minerals are common ones in the Drakensberg (Johnson *et al.*, 2006). White and red soils once collected need to be grinded, cleaned and separated by settling to get a texture similar to the ones observed on rock paintings. Finally once all the raw materials are processed, they are mixed with a liquid binder and applied with a brush or a similar tool in the case of San fine-line tradition; black being the last colour to be painted. Concerning Basotho black paints, made with charcoal, a piece of charcoal may have been used to draw the figures directly on the rock face. Then, weathering starts with the action of lichens, bacteria, rain and wind, producing calcium oxalates, calcium sulphates, and clay and depositing aerosol particles. Fires made in the rock shelters brought time to time soot on top of the figures.

Which of these paintings are suitable for dating? All carbon-based paintings that is to say charcoal, soot, carbon-blacks, cremated bones and calcite paintings may be suitable for radiocarbon dating. In the case of charcoal, the date obtained will be the date of the death of the tree, and not the date of the paintings. It will thus produce a maximum age. Concerning soot and carbon-blacks, as detailed above, they are more likely to have been manufactured by humans and thus will reveal the age of the paintings. However, Raman spectra obtained with the green laser showing weak amorphous carbon peaks, if not at all, and microscopic observations showing scattered black particles point to a very low proportion of carbon in these samples. Moreover, at Aral 166, particles of soot were identified at the surface of the

paint which may be due to posterior fires in the shelter. Samples from Aral 166 were not submitted for radiocarbon dating.

Cremated bones and calcite contain carbon but dating them should be a problem. Calcium carbonates from cremated bones are dated by radiocarbon but the rock itself contains calcium carbonates and they occur as weathering products too. It would thus not be possible to distinguish those from the cremated bones from those from rock or weathering products. The same problem occurs for calcite and moreover, the source of this calcite is not known. Calcite coming from egg or shell might be dated but the problem of calcium carbonates naturally present in the rock is still present. Thus they were not taking for radiocarbon dating.

In the case of OSL dating, thick dark red paint layers were found and should be good candidates for experimentations. Moreover, they are fine-grained with few quartz and feldspars grains which should prevent reflection and transmit light through the paint layer.

## 3.3 The Thune Valley, Botswana

In the Thune Valley, 56 paint samples were collected. 11 were black paint samples, 1 white paint sample, 1 green paint sample, and 43 red/dark red paint samples. Out of these samples, only the black paint samples were characterized because they were the most likely to content carbon-based pigments, and thus being datable with radiocarbon.

### 3.3.1 Rock and surface preparation

Paintings in the Thune Valley are found on sandstone from the upper part of the "Red beds", and on the Lebung series sandstone. Its composition is similar to Clarens Formation sandstone, but it contains high proportion of iron giving an orange or red hue to the rock (Johnson *et al.*, 1996). No study detailed surface alterations of this rock. They are expected to be similar as those encountered in sites in South Africa and Lesotho (clay, calcium sulphates, calcium oxalates).

Characterization of the rock support from one site and from samples of paint collected as detached flakes of rocks was conducted. White to orange layers or grey layers are found at the surface of the rock. It is composed of calcium sulphates, clay and feroxyhyte. This last

compound may be responsible for the grey colour. Eolian deposits under the form of quartz and feldspars (about 10-20 µm diam.) were observed too.

The rock itself is composed of quartz and K-feldspars in a matrix composed of calcium and iron. No albite or plagioclase was identified. Their size is between 50 and 200 µm diam. with the majority about 100 µm diam. Quartz are predominant in the rock, about 80% of the rock, K-feldspars being the other 20%. It has not been possible to determine the exact mineralogy of the K-feldspars composing the rock.

No preparation of the rock surface is visible. However, all the paintings were realized on the white or grey weathering crust visible at the surface of the rock and which may act as a preparation layer for the artists.

### 3.3.2 Black paints

#### 3.3.2.1 Microscope

Samples were first observed unprepared under the microscope with a magnification of x100 and x500. Two textures were observed: a fine-grained texture composed of tiny crystals, and a smooth texture composed of a uniform layer of paint (no grain can be seen even at x500 magnification) (Figure 3.52). The smooth texture was observed only on one sample (TD2-2012-21) collected on a human figure.

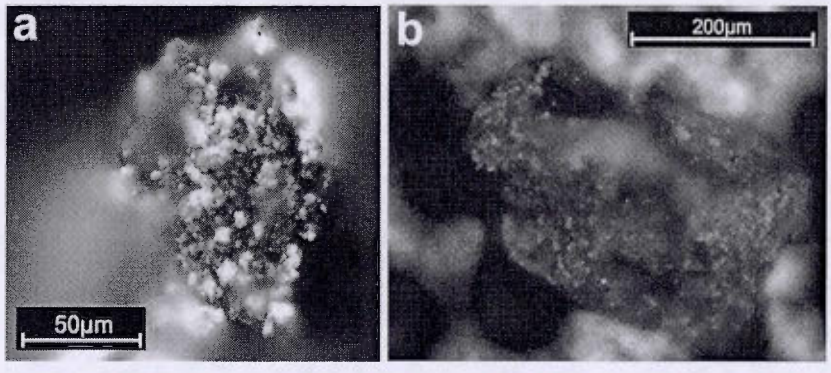


**Figure 3.52** Microscope images of black paints from the Thune Valley site, Botswana: a) fine-grained texture, b) smooth texture

All samples were mounted in cross-sections.

In cross-section, the black layers appear all with a fine-grained texture (Figure 3.53). They are from 10 µm to 200 µm thick. The thickness of the black layer is highly variable even in the same cross-section, reflecting the asperities of the rock support. The average is between 50 and 100 µm thick. The colour of the black layer is homogeneous except sample TD2-2012-19 which looks more grey than black. It may be intentional as the fish colour *in-situ* is grey too. White grains are seen in the black layer giving the grey colour.

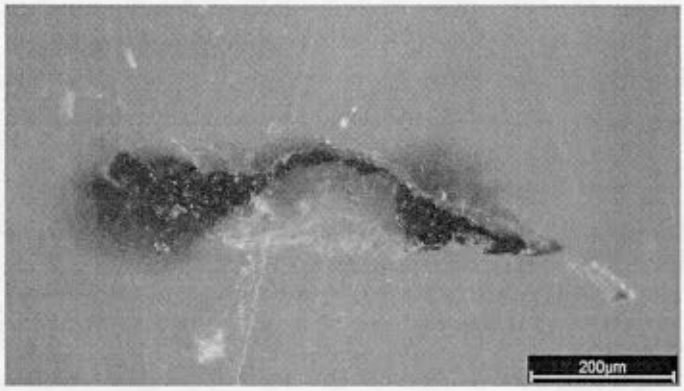


**Figure 3.53** Microscope image of black paint sample from the Thune Valley, mounted in cross-section

Red layer (1) and white layers (2) are present underneath the black layer. They are paints from the adjacent part of the figures. It reveals that in those cases, the black layer was made after the other colours.

3.3.2.2 SEM-EDS

The black layers show four different textures under SEM: a smooth texture (1), small balls about 0.5 µm diam. (2), a fine-flaky texture with flakes about 0.5 to 1 µm diam. (6), and a flaky-texture with flakes about 5 µm diam. (5) (Figure 3.54). None of them present the texture of charcoal. The small ball texture is similar to the texture recorded on soot (Tomasini *et al.*, 2012).

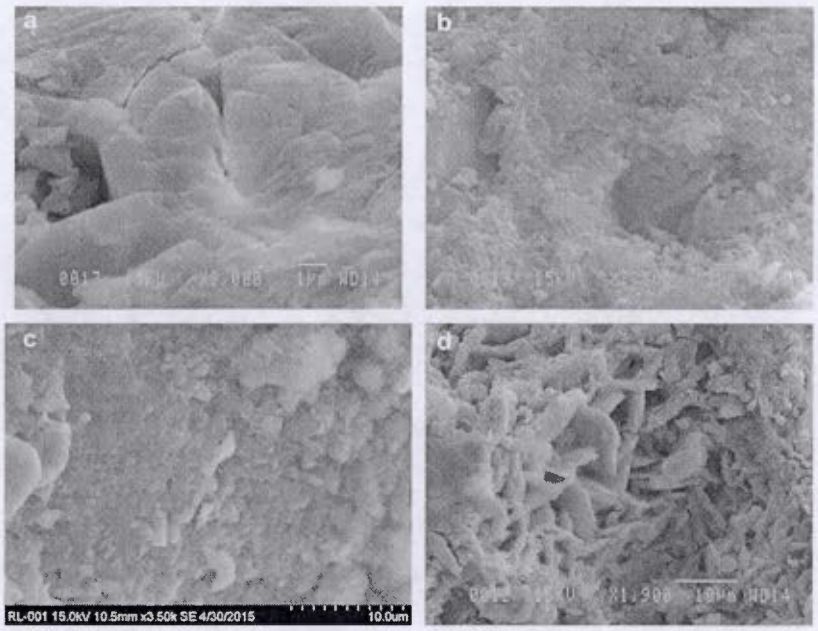


**Figure 3.54** Textures recorded on black samples from the Thune Valley (secondary electron images): a) smooth texture, b) small balls, c) fine-flaky texture, d) flaky texture

On all the samples, carbon has been recorded as the main component of the black layer. Calcium and sulphur were found too, and are identified as calcium carbonates, calcium sulphates and calcium oxalates. Cubic grains, long grains and small round grains were observed in and around the black layer.

On sample TD21-2012-2, a high proportion of phosphorus has been recorded. It was difficult to see on unprepared samples if it was related to carbon or not. EDS analysis from the cross-section showed that phosphorus is linked to calcium and not to carbon (Figure 3.55). It is spread around the black paint layer (on top and underneath), but is very little present in the paint layer itself. Thus phosphorus can be seen as a weathering product, under the form of phosphorus salts.

Sodium, aluminium, silicon, potassium, titanium and iron were found on each sample and are linked to the rock support of the paint or to aerosol particles.

In cross-section, all the black paint layers were found to be composed of carbon and calcium. The calcium comes doubtless from calcium oxalates, as weathering products. In two samples, TD12-2012-8 and TD12-2012-9, weak peaks of aluminium, silicon and phosphorus were recorded. They are attributed to weathering too.

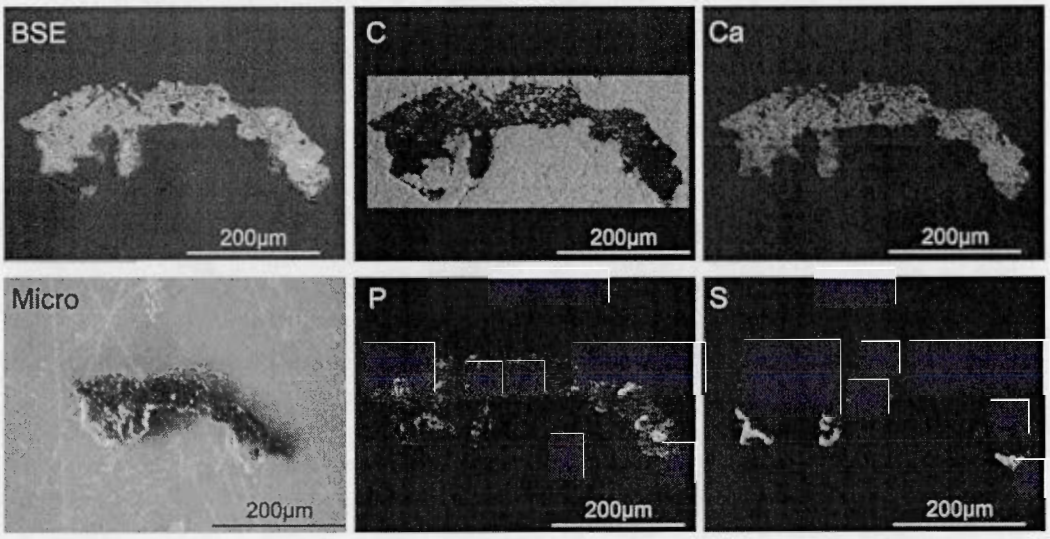


**Figure 3.55** Elemental map on a black paint from the Thune Valley, mounted in cross-section

3.3.2.3 Raman spectroscopy

Samples were analysed with both green (514 nm) and near-infrared (785 nm) lasers. Peaks of amorphous carbon were recorded on all samples with both lasers. Spectra were categorized as detailed previously in §3.1.2.3.

First, spectra recorded on unprepared samples are presented. With the green laser, all samples show type 1 spectra, whereas with near-IR laser, all samples show type 3 spectra. It was not possible to get a proper spectrum with the green laser on 5 samples: TD2-2012-1, TD2-2012-20, TD2-2012-21, TD12-2012-6, and TD21-2012-2. As explained previously (§3.1.2.3), this difference in the shape of spectra is due to the type of excitation used and thus to the type of bonds excited.

Peaks at 1260, 1312, and 1625 $cm^{-1}$, which can be linked to clayish minerals were recorded in TD2-2012-21. No other paint was observed around the black layer, which seems to point to an intentional admixture made by the artists. However, EDS mapping realized on the cross-section reveal that a layer of silicon and aluminium in present on top of this sample, and may be the source of the clay peaks recorded.

In cross-section, all samples presented amorphous carbon with a type 1 shape with the 514 nm laser and amorphous carbon with a type 3 shape with the 785 nm laser (Figure 3.56).

Clay has been identified in two samples, TD2-2012-21 and TD12-2012-7.

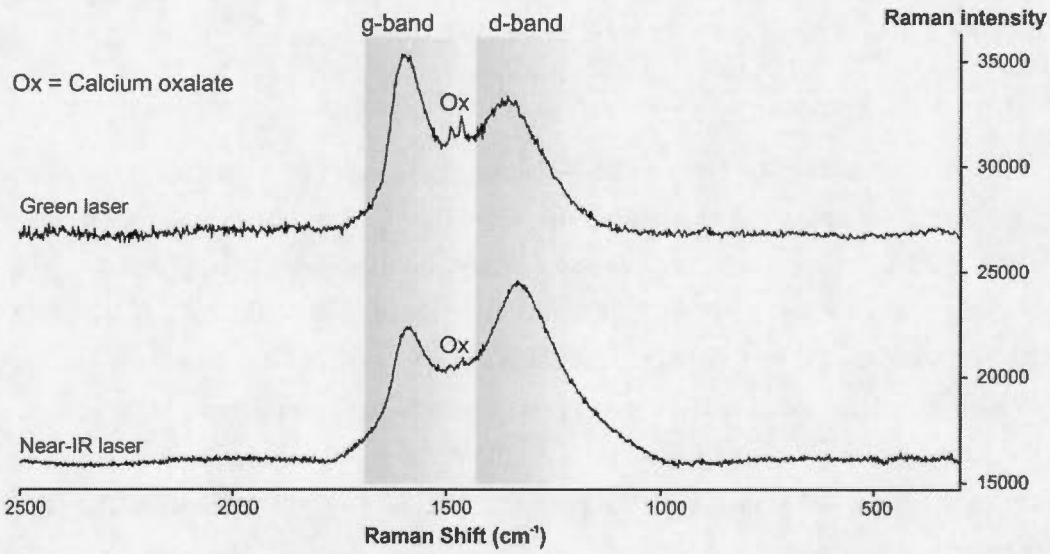


**Figure 3.56** Raman spectra recorded on black paints from the Thune Valley sites, Botswana

D and g-bands of carbon were deconvoluted using Grams using the same parameters as mentioned in §3.1.2.3.

With laser 785 nm, the d-band varies from 1322 and 1333 $cm^{-1}$ on unprepared samples and from 1321 to 1335 $cm^{-1}$ on cross-section. The g-band oscillates from 1586 to 1596 $cm^{-1}$ on unprepared samples, and from 1586 to 1600 $cm^{-1}$ on cross-section.

With laser 514 nm, the d-band varies from 1351 and 1364 $cm^{-1}$ on unprepared samples and from 1349 to 1361 $cm^{-1}$ on cross-section. The g-band oscillates from 1599 to 1608 $cm^{-1}$ on unprepared samples, and from 1592 to 1608 $cm^{-1}$ on cross-section.

These results are homogeneous whatever the preparation of the sample which points to a single type of pigments and to absence of posterior pollution by fires for example. Using data from positions, area and intensity of each peak, principal components analysis were carried out with JMP to see if any sub-group was distinguishable, with no successful results. The spectra recorded on the Botswana samples are homogeneous.

If compare to the study of carbonaceous matter by Coccato *et al.* (2015), the spectra recorded are attributed to charcoal and other flame carbons of different origins.

3.3.2.4 FTIR spectroscopy

Peaks at 914, 1004, 1033, 1107 $cm^{-1}$ associated to Si-O and Al-O bonds, and at 3620 and 3697 $cm^{-1}$ associated to OH stretching modes are present in all the samples, but they were not all recorded on the same spectrum. They are linked to the presence of quartz, feldspars and/or clayish materials. Except samples TD2-2012-20, TD12-2012-5, TD12-2012-6, and TD21-2012-3, were peaks are doubtless associated to clay and more precisely to kaolinite (Madejova and Komadel, 2001), it is not possible to give a final attribution to the peaks on the other spectra. These minerals can come from the rock, such as kaolinite has been observed in degraded sandstone (Johnson *et al.*, 2006), or may be intentional addition from the artists.

Peaks at 2770, 2856, and 2927 $cm^{-1}$ are present in all samples except three (TD2-2012-1, TD12-2012-7, TD12-2012-9). They are attributed to residues of methanol used to clean diamond micro-compression cells.

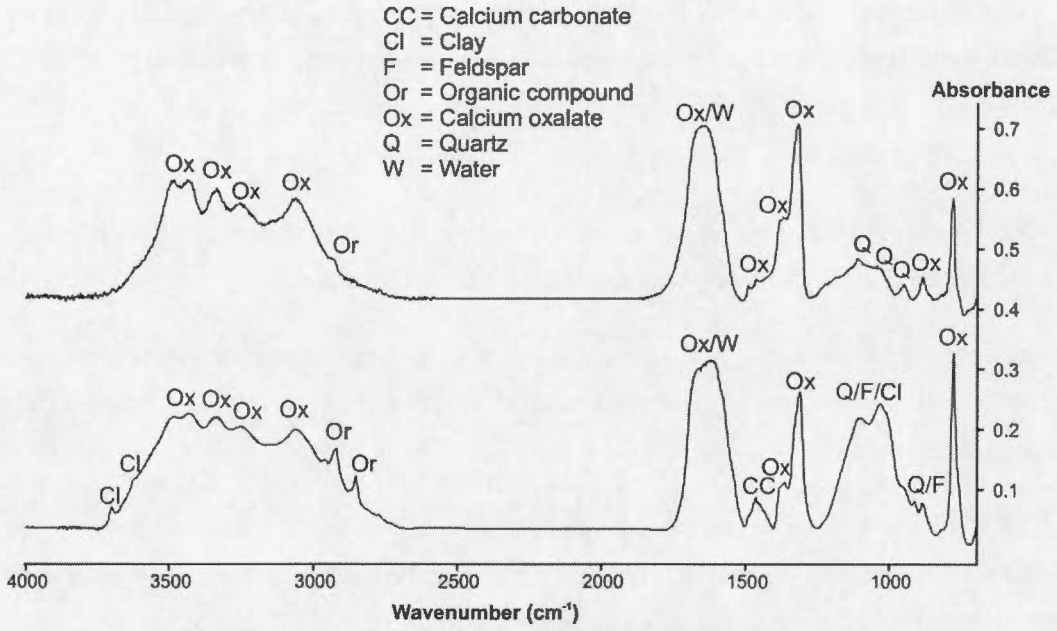


**Figure 3.57** FTIR spectra recorded on black paints from the Thune Valley sites, Botswana

3.3.2.5 Conclusion

The morphology of the black paint as flakes, the presence of carbon under EDS analyses and the presence of peaks of flame carbons with Raman analysis prove that 9 of the black paints are made of carbon-blacks, that is to say incomplete combustion of organic compounds such as fat, resin, wax, etc.

In the case of the two others, TD2-2012-19 and TD2-2012-21, whose morphology is as small balls, they are made of soot.

It is interesting to note that the morphology of the black paint under SEM is homogeneous in site TD12 with a fine-flaky texture, and in site TD21 with a flaky-texture, whereas site TD2 presents three different textures. It may reveal different periods of use of the site.

3.3.3 Weathering products and alterations

3.3.3.1 Microscope

Two samples from sites TD12 and TD21 present a thick orange/yellow layer on top of the black paint layer. They can be correlated to orange, red, white and yellow crystals which appear on top of the black paint layers in all the other samples and which are likely to be due to weathering alterations. These are present on the rock face too.

Under the black paint layer, an orange to yellow layer, thicker than the one observed on top of the layer, is present and may be a degradation crust from the rock.

Observations of the cross-sections show that on top of the black layer, a thin transparent layer (about 5-10 µm thick) is present on 3 samples (TD21-2012-3, TD21-2012-2, and TD12-2012-6).

Under the black layer, a weathering crust is present with colours from white/yellow to orange. It is between 50 and 100 µm thick but it may be thicker such as the samples were taken to get the pigment itself and not the entire crust underneath (Figure 3.58).

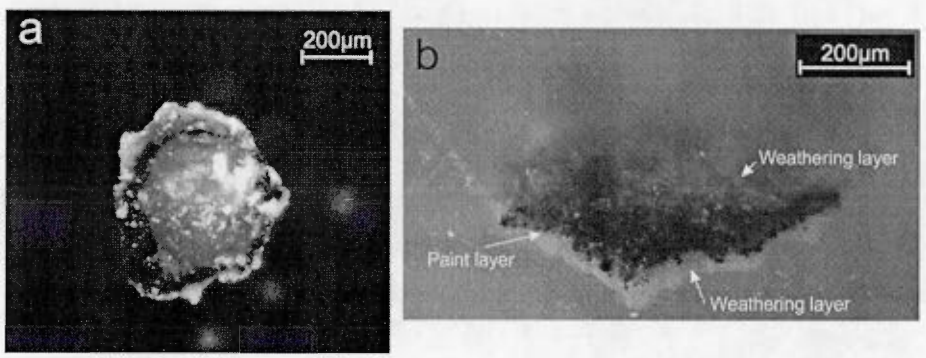


**Figure 3.58** Microscope observations of weathering products in black samples from the Thune Valley sites, Botswana: a) unprepared, b) cross-section

3.3.3.2 SEM-EDS

High proportion of magnesium was recorded on two samples, TD2-2012-1 and TD2-2012-21, which may be linked to hydromagnesite, a weathering product found previously on South African rock art (Bonneau *et al.*, 2012; Tournié *et al.*, 2011).

Magnesium, phosphorus, chlorine, and sulphur were recorded on all the samples and are identified as weathering products.

High proportion of phosphorus was found linked to calcium in TD21-2012-2, and high proportion of sulphur in TD12-2012-8. The presence of long crystals composed of sulphur and calcium in this sample points to calcium sulphates.

Aluminium and silicon are attributed to clayish minerals which are naturally weathering products of the rock (Johnson *et al.*, 2006).

In cross-section, on top of the black layer, a thin layer (5 to 10 µm thick) composed of calcium, or silicon, calcium and magnesium, or only silicon has been observed on 5 samples. Underneath the black paint, a weathering layer composed of aluminium, silicon, calcium, magnesium and phosphorus has been recorded with locally, the presence of sulphur concentrates in crystals. Grains composed of silicon (quartz) and of aluminium and silicon (feldspars) were observed too and are attributed to the rock support.

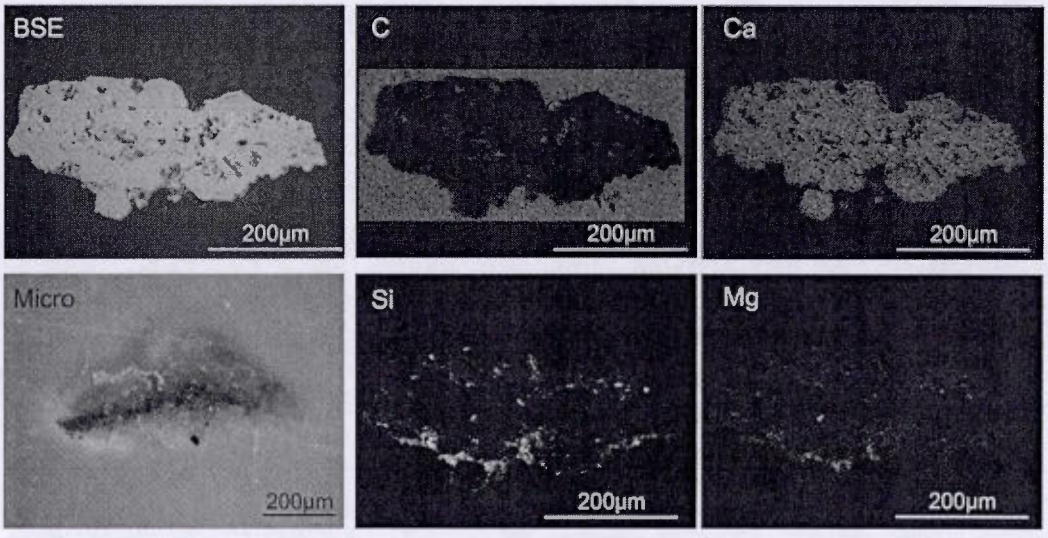


**Figure 3.59** Elemental maps on a black paint from the Thune Valley sites, mounted in cross-section

3.3.3.3 Raman spectroscopy

With the green laser, calcium oxalates (whewellite) were recorded on all samples, except TD21-2012-3.

With the near-IR laser, calcium oxalates (whewellite) were identified in TD2-2012-21, TD12-2012-6, and TD21-2012-2, and gypsum in TD12-2012-6, and TD21-2012-2.

With the green laser, on cross-sections, two series of peaks of calcium oxalates were recorded in the paint and surrounding weathering layers. They are attributed to whewellite and weddellite. Gypsum was recorded on sample TD21-2012-2.

With the near-IR laser, the same two series of peaks for calcium oxalates were recorded.

Sample TD21-2012-2 exhibits a peak at 963 $cm^{-1}$ linked to the presence of $PO_4$, in the white layer underneath the black layer. It is attributed to phosphorus salt.

3.3.3.4 FTIR spectroscopy

All the 11 samples contain calcium oxalates in high quantity (from 50 to 90% of the compounds recorded). For three samples, TD2-2012-1, TD12-2012-7, TD12-2012-9, peaks of calcium oxalates were almost the only ones recorded. Peaks of feldspars, quartz and calcium carbonates were found but are very weak.

Calcium carbonates were recorded on three samples (TD21-2012-2, TD21-2012-3, and TD2-2012-1). They can be seen as weathering products, matrix from the rock, or in the case of the two first mentioned samples, as part of the clay, however, in this last case, the peaks should be more intense than recorded.

Calcium sulphates were identified only on the two samples from TD21. Its presence may be explained by the shape of this shelter, which his more cave-like than a shelter, thus the weathering products may be different. Calcium carbonates are present in this site too.

A peak at 1684 $cm^{-1}$ was recorded on TD12-2012-8. This peak can be attributed to OH-deformation of water previously recorded at the surface of the rock.

The presence of clay has been observed in 6 samples. Peaks were attributed to kaolinite for samples TD2-2012-20, TD12-2012-5, TD12-2012-6, and TD21-2012-3.

#### 3.3.3.5 Conclusion

In conclusion, weathering crusts have been mostly observed underneath the paint layer were they are the thickest but thin crusts are present on top of the paint layer in TD12 and TD21. These layers are thinner, about 5-10 µm thick, and are mostly composed of calcium oxalates and clay.

The weathering crust underneath the paint layer is composed of clay, mostly kaolinite, with calcium oxalates, calcium carbonates and gypsum. Phosphorus salts were recorded only in sample TD21-2012-2, located in a kind of cave and less exposed to weathering. Phosphorus may come from dripping waters on thermites nests, observed at the roof of the "cave".

The presence of magnesium has been recorded too but its exact mineralogy has not been found. It can be hydromagnesite, as this weathering product has been previously recorded on San rock art in South Africa (Bonneau *et al.*, 2012; Tournié *et al.*, 2011) and in this Ph.D. on other southern African sites.

In the black layer, only calcium oxalates were recorded. They are weathering products made by lichens and bacteria. The fact that both whewellite and weddellite were found, points to weathering products and not to intentional addition by the artists such as previously postulated by Arocena *et al.* (2008) for San paintings in South Africa.

### 3.3.4 Discussion about paints in Botswana

Carbon-black and soot were identified as the pigments used to make black paints in three sites of the Thune Dam valley. These kinds of pigments have been previously reported as possibilities in Rudner's studies (1982, 1983) but no chemical study of black paintings have been reported on San rock art in Botswana until now.

Even carbon-blacks were previously identified in San rock art (Bonneau *et al.*, 2012), it is the first time that soot is identified.

Black paints are homogeneous within one site in TD12 and TD21, but not in TD2. However, in this last site, the black paints are homogeneous within one panel which points to homogeneity in the pigments used. It may be correlated to different periods of use of the rock-shelters.

The black paints studied here were all applied on top of other colours when the representations were polychrome. Only three examples were found here, but in those cases, it proved that the black colour was the last one to be added.

Weathering products identified are mostly calcium oxalates with depending on sites and panels, calcium carbonates, gypsum, phosphorus salts and possibly hydromagnesite. All of them have been previously reported on San rock art in South Africa (Bonneau *et al.*, 2012; Hall *et al.*, 2007; Hoerlé, 2005; Prinsloo *et al.*, 2008; Tournié *et al.*, 2011). The main difference with South Africa sites is the predominance of calcium oxalates against gypsum and calcium sulphates more generally. It may be due to differences in the weather. Indeed, the Kalahari Desert is less humid that the Drakensberg Mountains, bringing less rain and less acidic rain needed to the formation of calcium sulphates.

Using all of these results, it is possible to give some steps of the *chaîne opératoire* used to realize these paintings. First, the rock chosen has got a white or grey layer on top. The surface does not seem to have been prepared as a natural layer in found at its surface, and acts perfectly as preparation layer. Then the black paints are made from soot, possibly collected by putting a piece of rock or shell or egg on top of a fire, or from carbon-blacks, made by burning organic compounds. Three different morphologies were observed which may be linked to three different compounds burnt, but it is not possible to give more details. Paint is finished by adding a liquid binder and applied on the rock surface doubtless with a brush, looking at the details of the representations. Black paint is applied at the end when polychrome figures are realized. Then lichens, bacteria, rain, etc. with time degrade paints and binders which results in the formation of calcium oxalates and calcium sulphates. As rock continues to degrade, clay minerals percolate with rain on top of the paint layers. Finally, aerosol particles are deposited on top of the paint layer too.

These samples are carbon-based and thus can be dated with radiocarbon. The homogeneity of their composition through Raman analysis proves that no further soot or other carbon-based materials has been deposited on the paint layer which would influence the date. Soot samples should be regarded carefully as they are known to contain little carbon. Large samples are needed to get a proper date. It is confirmed by the impossibility to record amorphous carbon peaks during Raman analysis using the green laser. As the sites were about to be flooded by dam construction, samples were collected through the entire figure in each case. The proportion of weathering products as calcium oxalates and calcium carbonates is estimated following the protocol detailed in chapter IV to adjust the chemical pre-treatment.

### 3.3.5 General discussion about paints in southern Africa

Characterization of paint in three different areas of southern Africa shows that the raw materials used to make black, red and white paints are similar. Indeed, all the black paints analysed are carbon-based, and made from charcoal (Maclear district and Lesotho), soot (Lesotho and Botswana) and carbon-blacks. Red and white paints were studied only on sites from Lesotho and South Africa but they reveal similar recipes (Figure 3.60).

Moreover, when reconstructing steps of the *chaîne opératoire* of the sites, the acquisition and the preparation of raw materials to make paint are similar and can in the case of one site in the Phuthiatsana Valley be correlated with a grindstone found during excavations in this rock shelter.

Within one single panel/superposition layer, paintings with the same colour have the same composition. This homogeneity in the type of paints used is useful as it can correlate scenes, panels and sites together indicating a similar recipe for the paint and maybe by extension the same artist(s). This homogeneity can be of great help when superpositions are not present or when they are difficult to interpret.

As carbon-based paints were used to make the paintings, radiocarbon dating can be used. However, radiocarbon contaminants were observed in these samples, the main one being calcium oxalates. Moreover, humic acids and calcium carbonates appear on some samples. They should be removed before any attempt of radiocarbon dating (detailed in Chapter IV).

In the case of OSL dating, red paints in the Phuthiatsana Valley are thick and dark, which might have made a protection for quartz and feldspars grains at the surface of the rock.

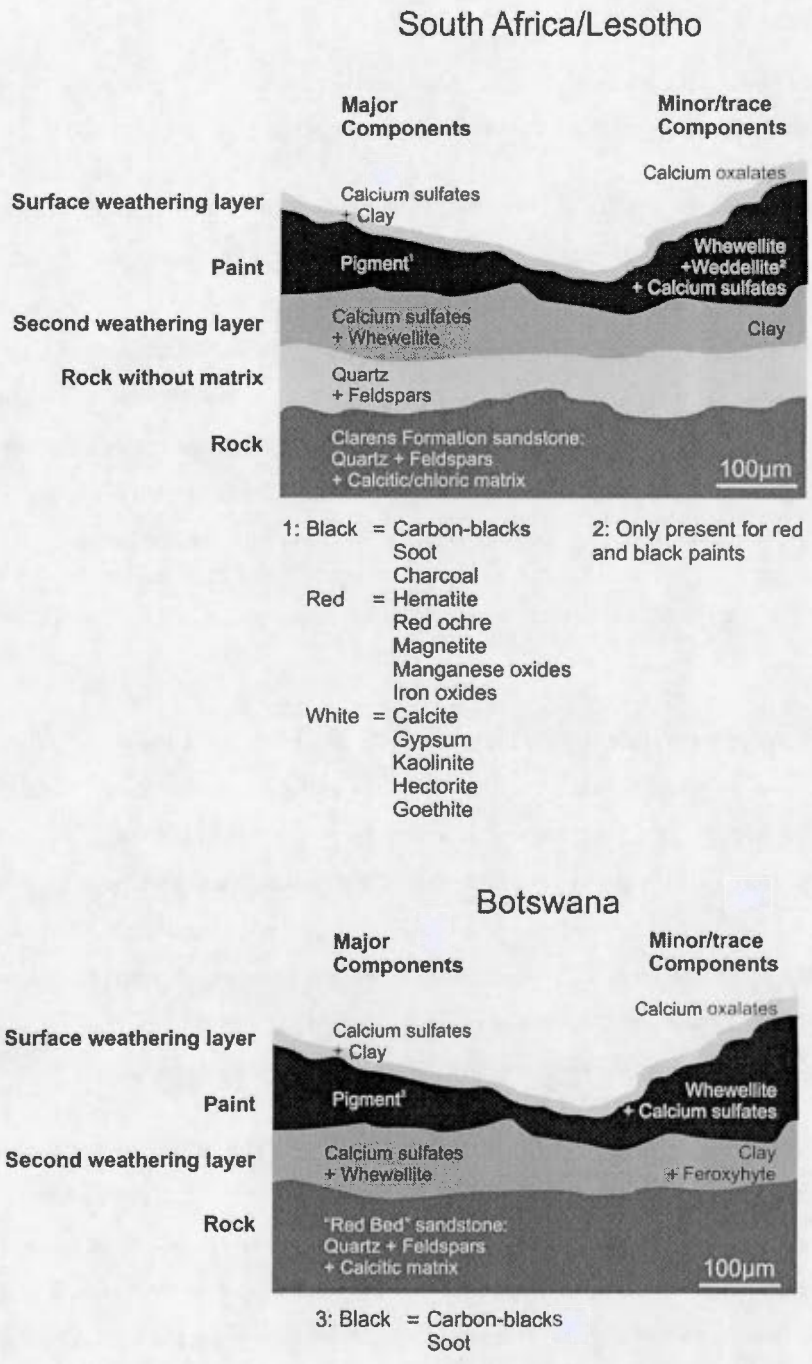


**Figure 3.60** Schematic cross-section of paintings analysed in South Africa, Lesotho and Botswana

## 3.4 Discussion about the characterization protocol

The characterization protocol used in this study is based on the use of complementary instrumentations on samples both unprepared and mounted as polished cross-sections.

The complementarity of the instruments has been proved through this chapter by the possibility to make sub-groups in a single mineralogical or molecular attribution as for carbon-based paint which can be charcoal, soot or carbon-blacks, or for hematite with different geological history, or for clay found to be either kaolinite, or montmorillonite, or hectorite. Carrying out analysis on both unprepared and cross-sections make it possible to distinguish the layers composing the paints, evaluate possible repaints or superpositions, and to track a specific compound such as calcium oxalates. All of these results are of great importance to choose the dating method to apply and to adjust it to the sample.

However, some improvements can be thought for future analysis. They are detailed step by step.

SEM-EDS analysis conducted with the table SEM TM3000 prove to be a great help to make a first selection of samples and to recognize paints composed of charcoal, even if all cannot be identified with it due to its magnification limits. Moreover, this table SEM-EDS provides only backscattered electron images which makes difficult to see the shape of carbon-blacks or iron oxides. The use of conventional SEM-EDS is required and coating cannot be avoided as secondary electrons are needed. In the case of black paints, as the objective is to track carbon, carbon coating should be avoided and gold or another metal preferred. A coating with gold/palladium was available at Université Laval, and thus was the one used.

Elemental maps on cross-sections were added to the protocol at the end of the project with the new acquisition of a Hitachi SEM-EDS, at the Département des Sciences de la Terre et de l'atmosphère, Université du Québec à Montréal. They proved to be extremely useful at tracking chemical elements and complement Raman analysis on cross-sections. Moreover, semi-quantitative analysis can be extracted from them, reducing the operating time. On the other hand, as no external standard was used, large systematic errors (5%) had to be added to the results to cover the uncertainties of the measurement. Adding an external standard

measurement in the protocol would help at reducing these errors and give a more precise estimation of the proportion of each element. However, to select suitable sample for radiocarbon dating and OSL, this protocol is efficient.

Raman analysis on cross-sections raises the problem of interferences of peaks from the resin used. They hide most of the peaks of clay and interfere in the deconvolution realized on carbonaceous matter peaks. On the other hand, the deconvolution did not brought interesting information that can be used to differentiate carbon-blacks or to evaluate their amount of carbon, but it provides information about the homogeneity of the carbon in the paint layer, needed to ensure that the paint was made with a single compound and not with a mixture which would result in an unreliable radiocarbon date. Other resins should be tested to see if their peaks still interfere, but they should be enough porous to maintain the sample during polishing, with very small retraction rate, with a transparent colour, and should dry at room temperature without ultra-violets rays which can alter the paint layer. The use of both green and near-IR lasers proves its importance in recording the different weathering products and components of the paints. However, in the case of clay, the use of infra-red laser would have brought more information about its mineralogical structure.

The use of FTIR analysis was of great help to complement Raman analysis on mineral identification and to estimate the proportion of radiocarbon contaminants but the instrument at the Université de Montréal starts recording spectra from 700 $cm^{-1}$, which prevent from any detailed interpretation of the minerals presents in clay and in the samples themselves as most of the determining peaks for minerals are between 300 and 1000 $cm^{-1}$. A suitable micro-FTIR was used at Parks Canada, for characterization on Canadian rock art (see chapter VI). A similar instrument should be found in the future. On the other hand, the possibility to access micro-FTIR with diamond micro-compression cells helps at reducing the samples needed for FTIR analysis and makes it possible to reproduce analysis when needed.

Each step of this characterization protocol should be done to provide the best characterization possible and thus evaluate the dating method to apply. It proves to be efficient at selecting samples for radiocarbon dating (more details in chapter IV) and at providing enough details about the *chaîne opératoire* to provide information about the techniques of paint to propose

interpretations of the realization of a site when dating methods cannot be applied (see chapter VI).

# CHAPTER IV

# RADIOCARBON DATING ON ROCK ART

This chapter deals with the development of a new protocol to select and prepare rock art samples for radiocarbon dating. Indeed, where the use of radiocarbon to date rock art has been previously applied (Valladas, 2003; Valladas *et al.*, 2001), the choice of samples, the estimation of radiocarbon contaminants, the quantity of sample to be taken, and the chemical pre-treatments vary between studies. In almost every case, if black paints contain carbon, they have been considered as charcoal and treated as such. However, it does not take into account the particularities of sites such as weathering products, adjacent paintings, and repaints, which may influence the date and its interpretation. Thus a careful characterization of the paint and its environment and alterations is needed. Such characterization has been developed in this Ph.D. project along with a model to select and estimate the quantity of sample needed for radiocarbon dating. An adapted chemical pre-treatment to optimize the chance of getting a reliable date with radiocarbon complements this model.

## 4.1 Interpreting characterization results

### 4.1.1 Type of pigment

The characterization protocol comprises optical microscope and SEM observations, along with SEM-EDS, Raman spectroscopy and FTIR spectroscopy analysis on both unprepared samples and cross-sections. Details about each step are given in section 2.3 of chapter II.

Results presented in chapter III show that both black and white paints may be suitable for radiocarbon dating: black being made with carbon-based pigment, and white with cremated bones (for information about the other kinds of pigments identified, please refer to chapter III). These pigments have been found only on southern African rock paintings, and thus only

these are described in this chapter (see chapter VI for more details about Canadian Shield sites).

SEM-EDS observations and analysis, followed by Raman spectroscopy analysis make it possible to identify the type of carbon-based pigment. In this study, the black pigments characterized were mostly found to be carbon-blacks (89 of 101), that is to say an incomplete combustion of an organic compound. Charcoal (6 out of 101) and soot (6 of 101) were identified too. This characterization is essential to interpret the radiocarbon dates obtained. Indeed, if a date is produced from charcoal painting, it will reflect the age of the death of the tree which can potentially be much older than the painting. Thus, the date will provide a maximum age for the paint. On the other hand, dates obtained on carbon black and soot paints will most likely reflect the time of painting. Carbon black may be found in nature but will not survive more than two or three months. Most of the time, this kind of pigments is thought to be made by humans (Garate *et al.*, 2004).

Four white figures, from three different sites in the Phuthiatsana Valley, Lesotho, were found to be made of cremated bones. Just as for charcoal, the use of old bones can be an issue when using such samples for dating. Moreover, Zazzo *et al.* (2009) proved that the carbon dated from cremated bones comes mainly from the original carbonates composing them and that the exchange of carbon with wood is low. Thus the date will reflect the age of the bone (i.e. the date of death of the animal) and not of the paint. However, to date cremated bones, carbon from calcium carbonates is used. In this project, paintings are made on rock with a calcitic matrix and calcium carbonates have also been identified as weathering products. They may bring carbon from other sources to the sample collected, and hence influence the date. Thus, a focus was given to black paints in this study.

Once suitable samples were found for radiocarbon dating, their environment and alterations were characterized to identify possible radiocarbon contaminants.

### 4.1.2 Identification of radiocarbon contaminants

Depending on the areas studied, weathering products surrounding paint layers were similar, even if their repartition and proportions were different between sites. A quick review of the results is given here, and further details can be found in chapter III.

In southern African sites, the most common weathering product found in and surrounding paint layers is calcium oxalates under the form of whewellite ($Ca(C_2O_4).H_2O$) or weddellite ($Ca(C_2O_4).2H_2O$). Calcium sulphates more or less hydrated ($CaSO_4.xH_2O$), calcium carbonates (CaCO3), humic acids, and hydromagnesite ($Mg_5(CO_3)_4(OH)_2.4(H_2O)$) were observed too.

Amongst them, only calcium oxalates, humic acids, hydromagnesite, and calcium carbonates contain carbon and should be removed before radiocarbon dating.

Calcium carbonates are present at the surface of the rock and doubtless come from the rock which has a calcitic matrix. They are few in quantity and their carbon is old carbon linked to the formation of the rock, several millions years ago. On the other hand, they may form as weathering products and include recent carbon.

Calcium oxalates are the results of different processes involving lichens, bacteria, percolating water, rock support and paint binders. In this case, it is impossible to track the provenance of their carbon. Moreover, the presence of the two forms of calcium oxalates in and surrounding the same paint layer proves that several formation processes are involved, and thus several sources of carbon. These calcium oxalates have been previously radiocarbon dated on rock art sites in southern Africa and gave *termini ante-quos* and *post-quos* (Mazel, and Watchman, 1997; Mazel and Watchman, 2003). However, considering the results given by these studies and the debate about the provenance of carbon metabolised, it has been chosen to remove them in this project.

Humic acids come from degradation of the carbon matter making up the paint. Just as for calcium oxalates, the sources of carbon metabolized are multiple and they should be removed prior to radiocarbon dating. On the other hand, the humic fraction containing humic acids, once separated from the paint can be dated too, to see to what degree the initial pigment

sample might have been contaminated (Valladas *et al.*, 2001). However, in our project, the humic fraction is too small and has not been considered.

Using these results a sampling and characterization protocol has been developed to select and collect the samples which are the most likely to be dated by radiocarbon.

### 4.1.3 Selecting the best sample for radiocarbon dating: the characterization protocol step by step and discussion

To avoid extensive sampling which would damage the rock paintings, a two-step strategy has been developed: first, a barely visible sample is collected in-situ. The initial sample is about 0.5 $mm^2$. It is collected from parts of the figure already damaged by weathering with a scalpel cleaned with distilled water and stored in a gelatine capsule. Characterization is carried out on this sample unprepared and in cross-section. Then, based on the results, an estimation of the quantity of paint needed is made and, if agreed by the relevant heritage authority, collected for radiocarbon dating.

The initial sample is about 1 $mm^2$. It is collected from parts of the figure already damaged by weathering. This sample is then analysed unprepared and in cross-section.

Observations under the microscope make it possible to see some eolian deposits, such as soils or sand grains and sometimes charcoal pieces. If charcoal pieces are visible at the surface of the sample, it should be discarded as these may reflect posterior deposition by fire in the rock-shelter, and will thus not reflect the date of the paint.

The cross-section is used to assess the homogeneity of the paint layer and any possible overpainting episodes. These episodes are easily visible most of the time under microscopic observation as two paint layers are visible, separated by a transparent or white layer composed of weathering products. However, in a few cases, this weathering layer is too small to be seen and can be detected only by SEM elemental mapping, conducted later in the characterization protocol. If a layer of repainting is present and if this layer is composed of carbon-based paint then the sample is discarded as the date obtained would be a mixture of the two layers.

In this study, only one sample has multiple layers of repainting composed of carbon-based paint, but 10 black paint layers were found to have red paint layers underneath them.

At this step, the thickness of the paint layer is estimated and the microstratigraphy observed: is the paint made directly on top of the rock? Was there a preparation of the rock surface? Is there a crust or eolian deposits on top of the black layer? All of these details need to be answered since, when collecting the sample, despite taking a lot of precautions, these layers surrounding the paint will be collected too.

Raman spectroscopy is used to identify the components comprising the paint and the surrounding layers. Characterization should be conducted with both green and near-IR lasers to give a complete understanding of the sample, as they do not excite the same chemical bonds.

For a carbon-based paint (i.e. charcoal, carbon-blacks, soot), two broad peaks centred around 1320 and 1590 $cm^{-1}$ are recorded. At this step, the green laser should be preferred as the near-IR laser is able to excite the chemical bonds of organic matter present in the sample, presenting the same peaks, even though they are not part of the paint. Furthermore, if the paint is made of a carbon-based pigment but contains little carbon, as is the case for soot for example, obtaining a spectrum with the green laser would be difficult. Finally, a long exposure to the green laser can burn the sample and amorphous carbon peaks will then appear without correlations with the original paint.

If the paint is not carbon-based, but made of iron oxides, manganese oxides or other minerals, they may not always react to green laser stimulation or to near-IR stimulation (e.g. hematite reacts better to the near-IR laser than to the green laser (Bonneau *et al.* 2012)). As a result, it is necessary to use both lasers to achieve the best characterization possible.

To try to make distinctions between carbon-based paints, deconvolution of the two broad peaks (called the D-band and G-band) is performed following the parameters detailed by Coccato *et al.* (2015): Lorentzian curves are used to model the peaks, a linear baseline is subtracted from 800-1800 $cm^{-1}$, Grams is used as software. The positions of the peaks, their intensity and their area are collected with Grams and treated with Excel. These data do not

make it possible to distinguish carbon-based compounds between carbon-blacks and charcoal. The peaks are too similar for a proper distinction. However, if compared to Coccato *et al.*'s study (2015), the peaks in our study are all in the group for charcoal and flame carbons, which confirms their attribution to carbon-blacks and charcoal, and the absence of graphite, i.e. mineral carbon. In the case of soot, a distinction can be made in a few cases with this deconvolution process as the positions may be slightly different from those of carbon-blacks and charcoal (Figure 4.1). This should, however, be coupled with SEM observations to assess the identification.

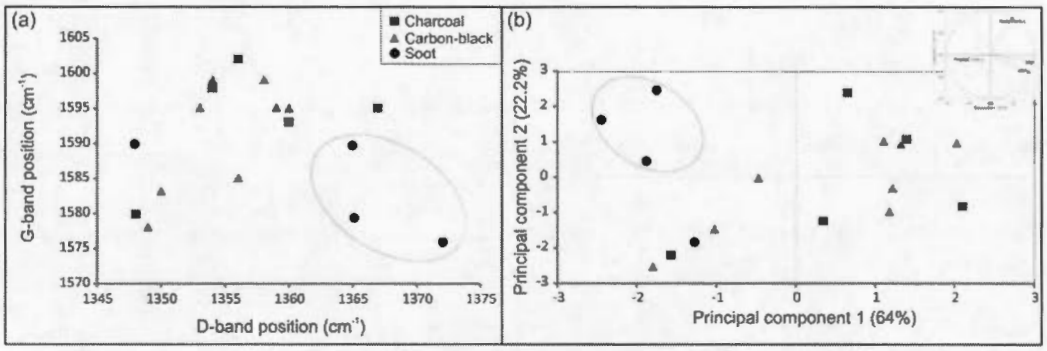


**Figure 4.1** a) D-band Raman peaks plotted against G-band Raman peaks for distinction between soot, charcoal and carbon-blacks (samples from Lesotho; the final identification of the paint was obtained by SEM observations); (b) Principal component analysis of the same samples obtained from D-band position, G-Band position, Area ratio, and Intensity ratio (analysis carried out with JMP)

Nevertheless, the fact that soot may exhibit slightly different peak positions may serve to discard samples contaminated at the surface with soot crusts from firewood, in the event that soot itself was not the pigment used. In this case, data obtained on unprepared samples and samples in cross-sections are compared and should reveal that the results are the same, within 10cm-1, in the positions of peaks, and within 10% in intensity and area ratios. This is considered acceptable and tends to prove that the pigments used are chemically homogeneous with no carbon-based deposits at their surface. Only two samples did not match these requirements and thus were not sampled for 14C dating.

Carbonaceous matter peaks are sometimes influenced by the presence of peaks of clay minerals coming from a thin weathering layer on top of the black paint layer, or from intentional admixtures. These peaks modify the aspect of carbonaceous matter peaks and cannot be separated from them, even with deconvolution. Hence these spectra are discarded for the deconvolution process.

The disadvantage of cross-sections at this step is the presence of epoxy resin that penetrates the sample and sometimes masks carbon peaks. Only spectra without resin peaks were used for deconvolution. On the other hand, analysis of both forms of the sample (raw and cross-section), as previously detailed, allows assessment of the chemical homogeneity of the paint, which is essential for radiocarbon dating.

Peaks may be influenced by the presence of humic acids too, as was the case for the Lesotho samples. There was no way to remove them from the spectra before the deconvolution process, introducing larger errors in the peak positions, intensity and area ratios determined. Luckily, humic acids were present only in a few samples and detected with FTIR spectroscopy analysis, making it possible to have a better understanding of the deconvolution results.

Raman analysis with the green laser makes it possible to estimate the percentage of carbon present in the sample. Indeed, the tests performed, show that if no or only weak peaks of carbonaceous matter are recorded with the green laser, the quantity of carbon present after pre-treatment will be less than 3%.

Raman analysis conducted on the layers surrounding the paint and on the paint itself identifies their components (clay, calcium carbonates, calcium sulphates, calcium oxalates, etc.) and thus determines which should be removed before radiocarbon dating.

SEM-EDS is used for both observations and elemental analysis. Coating should be made with gold or other metals. Carbon coating should be avoided as this element is tracked during analysis.

Elemental analysis and mapping (of cross-sections only) show the repartition of chemical elements in the sample. This provides details about the chemical elements making up the paint and the surrounding layers. If compared to Raman results, this makes it possible to understand the place of each compound and the feasibility of excluding them prior to dating.

Semi-quantitative data on calcium and sulphur were collected from elemental maps. To be able to get reproducible results, maps are taken for 2000 µs per point, in a frame of 512 x 384 pixels, and 10 frames were acquired. If compared with conventional semi-quantitative EDS analysis conducted on the same part of the sample for 300 s, the results are within a 5% error. The proportions of calcium obtained from the different sites range from 2 to 24% (± 2%).

On unprepared samples, the morphology of the particles making up the samples is observed. In the case of carbon-based pigments, it is possible to distinguish between charcoal (long pieces with holes inside), soot (small balls) and carbon-blacks (flakes of different sizes) (Figure 4.2). This distinction has been previously reported by Tomasini *et al.* (2012).

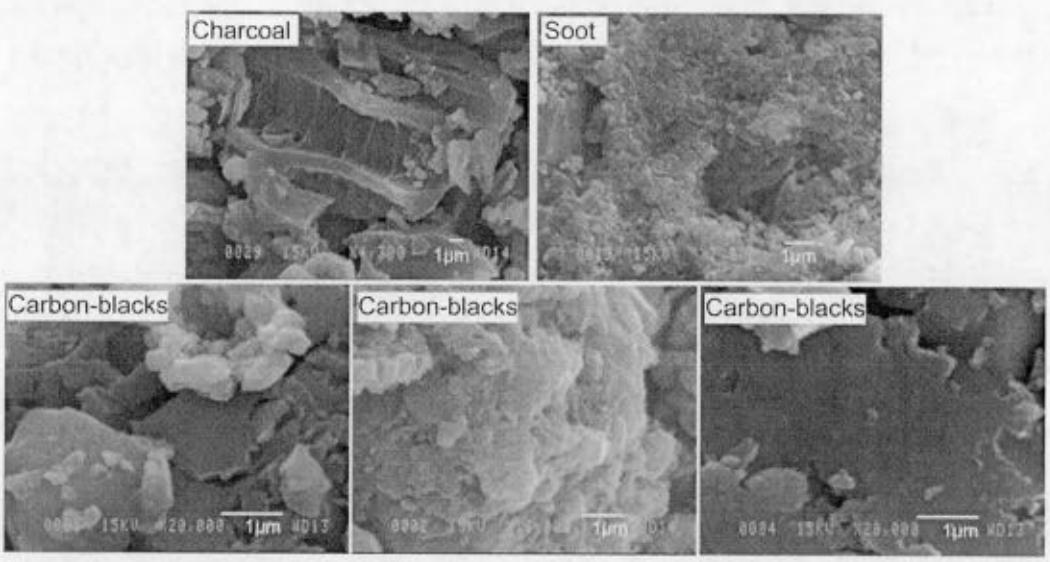


**Figure 4.2** Five different morphologies for carbon-based samples recorded in this thesis (Secondary electron SEM observation)

FTIR analysis is conducted to confirm the presence of radiocarbon contaminants such as calcium oxalates and humic acids, and to give an approximation of their abundance in the sample to be collected.

FTIR analysis, by definition, is quantitative as it compares the absorption of a beam of wavelengths by a sample and a second beam with the same wavelengths without the sample. One needs, however, to take into account the molecular extinction coefficient (ε). It is thus possible to make a ratio between the calcium oxalate peaks, calcium carbonate peaks, and calcium sulphate peaks (the three compounds of the sample containing calcium, the rate of calcium, and sulphur being calculated previously during SEM-EDS analysis).

To calculate this ratio, the absorption of the main Ca-X bond peak of each compound (that is to say, the peak at 1618 $cm^{-1}$ for calcium oxalates, peak at 1114 $cm^{-1}$ for calcium sulphates, and peak at 1400 $cm^{-1}$ for calcium carbonates) is normalized against the sum of the intensities of the three compounds (Equation 4.1):

$$\%_{ox} = \frac{I_{ox}}{(I_{ox} + I_{ca} + I_{sul})} \times 100 \qquad (4.1)$$

where $\%_{ox}$ is the percentage of calcium oxalates in the FTIR spectrum, $A_{ox}$ the absorption of the main peak of calcium oxalates, Aca the absorption of the main peak of calcium carbonates, and $A_{sul}$ is the absorption of the main peak of calcium sulphates. $A_{ox}$, $A_{ca}$, and $A_{sul}$ are calculated by applying the Lambert-Beer law and using molecular extinction coefficients calculated from samples of known concentrations of each compound.

Percentages of each compound are calculated and then the proportion of each of them in the sample is estimated using the proportion of calcium obtained during SEM-EDS analysis (Equation 4.2):

$$P_{ox} = \frac{SEM_{Ca} \times \%_{ox}}{100} \qquad (4.2)$$

where $P_{ox}$ is the percentage of calcium oxalates estimated in the whole sample, $SEM_{Ca}$ is the proportion of calcium obtained with SEM-EDS.

In this project, $P_{ox}$ was used with a systematic error of 20% due to large uncertainties in the determination of the proportion of calcium with SEM-EDS, since no standard was used for semi-quantitative determination.

This determination is made on the whole sample as, when collection of the sample is carried out in-situ, all the surrounding layers will be taken at the same time. Hence, the proportion of calcium may be calculated for each layer composing the sample, but only the result on the whole sample is used. We also chose to conduct FTIR analysis on unprepared samples for the same reasons. Micro-ATR (Attenuated Total Reflectance) germanium may be used to focus on the different layers, but does not reflect the entire composition of the material to be sampled.

Following FTIR analysis, it was possible to determine the proportion of calcium oxalates, calcium sulphates and calcium carbonates in the collected samples: from 2 ± 0.5% to 21 ± 4% for calcium oxalates, from 2 ± 1% to 7 ± 1% for calcium sulphates, and from 2 ± 1% to 4 ± 1% for calcium carbonates.

In the case of humic acids, very weak peaks were observed in just a handful of samples. They are thought to be present in about 5% of the samples, and can be easily removed with NaOH. Thus, no more detailed estimation has been conducted.

Having undertaken all of the stages outlined above, paints, their alterations, and their weathering products are now identified. Following the initial tests conducted (Bonneau et al. 2011), a modified ABA (Acid-Base-Acid) pre-treatment was established. However, to try to reduce the quantity of sample to be taken, tests were further undertaken to adjust the length of each step to avoid as much as possible the loss of sample.

## 4.2 Chemical pre-treatment

Chemical pre-treatment is almost certainly the key element in precision radiocarbon dating.

There are essentially two important questions to be asked of any pre-treatment method (Bronk Ramsey *et al.*, 2004):

- Does the method remove contamination present in the sample (acceptable levels will depend on the relative age of the contaminants but are likely to be <1–5%)?

- Does the method add significant levels of contamination (acceptable levels are <0.1% since $^{14}C$ concentration (i.e. "modern" carbon) is usually radically different)? (For example, a sample containing 10 mg C needs to keep any added contaminants below 10 μg).

To answer the first question, FTIR analyses were conducted on each sample (if large enough) after pre-treatment to assess the absence of the previously recorded radiocarbon contaminants.

To answer the second question, level of residual carbon in tin capsules, iron balls and other tools used during the different steps of radiocarbon preparation were checked with EA-IRMS. They are part of the radiocarbon laboratory routine at the Oxford Radiocarbon Accelerator Unit (ORAU) and gave results within acceptable levels mentioned.

Radiocarbon contaminants found in our samples are: calcium carbonates, humic acids and calcium oxalates. The first two are commonly found in samples from various origins and thus their removal using chemical pre-treatments has been widely studied (Brock *et al.*, 2010). On the other hand, calcium oxalates have received very little attention as they are rarely identified in common radiocarbon samples. During the initial project at the RLAHA/ORAU, preliminary tests were conducted on calcium oxalates and published by Bonneau *et al.* (2011).

Tests conducted in this Ph.D. project aim at reducing the time that samples are immersed in acids and bases while efficiently removing the radiocarbon contaminants. The emphasis was placed on calcium oxalate removal as this was the main contaminant for our samples.

### 4.2.1 Investigations on calcium oxalates

Aliquots of pure calcium oxalates (Calcium Oxalate Monohydrate 98%, ACROS Organics) of different weights (1, 3, 5, 10, 30, 50, 100 mg) were added to sample tubes. 1M HCl is added and samples are left for dissolution in three different conditions: 80°C heating, ultrasonic bath with no heating, and ultrasonic bath at 80°C.

Results are plotted in figure 4.3. They are all very similar to each other. The ultrasonic bath with no heating proves to take a bit more time to dissolve calcium oxalates than heating. The addition of heating to ultrasonic bath produces results similar to only heating. The results follow an exponential curve.

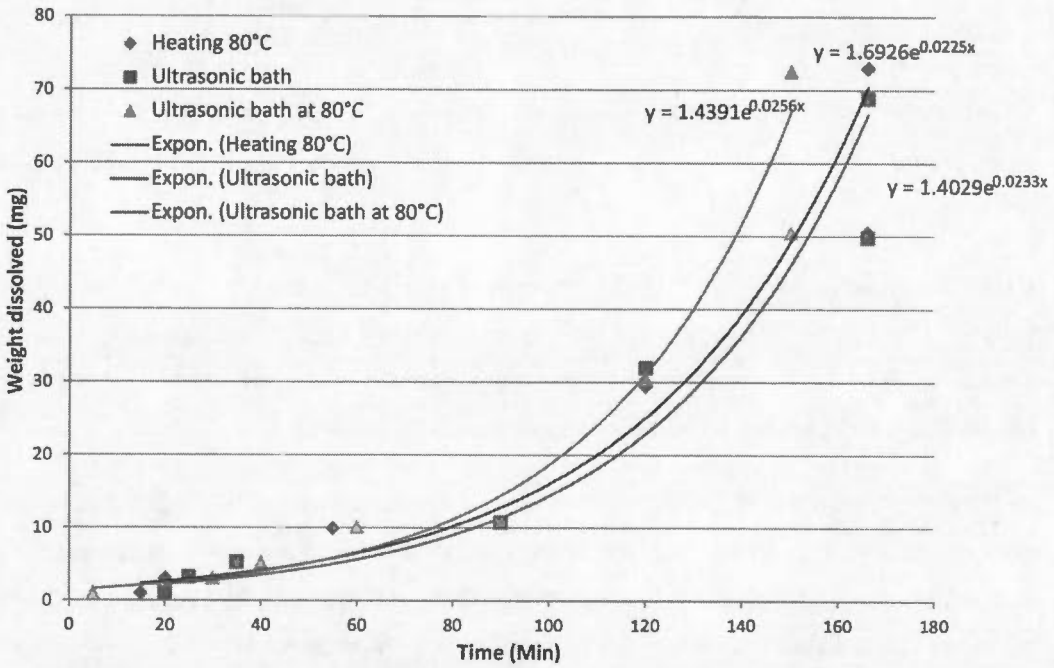


**Figure 4.3** Weight of calcium oxalates dissolved against time in three different conditions (plots include uncertainties)

### 4.2.2 Experiments on artificial mixtures

Tests were conducted on charcoal in 1M HCl to evaluate the impact on carbonaceous matter.

5 mg aliquots of charcoal were prepared in two series of 14 tubes with 1M HCl. The first set was heated at 80°C, whereas the second set was put in an ultrasonic bath at 80°C, for 10 to 120 min.

Then samples were cleaned 3 times with distilled $H_2O$ and weighed. However, when pipetting cleaning distilled water, pieces of charcoal may be taken. Hence, distilled water

used to clean each sample was evaporated and pieces of charcoal present in it weighed too, to make a correction between dissolving and pipetting actions.

Results are plotted in figure 4.4. Results are presented corrected with the proportion of charcoal pipetted that is to say between 0.5 and 2% depending on samples.

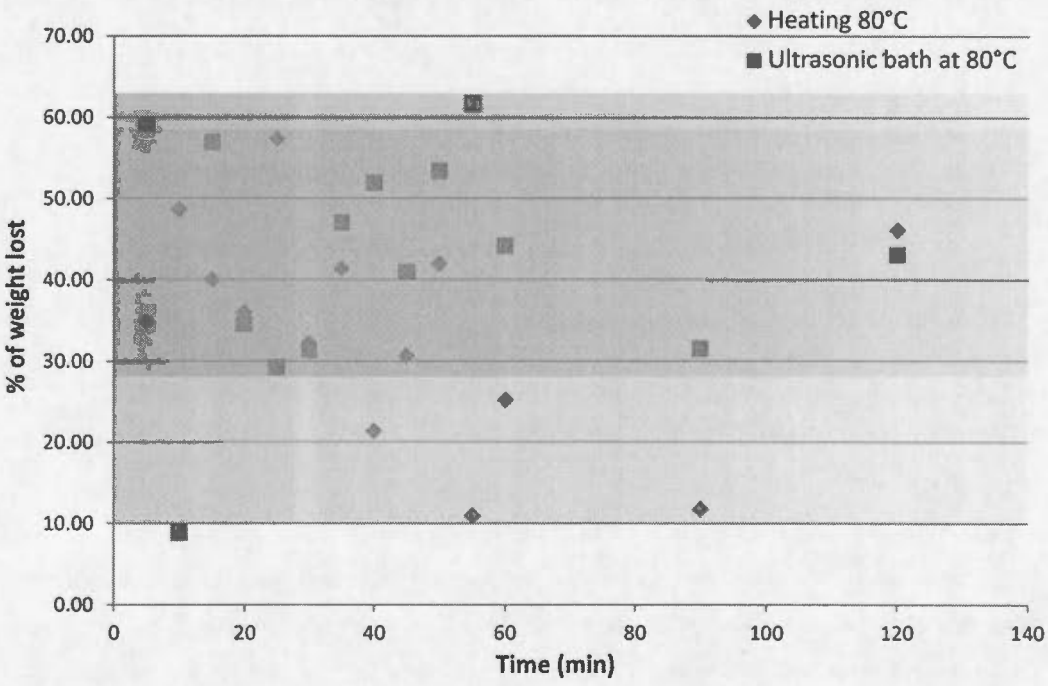


**Figure 4.4** Loss of charcoal during pre-treatment.

Using only heating, the loss of sample is 34 ± 13%, whereas it is 42 ± 14% for the ultrasonic bath with heating, irrespective of time spent in the HCl. This higher loss of sample is due to the permanent moving of the particles which makes the acid more efficient at reacting with them. However, it seems that the impact on calcium oxalates is less than on charcoal, calcium oxalates being more resistant than charcoal to HCl.

Hence to dissolve calcium oxalates, only heating has been chosen.

### 4.2.3 Experiments on real samples and results

46 samples were pre-treated for radiocarbon dating using the following protocol:

- 1M HCl at 80°C for 20 to 90 min depending on the quantity of radiocarbon contaminants estimated.
- Rinsing with ultrapure Milli-Q™ water (Millipore Corp.) until neutrality.
- 0.1 NaOH at room temperature for 10 to 20 min depending on the estimation of the presence of humic acids.
- Rinsing with ultrapure Milli-Q™ water until neutrality.
- 1M HCl at 80°C for 60 min.
- Rinsing with ultrapure Milli-Q™ water until neutrality.

When grains from the rock support were present, they were previously removed physically with a sterile scalpel blade under binocular glass.

FTIR analysis conducted on each of these samples after pre-treatments proves that all of the radiocarbon contaminants were successfully removed, except for sample PRH1-2013-C4. This sample had a high proportion of calcium oxalates and calcium carbonates. A first 1M HCl acidification was conducted for 90 min but was not enough to remove all contaminants, thus this step was repeated with fresh 1M HCl for a further 90 min, and still some contaminants remained. However, these two steps considerably reduce the proportion of carbonaceous matter to be dated. A date was attempted for comparison.

Using this entire pre-treatment protocol and including the sampling of a tiny piece for FTIR analysis, the loss of sample in weight is 61 ± 22%. It is highly dependent upon the proportion of contaminants estimated. For example, from Botswana sites where calcium oxalates represent about 20% of each of the samples, the loss of sample during pre-treatment was more than 70%. Moreover, charcoal and soot seem to be more affected by this pre-treatment than carbon-blacks, maybe due to the difference in the heating process used to manufacture them.

This loss is slightly lower than that reported by Valladas *et al.* (2001): loss of about 90% of the sample during pre-treatment of Paleolithic cave paintings made of charcoal. However, a

part of this loss is due to the presence of humic acids which are extracted to be dated separately.

This pre-treatment leaves us with between 0.05 and 3.8 mg for AMS targets (in the case of the largest samples, targets were reduced to 1.9 mg). Four more samples are less than 10µg of carbon in the AMS targets. They were dated for experimental purposes but the dates obtained are not considered as the level of contamination in them would be extremely high in proportion, compared to conventional targets.

## 4.3 Results and discussion

### 4.3.1 Rock art sample selection model

The characterization and pre-treatment selection model was improved during this Ph.D. Figure 4.5 resumes the different steps of the selection and pre-treatment protocol.

Lesotho and Botswana samples make it possible to test the possibility of obtaining a date even on samples which would not have been chosen by this model. And indeed, these samples resulted in the four dates on extremely small amounts of carbon.

On the other hand, it makes it possible to do replicate dates to assess the reproducibility of our protocol which gives good results on each area studied (see below on dedicated sections for more details on the dates).

Out of 54 samples submitted for the entire project for dating, 7 failed, mostly in the first stages of the project and amongst them 4 would not have been chosen following the model requirements.

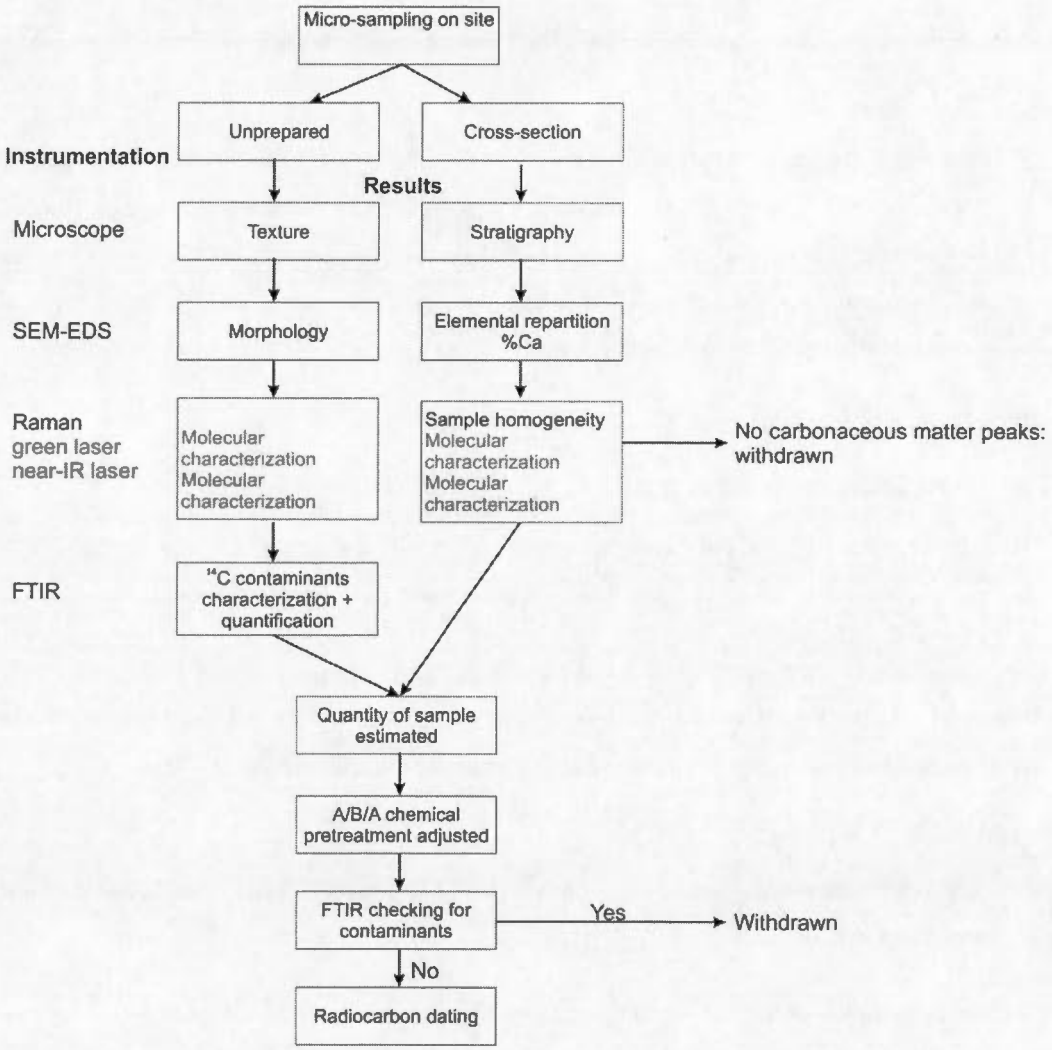


**Figure 4.5** Sample selection and pre-treatment protocol.

Finally, the question arises about the size of the sample to be collected on site. First, to get a radiocarbon date with an acceptable error, ≥ 0.5 mg of carbon is needed for the AMS target. Raman analysis with the green laser makes it possible to estimate the percentage of carbon present in the sample. Indeed, the tests performed, show that if no or weak peaks of carbonaceous matter are recorded with the green laser, the quantity of carbon present after pre-treatment will be less than 3%. In fact, in this study most of the samples used for dating (including the ones for tests) were composed of between 0.5 and 15% of carbon after pre-

treatment. So coming back to the 0.5 mg needed, if 3% of the sample is carbon, it means that the sample after pre-treatment should be at least 17 mg. The pre-treatment removes on average 61% of the sample, and thus the initial sample collected should be 35 mg.

However, it is possible to adjust this estimation, firstly, by using the SEM morphology. Soot samples are those with less carbon and which are the most affected by the chemical pre-treatment. Hence, they would require more than 35 mg of sample. In the case of carbon-blacks with fine-flaky texture, the percentage of carbon is most of the time between 8 and 15% of carbon after pre-treatment, and thus should require less than 35 mg starting weight.

Finally, a proper estimation of the radiocarbon contaminants and the time immersed in acids and bases can reduce the loss of sample to only 40% during pre-treatment. Hence, a sample of 20 mg would be required, which is estimated to an area of 2 to 3cm², depending on the thickness of the paint layer.

This collection area should be discussed with the people in charge of the sites. The use of already damaged parts and collection in the deepest part of the rock should be preferred. Moreover, the integrity of the representation should be maintained (Figure 4.6).

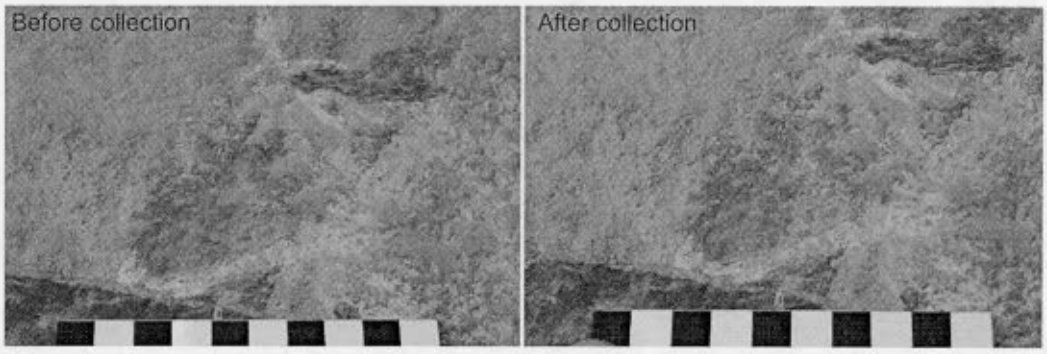


**Figure 4.6** Paintings before and after collection for radiocarbon dating

### 4.3.2 Dates obtained

46 measurements on 42 figures were obtained. Four of these were obtained on AMS targets of less than 10 µg and are therefore the least reliable, but are nevertheless used for discussion purposes. 38 samples were obtained on "very small graphite" targets (that is to say AMS targets < 0.5 mg C), 5 on "small graphite" targets (that is to say AMS targets between 0.5 and 0.9 mg C), and 3 on "large graphite" targets (that is to say AMS targets between 1.6 and 1.9 mg C). Out of the 38 very small graphite determinations, 13 were obtained on AMS targets between 0.05 and 0.1 mg of carbon. The determinations obtained should be treated with high precaution as the effect of contamination is higher.

Dates obtained for each area are detailed in the following sections. All radiocarbon determinations were calibrated using the Southern Hemisphere SHCal13 calibration curve (Hogg *et al.*, 2013) and OxCal v 4.2 software (Bronk-Ramsey, 2009). As the chemical pre-treatment was under development, most of the dates obtained were 'OxA-X-'ed in the ORAU database that is to say that these dates were obtained using an unconventional protocol and thus should be regarded with caution. Moreover, very small graphite dates are automatically 'OxA-X-'ed.

#### 4.3.2.1 Botswana

Nine dates were obtained in Botswana on eight different figures from three sites. They are detailed in table 4.1.

**Table 4.1** Radiocarbon ages obtained in the Thune Valley, Botswana

| Sample | Lab number | Start weight (mg) | % carbon | To AMS (mg) | $\delta^{13}C$ (‰) relative to PDB | Conventional $^{14}C$ age BP (±1σ) | Calibrated age BP (95.4% range) |
|---|---|---|---|---|---|---|---|
| TD12-2012-6 | OxA-X-2555-46 | 17.57 | 0.6 | 0.046 | -25.3 | 4500±260 | 5723-4420 |
| TD12-2012-7 | OxA-X-2555-45 | 19.01 | 2.1 | 0.111 | -25.8 | 2500±100 | 2754-2332 |
| TD12-2012-8 | OxA-29182 | 37.90 | 13.2 | 0.667 | -17.3 | 3060±30 | 3343-3284 (19,1%), 3274-3105 (72,2%), 3096-3077 (4,2%) |
| TD12-2012-9 | OxA-X-2543-6 | 38.10 | 12.8 | 0.882 | -18.4 | 2580±390 | 3593-1712 |
| TD2-2012-1 | OxA-X-2555-49 | 60.10 | 1.0 | 0.386 | -25.0 | 1250±80 | 1276-962 |
| TD2-2012-19 | OxA-X-2555-48 | 30.28 | 4.2 | 0.224 | -22.4 | 2130±90 | 2320-1878 |
| TD2-2012-21 | OxA-X-2555-47 | 19.02 | 2.1 | 0.111 | -23.5 | 2960±160 | 3448-2751 |
| TD21-2012-2 | OxA-X-2555-44 | 7.23 | 16.8 | 0.086 | -26.7 | 2580±130 | 2923-2906 (0,6%), 2891-2327 (94,8%) |
| TD21-2012-3 | OxA-X-2555-43 | 6.06 | 2.1 | 0.048 | -25.1 | 2630±230 | 3325-3296 (0,6%), 3253-2147 (94,5%), 2126-2109 (0,3%) |

*TD 2*

This site is a large, north-facing shelter, approximately 80 m in length.

TD2-2012-1 was collected from a human figure painted in black. TD2-2012-19 was collected from forward of the tail along the dorsal line of a fish painted in black and white. TD2-2012-21 was collected from the torso of a human figure painted in black (Figure 4.7).

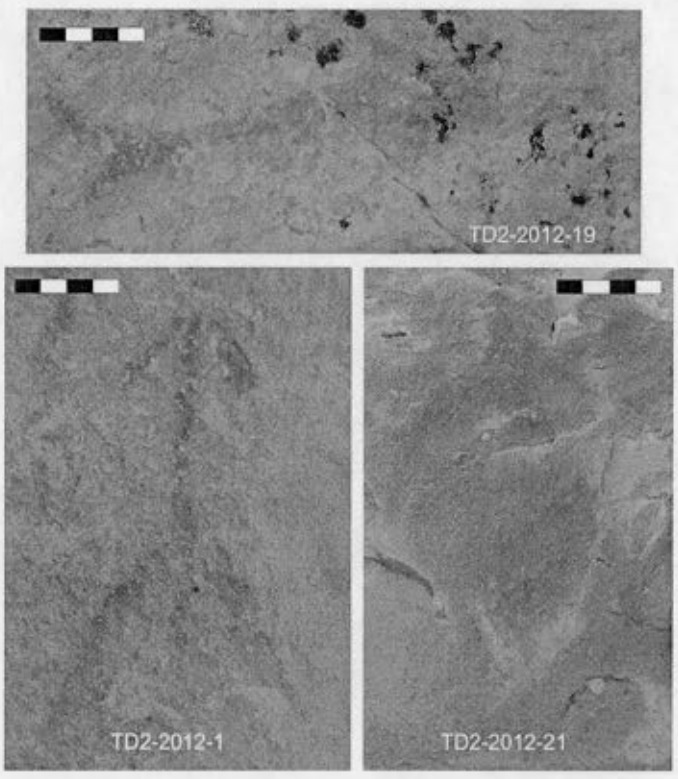


**Figure 4.7** Figures dated at site TD2, Botswana

According to the placement of the figures in the site, the oldest part seems to be the western-end part and the youngest the eastern-end. The two oldest samples were collected close to each other, whereas the younger sample is from a human figure at the other side of the site. This distinction is visible in the paint recipe used too: the two oldest figures being made with soot whereas the youngest figure is composed of carbon-blacks exhibiting a smooth texture.

Dates were modelled using OxCal (Bronk-Ramsey, 2009) as three separate phases, three contiguous phases, two separate phases, two continuous phases, and one single phase. As only three dates were obtained on this site, modelling suffers from large uncertainties. However, the model with two contiguous phases is in agreement with the style of the paintings, and corroborates characterization results (Figure 4.8).

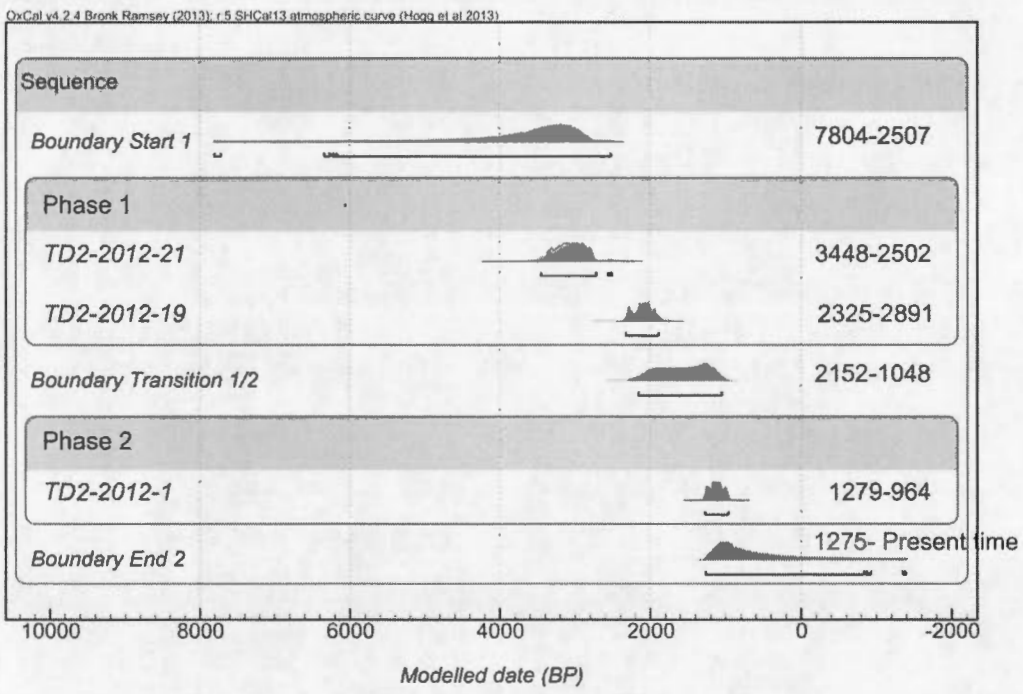


**Figure 4.8** Bayesian modelling for dates obtained at TD2

This model confirms that the last period of paint is from around 1000 cal. BP with the black figure. This black figure is found close to representations of sheep which, following archaeological data, cannot be older than 2200 cal. BP (Walker, 2009). This result is in good agreement with archaeological data in this area.

Whatever the modelling chosen, the dates suggest that the site has been used for more than 1500 years, maybe by two different populations or by the same population whose paint recipes changed through time.

*TD12*

TD12 is a small rock shelter on a rocky outcrop. It contained a few paintings, most prominent of which was a fish painted in black with red details.

TD12-2012-6 was collected from a human figure painted in black. TD12-2012-7 was collected from a second human figure painted in black. TD12-2012-8 was collected from behind the head along the dorsal edge of the black fish painting, while TD12-2012-9 was collected from behind the head along the ventral edge of the same image (Figure 4.9).

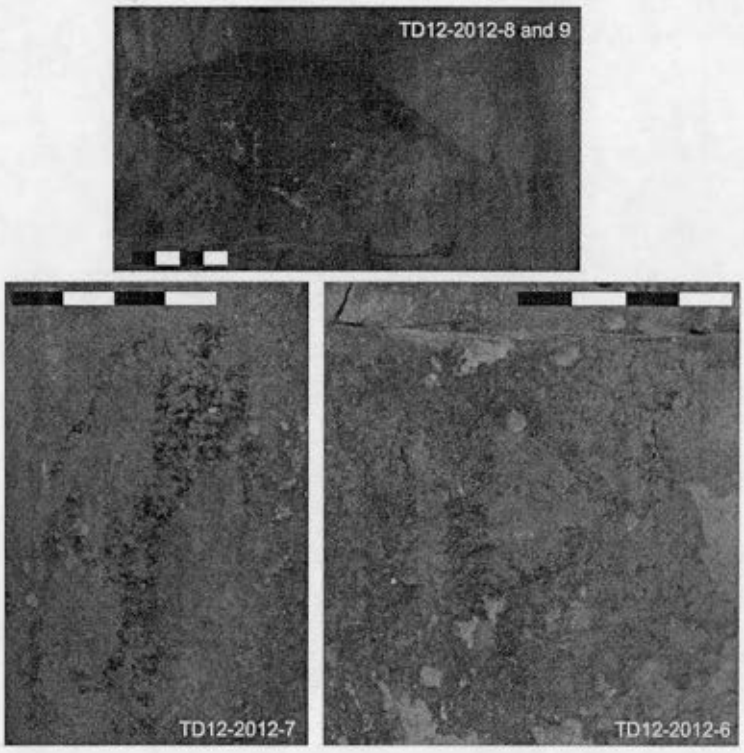


**Figure 4.9** Figures dated at site TD12, Botswana

TD12-2012-8 and TD12-2012-9 are two separate dated samples from the same painting. The date on TD12-2012-9 suffers from a large uncertainty because of a problem during the pressing of the AMS target, resulting in a low current during AMS determination. However, the two dates obtained are in close agreement. The two dates were combined giving a result

of 3057 ± 30 BP, which calibrates to 3357–3180 cal. BP. This date is considered as the most probable for the fish figure, on which the samples were taken.

A Bayesian modelling was attempted with three continuous phases of paints (Figure 4.10). The results suggest that three periods of painting may be represented at this site, which in fact correspond to three different panels on which the samples were collected. On the other hand, the paint recipe is the same through the entire site pointing to the use of this site by one continuous population.

The results point to utilisation of the site for more than 2500 years, as for the use of the black paint recipe composed of carbon-blacks with a fine-flaky texture.

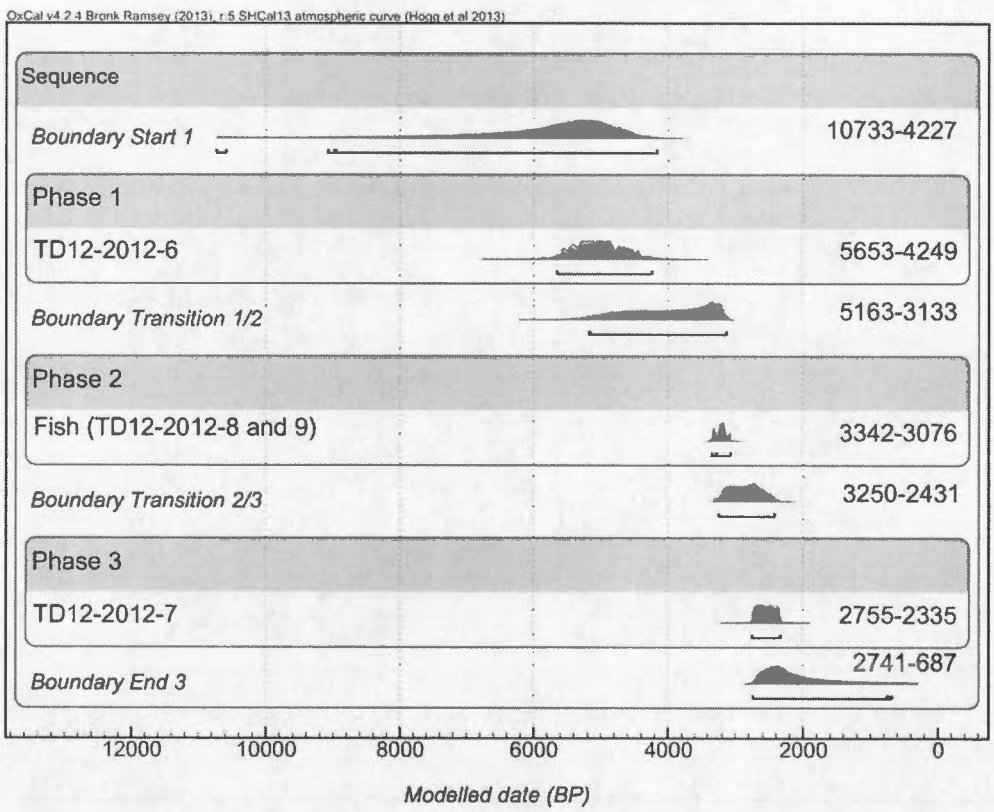


**Figure 4.10** Bayesian modelling of dates obtained at TD12

*TD21*

Most of the length of TD21 consists of a small overhang with a relatively low vertical face. At its western end, the shelter is deeper and contains several large fallen rocks.

TD21-2012-2 was collected from the head and shoulders of a human figure painted in black. TD21-2012-3 was collected from the legs of a human figure painted in black. Both images were located in the deeper part of the shelter (Figure 4.11).

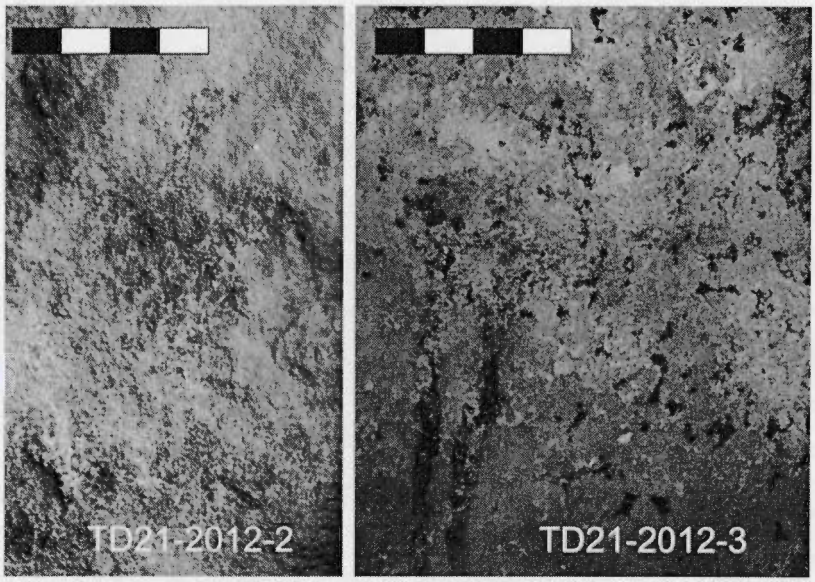


**Figure 4.11** Figures dated at site TD21, Botswana

The two dates obtained are in good agreement, despite the small quantities of carbon dated. As the paintings were found close to each other in the shelter, they were expected to have been made at the same time. Moreover, they were painted with the same recipe, composed of carbon-blacks exhibiting a flaky texture. As figures were close to each other and made with the same recipe, it points again to a single period of painting, confirmed by the dates obtained.

Bayesian modelling on the two dates as part of the same phase gives modelled dates of 2875 – 2340 cal. BP and 3139 – 2184 cal. BP, respectively. It is possible to conclude that the most probable period of creation for these two paintings is 2900 – 2300 cal. BP.

*Discussion of the dates obtained in the Thune Valley*

Looking at the dates obtained around the Thune Valley, three to five periods seem evident.

Bayesian modelling has been used to see which of these options are the most probable and to better define the periods themselves.

Three models were carried out: one with three contiguous phases (Figure 4.12), one with four contiguous phases (Figure 4.13), and the last one with five contiguous phases (Figure 4.14).

All of these models have got good agreement indices (between 98.0 and 99.9), meaning that they are all possible. Following these results, it is possible to give a preliminary chronology of the use of sites in Thune Valley. These results show that a human figure at TD12 would have been the first of the set of paintings studied to be painted at about 5000 cal. BP, which constitutes the oldest direct date so far obtained on San rock art. Then seven figures (human figures and fishes) were painted in TD2, TD12 and TD21 during a period between 3500 and 2000 cal. BP years ago. Finally, a last human figure, very stylized has been realized on site TD2, next to sheep representations.

TD21 is the only site which seems to have been used for only one period, whereas the two others were used for two periods. TD2 is the last one to be used. Looking on a map (Figure 1.11), TD12 and TD21 are only 1 km from each other. The fact that these sites would have been used at the same time for painting is highly possible and it can be noted that they are on each bank of the Thune River.

TD2 is about 4 km far from the two other sites. Even though it is a short distance for San hunter-gatherers, it may be part of another set of sites used at the same time and later preferred compared to the two others.

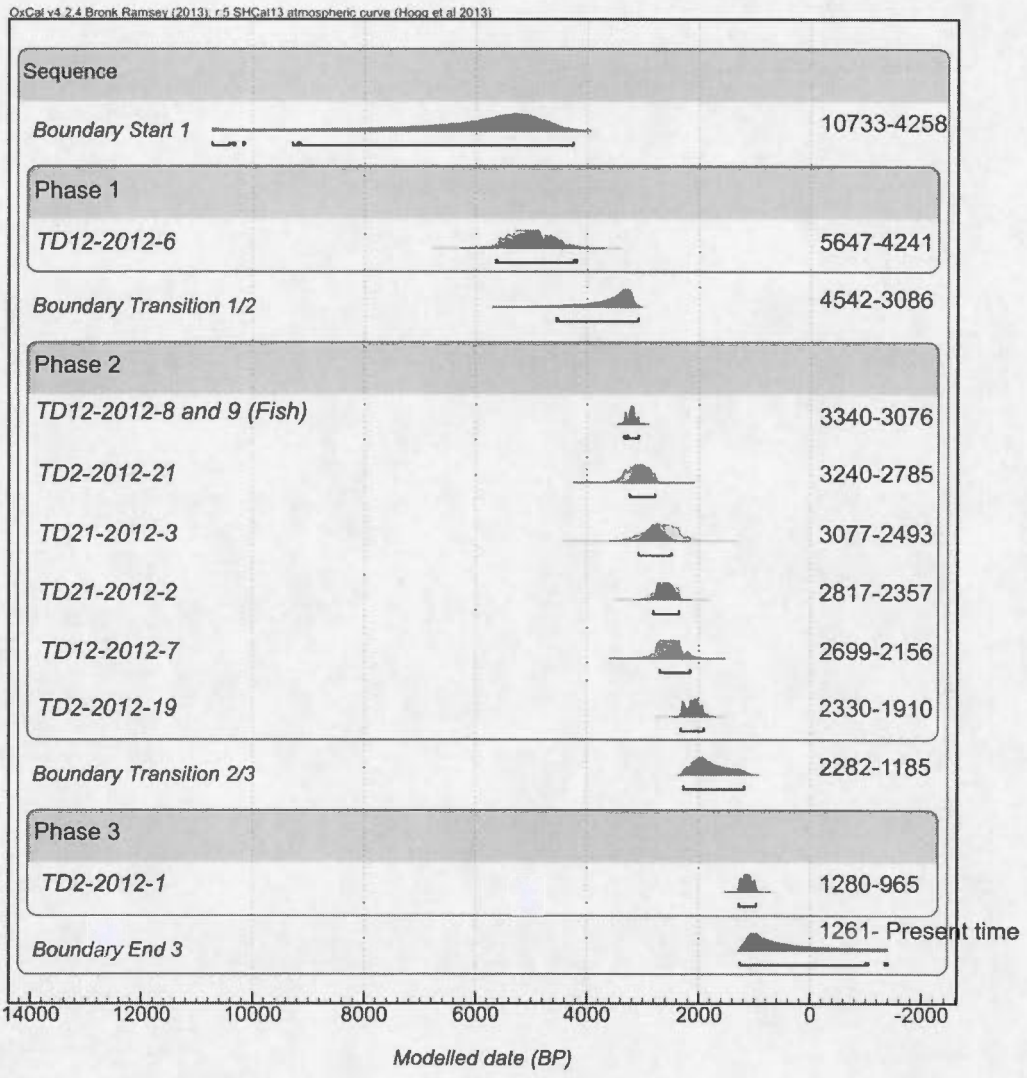


**Figure 4.12** Bayesian modelling of dates obtained in the Thune Valley (three contiguous phases)

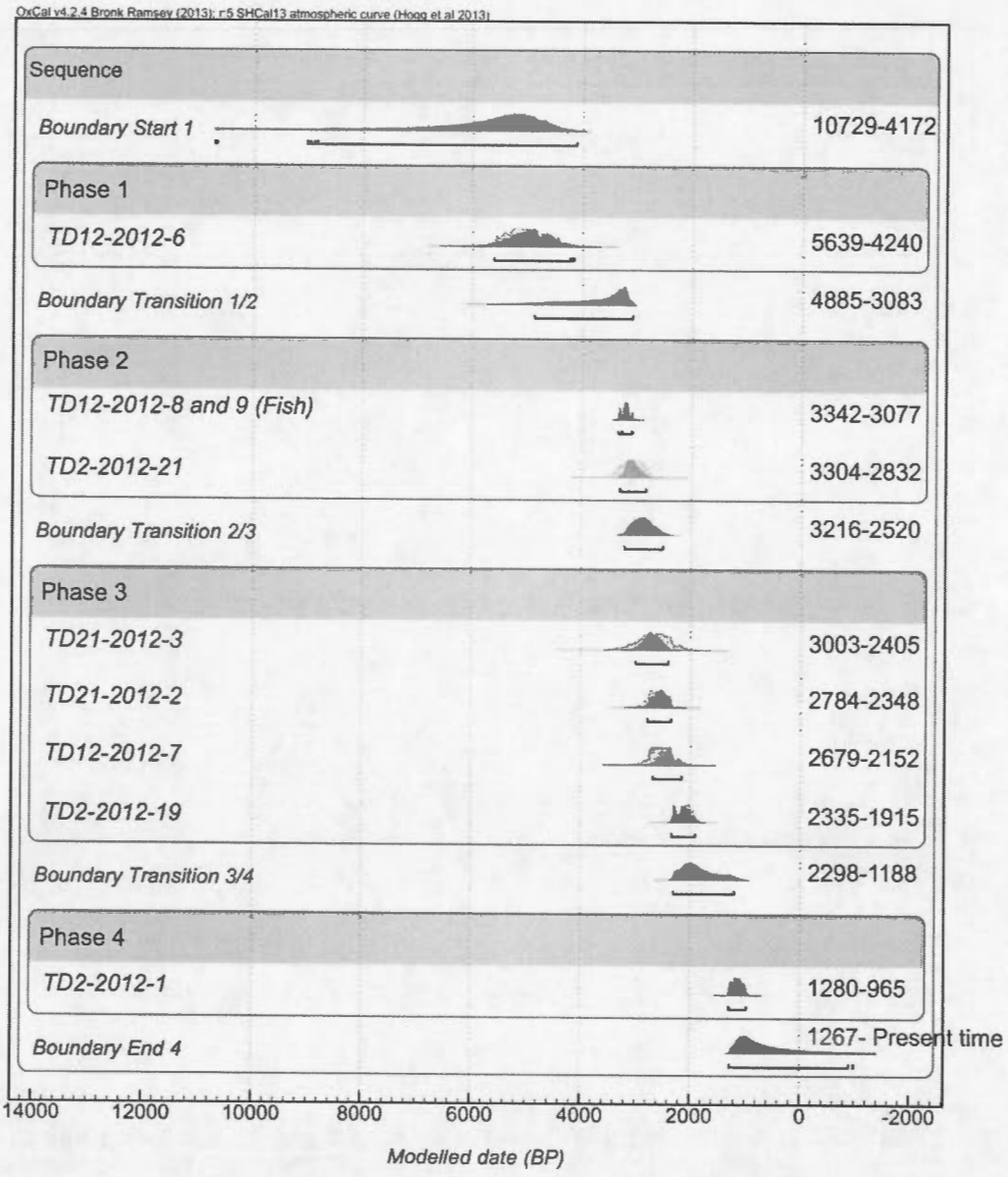


**Figure 4.13** Bayesian modelling of dates obtained in the Thune Valley (four contiguous phases)

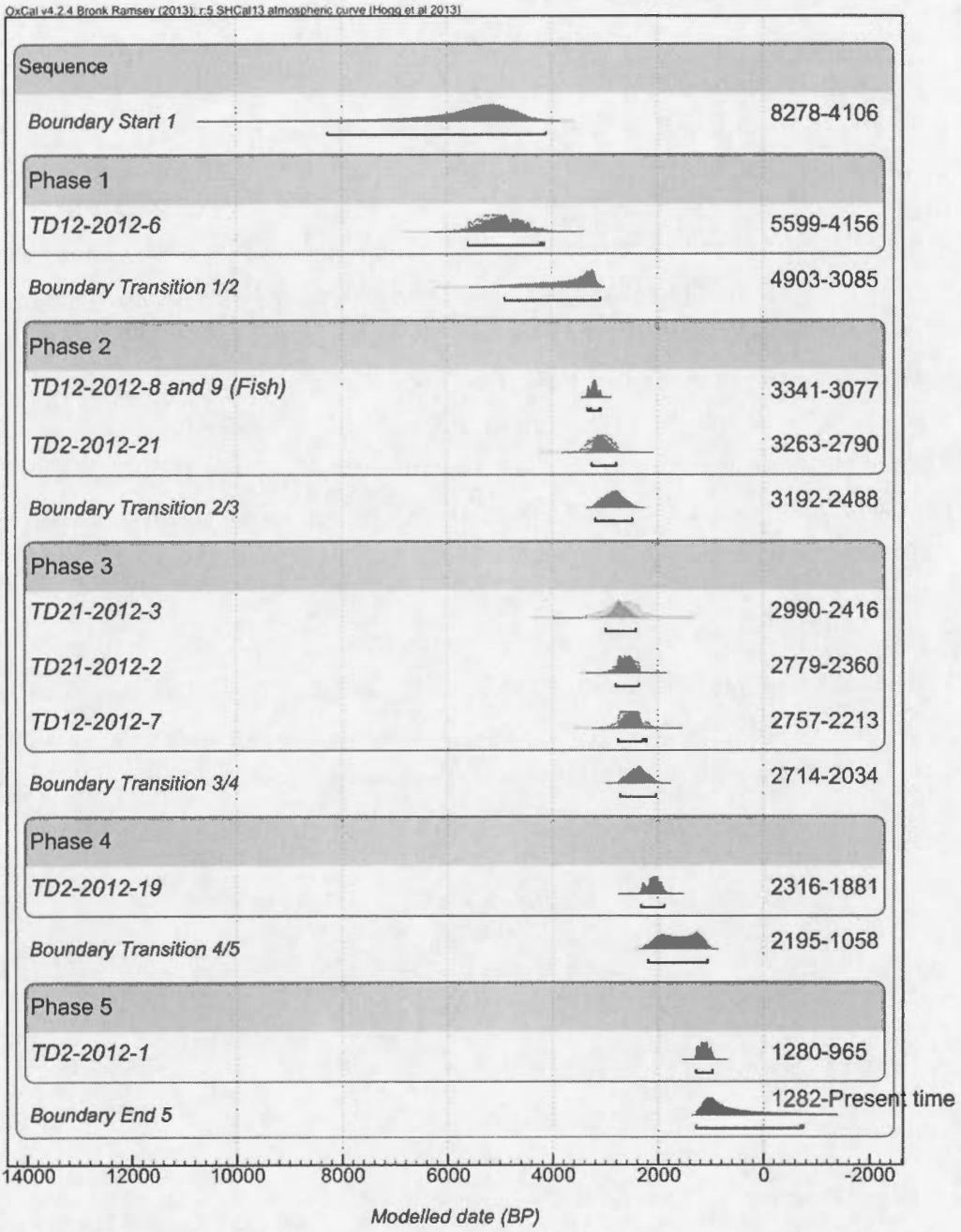


**Figure 4.14** Bayesian modelling of dates obtained in the Thune Valley (five contiguous phases)

These hypotheses are based on only nine dates and need to be correlated with archaeological excavations performed by a commercial archaeology team. Nevertheless, TD2 (also called Pepe Cave) was the only site excavated. Later Stone Age material correlated to San hunter-gatherers was found, but no more dating information is provided (Water Resources Consultants, 2009).

Comparing these periods with paint characterization, it appears that at least three recipes were used at the same time in the Thune Valley, which by extension may reveal the presence of three populations painting at different sites at the same time. This interpretation of the dates is based on the assumption that a recipe was shared by a single population, which would be coherent with the definition of the San people as numerous populations using different languages and sharing common habits. Paint characterization on the other colours (red and white) may help to providing clues about the production of sites. They are part of a future project.

#### 4.3.2.2 Lesotho

12 measurements were obtained on 11 different figures from 5 different sites. They are presented in table 4.2. Out of these 12 dates, 4 were obtained on extremely small quantity of carbon, <10µg. They are not considered to represent authentic ages but are discussed to give a clue about the period of paint.

**Table 4.2** Radiocarbon ages obtained on sites in the Phuthiatsana Valley, Lesotho

| Sample | Lab number | Start weight (mg) | % carbon | To AMS (mg) | $\delta^{13}C$ (‰) relative to PDB | Conventional $^{14}C$ age BP (±1σ) | Calibrated age BP (95.4% range) |
|---|---|---|---|---|---|---|---|
| ARAL171C1 | OxA-X-2470-50 | 68.2 | 0.4 | 0.065 | -22.3 | 1210±90 | 1274-927 |
| ARAL172C1 | OxA-X-2479-37 | 3.8 | 0.5 | 0.010 | n/a | 1700±310 | 2325-965 |
| ARAL175C1 | OxA-X-2479-49 | 73.4 | 2.1 | 0.296 | -24.3 | 300±65 | 495-250 (74,6%), 229-140 (19,5%), 113-105 (0,4%), 84-72 (0,7%), 18-12 (0,3%) |
| ARAL175C2 | OxA-X-2470-48 | 73.2 | 1.0 | 0.152 | -24.1 | 390±70 | 516-291 |
| ARAL175C2 | OxA-X-2495-27 | 195.8 | 0.7 | 0.454 | -22.9 | 470±90 | 630-601 (2,7%), 564-300 (92,7%) |
| ARAL175-2012-1a | OxA-X-2555-40 | 130.1 | 0.4 | 0.254 | -24.6 | 760±120 | 905-855 (4,8%), 844-518 (90,6%) |
| ARAL175-2012-2a | OxA-X-2555-39 | 110.1 | 0.1 | 0.274 | -25.4 | 410±130 | 635-594 (2,5%), 569-239 (80,5%), 231-138 (9,2%), 114-102 (0,6%), 92-68 (1,3%), 25-now (1,3%) |
| ARAL175-2012-3a | OxA-X-2555-26 | 150.1 | 0.7 | 0.315 | -22.9 | 575±75 | 664-460 |
| ARAL249-2012-1 | OxA-X-2555-24 | 20.8 | 4.0 | 0.145 | -24.9 | 770±90 | 897-890 (0,4%), 883-873 (0,6%), 803-540 (94,4%) |

| Sample | Lab number | Start weight (mg) | % carbon | To AMS (mg) | $\delta^{13}C$ (‰) relative to PDB | Conventional $^{14}C$ age BP (±1σ) | Calibrated age BP (95.4% range) |
|---|---|---|---|---|---|---|---|
| ARAL252C1 | OxA-X-2479-34 | 4.2 | 2.4 | 0.004 | n/a | 5300±2000 | 13579-1591 |
| ARAL252C2 | OxA-X-2479-35 | 7.1 | 0.4 | 0.009 | n/a | 5700±1000 | 9003-4226 (95,3%), 4201-4177 (0,1%) |
| ARAL252C4 | OxA-X-2479-36 | 4.2 | 2.7 | 0.010 | n/a | 2640±390 | 3691-3659 (0,4%), 3649-1806 (94,8%), 1772-1748 (0,3%) |

*ARAL 171*

ARAL171 lies on the north bank of the Phuthiatsana River in the Berea District section of the Metolong Dam's catchment close to the village of Ha Seeiso.

Sample ARAL171C1 was collected from a human figure depicted wearing skin cloaks (*karosses*) (Figure 4.15).


**Figure 4.15** Figure dated at site ARAL 171, Lesotho

One single date has been obtained for this site, 1274-927 cal. BP. The pigment dated is made of charcoal, meaning that the date obtained is a maximum age: the paint had not been made before, but may be much younger. At the surface of the shelter, a small assemblage of 19 stone artefacts containing a single thumbnail scraper was found. It has been defined as a Final Late Stone Age technocomplex, that is to say that it has been made within the last 4000 years, which is consistent with the date obtained.

*ARAL172*

ARAL172 is a small (39 x 17 m) rock-shelter on the south bank of the Phuthiatsana River, in the Maseru District section of the Metolong catchment. A series of six panels was recorded.

Sample ARAL172C1 was collected on the hoof of a polychrome eland (Figure 4.16).


**Figure 4.16** Figure dated at site ARAL172

The date was obtained on less than 10µg of carbon, which makes the effect of contamination extremely high in comparison of larger samples. Large error is associated to this date too. However, using the calibrated date 2325-965 cal. BP, it is possible to conclude that this painting was created during the last 2000 years.

*ARAL 175*

ARAL175, known to some local residents as Lepoqong and in the rest of the archaeological literature as Ha Makotoko after a nearby village, is by far the largest rock-shelter in the Metolong catchment. Despite its large size, the shelter preserved relatively little rock art.

Five samples were selected for dating. All of the samples analysed came from black-painted figures in the north-eastern end of the rock-shelter in Panel F (Figure 4.17).

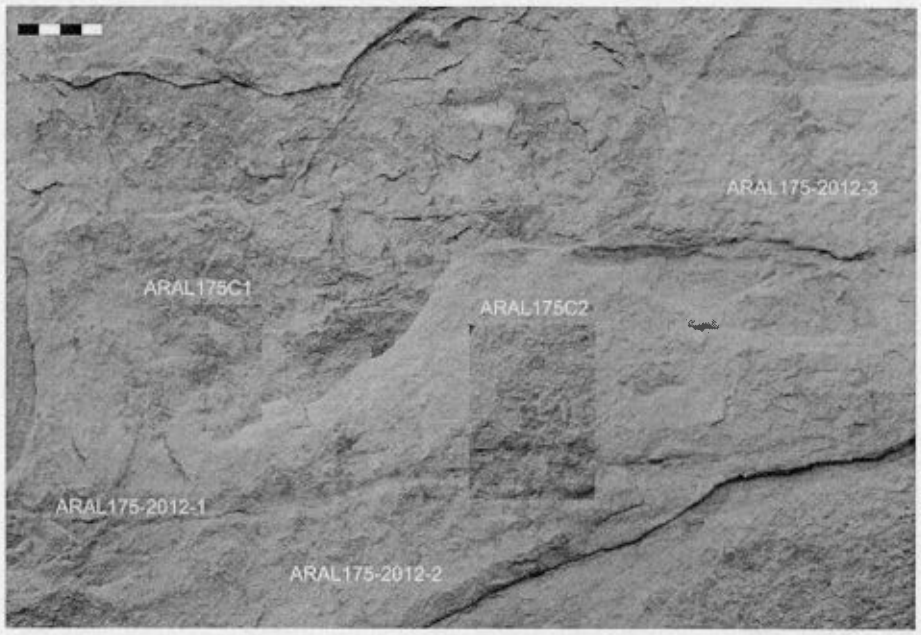


**Figure 4.17** Figures dated at site ARAL 175, Lesotho

Due to large sample collected on ARAL175C2, it was possible to obtain two replicate dates out of one sample. They are in good agreement which confirms that our protocol removes radiocarbon contaminants and that it does not introduce significant contaminant during its process.

The two dates were combined giving a result of 420 ± 56 BP, which calibrates to 538-315 cal. BP.

As horses are depicted in this panel, an attribution to the historic period has been previously assumed. Moreover, historical evidence also constrains the likely age of some of the samples since San hunter-gatherers were absent from the Metolong catchment after the end of the 1830's (Vinnicombe, 1976; Arthur and Mitchell, 2010). The five dates were modelled using Bayesian modelling in one single phase, and a known age constraint has been added at AD1840 ± 10 (Figure 4.18). This modelling shows that all of the paintings are likely to have been made in a single period, with a start between 993 and 486 cal. BP and an end between 494 and 100 cal. BP (this limit comes from the age constraint added to the model).

Comparing with paint characterization, three different recipes were used to paint. The main recipe is carbon-blacks with a smooth texture (3 samples), whereas carbon-blacks with a flaky texture and soot were found on only one figure. These three recipes were used to paint during one single period, which if applying the assumption given for the Maclear district, points to the use of this shelter by three different populations.

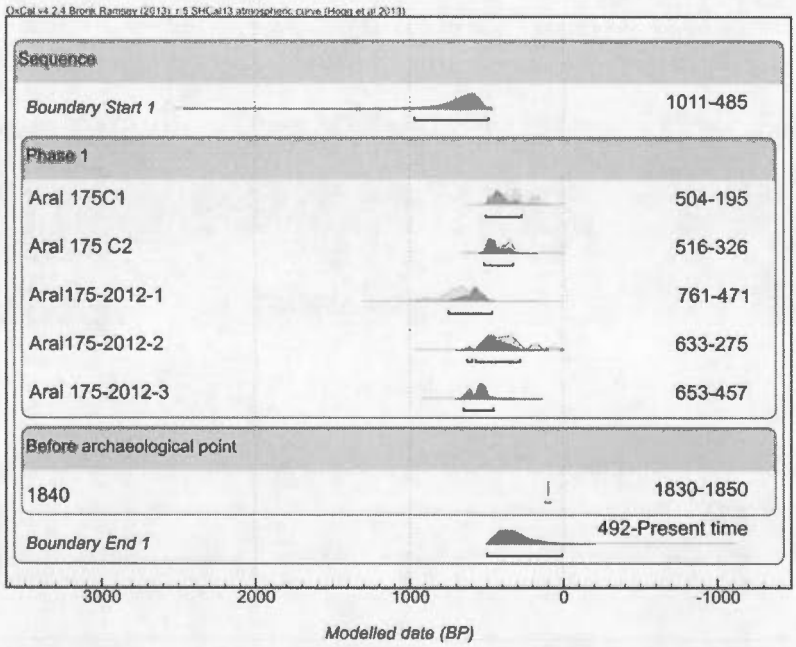


**Figure 4.18** Bayesian modelling of dates obtained at ARAL175

*ARAL 249*

This site lies in the central part of the catchment impounded by the Metolong Dam directly below Ha Masakale village. Only a single painted image of a large eland was present, from which the sample was collected (Figure 4.19).

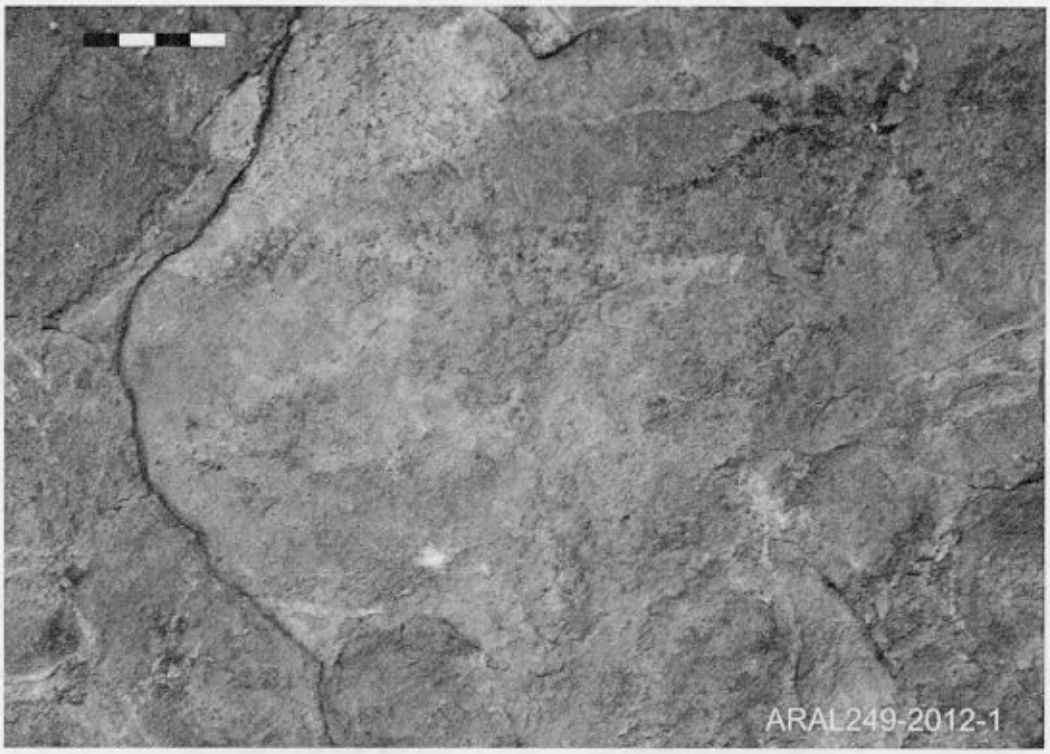


**Figure 4.19** Figure dated at site ARAL 249, Lesotho

One single date was obtained on this eland, 770 ± 90 $^{14}$C years BP. ARAL 249 contained no archaeological deposits or surface finds. However, excavations at Ntloana Tšoana, on the opposite bank of the river, identified a broadly equivalent hunter-gatherer occupation dated to 650 ± 20 $^{14}$C years BP (UGAMS-8973) (Peter Mitchell and Charles Arthur, personal communication, 2015). This date is in good agreement with the one obtained on the eland. This painting may be the creation of this hunter-gatherer group.

*ARAL252*

ARAL252 is situated in the upper end of Metolong Dam Catchment, on the north bank of the small Sephiri River, a tributary of the Phuthiatsana.

Dating of four samples was attempted at ARAL252. Three were black human figures, one shown bending forward at the waist, and the fourth a vertical black line. ARAL252-C1 and ARAL252-C2 came from Panel H, while ARAL252-C4, a black human figure, came from Panel G (Figure 4.20). Panel G consisted of 21 human figures and a small quadruped, and Panel H of two elands, one human and a row of long and short lines. Due to an insufficiency of carbon, one of the samples could not be successfully dated and the reliability of the determinations obtained from the other three is uncertain.

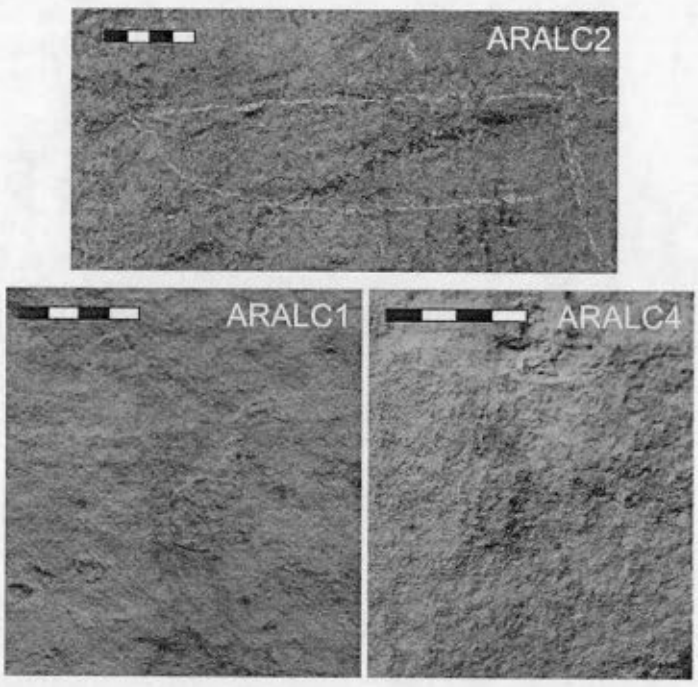


**Figure 4.20** Figures dated at site ARAL 252, Lesotho

The three dates obtained suffer from large uncertainties as they were obtained on very small amount of carbon. Moreover, the potential contamination is very high for such samples. However, a period of paint seems evident from these dates: 4000 to 1500 cal. BP, with more probabilities about 2500-1500 cal. BP. This period is similar to the one suggested for ARAL 172, but its date was on a very small amount of carbon too.

Two interpretations stem out of these dates on very small amount of carbon:

- The dates obtained are from contaminants and thus do not reveal the age of the paints.

- The homogeneity of the dates, despite the large uncertainties, points to a period of creation about 2500-1500 cal. BP.

It is impossible to conclude about one or other of these interpretations. More dates should be performed to ascertain the right one.

*Discussion of the dates obtained in the Phuthiatsana Valley*

Due to the large uncertainties attached to most of the dates obtained in the Thune Valley, no Bayesian modelling has been conducted. However, it is possible to identify at least two and maybe three periods of paints in the Metolong catchment of the Phuthiatsana Valley:

- One period between 2500 and 1500 cal. BP, and one period between 1200 and 100 cal. BP.

- Or, one period between 2500 and 1500 cal. BP, one period between 1200 and 1000 cal. BP, and one period between 1000 and 100 cal. BP.

Comparing the dates with the locations of the sites around the valley, it seems that sites, even separated by 3 to 5 km, were used during the same period. On the other hand, paintings created at the same time were not made with the same recipe. It may be suggested that two or three populations were painting in different shelters at the same time but using different recipes. Interestingly, when comparing to archaeological data, no evidence of San hunter-gatherer occupation has been found after 5600 BP in the Metolong catchment, and the wider Phuthiatsana basin (See §4.3.3).

Only one figure dated was polychrome, an eland from Aral 172. The white paint from this eland has been identified as gypsum. Thus it is possible to conclude that gypsum was used to make white paint in the Phuthiatsana Valley at least between 2325 and 965 BP.

#### 4.3.2.3 South Africa

22 measurements on 20 different figures from 6 sites were obtained (Table 4.3). 3 dates on painted flakes found on the floor of the RSA TYN2 shelter were obtained during the initial project in 2010 and published by Bonneau *et al.* (2011), and are added for discussion purposes.

**Table 4.3** Radiocarbon ages obtained on sites in the Maclear district, South Africa (*: available quantity, reduced to 1.9 mg).

| Sample | Lab number | Start weight (mg) | % carbon | To AMS (mg) | $\delta^{13}C$ (‰) relative to PDB | Conventional $^{14}C$ age BP (±1σ) | Calibrated age BP (95.4% range) |
|---|---|---|---|---|---|---|---|
| CHA1C1 | OxA-X-2590-20 | 4.58 | 2.8 | 0.070 | -24.6 | 2590±110 | 2848-2352 |
| FRE4-2013-C3 | OxA-X-2555-72 | 13.20 | 1.5 | 0.049 | -39.5 | 1160±140 | 1297-768 |
| FRE4-2013-C4 | OxA-X-2555-21 | 24.10 | 1.2 | 0.067 | -41.8 | 770±100 | 903-865 (3%), 815-531 (92,4%) |
| FRE4-2013-C6 | OxA-X-2555-20 | 28.64 | 0.9 | 0.128 | -35.0 | 510±90 | 641-590 (9,6%), 572-318 (85,8%) |
| FRE4-2013-C7 | OxA-X-2555-19 | 25.34 | 1.4 | 0.108 | -36.8 | 290±90 | 494-134 (85,1%), 119-58 (6,8%), 28 to now (3,6%) |
| FRE4-2013-C8 | OxA-X-2555-18 | 25.16 | 0.3 | 0.049 | -43.4 | 1420±140 | 1561-977 |
| LAB1C1 | OxA-25960 | 8.01 | 6.6 | 0.054 | -27.7 | 2040±120 | 2308-2220 (6,5%), 2212-1705 (88,9%) |
| LAB1C2 | OxA-25961 | 9.02 | 6.2 | 0.097 | -24.5 | 1620±90 | 1700-1649 (5,3%), 1625-1305 (90,1%) |
| LAB1-2013-C3 | OxA-X-2555-17 | 18.05 | 8.8 | 0.134 | -32.8 | 1530±90 | 1585-1266 (94,2%), 1210-1189 (1,2%) |
| LAB1-2013-C5 | OxA-X-2555-16 | 10.03 | 7.3 | 0.103 | -34.9 | 2690±100 | 2998-2428 (95%), 2392-2381 (0,4%) |
| LAB7-2013-C1 | OxA-28977 | 21.46 | 44.2 | 3.805* | -25.6 | 147±23 | 263-222 (20,5%), 147-now (74,9%) |
| LAB7-2013-C2 | OxA-28978 | 27.60 | 22.4 | 2.715* | -25.1 | 124±23 | 254-225 (13,8%), 143 to now (81,6%) |

| Sample | Lab number | Start weight (mg) | % carbon | To AMS (mg) | $\delta^{13}C$ (‰) relative to PDB | Conventional $^{14}C$ age BP (±1σ) | Calibrated age BP (95.4% range) |
|---|---|---|---|---|---|---|---|
| PRH1-2013-C1 | OxA-28980 | 35.66 | 5.0 | 2.421* | -23.7 | 447±28 | 509-449 (87,9%), 355-338 (7,5%) |
| PRH1-2013-C2 | OxA-29186 | 18.63 | 8.7 | 1.126 | -23.1 | 308±40 | 452-351 (50,9%), 342-280 (41,9%), 203-195 (0,8%), 167-155 (1,8%) |
| RP/2009/003/13 | OxA-X-2370-29 | 13.53 | 8.4 | 0.883 | -25.3 | 2072±32 | 2081-2074 (1%), 2060-1919 (94,4%) |
| RP/2009/003/14 | OxA-X-2370-30 | 17.48 | 2.3 | 0.526 | -24.1 | 2100±140 | 2148-1926 |
| RP/2009/003/29 | OxA-X-2370-31 | 12.86 | 1.8 | 0.414 | -23.6 | 2083±130 | 2093-1920 |
| TYN2C1 | OxA-25962 | 7.40 | 8.4 | 0.156 | -24.6 | 2390±90 | 2748-2080 (94,9%), 2073-2060 (0,6%) |
| TYN2C2 | OxA-25963 | 20.22 | 1.6 | 0.182 | -25.7 | 2500±90 | 2841-2827 (0,4%), 2795-2298 (91,4%), 2260-2177 (3,4%), 2169-2162 (0,2%) |
| TYN2C3 | OxA-25964 | 24.37 | 3.3 | 0.125 | -24.8 | 2080±90 | 2306-2231 (6,8%), 2207-1820 (87,9%), 1765-1754 (0,6%) |
| TYN2C5 | OxA-25965 | 14.88 | 1.1 | 0.185 | -23.5 | 1940±110 | 2050-1607 |
| TYN2C6 | OxA-25966 | 58.79 | 14.8 | 0.357 | -24.2 | 1900±23 | 2002-1586 |
| TYN2C7 | OxA-25967 | 61.17 | 6.3 | 0.073 | -26.2 | 2290±35 | 2699-2633 (3,3%), 2617-2587 (1,3%), 2539-1998 (90,6%), 1947-1941 (0,2%) |

*RSA CHA1*

RSA CHA1 is approximately 20 m long, but only a few meters deep. The painted panels comprise two vertical rock faces, almost at right angles to each other. Both faces are densely painted, with the images extending both vertically and horizontally over most of the rock face. The site contains 424 individual figures.

Sample CHA1-C1 was collected from the black hoof of one of the forelegs of a shaded polychrome eland (Figure 4.21), providing one single date for this site, 2848-2352 cal. BP.


**Figure 4.21** Figure dated at site RSA CHA1, South Africa

It provides here a chronological point about the use of this shelter, but its period of use may be much longer.

*RSA FRE4*

RSA FRE4 is a small rock shelter of about 15 m in overall length, although it is 'bent' around the corner of a drainage line in the side of a valley. There are small numbers of paintings scattered throughout the site. The dated paintings come from two groups of human figures holding iron-bladed spears and axes and knobkerries.

FRE4-2013-C3 was collected from the body of a human figure painted in black. The figure holds a knobkerrie and a shield. This is the only date obtained from the first group of human figures. In the second group of figures, FRE4-2013-C4 was collected from the head of a human figure painted in black. The figure holds a bow and arrow and has a hunting bag with further arrows on its back. FRE4-2013-C6 was collected from the body of a human figure painted in black. FRE4-2013-C7 was collected from the body of a human figure holding in one hand an iron bladed axe and in the other what is probably an iron bladed spear. FRE4-2013-C8 was collected from the head and body of a human figure painted in black, also part of the second group (Figure 4.22). The figure holds an iron bladed axe.

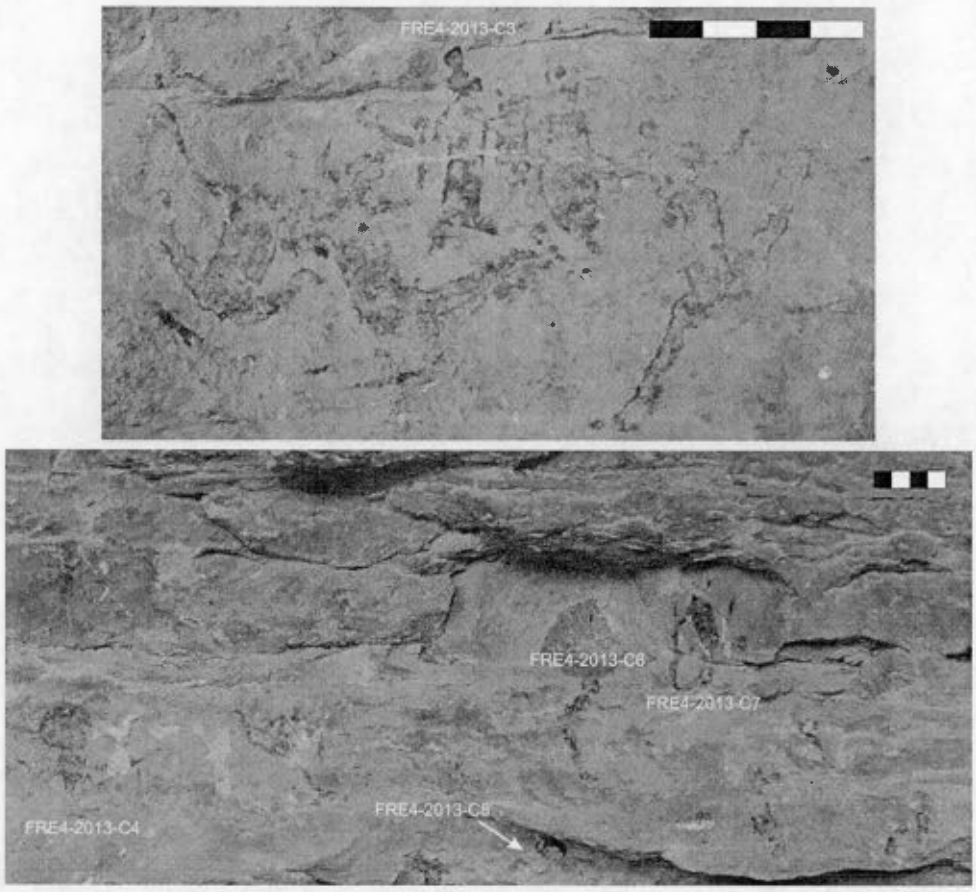


**Figure 4.22** Figures dated at site RSA FRE4, South Africa

Iron-working Farming Communities were present in lower-lying parts of the Eastern Cape Province to the east of the Maclear area from around 1500 cal. BP and using historical evidence, San hunter-gatherers are known to have been absent from the area after the late nineteenth century (Mitchell and Whitelaw, 2005).

The first group of figures, including FRE4-2013-C3 appears to be painted at the same time, considering the proximity of the figures and their apparent link in the same scene. It is possible to conclude that this panel was realized between 1297 and 768 cal. BP.

The second group of figures is made of scattered figures and the dates obtained confirm that they were not painted at the same time. FRE4-2013-C8 and maybe FRE4-2013-C4 seem to date from the same period as the first group of figures, which is corroborated by the fact that they were made with the same paint recipe; whereas the two other figures are more recent and can be attributed to historical times. These were painted with another recipe composed of carbon blacks with a smooth texture. These dates are in good agreement with archaeological evidences reported by Mitchell and Whitelaw (2005) and it may be possible that the site was created in two periods by one population whose paint techniques changed through time, or by two populations who painted during two different periods with two different paint recipes.

*RSA LAB1*

RSA LAB1, also known as 'Storm Shelter', is a rock shelter approximately 80 m in length and of variable height and depth. Paintings are scattered throughout the shelter, although the best-preserved panel, about 5 m long, containing the majority of paintings, is at the northern end of the shelter. This main panel consists of 231 individual paintings of a variety of subjects. The dates reported are all from this main panel.

LAB1-C1 was collected from the horn of a painting of an eland antelope. LAB1-C2 was collected from the black back-line of the same painted eland. LAB1-2013-C3 was collected from the second horn of the same painted eland. LAB1-2013-C5 was collected from the face of a second painted eland in close proximity to the first, but underneath if considering the superposition of the paintings (Figure 4.23).

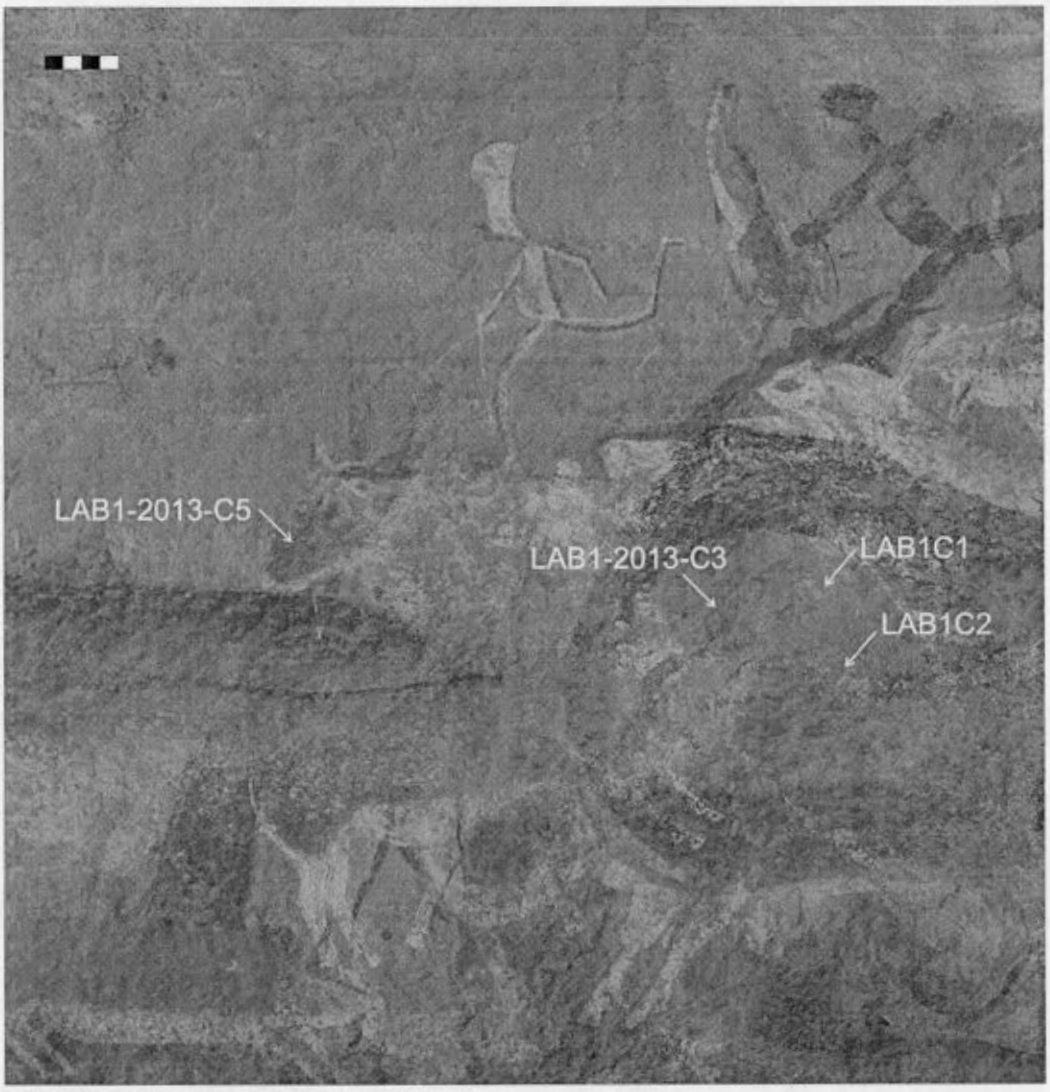


**Figure 4.23** Figures dated at site RSA LAB1, South Africa

LAB1C1 and LAB1C2 are samples from the same painted eland. The calibrated date ranges, however, do not overlap. They were collected in September 2011 at the beginning of the project and characterized at the University of the Witwatersrand in Johannesburg. It was not possible to make cross-sections. Following these results, a new sample was collected at the same place as LAB1C2. A cross-section was made showing a superposition of two black

paint layers (Figure 4.24). The section of the eland backline from which sample LAB1-C2 was collected overlying an earlier black painting.

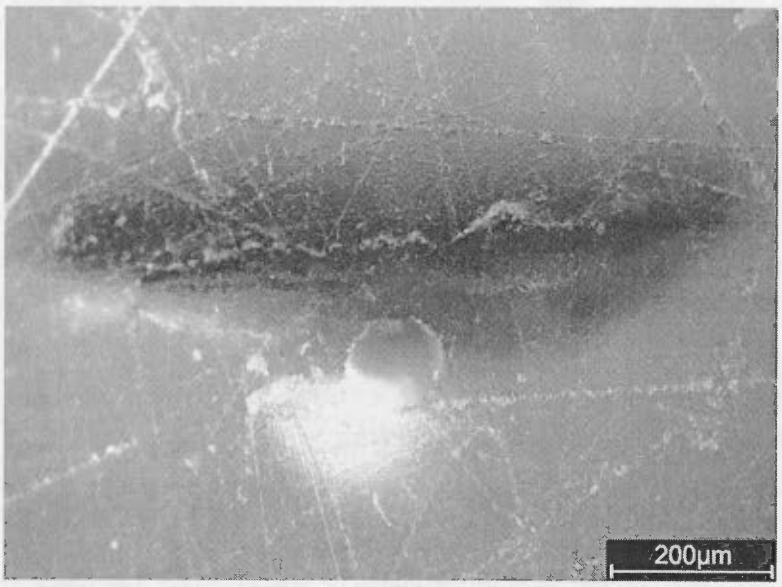


**Figure 4.24** Cross-section of LAB1-C2 (sample retaken in 2012), light microscope image.

To clarify the matter, a third sample was collected from the same painting, from the second horn (LAB1-2013-C3). Unfortunately, when calibrated, this determination also fails to overlap with that obtained from LAB1-C1. It does, however, overlap with LAB1-C2, which we believe to be incorrect. No calcium oxalate remained in any of these samples after pre-treatment according to FTIR analysis, and therefore these incompatibilities are attributed to the small amount of carbon available for dating LAB1-C1 and LAB1-C2. Given the larger sample size, we conclude that LAB1-2013-C3 best dates the eland in question.

This example is very interesting as it proves firstly the necessity to make cross-sections to evaluate potential repaints which would influence radiocarbon dating, and secondly that the use of very small amounts of carbon, for which the possibility of introducing contamination during laboratory processing is higher, should be avoided as much as possible.

The four dates obtained from this site point to at least two periods of production for this panel: one about 3000-2500 cal. BP and another about 1500-1000 cal. BP, which are corroborated by the use of two different black paint recipes. Considering the high level of superposition of this site and the number of figures present, it is difficult to give further interpretation, but it proves that the site was used for at least 1000 years and doubtless much longer. The dates are coherent with the superposition of the figures.

This site was first selected for the presence of Eldritch figures and LH-SDFs. No black paint was found on Eldritch figures and as only black paints were investigated in the Maclear District according to the archaeological permits, it was not possible to give a chronological attribution to these figures. One LH-SDF was found on top of two black horns of an eland. Dating these horns would have provided a maximum age for this figure. However, the sample once collected and pre-treated was too small to attempt radiocarbon dating and was withdrawn.

*RSA LAB7*

RSA LAB7 is a rock shelter of about 30 m in overall length. It is located in dense bush, just above the level of a stream. There are many paintings in the shelter, although most of those located low on the wall have been rubbed and severely damaged by livestock.

LAB7-2013-C1 was collected from the area behind the head of a large (approximately 70 cm) painting of an elephant. LAB7-2013-C2 was collected from an area one-third of the way along the back of the same image (Figure 4.25).

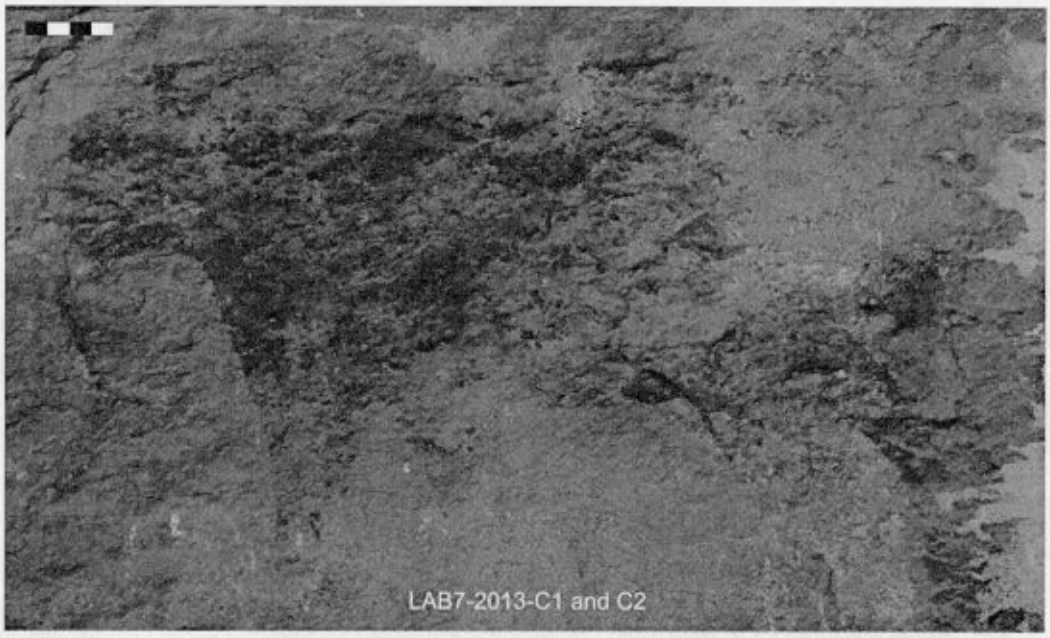


**Figure 4.25** Figure dated at site RSA LAB7, South Africa

The two dates from samples collected on the same elephant are in close agreement. They were combined giving a result of 136 ± 17 BP, which calibrates to 273–10 cal. BP.

Many stone artefacts are currently washing out at the drip line of this shelter. They appear to be of Later Stone Age origin, but have not been attributed to a particular industry. Several small pieces of black, thin-walled pottery were noted. At other sites in the area, this type of pottery has been linked to Later Stone Age communities and date to within the last 2000 years. There were in addition two small fragments of red pottery probably related to Farming Communities (David Pearce, personal communication, 2015). These remains may relate to the dated elephant.

*RSA PRH1*

RSA PRH1 is a large rock shelter, the main section being 15 m long, up to 10 m deep and up to 8 m high, with smaller depressions along the back wall.

PRH1-2013-C1 was collected from the hindquarters of a large (approximately 50 cm) painting of an elephant in grey-coloured paint, while PRH1-2013-C2 was collected from the top of the head of the same image. PRH1-2013-C4 was collected from the upper torso of a human figure painted in red, white and black (Figure 4.26).


**Figure 4.26** Figures dated at site RSA PRH1, South Africa

The two samples from the same painted elephant provided comparable calibrated date ranges, although as the calibration curve at this time is fairly flat this results in quite large calibrated date ranges. The two dates were combined giving a result of 406 ± 20 BP, and a bimodal calibrated distribution: 512–453 (89.5%) and 349–335 (5.9%) cal. BP. The third sample from this site, PHR1-2013-C4, retained a few calcium oxalates after pre-treatment (about 5% of the sample). It has been dated at 3137-2873 cal. BP. but was considered an unreliable result.

*RSA TYN2*

RSA TYN2 is a rock shelter approximately 25 m long, 3 m high and 6 m deep. Paintings are scattered throughout the shelter, although the majority are clustered into two panels towards the centre of the shelter. The more eastern of the two central panels is now undergoing severe spalling.

To date, 192 painted flakes of rock have been collected from beneath this panel. Unfortunately, none contains a complete painted image and in most cases the painted areas cannot be recognized as parts of particular subjects, nor can any of them be matched to paintings remaining on the shelter wall. Samples RP/2009/003/13, RP/2009/003/14 and RP/2009/003/29 were collected from three of these flakes and dated as part of the initial project in 2010 (Bonneau *et al.*, 2011).

The other samples were collected in 2011. TYN2-C1 was collected from the lower torso of a human figure painted in black. TYN2-C2 was collected from the lower torso of a second human figure painted in black. TYN2-C3 was collected from the black hoof of a painted eland. TYN2-C5 was collected from a short diagonal black line that is the remains of the leg of a human figure that has almost completely flaked off from the shelter wall. TYN2-C6 was collected from the arm of a red and black painted human figure, partly flaked away from the rock surface. TYN2-C7 was collected from a bag hanging from a black painted human figure immediately next to the figure from which TYN2-C6 was collected (Figure 4.27).

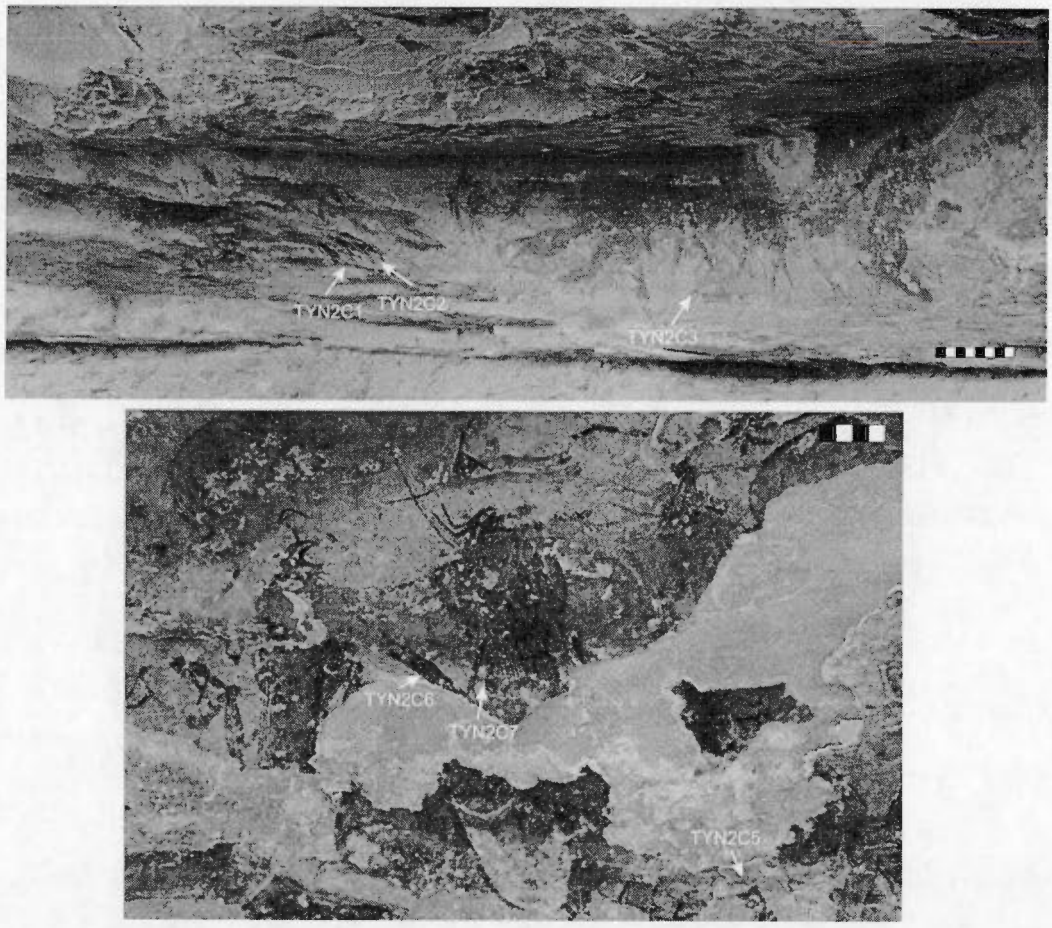


**Figure 4.27** Figures and painted flakes dated at site RSA TYN2, South Africa

Bayesian modelling has been used to try to reconstitute the timing of paint production of this shelter. Three phases were identified from the results (Figure 4.28 and Figure 4.29).

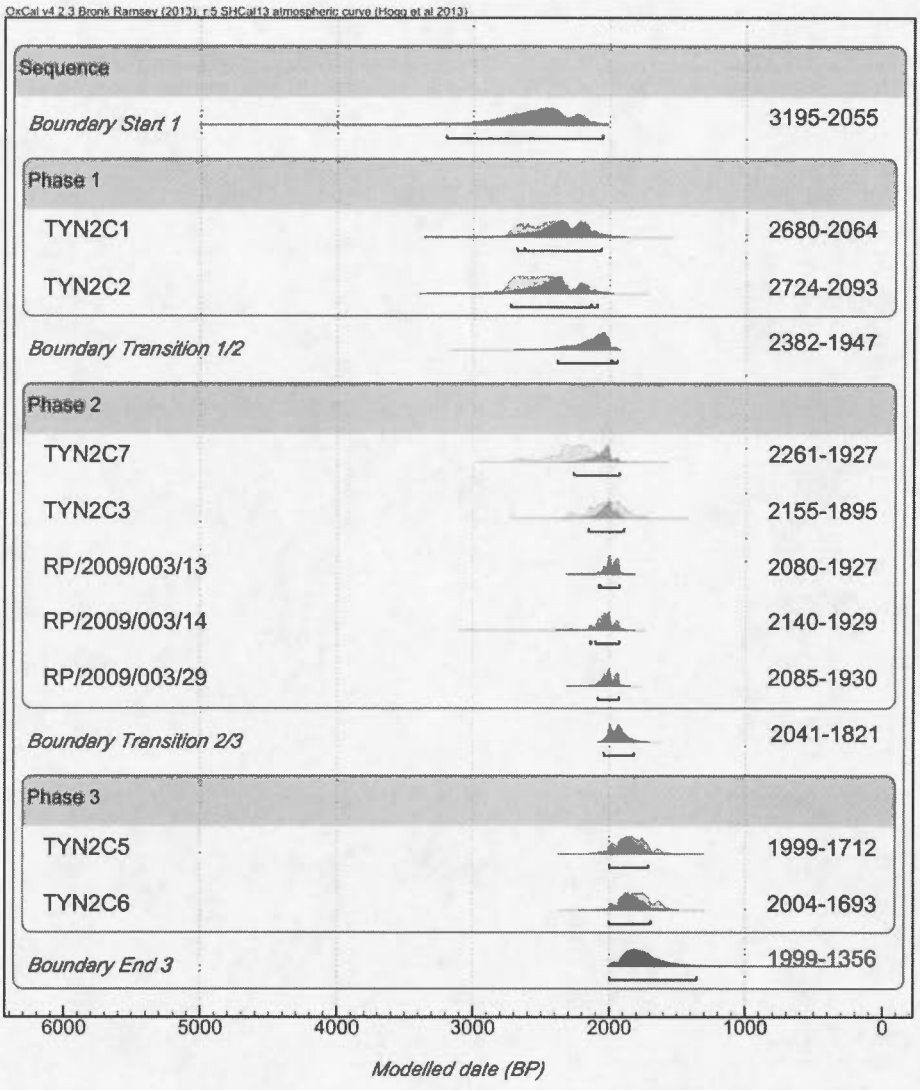


**Figure 4.28** Bayesian modelling of dates obtained at RSA TYN2

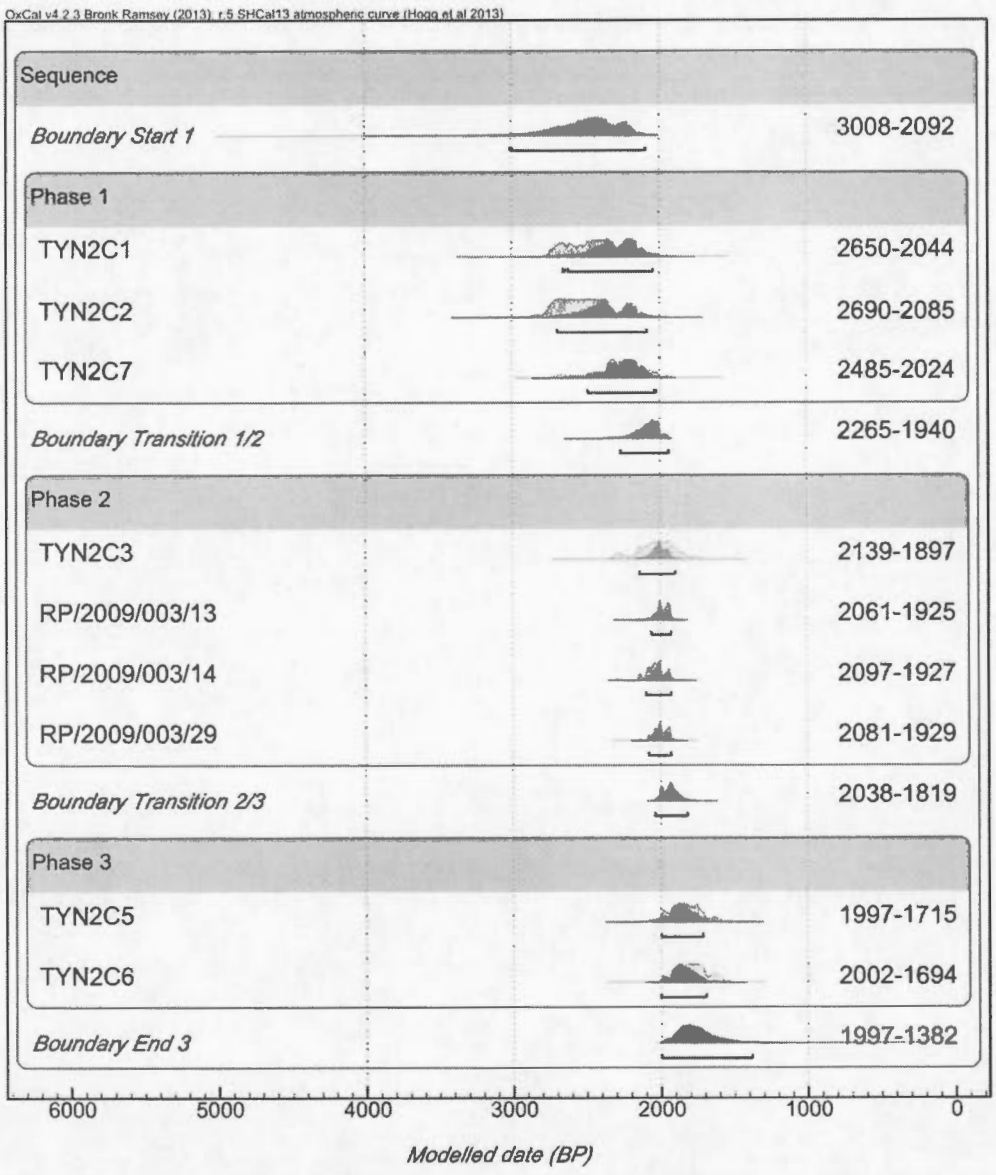


**Figure 4.29** Bayesian modelling of dates obtained at RSA TYN2, second possibility

Both models have got good agreement indices (97 and 97.9). They point to the same model for shelter realization. The first panels were made on the western end of the site, between 3000 and 2000 cal. BP. Then both parts of the site were in use during a period between 2300

and 1800 cal. BP. The flakes found on the floor and dated in 2011 belong to this period. Then a final stage focused on the eastern end (panel now undergoing severe spalling), from 2000 to 1400 cal. BP. It is interesting to note that the black monochrome figures are the oldest dated in this site, whereas the polychrome ones are younger. But some monochrome and polychrome figures also date from the same periods.

The use of this shelter was for more than 1500 years.

The paint characterization shows that two recipes were used to make the black paintings: carbon-blacks with a fine-flaky texture and carbon-blacks with a flaky texture (textures and results on black paints are detailed in Chapter III). Interestingly, the former is found in figures dating from the three periods of time, whereas the latter is found only for the last two phases. As previously mentioned, it may be assumed that these recipes are linked to two different San populations who painted in the shelter at the same time but with two different recipes. Moreover, during the initial project conducted in 2010, two different red paint recipes were identified on painted rock fragments fallen to the rock-shelter floor and found mostly under the second panel, suffering from major rock flaking. They might be linked with the two carbon-black recipes found in this site, but as it was not possible to correlate flakes with the existing rock paintings, the comparison cannot be further pursued.

*Discussion of the dates obtained in the Maclear District*

Interestingly, the three periods of paint described for RSA TYN2 can be extended to the other sites dated in the Maclear district and two other periods: one between 1300 and 700 cal. BP, and one during historical times with a limit at the late nineteenth century, as San were absent from this area according to archaeological and historical evidences (Mitchell and Whitelaw, 2005).

Using this chronology, RSA CHA1, RSA TYN2 and RSA LAB1 were the first shelters to be painted in the first period. Then the second period comprises only RSA TYN2. The third period contains paintings from RSA TYN2, RSA LAB1 and perhaps RSA FRE4. RSA FRE4 is the only one in the fourth period and the fifth period comprises RSA FRE4, RSA LAB7 and RSA PRH1.

Dates obtained, even if they are few in comparison to the number of paintings and sites in this area, show a long tradition of painting and occupation of this region, from 3000 cal. BP to historical times. It covers more than 2500 years with sites being occupied for more than 1500 years. It is in good agreement with the date of ~3600 BP (uncalibrated) at Steenbokfontein Cave (Jerardino and Swanepoel, 1999), obtained for collapsed wall paintings in archaeological layers.

If monochrome figures are the oldest at RSA TYN2, it is not the case of other sites as RSA LAB1. No pattern was found by comparing the style of the figures with their age in this area, except maybe for the two elephants which date from the historical period.

Comparing dates and paint characterization, carbon-blacks with a smooth texture and carbon-blacks with a fine-flaky texture were found to be used through all the five periods proposed for sites studied in the Maclear district whereas carbon-blacks with a flaky texture seem to be limited to the third and fourth periods. This distinction may be a bias given by the lack of dating on other sites, but may be seen as a change in the paint techniques or as the arrival of another San population in this area at a specific period of time.

Using radiocarbon dating on the black paint, it is possible to give a date for the use of the white paints composing polychrome figures. This comparison can be done only at RSA PRH1 on an elephant, whose tusks were made with kaolinite. Thus it is possible to conclude that kaolinite was used to paint in the Maclear district at least from 512 to 335 cal. BP.

### 4.3.3 Dates in context: implications for San rock art sites

The oldest date obtained in this study is from site TD12 in Botswana, with an age of 5723-4420 cal. BP. The same period has been recorded on two samples in ARAL 252, Lesotho, but as the amount of carbon was very low, they are not considered reliable. More dates should be provided to assess the presence of San in this part of Lesotho at this period.

The next oldest figures were again observed in Botswana on sites TD2 and TD12 and date between 3500 and 3000 cal. BP.

Then a period between 3000 and 2000 cal. BP comprises sites from Botswana and South Africa. It proves that San were present in both places at this time.

Then between 2000 and 1000 cal. BP, Lesotho, Botswana and South Africa sites were painted, and finally only South Africa and Lesotho sites were found to be painted after 1000 cal. BP.

To summarize, southern African hunter-gatherers were creating images on rock-shelter walls as long ago as 5723–4420 cal. BP in south-eastern Botswana, 2326-965 cal. BP in western Lesotho, and 2998–2381 cal. BP in the Maclear region of South Africa. This chronology falls in the same period as minimum and maximum ages obtained on calcium oxalates in the Kwa-Zulu Natal Drakensberg, South Africa, sites by Mazel and Watchman (1997, 2003) but gives direct ages to the figures.

Interestingly, black paintings dated in this study are only monochrome figures in Lesotho, and Botswana, except for two fishes in Botswana which were polychrome. On the other hand, South African paintings dated from the same period are mostly polychrome representations. Moreover, the representations in the Maclear district are mostly more detailed than their acolytes in Botswana and Lesotho. Can it be concluded that at least two different traditions of paint were present at the same time in areas as close to each other as are the Maclear district and the Phuthiatsana Valley? It is highly possible as each San population had their own tradition, even though they shared common beliefs. Moreover, the fact that similar black paint recipes were found in both areas corroborates possible exchanges or migrations.

These dates open up space for developing a chronometrically grounded approach to diversity and change within San rock art. Because the meaning of San rock art is so well understood, these chronological changes should be understood in social terms. This part is left in the hands of archaeologists.

Finally, these dates allow archaeologists to start developing a dialogue between the records of hunter-gatherer activity preserved in paint and that preserved in excavatable deposits. In the case of Lesotho's Metolong Dam catchment, for example, previous work there and in the wider Phuthiatsana Basin struggled to identify hunter-gatherer sites dating to the second half

of the Holocene, and completely failed to locate any at all for the period 5600–700 cal. BP (Mitchell, 1994), notwithstanding their presence in an environmentally very similar area directly across the Caledon River in South Africa (Wadley, 1995). These results (from ARAL171 and, though more cautiously, ARAL172) now show that hunter-gatherers *were* present for at least part of this period, implying that faulty survey methodologies and/or post-depositional changes of the regional landscape or specific site stratigraphies have hindered detection of *in situ* archaeological deposits.

### 4.3.4 Discussion on the methodology and radiocarbon dates

The methodology used to select samples has been advanced through the entire project and has been revealed to be very efficient at selecting the best candidates for radiocarbon dating and at assessing their type and homogeneity to interpret correctly the date obtained. However, this necessitates a wide number of instruments which are commonly found in universities around the world but in different departments which may make their access challenging at some points.

Furthermore, it requires a good understanding of the operation and limits of each of these instruments.

Each step of the characterization protocol is needed. The experiment at the beginning of the project performed at the University of the Witwatersrand, without us having the possibility of making cross-sections led to an unreliable date, as two carbon-based black paint layers where taken in the same sample (LAB1-C2).

The chemical pre-treatment protocol is now well established and following the proportion of radiocarbon contaminants estimated and the dissolution curve, it is possible to finely adjust the time needed in the acid to remove the contaminants, whilst securing as much as possible of the sample.

This protocol aims at reducing as much as possible the size of the sample to be taken. However, an area of at least 2 $cm^2$ is still needed. On the other hand, collection is done in conversation with archaeologists in charge of the sites, using cracks already present and in

parts of the figure where the paint layer seems to be the thickest, conserving the integrity of the representation.

The addition of FTIR analysis after pre-treatment proves to be very useful to check the presence of residual contaminants. This technique has its own limits as it cannot detect chemical bonds which represent less than 2 to 5% of the sample. However, it proves to be very efficient at detecting calcium oxalates, calcium carbonates and humic acids. The fact that none of their peaks are detected proves that they were, if not totally removed, reduced to an amount which is negligible for radiocarbon determination.

Dates obtained were mainly on "very small graphite" targets, with less than 500 μg of carbon, introducing larger uncertainties in the dates obtained, and raising the question of the proportion of contamination versus the carbon coming from the sample to be dated. For dates obtained on less than 100 μg of carbon, it is difficult to ensure that the level of contamination will be under 0.1% as required by Bronk Ramsey *et al.* (2004). However, the dates obtained are consistent with each other and with dates obtained on higher yielding samples, which would not be expected if contamination was an issue. Moreover, three replicates were made on three different figures from the three southern African areas studied, providing dates in good agreement with each other, proving that the protocol is efficient at removing radiocarbon contaminants and do not bring significant amount of contamination. Only one figure makes an exception, the eland at RSA LAB1, collected at the beginning of the Ph.D. project. Another date had to be measured with a larger amount of carbon to determine the most probable date of this figure.

With the improvements added to the characterization and pre-treatment protocols, the amount of carbon dated is larger and thus dates obtained have got smaller uncertainty.

In this project, some dates have large uncertainties due to the small amounts of carbon dated. But considering the estimation of the age of the sites was previously very wide, from 8000 to 100 BP, even determinations with large uncertainties provide enhanced chronological understanding and the use of Bayesian modelling further helps at determining the phases of painting within and between sites.

This protocol has been demonstrated to be successfully applied on *in situ* parietal paintings, in different regions of southern Africa where paint preparation, geology, weathering conditions, and contaminants vary. It is therefore likely that the same protocol could be used anywhere else in the world if carbon-based paints are found.

Moreover, by comparing the paint recipes identified and radiocarbon ages, it is possible to conclude that the same recipe was used in a single panel dating from one single period. Hence, there is homogeneity in the paint recipes through a single panel. This makes it possible to postulate that if a panel, which is made of figures having the same colour, is in fact shown to be made of different paint recipes, it would have been made either through different periods, or by three different populations at the same time, or a combination of both. In any of these cases, and if no dating method is applicable, the detailed characterization protocol established provides important information about the realization of the site and hence may influence the interpretation of this site. Following this ascertainment, and as none of the dating methods selected in this project were applicable at the *Mikinak* site, Quebec, Canada, the results of the characterization protocol were used to propose key information about the realization of the site (Chapter VI).

# CHAPTER V

# OPTICALLY STIMULATED LUMINESCENCE DATING ON ROCK ART: A FEASABILITY STUDY

This chapter deals with experimentations conducted on rock surfaces and rock painted surfaces to assess the possibility to use optically stimulated luminescence (OSL) as a tool to date rock art by using grains of quartz and feldspars from the rock on which paints were made. The working hypothesis is given as follow: rock faces on which rock art was made, are exposed to daylight every day for several hours, and hence have no residual luminescence signal. If paint is made on top of this rock face, it may protect rock face from daylight and thus a luminescence signal will accumulate in minerals according to time and natural radioactivity. The two parts of this hypothesis are investigated in this chapter, preceded by suitability tests of rock supports for luminescence dating. Details on instrumentations and samples preparations are given in chapter II.

## 5.1 Preliminary investigation

### 5.1.1 Geology of the sites

Studied sites are from two different climatic and geological areas: the Canadian Shield and the Karoo Supergroup, in South Africa. In the Canadian Shield, rock supports are gneiss and granodiorite mainly composed of quartz, whereas southern African rocks are sandstones composed of potassium feldspars (K-feldspars) and quartz in variable proportions (more details about the geology of each site can be found in Chapter I).

Even if these rocks contain minerals which are commonly used for OSL dating (quartz and K-feldspars: Table 5.1), their suitability needs to be tested.

**Table 5.1** Minerals and their grain size selected for each area studied

| Studied area | Minerals | Grain size |
|---|---|---|
| Cliff Lake | Quartz | 150-250µm |
| Lake Wapizagonke | Quartz | 150-250µm |
| Thune Valley, Botswana | Quartz<br>K-feldspars | 90-150µm |
| Phuthiatsana Valley, Lesotho | Quartz<br>K-feldspars | 90-150µm |
| Maclear district, South Africa | Quartz<br>K-feldspars | 90-150µm |

### 5.1.2 Suitability of quartz and K-feldspars for OSL/IRSL analyses

To test the suitability of quartz and K-feldspars in the different rocks, sensitivity tests and dose recovery tests were conducted. Sensitivity tests consists on doing a measurement of the OSL/IRSL signal of quartz and feldspars taken from the inner core of the rocks, where the natural signal is supposed to be saturated. This is followed by a test dose measurement. For quartz, an IRSL lecture is carried out before the OSL one, to see if there is any contamination with feldspars minerals, which would require further preparation. Indeed, feldspars emit luminescence when stimulated either by blue or by infrared light sources. Hence, if they are present in a sample, their signal will interfere with quartz OSL.

To conduct the tests, the Single-Aliquot Regenerative (SAR) protocol has been used. It is constituted of a set of cycles being themselves composed of two OSL measurements and one laboratory dose given. A cycle begins with the first OSL recording (Ln for the natural signal, Lx for regenerative doses). It can be preceded by preheat. Then, the signal read is normalized by adding a known laboratory dose, called test dose, which stays constant during all the protocol, and by recording the induced OSL signal, called Tn for the natural signal, Tx for regenerative doses. As for Ln/Lx, the OSL recording can be preceded by preheat. The first

cycle records the natural signal. Then to evaluate its equivalence to the radioactive dose received, known laboratory doses (called regenerative doses) are given to the aliquot and a cycle of recording is carried out after each regenerative doses. Ratio of signals Ln/Tn and Lx/Tx are plotted in a graphic against regenerative doses and the original dose received by the sample is extrapolated from the curve, called "growth curve".

Dose recovery test consists on zeroing the initial signal in the sample, giving it a known laboratory dose and trying to recover it. The SAR protocol (Murray and Wintle, 2000) is implemented to measure the apparent dose. The results are expressed as a dose recovery ratio (dose recovered/dose given). If it is in a scale of 10%, the sample is considered as suitable. Further parameters are investigated during dose recovery tests: recycling and recuperation.

The recuperation is the ratio of the 0 Gy regeneration dose to the corrected natural signal. It expresses the thermally transferred charges from shallow light-insensitive traps by the test dose and preheat. This value should not exceed 5% (Murray and Wintle, 2000).

In the SAR cycle, the first Lx/Tx is repeated at the end of the cycle to validate the SAR protocol as it should yield a similar value as the first one. If this recycling ratio is between 0.9 and 1.1, the SAR protocol is validated (Murray and Wintle, 2000).

#### 5.1.2.1 Quartz

*Sensitivity tests*

The sequence (Ln/Tn) used for quartz sensitivity is detailed in table 5.2. In the case of Cliff Lake and Lake Wapizagonke rocks, no OSL signal was recorded, thus new discs were made and a dose of 2 000 Gy was given to assess the suitability of quartz for OSL dating.

**Table 5.2** Sequence used for quartz sensitivity

| Step | Treatment |
|---|---|
| 1 | Preheat 240°C for 10s |
| 2 | IRSL at 50°C for 100s |
| 3 | OSL at 110°C for 40s |
| 4 | Test dose, 20Gy |
| 5 | Preheat 160°C for 10s |
| 6 | IRSL at 50°C for 100s |
| 7 | OSL at 110°C for 40s |

**Lesotho rocks**

Rocks taken at sites ARAL 169 and 172 have been tested and reveal a strong OSL signal and no IRSL signal, confirming no feldspars contamination.

**Maclear rocks**

Tests were conducted on rocks from sites RSA LAB1 and RSA MEL8. OSL signals were recorded for RSA LAB1 but with a very small intensity (less than 4000 counts) for minerals which are supposed to be saturated. However, the quartz of the RSA MEL8 rock yields a strong OSL signal and no IRSL signal. Thus, tests were continued only on quartz from RSA MEL8 rocks.

**Botswana rocks**

Tests were carried out on rocks collected at site TD 20. An OSL signal was recorded and a small IRSL signal. After a second HF pre-treatment, the IRSL signal disappeared. The first IRSL signal was due to the presence of feldspars which have not been dissolved by the first HF pre-treatment.

**Cliff Lake rocks**

As rock supports in Canada sites were different, the results are detailed in two paragraphs. Rocks collected around the Cliff Lake show almost no OSL signal even with a given dose of 2 000 Gy (Figure 5.1). No IRSL signal was recorded too.

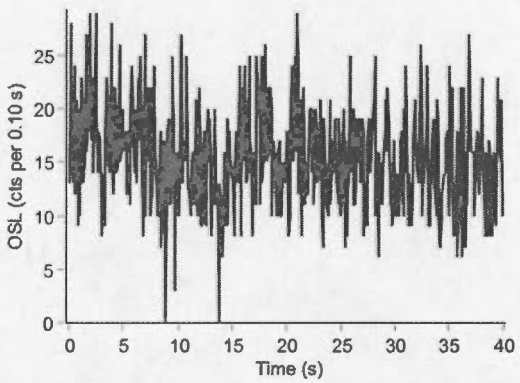


**Figure 5.1** Example of OSL signal recorded for Cliff Lake quartz.

Tests conducted on possible feldspars inclusions in quartz gave no exploitable results, the grains having no IRSL, neither OSL signal. Thus, Cliff Lake quartz were considered not suitable for OSL dating.

**Lake Wapizagonke rocks**

As for Cliff Lake rocks, almost no OSL signal was recorded on Lake Wapizagonke samples, even with a given dose of 2000 Gy. However, a strong IRSL signal is present. This signal was not present after a second HF cleaning, meaning that it was the result of feldspars contamination. Thus, Lake Wapizagonke quartz were considered not suitable for OSL dating.

**Conclusion about sensitivity tests for quartz**

No OSL signal was recorded on quartz from Canadian sites, whereas an intense signal was found on southern African rocks. It can be explained by the nature and geological history of the rocks. Indeed, southern African rocks are sedimentary rocks which originate from eolian and marine deposits. Canadian rocks are metamorphic rocks which did not experiment exposure and burial cycles and are much older than southern African ones. Quartz sensitivity may be a function of these cycles undertaken by the rocks. Hence, for primary rocks such as the ones in the Canadian Shield, no OSL signal is expected for quartz (Tsukamoto *et al.*, 2011). In the study conducted by Sobati *et al.* (2011), no exploitable OSL signal was recorded on metamorphic rocks too.

On the other hand, the sensitivity of quartz in the Maclear district rocks may be explained by annual fires, start up by farmers to renew grass for their herds. This may explain the difference noticed between rocks from two different sites in the Maclear district. However, this practice does not exist for the Botswana and Lesotho sites studied. Thus, the OSL signal from quartz is more likely to originate from the nature of the mineral and not from posterior fire exposures, which are likely to act as bleaching cycles.

Only Lesotho and South African rocks were selected from further tests as they contained K-feldspars too, which makes comparisons possible.

*Bleaching tests*

Dose recovery tests imply to reset the OSL signal naturally present in the sample. To know when the signal is the smallest, discs were made and put under a lamp reproducing daylight, SOL 2, from 30 min to 4 h. Natural signal was recorded too. Three discs were made for each period of time for Lesotho and South Africa rocks. The sequence applied is described in table 5.3.

**Table 5.3** Sequence applied for bleaching tests on quartz

| Step | Treatment |
|---|---|
| 1 | Preheat 240°C for 10s |
| 2 | IRSL at 50°C for 100s |
| 3 | OSL at 110°C for 40s |
| 4 | Test dose, 1Gy |
| 5 | Preheat 160°C for 10s |
| 6 | IRSL at 50°C for 100s |
| 7 | OSL at 110°C for 40s |

IRSL recording is conducted before each OSL lecture to assess the absence of IRSL signal which may influence the OSL results. No IRSL signal was recorded.

In both samples, the OSL signal comes to a plateau before 30 min of exposure (Figure 5.2). The shape and intensity of the curves are in good agreement, which is to be expected for rocks from the same geological formation even separated from hundreds of kilometres. This result is conformed to what should be expected for quartz. Similar tests carried out by Godfrey-Smith *et al.* (1988) showed a rapid decay of the OSL signal in quartz, even after few seconds. A plateau was reached before 30 min. Following these results, a bleaching time of 1 hour was selected for quartz samples.

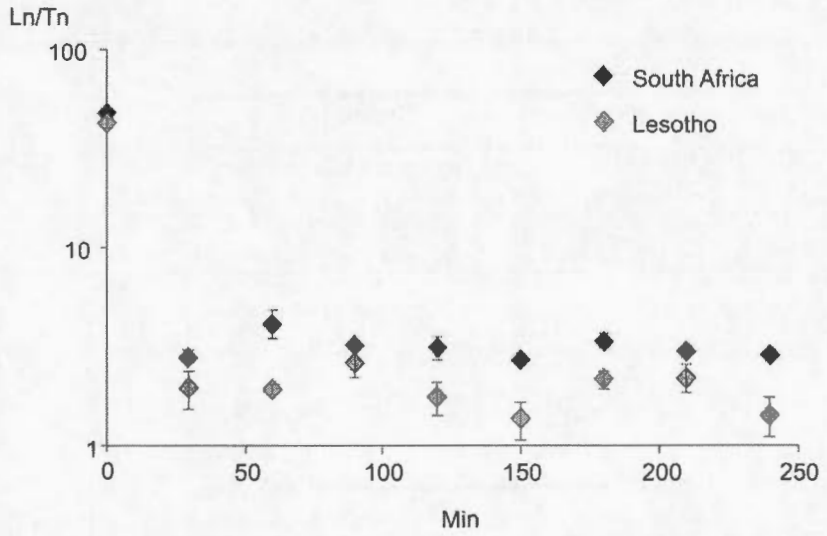


**Figure 5.2** Decay of OSL signal in quartz to daylight exposure

*Thermal transfer*

According to the archaeological data available, paintings studied may date from 200 to 8000 BP. In the case of young paintings, it is possible that thermal transfer would interfere in the equivalent dose determination. It has been investigated to help at selecting the correct preheat temperature for quartz.

Thermal transfer is a transfer of charges to luminescence sensitive traps during preheating. These electrons originate from deposition, radiation dose since deposition, and trapped electrons that are excited during the laboratory bleach (Rhodes and Bailey, 1997). Three aliquots were mounted for each preheat temperature (160°C to 240°C) and each rock (Lesotho and South Africa), bleached for 1 hour under the SOL 2 lamp, and then thermal transfer was recorded using a SAR protocol as detailed in table 5.4.

**Table 5.4** Thermal transfer sequence for quartz

| Step | Treatment |
|---|---|
| 1 | Preheat at 160-240°C for 10s |
| 2 | IRSL at 50°C for 100s |
| 3 | OSL at 110°C for 40s |
| 4 | Test dose, 1Gy |
| 5 | Preheat 160°C for 10s |
| 6 | IRSL at 50°C for 100s |
| 7 | OSL at 110°C for 40s |
| 8 | Regenerative dose: 1Gy/5Gy/10Gy/0Gy/1Gy |
| 9 | Return to step 1 |

For both rocks, thermal transfer is negligible until preheat of 200°C. It gets higher but still relatively weak (0.60 and 1.20 Gy) after preheat of respectively 220°C and 240°C (Figure 5.3). A preheat of 200°C or less should thus be used. Following these results, investigations continued on preheat plateau and dose recovery tests.

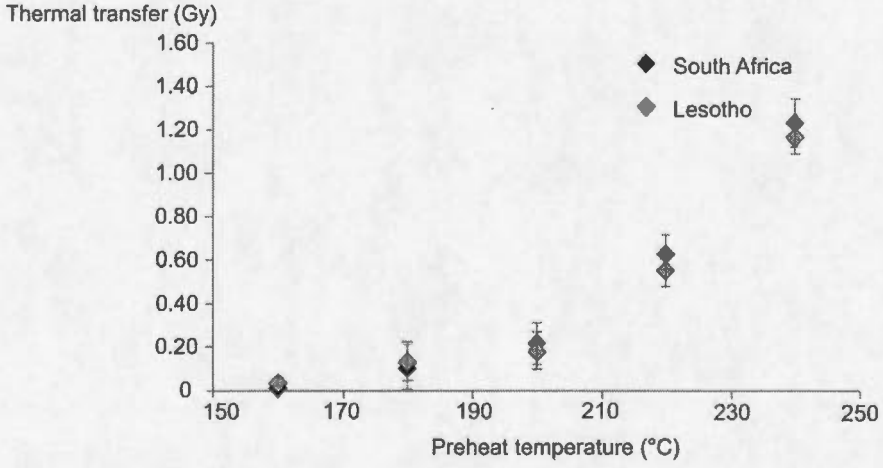


**Figure 5.3** Thermal transfer recorded on Lesotho and South African quartz samples

*Dose recovery tests/Preheat plateau tests*

Dose recovery consists of bleaching a sample, giving it a known laboratory dose, and then of conducting an equivalent dose determination to see if the dose recovered is similar to the one given. It assesses the possibility to use a sample for OSL dating. An evaluation and modifications of the SAR protocol can be then proposed in order to yield the expected result. This test was conducting with different preheat temperatures, resulting in a graphic of equivalent doses plotted against preheat temperatures showing a plateau.

Three aliquots were mounted for each preheat temperature (160°C to 240°C) and each rock (Lesotho and South Africa), and bleached for 1 hour under the SOL 2 lamp. The sequence used for dose recovery is given in table 5.5. Two series of dose recovery tests were conducted: first, one with a given dose of 20 Gy which correspond to the dose expected for a 10 000 year-old painting (slightly older than the archaeological expectation); secondly with a given dose of 2 Gy which correspond to a 1 000 year-old painting (the most likely date referring to the radiocarbon dates detailed in Chapter IV).

**Table 5.5** Dose recovery sequences for quartz

| Step | Treatment |
|---|---|
| 1 | Given dose, 2Gy |
| | Given dose, 20Gy |
| 2 | Preheat at 160 to 240°C for 10s |
| 3 | IRSL at 50°C for 100s |
| 4 | OSL at 110°C for 40s |
| 5 | Test dose, 1Gy |
| | Test dose, 3Gy |
| 6 | Preheat 160°C for 10s |
| 7 | IRSL at 50°C for 100s |
| 8 | OSL at 110°C for 40s |
| 9 | Regenerative dose, 1Gy/5Gy/10Gy/0Gy/1Gy |
| | Regenerative dose, 10Gy/50Gy/30Gy/0Gy/10Gy |
| 10 | Return to step 1 |

The first series show dose recovery ratios (dose recovered/dose given) within 10% for both Lesotho and South African rocks (Figure 5.4). The recycling ratios are within 10% and recuperations are 3.17 ± 0.57% for Lesotho rocks and 4.34 ± 0.36% for South African rocks.

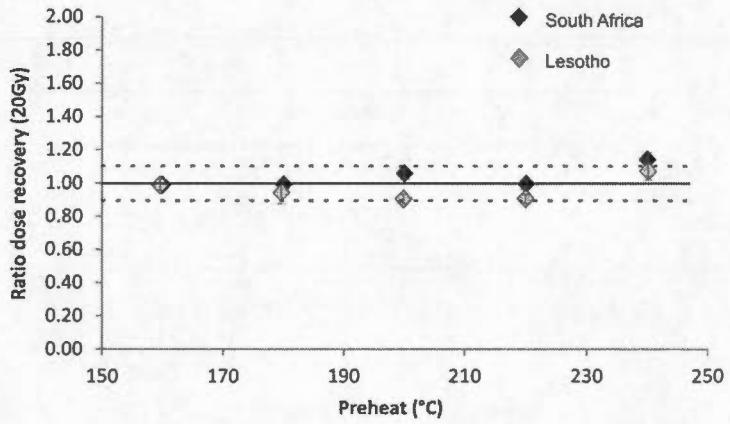


**Figure 5.4** Dose recovery ratios (20 Gy) for Lesotho and South African rocks

These results were plotted against equivalent doses to observe a preheat plateau (Figure 5.5). According to figure 5.5, the preheat temperature is 200°C for Lesotho rocks and 180°C for South African rocks. However, looking at the dose recovery ratio, for Lesotho, a better preheat temperature would have been 180°C. It is under the 200°C limits determined during thermal transfer experimentations.

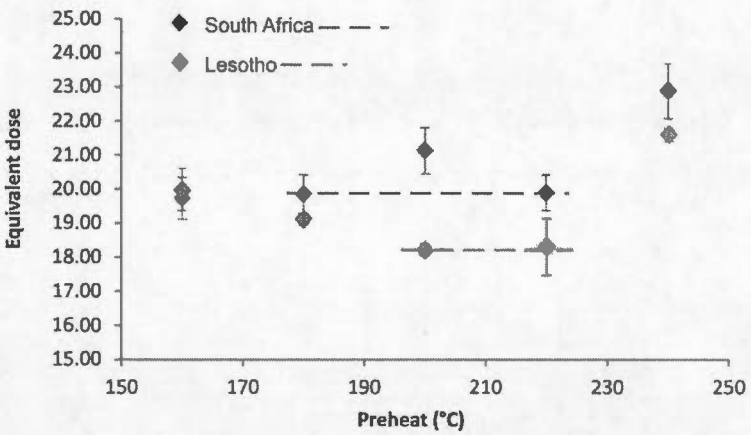


**Figure 5.5** Equivalent doses obtained for a range of preheat temperatures for Lesotho and South African rocks

These results show a good suitability for these rocks for OSL dating in the case of old paintings. But is it still the case for smaller doses? Thus investigations continued with given doses of 2 Gy.

Dose recovery ratios are within 10% for all preheat temperatures except 240°C for Lesotho rocks, whereas they are acceptable only for preheats at 180°C and 200°C for South African rocks (Figure 5.6). Recycling ratios are within 10% in all cases but the recuperation is at 15 ± 5% in all samples at all preheat temperatures.

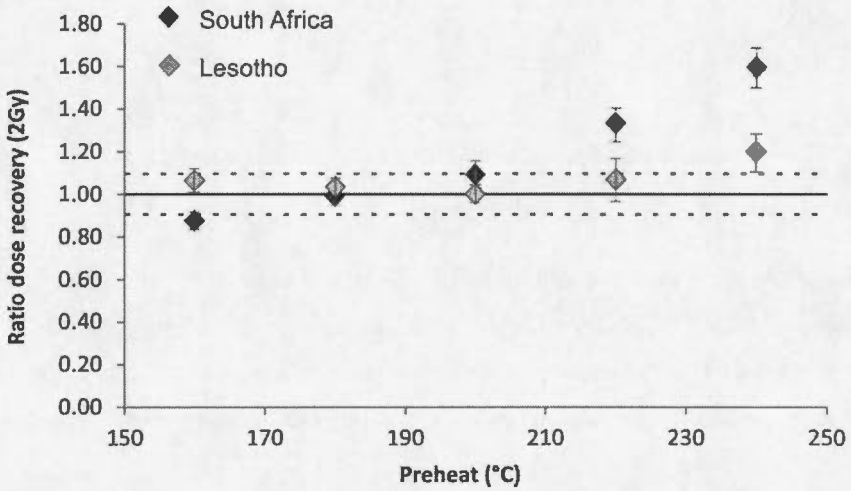


**Figure 5.6** Dose recovery ratios (2 Gy) for Lesotho and South African rocks

The preheat plateau is more complicated to see than with the previous series of results, especially for South African rock, where no plateau is particularly visible. However, it gives almost the same results with a preheat temperature of 180°C for South African rocks, and a preheat temperature of 200°C for Lesotho rocks (Figure 5.7).

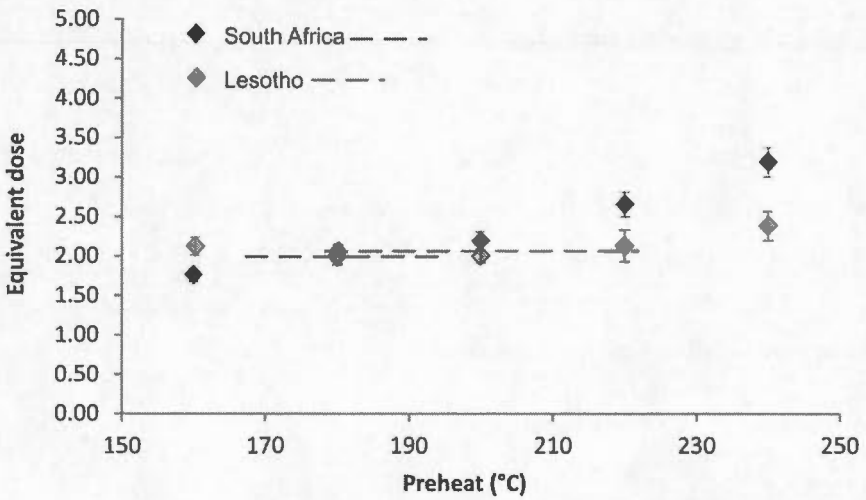


**Figure 5.7** Equivalent doses obtained for a range of preheat temperatures for Lesotho and South African rocks

In the aim of reducing the recuperation under 5% as it should be, another dose recovery test (2 Gy) was conducted on South African rock with addition of a 300s bleach between each Ln/Lx and Tn/Tx. The preheat temperature for Ln/Lx was 180°C. The results were not conclusive. Recuperation was still about 15% and the dose recovery ratio was about 20%. So this type of sequence was abandoned for quartz.

This part allows us to considered quartz from Lesotho and South African rocks suitable for OSL dating with specific preheat temperatures. The high level of recuperation for small doses is due to the weak signal observed in quartz. Moreover, even if it is about 15%, the error of 5% associated to it proves that this level is more an artefact of calculation due to the weakness of the signal rather than a real transfer of charges.

Potassium feldspars suitability for dating is now investigated, using the same series of tests.

5.1.2.2 Potassium feldspars (K-feldspars)

*Sensitivity tests*

Such as for quartz, K-feldspars sensitivity was tested giving a strong IRSL signal (between $5.10^4$ and $10^5$/sec.) for all the rocks tested. However, no more tests were conducted on Lake Wapizagonke rocks as only very few K-feldspars are present in this rock, thus very large samples (cores about 5 cm diam. and 3 cm long) would have been needed to continue the tests. These were not allowed by the person in charge of the site.

For comparison purpose, further experimentations were carried out only on Lesotho and South African rocks. It follows the same path than previously used for quartz suitability.

*Bleaching tests*

Aliquots were mounted and put under a lamp reproducing daylight, SOL 2, from 30 min to 4h. Natural signal was recorded too. Three discs were mounted for each period of time for Lesotho and South Africa rocks. Two rocks were tested for the South African area: one from RSA MEL8 and one other from RSA LAB1. Sequence applied is described in table 5.6.

**Table 5.6** Sequence applied for bleaching tests on K-feldspars

| Step | Treatment |
|---|---|
| 1 | Preheat 210°C for 60s |
| 2 | IRSL at 50°C for 100s |
| 4 | Test dose, 1Gy |
| 5 | Preheat 210°C for 60s |
| 6 | IRSL at 50°C for 100s |

Lesotho rock and South African rocks whatever the sites they come from, show the same pattern. At least 180 min (3h) are needed to reach a plateau in the residual dose (Figure 5.8). Thus, a 4-hour bleaching period was selected for our K-feldspars samples to be sure to reach this plateau.

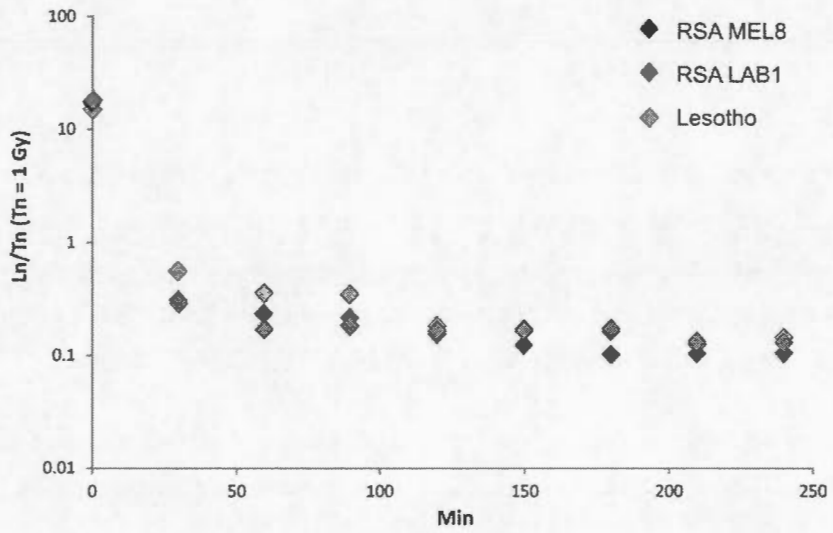


**Figure 5.8** Decay of IRSL signal in K-feldspars to daylight exposure (symbols include errors)

*Thermal transfer*

Such as detailed previously for quartz, K-feldspars may have significant thermal transfer which may interfere in the determination of equivalent dose of young paintings. Samples were bleached under artificial sunlight for 4 hours and then the sequence presented in table 5.7 was applied.

**Table 5.7** Thermal transfer sequence on K-feldspars

| Step | Treatment |
|---|---|
| 1 | Preheat at 0 - 230°C for 60s |
| 2 | IRSL at 50°C for 100s |
| 3 | Test dose, 1Gy |
| 4 | Preheat at 0 - 230°C for 60s |
| 5 | IRSL at 50°C for 100s |
| 6 | Regenerative dose: 1Gy, 5Gy, 10Gy, 0Gy, 1Gy |
| 7 | Return to step 1 |

Lesotho and South African rocks present the same pattern (Figure 5.9). Thermal transfer decreases with preheat temperature, which is to be expected as it is due to transfer of charges during preheat. A plateau is reached with a preheat at 90°C for 60s. The two points at the smallest temperatures are higher but these values are due to bias in the calculations as the signals recorded were extremely weak and thus integrations suffer for large errors. Recycling ratios are within 10% for all samples at all preheat temperatures, and recuperation is within 5% for all samples at all preheat temperatures except for preheats at 60, 30, and 0°C, which is due to the weakness of the signal recorded.

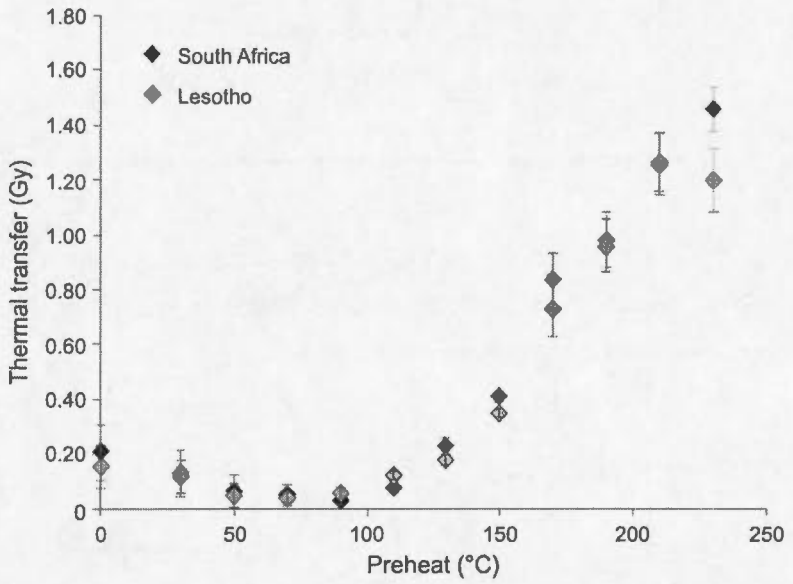


**Figure 5.9** Thermal transfer for Lesotho and South Africa K-feldspars

Thermal transfer recorded for each rock is high in comparison of the signal we are expected to analyse. Preheat temperatures can be reduced but an intense TL peak from instable traps is present in feldspars at 210°C (Duller, 1997). If samples are not enough preheated, they will suffer from interferences from these unstable traps. Thus, to try to reduce thermal transfer transmitted through SAR cycles, a bleach was introduced between each Ln/Lx and Tn/Tx, as previously done for Amerindian potteries by Forget Brisson *et al.* (2015). The bleach was done directly with the lamp inside the Lexsyg machine for 300 s. The sequence applied is detailed in table 5.8.

**Table 5.8** Modified thermal transfer sequence on K-feldspars

| Step | Treatment |
|---|---|
| 1 | Preheat at 170 - 230°C for 60s |
| 2 | IRSL at 50°C for 100s |
| 3 | Bleach for 900s |
| 4 | Test dose, 1Gy |
| 5 | Preheat at 170 - 230°C for 60s |
| 6 | IRSL at 50°C for 100s |
| 7 | Bleach for 900s |
| 8 | Regenerative dose, 1Gy, 5Gy, 10Gy, 0Gy, 1Gy |
| 9 | Return to step 1 |

For both Lesotho and South African rocks, the thermal transfer is about 10% less intense with the modified IRSL sequence (Figure 5.10). It helps to reduce transfer of charges during repeated preheat cycles, but it does not remove the initial thermal transfer.

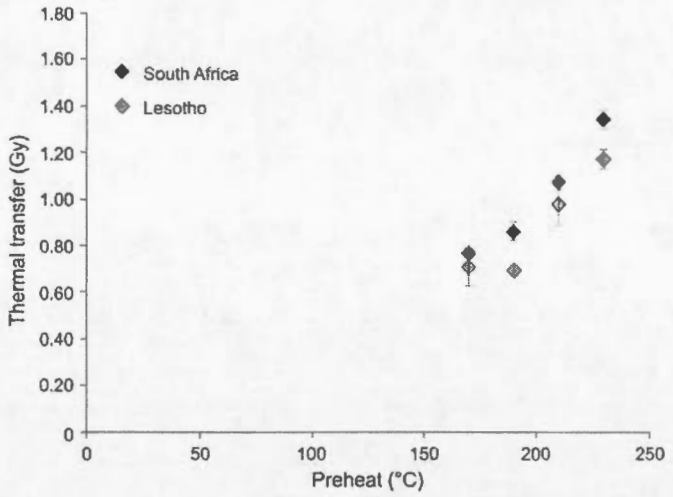


**Figure 5.10** Thermal transfer for Lesotho and South Africa K-feldspars with the modified sequence

Another way to estimate the thermal transfer contribution is to use the SARA protocol: Single-Aliquot Regeneration and Added dose (Murray and Mejdahl, 1999). In that aim, dose recoveries were carried out with the following given doses (three aliquots per dose): 0 Gy, 2 Gy, 5 Gy, 10 Gy and 15 Gy. The modified sequence with bleach and a preheat at 210°C for 60s was used. Doses recovered were plotted and extended to the x-axis to estimate thermal transfer value. It gives a result of 1.31 ± 0.12 Gy for the South African rock, and 1.20 ± 0.09 Gy for the Lesotho rock (Figure 5.11). They are slightly higher, but in the same range than thermal transfers previously recorded.

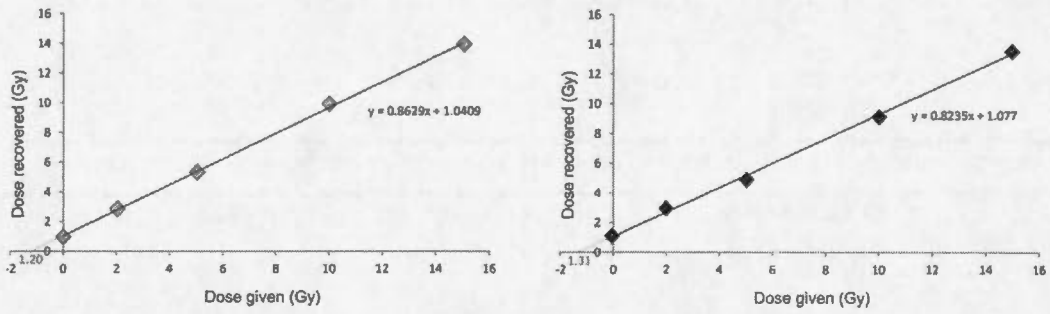


**Figure 5.11** Thermal transfer estimation using SARA: Right = South African rock; Left = Lesotho rock (symbols include errors)

Thermal transfer is about 1 Gy for each rock studied. It represents the equivalent of a 500 year-old signal already present in the samples and thus implies high errors in the case of recent ages. In previous studies on the evolution of luminescence signal in the rock (Sohbati *et al.*, 2011; Sohbati *et al.*, 2012), few or no thermal transfer was recorded in K-feldspars samples.

For dose recoveries tests, thermal transfer is subtracted from the results obtained to get a better estimate of the suitability of K-feldspars for IRSL dating.

*Dose recovery tests*

Dose recovery tests with a given dose of 20 Gy give good results for both rocks with a dose recovery ratio of 0.96 ± 0.07 Gy for the South African rock, and 1.07 ± 0.07 Gy for the Lesotho rock. Recycling ratios are respectively of 1.02 ± 0.03 and 0.97 ± 0.03, and recuperation varies between 3 and 4% in both cases.

Then, such as previously done with quartz, dose recovery tests were conducted with a given dose of 2 Gy. Two series were conducted: one with a conventional SAR sequence, and one other with the modified SAR sequence presented above (Table 5.9).

**Table 5.9** Sequences applied for dose recoveries on K-feldspars

| Step | Treatment, Type 1: conventional SAR | Step | Treatment, Type 2: modified SAR |
|---|---|---|---|
| 1 | Preheat from 170 to 230°C for 60s | 1 | Preheat from 170 to 230°C for 60s |
| 2 | IRSL at 50°C for 100s | 2 | IRSL at 50°C for 100s |
| 3 | Test dose, 1Gy | 3 | Bleach for 900s |
| 4 | Preheat from 170 to 230°C for 60s | 4 | Test dose, 1Gy |
| 5 | IRSL at 50°C for 100s | 5 | Preheat from 170 to 230°C for 60s |
| 6 | Regenerative dose, 1Gy, 5Gy, 10Gy, 0Gy, 1Gy | 6 | IRSL at 50°C for 100s |
| 7 | Return to step 1 | 7 | Bleach for 900s |
| | | 8 | Regenerative dose, 1Gy, 5Gy, 10Gy, 0Gy, 1Gy |
| | | 9 | Return to step 1 |

With the type 1 sequence, dose recovery ratios are too high whatever is the preheat temperature used (Figure 5.12). It is only in the range between 0.9 and 1.1 when no preheat is done, which is to be expected such as no heating is used and thus no charge transfer is present. Recycling ratios are between 0.95 and 1 for South African rocks, whereas they are between 1.02 and 0.94 for Lesotho rocks. Recuperation is slightly high, ranging between 3 and 12%.

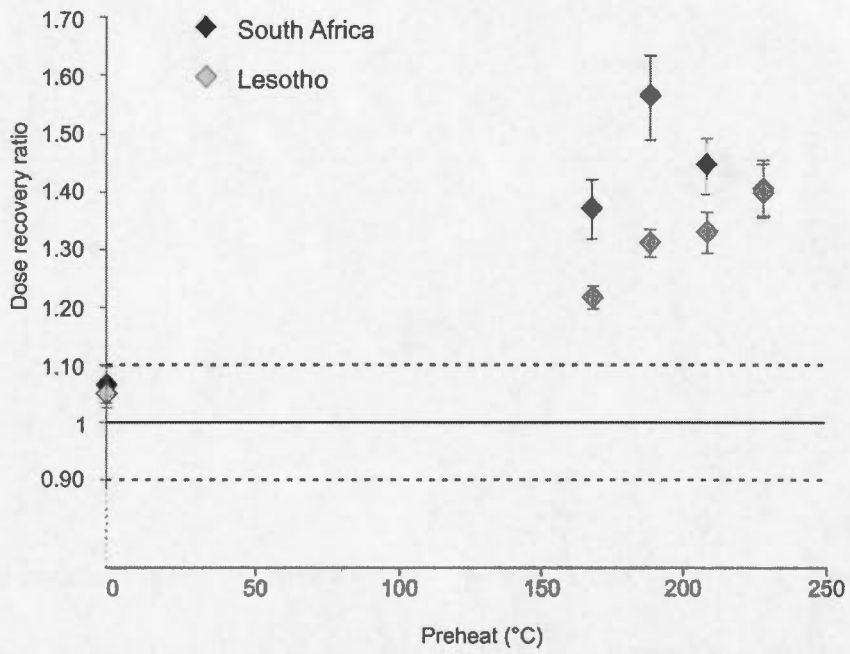


**Figure 5.12** Dose recovery ratios obtained with sequence type 1

Thermal transfers previously estimated were subtracted from doses recovered and dose recovery ratios were calculated again. Results are slightly better than previous dose recovery ratios but they are too small in comparison of what is to be expected (Figure 5.13). It seems that a too big part was subtracted to the dose recovered, and thus that the thermal transfer estimated previously contains another component. To see, if this component may come from the cycles of preheating, dose recovery tests were conducted using the modified SAR sequence (type 2).

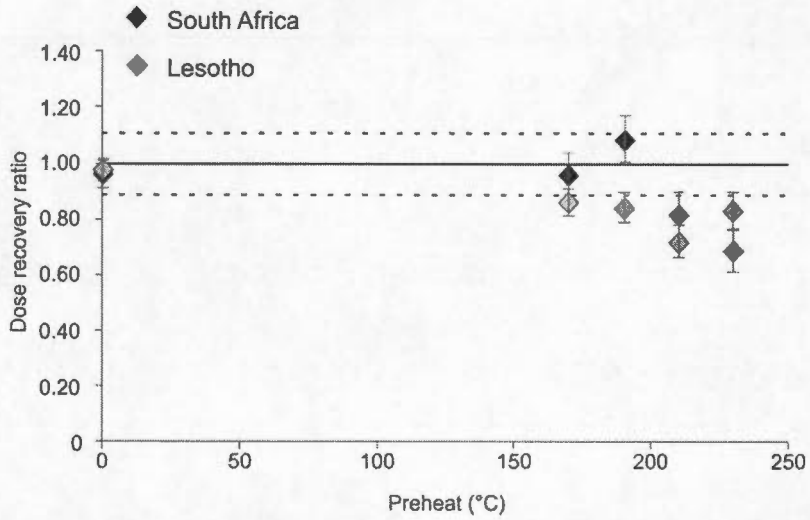


**Figure 5.13** Dose recovery ratios with thermal transfer subtracted (Sequence type 1)

Dose recovery ratios obtained with sequence type 2 are better than those of sequence type 1 (between 0.69 and 1.09 for South Africa, and between 0.71 and 0.97 for Lesotho), however, they are still mostly out of the range of 0.9 to 1.1 proposed in the ongoing SAR method (Figure 5.14). Recycling ratios are between 1.01 and 0.95 for South African rocks, and between 1.04 and 0.98 for Lesotho rocks. Recuperation is much better with sequence type 2, as it stays between 2 and 4% for both samples.

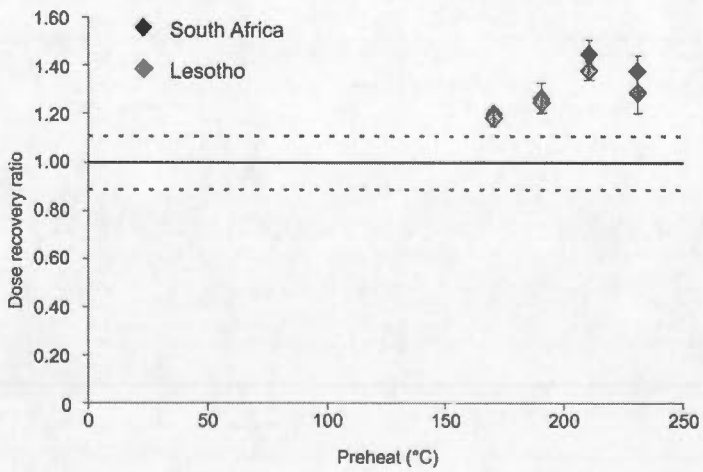


**Figure 5.14** Dose recovery ratios obtained with sequence type 2

When thermal transfer estimations are subtracted to doses recovered, the dose recovery ratios are in the range of accepted data for preheats at 180°C and 210°C for Lesotho rocks, and at 210°C for South Africa rocks (Figure 5.15). Because of the TL peak of K-feldspars at 210°C, preheat temperature selected was 210°C for 60s, to reduce as much as possible this unstable contribution.

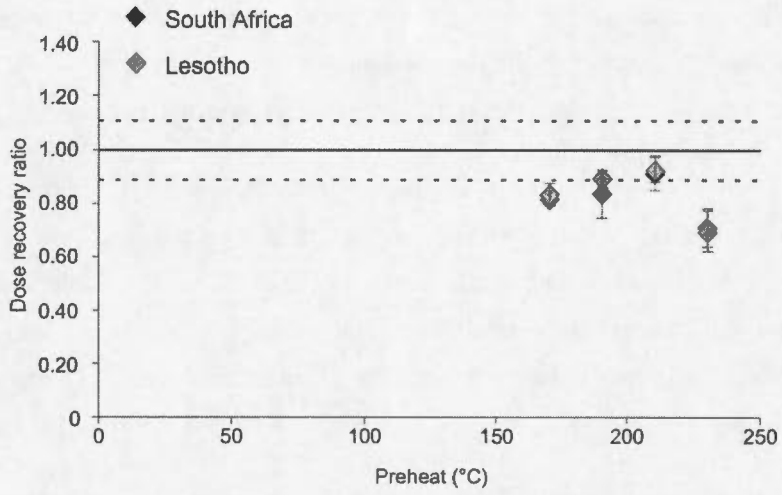


**Figure 5.15** Dose recovery ratios with thermal transfer subtracted (Sequence type 2)

K-feldspars from Lesotho and South Africa are suitable for IRSL dating if analyses are conducted with a modified SAR sequence with a preheat at 210°C for 60s and a subtraction of thermal transfer. Thermal transfer estimations by SARA are too high and were not used for further analysis.

5.1.2.3 Discussion and conclusion on suitability of minerals for OSL/IRSL dating

Quartz and K-feldspars from rocks collected on all the areas studied were analysed for suitability for OSL and IRSL dating. Because of the nature of rocks and possibility of comparison between quartz and K-feldspars, only rocks from Lesotho and South Africa were selected for further tests.

Bleaching tests show that quartz bleach much quicker than K-feldspars, as previously reported in Godfrey-Smith *et al.* (1988). Thus quartz seem to be the best candidates for this

project. Moreover, they do not suffer from high thermal transfer. Preheat temperatures were chosen at 180°C for South African rocks, and at 200°C for Lesotho rocks. On the other hand, recuperation recorded was higher than normally accepted for a SAR cycle, about 15%.

Quartz OSL signal is activated by blue light which excite feldspars too. Both of their luminescence signals will be read at the same time. Thus, quartz samples need to be free of feldspars. HF pre-treatments are conducted to achieve it but in the case of our sample, with small quantities of grains, it lefts very few at the end. Tests with post-IR OSL were conducted to try to eliminate feldspars contribution without pre-treatment (see §5.2.1).

Tests were conducted in parallel on K-feldspars. They take more time than quartz to get bleached but in the case of sites studied, exposed to sun several hours per day, they are assumed to be well bleached (hypothesis tested in §5.2.2). Suitability results show that they are good for IRSL dating even for small doses, if a modified SAR protocol with a preheat at 210°C for 60s is used. Even if they suffer for high thermal transfer, it can be subtracted to get an acceptable dose recovery ratio.

Using the determined parameters, further analysis is conducted. First, the OSL and IRSL signals from the rock face to the inside rocks are investigated, to verify the first part of the working hypothesis: minerals at the surface of the rock face have no residual luminescence signal.

## 5.2 Luminescence transects inside of the rock faces

Cores of rocks collected on rock faces close to paintings were prepared and analysed millimetre per millimetre to document the OSL and IRSL signals inside rocks.

### 5.2.1 Quartz

A few grains are collected from each core millimetre, and HF pre-treatment reduce their number further which leaves just enough sample to mount 2 or 3 discs. In the aim to have larger sample to analyse, post-IR OSL sequence was tried on a core from South Africa.

Post-IR OSL is used on fine-grains polymineral samples to eliminate feldspar contribution. Wintle (2008) mentioned that an IRSL lecture of 5 min prior to OSL lecture, on 4-15 μm

polymineral samples has got the same effect than a 3-day etching with $H_2SiF_6$ (hexafluorosilicic acid). Quartz used in this study is much coarser (150-250 μm). The sequence applied is detailed in table 5.10.

**Table 5.10** Post-IR OSL sequence

| Step | Treatment |
|---|---|
| 1 | Preheat 180°C for 10s |
| 2 | IRSL at 50°C for 330s |
| 3 | Green OSL at 110°C for 40s |
| 4 | Test dose, 10Gy |
| 5 | Preheat 160°C for 10s |
| 6 | IRSL at 50°C for 330s |
| 7 | Green OSL at 110°C for 40s |
| 8 | Regenerative dose, 200Gy, 400Gy, 50Gy, 0Gy, 200Gy |
| 9 | Return to step 1 |

Tests were first conducted by reading Ln/Tn (Test dose = 3Gy) to see if the remnant quartz signal would be high enough after IRSL stimulation on rock from RSA MEL8. A weak but possibly exploitable signal was recorded. Addition of bleach or hotwash after Ln measurement did not help to get a better signal. Thus, a sample from the centre of the rock, where a dose of 273.03 ± 18.55 Gy was recorded by K-feldspars, was analysed with this sequence. The equivalent dose recorded was 78.80 ± 47.8 Gy. It is out of the K-feldspars equivalent dose determination and suffers for large incertitude due to the weakness of the signal even with high doses. Thus post-IR OSL was abandoned for further investigations.

Quartz prepared from 1 mm slices of rock cores were extremely few, not enough to make discs and get an exploitable signal. Thus further investigations were focused on K-feldspars.

### 5.2.2 K-feldspars

#### 5.2.2.1 Preliminary tests on fallen rocks

A core was sampled under red light from a rock collected on the floor of RSA LAB1, to investigate the evolution of the IRSL signal through depth. First, a Ln/Tn recording was conducted with a test dose of 10 Gy and a bleach of 900s after Ln measurement (Figure 5.16). It shows a bleach of the signal at the surface, through the 3rd millimetre, where the signal seems to reach a plateau. This profile is similar to those previously recorded by Freiesleben *et al.* (2015), and Sohbati *et al.* (2011, 2012).

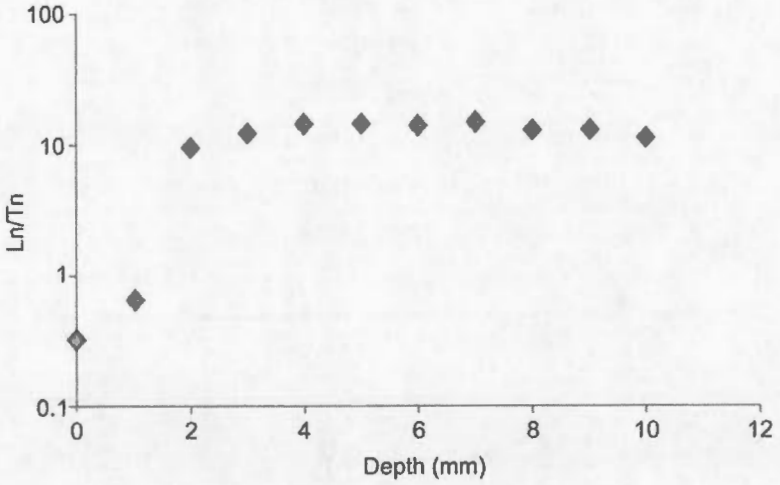


**Figure 5.16** IRSL profile in the rock from RSA LAB1 (logarithmic scale, symbols include errors, no thermal transfer subtracted)

Second, equivalent doses were recorded for the two first millimetres using the modified SAR protocol for K-feldspars, detailed in Table 5.9. They give respectively 0.91 ± 0.13 Gy for 0-1mm part, and 3.22 ± 0.57 Gy for the 1-2mm part. The equivalent dose calculated from the surface is in the range of the thermal transfer previously recorded. And thus, one can conclude that no IRSL signal is present at the surface. The result from the second millimetre shows an attenuation of the signal, as can be expected regarding the study on light penetration in Clarens formation rocks by Hall *et al.* (2010). Then, tests were pursued using cores collected *in-situ* from the rock face close to paintings.

5.2.2.2 Cores collected on the rock face close to paintings

Five cores from two sites, Aral 172 and Aral 175 were selected. At site Aral 172, two cores were taken around the figure of an eland well exposed to sunlight. At site Aral 175, three cores were collected around a human figure in a deeper part of the shelter but exposed to direct sunlight at least several minutes per day (observation made during my visit in 2012). During these tests, the Lexsyg instrument on which all the previous results were obtained, broke and its fixing required several months. Hence, tests were continued with the Risø instrument. Details about setting of this instrument and tests conducted to adjust the SAR sequence are given in Appendix B. The main changes were in the pre-heat temperature which was reduced to 200°C and in the use of a thermal wash step instead of a bleach step. The thermal wash consists on an IRSL recording at 225°C for 100s after each Ln-Lx and Tn-Tx.

First, a Ln/Tn recording was conducted on three disks per millimetre, with a test dose of 1Gy and a thermal wash after the Ln measurement (Figure 5.17). Then equivalent doses were calculated using the modified SAR sequence for Risø on three disks per millimetre (Table 5.11 and Figure 5.18).

**Table 5.11** Example of a modified SAR sequence for Risø (test doses and regenerative doses vary depending on the depth in the core)

| Step | Treatment |
|---|---|
| 1 | Preheat at 200°C for 60s |
| 2 | IRSL at 50°C for 100s |
| 3 | IRSL at 225°C for 100s |
| 4 | Test dose |
| 5 | Preheat at 200°C for 60s |
| 6 | IRSL at 50°C for 100s |
| 7 | IRSL at 225°C for 100s |
| 8 | Regenerative dose |
| 9 | Return to step 1 |

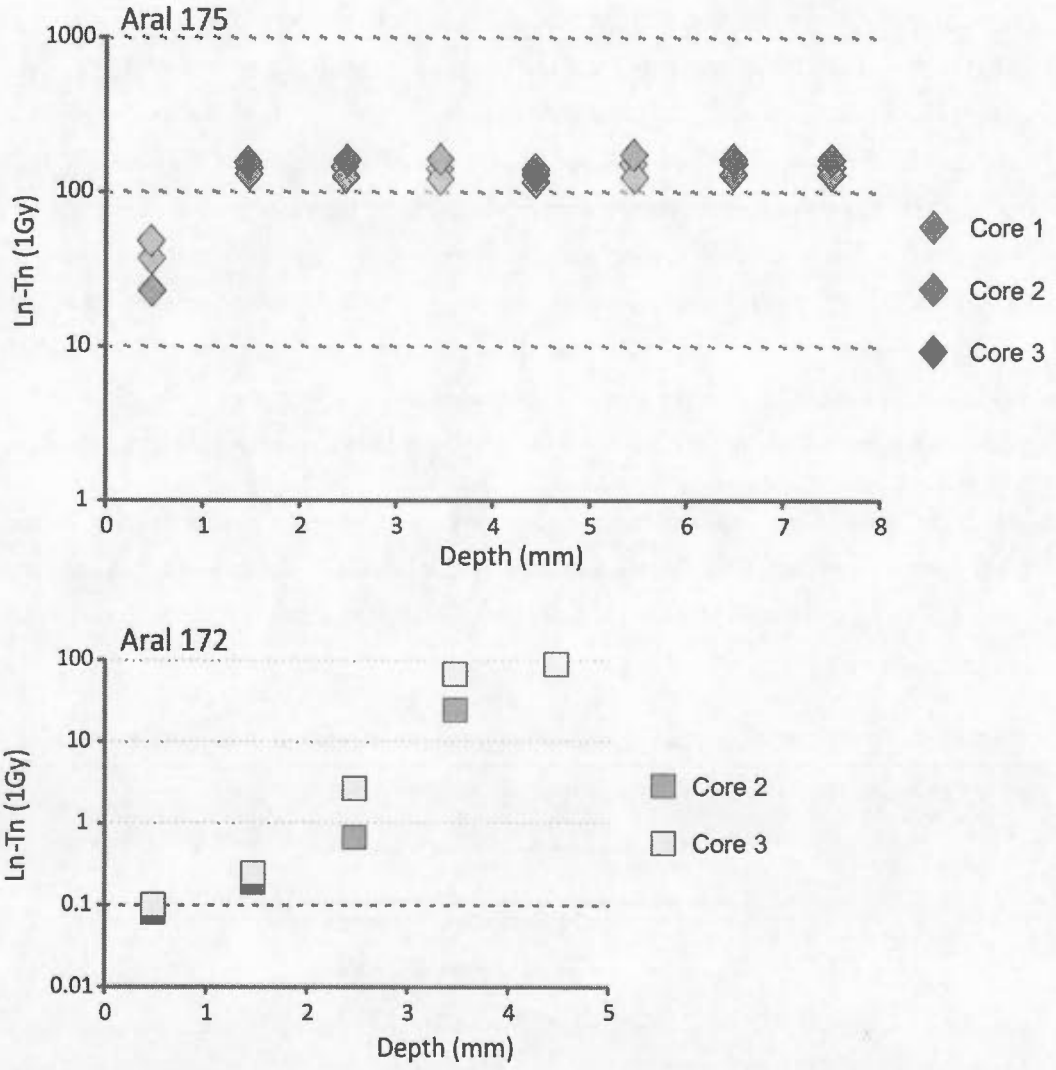


**Figure 5.17** Ln-Tn profiles of transects taken from rock face close to paintings from sites Aral 172 and Aral 175 (the red line represents the thermal transfer level observed for the rock)

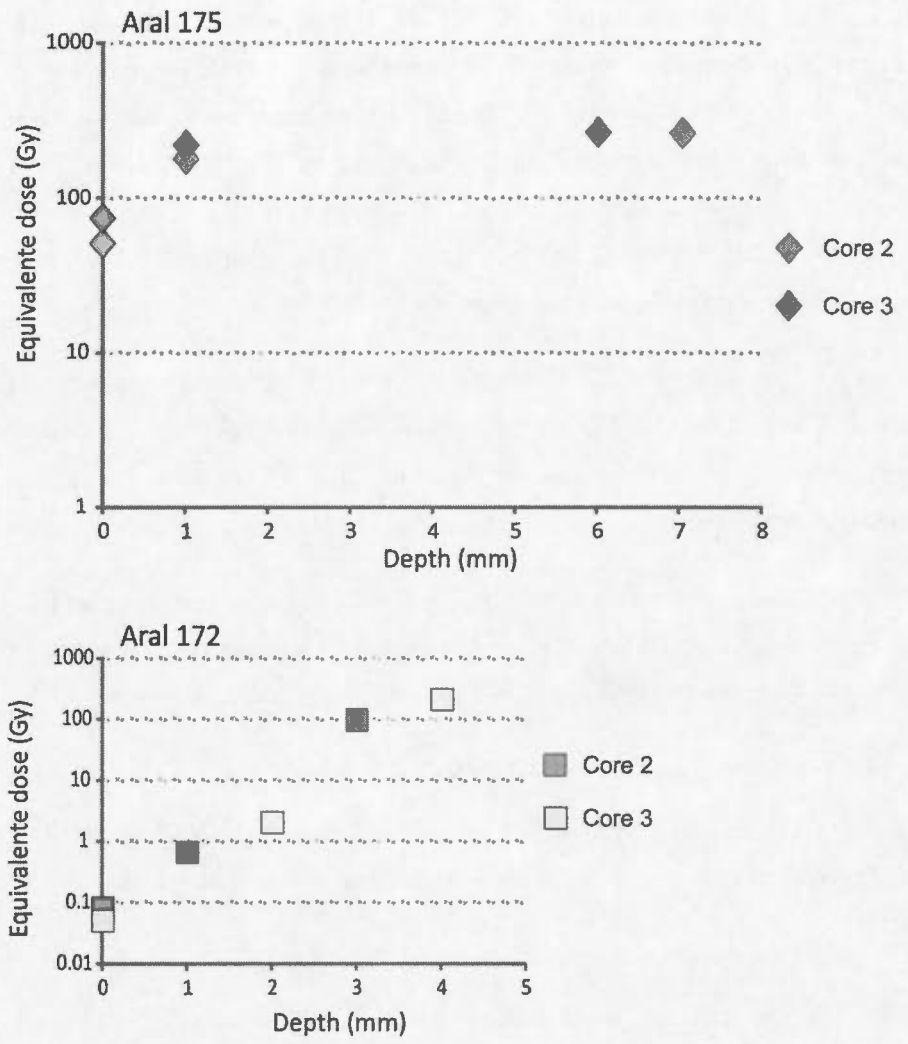


**Figure 5.18** Equivalent dose transects of cores taken from rock face close to paintings from sites Aral 172 and Aral 175 (thermal transfer subtracted)

The two series of cores do not exhibit the same pattern. At Aral 175, the signal at the surface is not completely bleached, and the determination of the equivalent dose shows a high dispersion in the results for core n°3 at the surface (85.4 ± 1.9 Gy, 72.1 ± 1.6 Gy, 69.8 ± 1.6 Gy). This dispersion is less visible for core n°2. It reveals different degrees of bleaching to which the grains constituting the rock face where exposed.

On the opposite, the two cores from Aral 172 show that they were bleached for the three first millimetres in depth, corresponding to the tests conducted on the fallen rock at RSA LAB1, and in agreement with Hall *et al.* (2010). Equivalent doses show that the bleaching is progressive through the three first millimetres reaching the saturated value of the rock at 4 mm in depth. These results proved that light can down up to 3 mm inside rock, and thus contribute to bacterial life and plant growing. Light penetrates through reflection properties of rock minerals, especially quartz and feldspars.

These results show the importance of checking the bleach of the rock face on which paintings were created. Even if the rock face seems exposed to direct sunlight several minutes or hours per day, on some sites, it is not enough to bleach minerals at the surface, especially K-feldspars which require longer exposure (as detailed in §5.1.2).

On the other hand, when exposition to daylight is sufficient, it can be concluded that 2 to 3 mm of rock is needed to make a proper protection against daylight. What about paint layers? Further tests investigate this second part of the working hypothesis.

## 5.3 Reproduction of rock paintings for tests

To test the hypothesis that a layer of paint protects against sunlight, artificial paintings had to be made to reproduce the conditions in the rock-shelter.

### 5.3.1 Paintings preparation and reproduction

Red and white soils collected in the vicinity of sites in the Phuthiatsana Valley, in Lesotho, are similar to those used by the artists, if previously crushed in mortar and separated by settling. Such pigments were prepared with soils R4 and W8 and then mixed with vegetal oil to make paints.

Two rocks were used for artificial paintings: one from RSA MEL8 and one other from ARAL172. As their size is about 15 cm diameter, minerals at their centre are supposed to be saturated and thus are good candidates for such experimentations. Indeed, to know if the paint layer can make a protection from the sun, a rock with a known and high natural dose

has to be used, to avoid thermal transfer of charges, and unstable contributions from laboratory doses.

The first one was cut with a saw under red light, and then paints were spread with pencils under red light too. Only one side was painted, the other side was left in a black plastic bag to have the original dose of the sample before exposure to daylight. Using this method, even with applying a high number of paint layers, the rock absorbed a part of the paints resulting in a very thin and sparse layer of paint (Figure 5.19). This absorption occurs too on rock face, but asperities retain the paint at the surface.

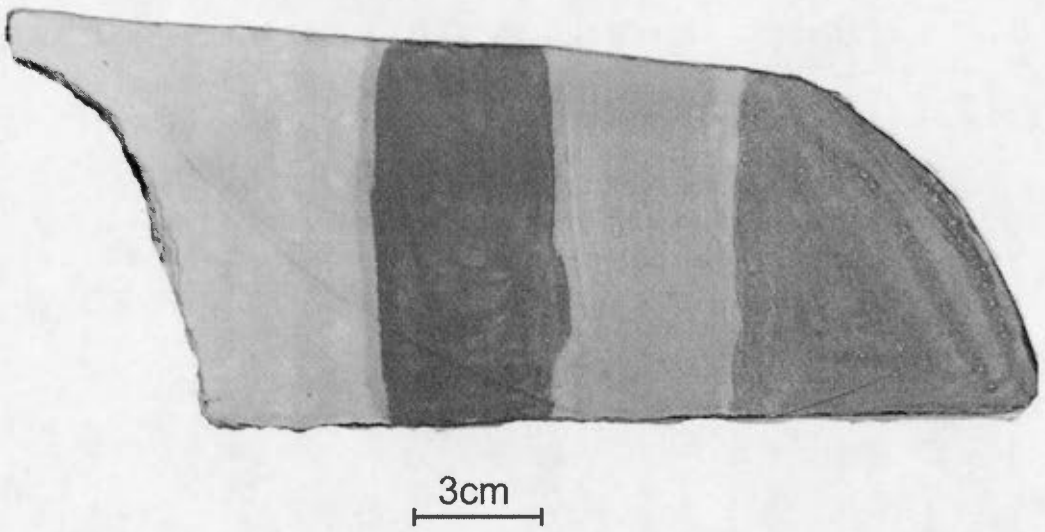


**Figure 5.19** Photo of the painted rock from RSA MEL8

The second rock, from ARAL172, was cut by a press under red light, resulting in a rough rock surface, giving a surface similar to those used by the artists. Then paint was made under red light as previously done for rock from RSA MEL8, resulting in a paint layer of about 100 μm thick.

The rocks were tapped with black tap to avoid daylight to penetrate in the rocks from another part than the painted surface, representing the rock face, and put under the SOL2 lamp for

24h, which represent the equivalent of 5 days continuous daylight exposure, in southern Africa.

Cores were taken from the painted and unpainted surfaces of these rocks and prepared as detailed in Chapter II.

5.3.2 Luminescence transects with paintings

5.3.2.1 Rock from RSA MEL8

Two cores (Ca3 and Ca4) from the stripes made with the red soil R8 were analysed. First, Ln/Tn ratios (Test dose: 1Gy, and a 900s bleach after Ln, analysis carried out with Lexsyg) on K-feldspars were recorded for each millimetre of cores (Figure 5.20).

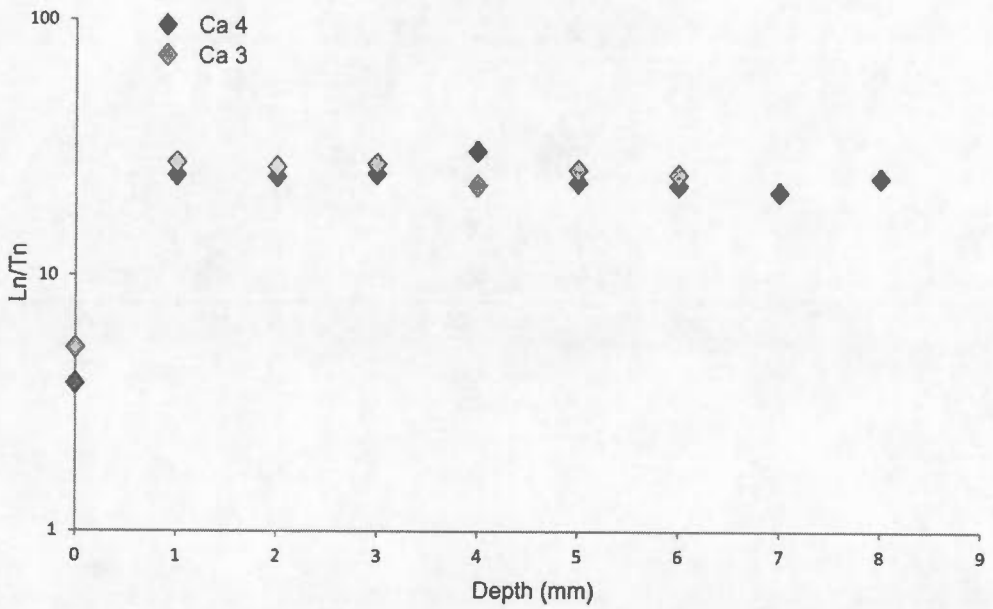


**Figure 5.20** Ln/Tn transects of cores with painted surfaces (RSA MEL8, Test dose: 1 Gy, symbols include errors)

Both cores give the same results: at the surface, the signal is partially bleached, and after the second millimetre, the signal comes to a plateau reflecting the dose from the inside of the rock. As the test dose used is small in comparison of the saturated signal expected for such part of the rock, equivalent dose determinations were conducted for parts 0-1, 1-2, and 6-7

mm (Figure 5.21). Thermal transfer estimation was subtracted from the equivalent doses obtained.

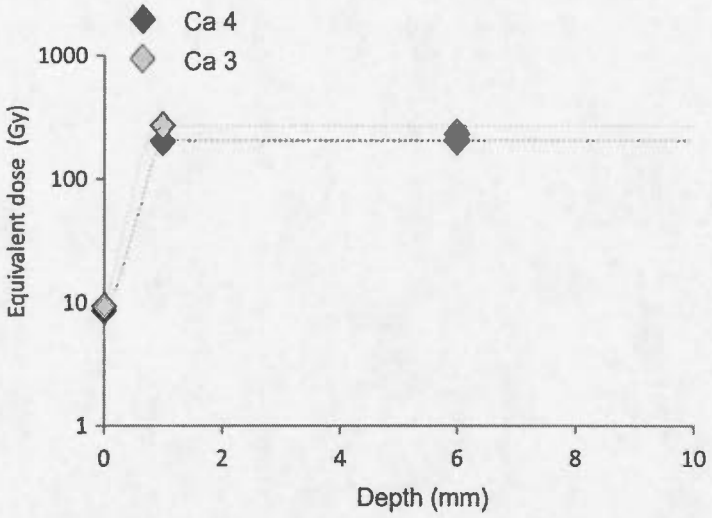


**Figure 5.21** Equivalent doses transects of cores with painted surfaces (RSA MEL8). Profiles were reconstructed by dot lines; symbols include errors.

The equivalent doses at the surface (thermal transfer subtracted) are 9.26 ± 1.06 Gy for Ca3 and 8.36 ± 1.62 Gy for Ca4. They are in close agreement and prove that the paint made a partial protection from daylight. The recovered signal is only 4% of the original dose, calculated at 232.74 ± 18.58 Gy for Ca3, and at 199.07 ± 6.92 Gy for Ca4.

Here, paintings were made on a smooth surface, which implies that the paint was absorbed by rock and thus results in a very thin layer of paint (less than 10 μm). The luminescence signal may be better protected on a coarser surface. However, these results show that even a thin layer on top of rock surface can influence the equivalent dose obtained.

5.3.2.2 Rock from ARAL 172

Painting was done only on 2/3 of the rock, living 1/3 exposed to direct light without protection. Four cores were taken from the painted parts and two from the unpainted part. Cores were collected and prepared as detailed in Chapter II.

First, Ln/Tn ratios (Test dose: 1 Gy, and thermal wash after Ln, analysis carried out with Risø) on K-feldspars were recorded for each millimetre of cores. However, a very weak signal was recorded on all cores whatever the depth of the slice. Only on one core from the painted part, a signal was recorded on three disks from different depths and plotted in Figure 5.22.

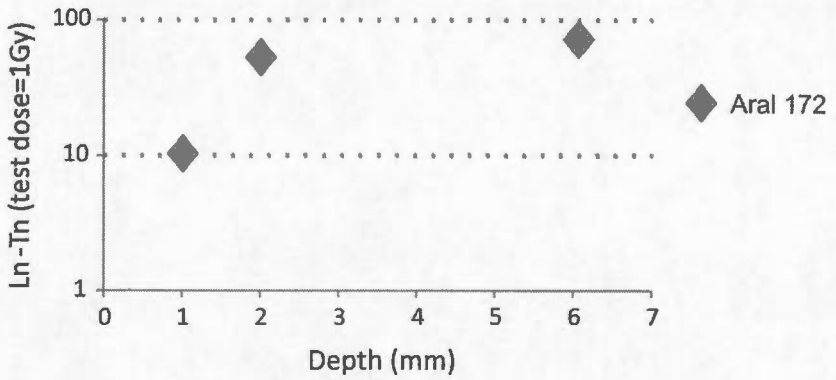


**Figure 5.22** Ln-Tn transect of core n°1 from the painted part of rock from Aral 172

To understand this lack of signal, 10 disks from different cores taken from the rock were analysed with SEM-EDS and Raman spectroscopy. It reveals that the grains constituting the disks and by extension the rock, were mostly anorthoclases ($(Na,K)AlSi_3O_8$). The presence of such feldspars has been previously reported in Clarens Formation sandstone (Bonneau *et al.*, 2012, and Chapter III). As they have a specific mineralogical structure, between K-feldspars and albite, they can emit luminescence with both blue and yellow wavelengths. However, in that case, a very weak emission was recorded in the blue and no instrument at the Lux laboratory has filters to test the presence of luminescence in the yellow part of the visible light spectrum.

Regarding the results from the Ln-Tn profile, it can be concluded that light penetrated and partially bleached at least the two first millimetres of the painted rock surface (paint layer being about 100 µm thick). However, it is not possible to push conclusion forward.

According to the two tests conducted from the painted rocks, one can conclude that the layer of paint makes a partial protection of rock face against daylight. Further tests should be conducted to estimate and model the protection made by a layer of paint.

Fading correction and annual doses were then investigated to complete the feasibility study conducted in this chapter.

## 5.4 Fading correction

Fading was calculated from the 0-1 mm part of Ca3 and Ca4 of rock from RSA MEL8. Three prompt and one delayed (7 days) measurements were done with a given dose of 20 Gy and a test dose of 3 Gy. Calculations of the *g*-value were carried out following equations in Huntley and Lamothe (2001). The *g*-value obtained is 0.4 ± 1.1%/decade for Ca3, and 4.4 ± 3.1%/decade for Ca4.

These values are relatively low and in close agreement with the ones calculated on soils from Wonderkrater, South Africa by Barré *et al.* (2012). This indicates that the luminescence signal recorded at the surface of the rock face, just underneath the paint layer, is close to the natural dose, with very little loss of electrons.

The last parameter to be evaluated in our protocol is the annual dose, also called dose rate.

## 5.5 Dosimetry and dose rates

As detailed in Chapter II, the dose rate for our samples has three individual components: rock, pigment and cosmic rays coming from the atmosphere (see Figure 2.12, in Chapter II). The water content was set at 1 ± 0.5 for southern African rocks, according to results from Hall *et al.* (2010), and at 10 ± 5 for soils and pigment. The percentage of internal potassium in K-feldspars was selected at 12.5 ± 5%.

### 5.5.1 Rocks

Each type of rocks from each studied area has been analysed with gamma spectrometry. To verify the homogeneity of the rock, a duplicate has been made on the same kind of rock but from another site in the same area. In the case of RSA BUX1 and the Botswana area, no duplicate has been made. Results are summarized in Table 5.12.

Getting the concentration of uranium and thorium, a high over-dispersion (20 to 60%) was recorded for RSA BUX1, Cliff Lake 1 and Lake Wapizagonke 1 and 2. It is due to the small intensity of the gamma peaks, and thus to the incertitude when fitting the peak to calculate the concentration. This introduces larger errors to the concentration but they stay in the order of magnitude of common results.

Results show a good homogeneity inside the same kind of rock, except the granodiorite from the Cliff Lake. Granodiorites of the Cliff Lake are coarse-grained igneous rocks which date from the Archean and which experienced various tectonics events and magmatic intrusions. Observed under microscope and SEM-EDS (see Chapter III), grains are various and inhomogeneous. This microscopic observation is confirmed by macro-observations *in-situ* were differences in colours, size of minerals, and feldspars/quartz veins were observed. So the heterogeneity of the Cliff Lake rock dose rate is doubtless attributed to the variations in composition into the rock itself. It implies that in case of OSL dating, the dose rate should be calculated with a sample of rock collected as close as possible from the paint, and another about 50 cm far to evaluate the homogeneity of the dose calculated.

If taking into account only sample Cliff Lake 1, its dose rate is similar to Lake Wapizagonke ones. Lake Wapizagonke rocks are pyroxene-rich gneisses. They were formed by metamorphisms of igneous rocks during the Precambrian, and their mineralogical compositions are similar with presence of quartz, alkaline-feldspars and plagioclases, and pyroxenes (see Chapter III and Appendix A for the characterization of the rocks).

**Table 5.12** Gamma spectrometry results and dose rate calculations for rocks

| Sample | U (ppm) | Th (ppm) | K (%) | Quartz dose rate (Gy/ka) | K-feldspars dose rate (Gy/ka) |
|---|---|---|---|---|---|
| RSA LAB1 | 4.11 ± 0.13 | 13.43 ± 0.4 | 1.96 ± 0.02 | 4.17 ± 0.16 | 4.76 ± 0.17 |
| RSA MEL8 | 6.1 ± 0.3 | 10.0 ± 0.2 | 1.93 ± 0.05 | 4.25 ± 0.19 | 4.85 ± 0.19 |
| RSA BUX1 | 0.90 ± 0.07 | 2.4 ± 0.4 | 0.35 ± 0.03 | 0.76 ± 0.05 | 1.28 ± 0.06 |
| TD20 | 0.58 ± 0.06 | 1.3 ± 0.1 | 0.71 ± 0.03 | 0.94 ± 0.06 | 1.46 ± 0.06 |
| ARAL 175 | 2.98 ± 0.13 | 5.1 ± 0.4 | 2.07 ± 0.05 | 3.17 ± 0.12 | 3.75 ± 0.13 |
| ARAL 169 | 4.17 ± 0.17 | 7.7 ± 0.2 | 1.71 ± 0.04 | 3.35 ± 0.14 | 3.93 ± 0.15 |
| Cliff Lake rock 1 | 0.37 ± 0.04 | 0.9 ± 0.4 | 0.15 ± 0.02 | 0.31 ± 0.05 | 0.83 ± 0.06 |
| Cliff Lake rock 2 | 3.80 ± 0.17 | 13.8 ± 0.3 | 3.22 ± 0.06 | 5.16 ± 0.19 | 5.78 ± 0.19 |
| Lake Wapizagonke rock 1 | 0.49 ± 0.05 | 0.6 ± 0.2 | 0.52 ± 0.03 | 0.68 ± 0.05 | 1.20 ± 0.06 |
| Lake Wapizagonke rock 2 | 0.49 ± 0.06 | 0.6 ± 0.2 | 0.51 ± 0.04 | 0.67 ± 0.05 | 1.19 ± 0.06 |

Interestingly, the dose rates of the Canadian rocks are similar to those of rock from Botswana and from RSA BUX1. These southern African rocks are sandstones. RSA BUX1 rocks are attributed to the Elliot Formation, and Botswana rocks to Lebung series, which are correlated to Elliot and Clarens Formations in South Africa. It is thus possible to deduce that rock art from the Thune Valley in Botswana was made on a sandstone which is more similar to the Elliot Formation ones, rather than to the Clarens Formation ones. Moreover, Elliot Formation sandstones are often called "red beds" because of their reddish colour, and Thune Valley sandstones are red sandstones. Comparing Canadian rocks and southern African rocks is much more complicated such as their mineralogical compositions are very different: igneous/metamorphic rocks on one side, sedimentary rocks on the other side. They are both composed of quartz and feldspars but the comparison stops there. It is possible to conclude that it is here only coincidence.

Lesotho and South African rocks (except RSA BUX1) have got the same and homogeneous dose rate, which is to be expected as they are from the same geological formation, the Clarens Formation.

The homogeneity of the dose rate through sites and regions are interesting in term of sampling method, such as close sampling will not be required in some cases and thus rock art panels will not suffer of large degradations.

### 5.5.2 Cosmic rays

Cosmic rays contribution was calculated only for sites where rocks dose rates were calculated, that is to say Cliff Lake 262, Lake Wapizagonke, TD20, RSA BUX1, RSA MEL8, RSA LAB1, ARAL 175, ARAL 169.

It was calculated with equations from Prescott and Hutton (1988, 1994). Results are given in Table 5.13.

**Table 5.13** Cosmic dose rates for sites studied

| Site | Latitude | Longitude | Altitude | Cosmic rate (Gy/ka) |
|---|---|---|---|---|
| Cliff Lake 262 | 50°N | 93°W | 357m | 0.310 ± 0.031 |
| Lake Wapizagonke | 46°N | 73°W | 214m | 0.303 ± 0.030 |
| ARAL169 | 29°S | 27°E | 1633m | 0.373 ± 0.037 |
| ARAL175 | 29°S | 28°E | 1636m | 0.372 ± 0.037 |
| TD20 | 22°S | 28°E | 599m | 0.306 ± 0.031 |
| RSA BUX1 | 31°S | 28°E | 1240m | 0.352 ± 0.035 |
| RSA LAB1 | 30°S | 28°E | 1700m | 0.379 ± 0.038 |
| RSA MEL8 | 30°S | 28°E | 1700m | 0.379 ± 0.038 |

Contribution from cosmic rays to dose rate is quite similar at all sites. The main difference is due to the altitude of the sites.

### 5.5.3 Pigment

Finally the dose rate from the pigment has to be calculated. Referring to characterization analyses presented in Chapter III, layers of paints are very small, from 20 µm to 300 µm. The aim is to assess if the contribution of pigment to the total dose rate is worth to be considered or not.

Two soils (Lesotho-2012-R4 and Lesotho-2012-W6), collected in the Phuthiatsana Valley close to the sites were crushed and analysed by gamma spectrometry. The dose rate calculation was the same as used for the rock samples. The results (Table 5.14) are in the same order of magnitude, and about three to four times less than the dose rates calculated for the rock supports.

**Table 5.14** Gamma spectrometry results and dose rate calculations for Lesotho soils

| Sample | U (ppm) | Th (ppm) | K (%) | Quartz dose rate (Gy/ka) | K-feldspars dose rate (Gy/ka) |
|---|---|---|---|---|---|
| R4 (red soil) | 0.39 ± 0.05 | 3.43 ± 0.6 | 0.39 ± 0.03 | 0.67 ± 0.06 | 1.19 ± 0.07 |
| W6 (white soil) | 2.34 ± 1.72 | 7.19 ± 0.8 | 0.05 ± 0.02 | 1.11 ± 0.10 | 1.64 ± 0.11 |

To make a comparison with a real sample, the dose rate for ARAL172-2012-10 (Dark red paint) has been calculated using the concentrations obtained by gamma spectroscopy and SEM-EDS for potassium (K) and by ICP-MS for uranium (U) and thorium (Th).

Such as the quantity of sample available was very small, 10.5 mg, the determination of the concentration of K with the gamma spectrometer failed with a result of 0.06 ± 2.47%. This large error comes to the weakness of potassium peak at 1461 keV, which even if visible was not enough defined to give a good evaluation of potassium content. Even a longer acquisition did not solve the problem. It however indicates that content of potassium is quite low in the pigment.

So another determination was tested on cross-section with the SEM-EDS. The result is 0.68 ± 0.12% of K (weight %).

ICP-MS determinations of U and Th concentrations are given in Table 5.15, along with dose rate calculation.

**Table 5.15** Pigment ARAL172-2012-10 dose rate calculation

| Sample | U (ppm) | Th (ppm) | K (%) | Quartz dose rate (Gy/ka) | K-feldspars dose rate (Gy/ka) |
|---|---|---|---|---|---|
| Aral 172-2012-10 | 0.568 ± 0.004 | 1.735 ± 0.010 | 0.68 ± 0.12 | 0.84 ± 0.07 | 1.36 ± 0.08 |

Values obtained are in close agreement with the ones obtained on soils collected close to sites in Lesotho.

### 5.5.4 Final dose rate calculations

The total dose rate is an addition of contributions from the rock, cosmic rays and the pigment with coefficients attached to them. The total dose rate is seen as a sphere of 50 cm diameter. In this sphere, the pigment represents a layer of between 20 to 300 μm thick, that is to say 0.04 to 0.6% of the dose, when rock and cosmic rays are 49.7 to 49.98% each. Results of calculations with each contribution and coefficient, for quartz and K-feldspars, are presented in Table 5.16.

In this calculation, the pigment contribution is considered the same for all sites. It is an approximation for this feasibility project. However, the weak contribution of it to final calculation (0.01 Gy/ka) points to not taking it into account.

Final annual doses can be dispatched in two series: one with annual dose rate about 0.5 Gy/ka for quartz and 0.7 Gy/ka for K-feldspars, and one with annual dose rate about 2 Gy/ka for quartz and 2.2 Gy/ka for K-feldspars. These dose rates are weak in comparison of annual dose rate of about 5 Gy/ka which can be found in other contexts and where objects are buried. They will be a limit to date recent paintings.

**Table 5.16** Final dose rates (CL= Cliff Lake, LW = Lake Wapizagonke)

| | | CL1 | CL2 | LW1 | LW2 | Aral 169 | Aral 175 | TD20 | RSA LAB1 | RSA MEL8 | RSA BUX1 |
|---|---|---|---|---|---|---|---|---|---|---|---|
| Quartz, 150-250μm fraction | Rock | 0.31±0.05 | 5.16±0.19 | 0.68±0.05 | 0.67±0.05 | 3.35±0.14 | 3.17±0.12 | 0.94±0.06 | 4.17±0.16 | 4.25±0.19 | 0.76±0.05 |
| | Pigment | 0.84±0.07 | 0.84±0.07 | 0.84±0.07 | 0.84±0.07 | 0.84±0.07 | 0.84±0.07 | 0.84±0.07 | 0.84±0.07 | 0.84±0.07 | 0.84±0.07 |
| | Cosmic rays | 0.310±0.031 | 0.310±0.031 | 0.303±0.030 | 0.303±0.030 | 0.373±0.037 | 0.372±0.037 | 0.306±0.031 | 0.379±0.038 | 0.379±0.038 | 0.352±0.035 |
| | Dose rate (Gy/ka): pigment 20μm | 0.31±0.04 | 2.73±0.11 | 0.49±0.04 | 0.49±0.04 | 1.86±0.09 | 1.77±0.08 | 0.62±0.05 | 2.27±0.10 | 2.31±0.11 | 0.56±0.04 |
| | Dose rate (Gy/ka): pigment 300μm | 0.31±0.04 | 2.72±0.11 | 0.49±0.04 | 0.49±0.04 | 1.86±0.09 | 1.77±0.08 | 0.62±0.05 | 2.27±0.10 | 2.31±0.11 | 0.56±0.04 |
| | Dose rate (Gy/ka): no pigment | 0.31±0.04 | 2.73±0.11 | 0.49±0.04 | 0.49±0.04 | 1.86±0.09 | 1.77±0.08 | 0.62±0.05 | 2.27±0.10 | 2.31±0.11 | 0.56±0.04 |
| K-feldspars, 90-150μm fraction | Rock | 0.83±0.06 | 5.78±0.19 | 1.20±0.06 | 1.19±0.06 | 3.93±0.15 | 3.75±0.13 | 1.46±0.06 | 4.76±0.17 | 4.85±0.19 | 1.28±0.06 |
| | Pigment | 1.36±0.08 | 1.36±0.08 | 1.36±0.08 | 1.36±0.08 | 1.36±0.08 | 1.36±0.08 | 1.36±0.08 | 1.36±0.08 | 1.36±0.08 | 1.36±0.08 |
| | Cosmic rays | 0.310±0.031 | 0.310±0.031 | 0.303±0.030 | 0.303±0.030 | 0.373±0.037 | 0.372±0.037 | 0.306±0.031 | 0.379±0.038 | 0.379±0.038 | 0.352±0.035 |
| | Dose rate (Gy/ka): pigment 20μm | 0.57±0.07 | 3.04±0.11 | 0.75±0.05 | 0.75±0.05 | 2.15±0.09 | 2.06±0.08 | 0.88±0.06 | 2.57±0.10 | 2.61±0.11 | 0.83±0.05 |
| | Dose rate (Gy/ka): pigment 300μm | 0.57±0.07 | 3.03±0.11 | 0.76±0.05 | 0.75±0.05 | 2.15±0.09 | 2.06±0.08 | 0.88±0.06 | 2.56±0.10 | 2.60±0.11 | 0.83±0.05 |
| | Dose rate (Gy/ka): no pigment | 0.57±0.07 | 3.04±0.11 | 0.75±0.05 | 0.75±0.05 | 2.15±0.09 | 2.06±0.08 | 0.88±0.06 | 2.57±0.10 | 2.61±0.11 | 0.83±0.05 |

## 5.6 Discussion and further work

In this project, a three-step testing protocol was used to assess the working hypothesis detailed in Chapter II.

First, quartz and K-feldspars composing rock supports of rock art studied were tested for suitability to OSL/IRSL dating. Quartz composing rocks from the Canadian Shield reveal no exploitable OSL signal. This lack of signal in quartz from metamorphic rocks was previously reported in Sobati *et al.* (2011) and Tsukamoto *et al.* (2011), and is explained by few exposure and burial cycles undertaken by the rocks. On the other hand, quartz composing rocks from southern Africa reveal an intense luminescence signal. Their rapidity to bleach and the absence of thermal transfer make them good candidates for this project. However, the HF pre-treatment needed to remove any feldspar component in the samples reduces substantially the number of grains available for tests, especially in the case of 1-mm-thick slices of rock cores, cut to investigate the evolution of the luminescence signal into the rock. In further works, larger samples (cores of at least 3 cm diam.) would be considered to get enough grains to investigate the potential of quartz for rock art OSL dating. Moreover, quartz were successfully used for surface dating in previous studies (Chapot *et al.*, 2012; Sohbati *et al.*, 2011; Sohbati *et al.*, 2012), and present less constraints in term of thermal transfer and preheat temperatures than K-feldspars.

Tests on K-feldspars show that a longer period of daylight exposure is needed to reach the minimum residual dose and K-feldspars from Clarens Formation sandstones suffer for high thermal transfer. Thus a modified SAR protocol was used. It implies to reduce preheat temperature at 210°C and to add a bleach of 900s after each Ln-Lx and Tn-Tx recordings. Combined with a subtraction of the thermal transfer, this SAR protocol proved that K-feldspars are suitable for IRSL dating even in the case of small doses. This protocol was adjusted at the end of the project, due to the necessity to change OSL instruments, from Lexsyg to Risø. The preheat temperature was changed to 200°C and the bleach step was replaced by a thermal wash step. However both of these SAR protocols have their limitations. Indeed, as thermal transfer is about 1 Gy and that the dose rate calculated for paintings created on Clarens Formation sandstones is about 2 Gy, historical paintings and paintings which are less than 1000 years old would be extremely difficult to date even impossible.

The second step was to test the bleaching of minerals at the surface of the rock. Investigations on cores collected from the rock face close to paintings prove that the IRSL signal can be only partially bleached. Moreover, light penetrates into the rock surface until 4 mm, but it is highly variable. Tests were conducted on rocks from the same geological formation: the Clarens Formation, and have all a similar mineralogical composition. Thus, light penetration in rock may be due more to orientation and exposition to daylight rather than to the mineralogical composition of the rock. On the other hand, this orientation may influence alterations of the rock and the growing of superficial deposits at the surface of the rock (clay, calcium oxalates and calcium sulphates). This layer may constitute a further "protection" against daylight. It has been here proved that a transect of rock from the rock face close to paintings is necessary to assess the bleach of minerals.

Comparing with previous studies on surface dating (e.g. Chapot *et al.*, 2012; Freiesleben *et al.*, 2015; Sohbati *et al.*, 2011; Sohbati *et al.*, 2012; Sohbati *et al.*, 2015), transects show similar shapes and intensities at the surface. However, on the opposite of simulation models presented in Sohbati *et al.* (2012), surface of rock is not deeper bleached depending on exposure time. In the case of cores from ARAL 172, whose surface is exposed to daylight since thousands of years, only the first 4 mm are bleached. This corresponds to an exposure of 10 days if referring to Sohbati *et al.* (2012)'s model. Hence, and it has been demonstrated in further studies (Chapot *et al.*, 2012; Freiesleben *et al.*, 2015; Sohbati *et al.*, 2015) and in this PhD, not only duration of exposition to daylight is to be taking into account when dealing with rock surface dating. Alteration, orientation and sheltering of the sites are to be investigated too.

Then, the third and last step was to test the protection made by a layer of paint, similar in composition as red paints encountered in sites from the Phuthiatsana Valley. Tests conducted on two cores from two artificially painted rocks point to an incomplete protection from daylight. Tests show that it maintains at least 5% of the initial signal, which is extremely small, and thus implies weak luminescence signals and large errors for young dates. On the other hand, even if only two tests are reported here and further analysis should be conducted, it suggests possible errors on OSL surface dating when weathering crusts are presents. Indeed, if such a thin layer of paint (about 20 to 100 µm) attenuates daylight penetration, in

the case of dating rock surfaces presenting thick weathering layers, minerals at the surface may exhibit a residual dose. Moreover, tests conducted on rock faces of two different rock-shelters prove that surface bleaching is not constant and is highly dependent of daylight exposition and surface alteration. This implies that the equivalent dose recovered would be higher than it is supposed to be, resulting in a too old age. It is particularly critical in the case of "young" samples and low annual doses.

Dating rock art using OSL on minerals found under the paint layer may be possible but it requires more investigations on the attenuation potential of the paint layer depending on its nature and thickness, and the construction of a mathematical model taking into account the cycle of exposition and "burial" of the rock face every day. Such a model for multiple burials and to recover their dates has been presented in Freiesleben *et al.* (2015). It may serve as a basis for more investigation.

Moreover, as suggested by Sohbati *et al.* (2015), pIRIR (post-Infrared, Infrared stimulated luminescence) may be used to complement IRSL recording as this luminescence signal comes from deeper traps which are thought to be more stable (and maybe less subjected to thermal transfer) than traps excited by conventional IRSL. On the other hand, to bleach such traps, longer exposure to daylight would be required, which may be a limitation of its use as we reported above that even in the case of well-exposed rock surface, the IRSL signal at the surface of the rock may be only partially bleached.

Another suggestion for further investigations would be to carry out analysis on single grains rather than on disks with a 2-mm-diameter circle of sample. It would make it possible to finer study bleaching at the surface and in depth in the rock, and the protection made by the paint layer.

CHAPITRE VI

# PIGMENT CHARACTERIZATION AS AN ALTERNATIVE TO INTERPRETE ROCK ART SITES WHEN DATING METHODS FAIL: THE CASE OF THE MIKINAK SITE, LAKE WAPIZAGONKE, QUEBEC, CANADA

Adelphine BONNEAU[1-2], Joy MOYLE[3], Kenza DUFOURMENTELLE[3], Daniel ARSENAULT[4], Charles DAGNEAU[5], Michel LAMOTHE[1]

[1]Département des Sciences de la Terre et de l'atmosphère - Université du Québec à Montréal, Montreal, Quebec, Canada

[2] Rock Art Research Institute - University of the Witwatersrand, Johannesburg, South Africa

[3]Collections, Curatorial and Conservation Branch - Heritage Conservation and Commemoration Directorate - Parks Canada, Ottawa, Canada

[4] Université du Québec à Montréal, Montreal, Quebec, Canada

[5] Underwater Archaeology Team - Parks Canada, Ottawa, Canada

*Corresponding author: adelphine.bonneau@gmail.com

Keywords: Canadian Shield rock art, Pigment characterisation, Raman spectroscopy, FTIR spectroscopy, Radiocarbon dating, OSL dating

Article in press, *Archaeometry*

Abstract

Dating is maybe the most frequently asked question in rock art studies, but still one of the most difficult to answer. However, chronology is vital to understand and interpret rock art sites. Attempts at dating the *Mikinak* site, at Lake Wapizagonke, Quebec, Canada, were unfortunately unsuccessful. But a multi-instrumental protocol applied to characterize paintings show that at least three different paint recipes were employed to create the site. These may reflect three different phases of paintings and that at least three different artists contribute to the production of this site.

## 6.1 Introduction

Dating is maybe the most frequently asked question in rock art studies, but still the most difficult to answer. Few dating methods are available and these are dependent upon specific environment and/or components in the paintings. There are more than 750 rock art sites in the Canadian Shield and very few of them are dated. These dates are based on testimonies collected from descendants of the artists or from the identification of certain representations such as guns, horses, or historical events (Lemaitre, 2013). Thus, the need for dates to interpret and understand rock art sites is critical. Few attempts have been conducted to date: only two radiocarbon dates have been reported on organic matter found in silica crusts at the Nisula Site, Quebec (Aubert *et al.*, 2004).

In this on-going project, two dating methods (radiocarbon and optically stimulated luminescence) were tested in order to date rock art in the Canadian Shield. In choosing and adapting the dating methods, a detailed characterization protocol combining a set of complementary instruments, has been developed. It was systematically applied on sites before any sampling for dating took place. It has proven to be a good alternative in understanding a rock art site when dating methods failed to provide absolute dates.

Even though ethnographic researches were conducted during the 18th and 19th centuries, the first chemical studies of rock art were carried out by H. Moissan at the beginning of the 20th century (Clottes *et al.*, 1990). Since then, worldwide, rock paintings were characterized to reveal the techniques and recipes used by the artists (e.g. Taylor *et al.*, 1974, Wainwright,

1990, Prinsloo *et al.*, 2008, Tournié *et al.*, 2011, Arias *et al.*, 2011, Menu and Walter, 1992, Menu *et al.*, 1993, Vignaud *et al.*, 2006, Ford *et al.*, 1994, Huntley *et al.*, 2015)

To pursue this long history of rock paintings characterization, this article intends to present the preliminary characterization results and dating attempts at the *Mikinak* Site, Lake Wapizagonke, Quebec, Canada.

## 6.2 Description of the site

Lake Wapizagonke is located in the Parc National de la Mauricie, about 100 km north of Trois-Rivières (Figure 6.1). The site (CdFg-05, also called 25M in the Park Canada identification system) has been called *Mikinak*, an Algonquian name, in reference both to the turtle depicted on the rock surface and to the profile shape of a hill seen on the opposite shore of the lake.

Jacques Béland, a naturalist, was the first to describe this site in 1951 (Béland, 1959). In the 1960s, excavations were conducted on the lake banks, revealing several occupations dating from the Woodland period (200 BC-1200 AD). More recent excavations, conducted in the last decades, revealed occupations by hunter-gatherers tribes from the Archaic Period to the second half of the 19$^{th}$ century (Dagneau, 2010). Early in the 1970's, René Ribes, Selwyn Dewdney, and Gilles Tassé recorded the site and mentioned that some of the paintings had disappeared since its discovery (Tassé and Dewdney, 1977, Lemaitre, 1996).

During these fieldworks, flakes of rocks with paint which had fallen into the lake were collected and stored for analysis. Thereafter a few analyses were carried out by the Canadian Conservation Institute under the supervision of Taylor et al. (1974) and more recently of Helwig (2011). Results showed that paintings were created with hematite-based pigments and subsequently surrounded by amorphous silica crusts from weathering. Finally, in 2010, a subaquatic investigation was conducted by Parks Canada's underwater archaeologists. New fragments with paint remains were collected in a square of 90cm x 75cm in the sediments of the lake (Dagneau, 2010).

Rock paintings were created by applying paints with fingertips. Zoomorphs, anthropomorphs and geometric figures are represented. A rock art analysis conducted by Arsenault and

Lemaitre (1996) points to the shamanic characteristics of these Algonquian graphics. They based their interpretation on a series of motifs suggesting the depiction of a shamanistic ceremony, where some characters are visible: an anthropomorph with a birdlike head identified as a non-human entity named *Memegueshuk*, an upside down human figure, with his or her paraphernalia, representing a shaman travelling to the world of the spirits, and two other figures associated with the supernatural world, the turtle and the thunderbird. Béland (1959) mentioned the presence of another panel underwater. Thanks to hot summer conditions, in 1997, photos of this panel showing red stains were obtainable. Nevertheless, no representation was distinguishable.

Despite the site's long history of recording and analysis, the question of its age is still unresolved and previous characterization studies focused only on two or three samples.

Samples used in this study are painted fragments from the Parks Canada collection, comprising those collected in the 1985 and in 2010. 17 fragments present red paint while one has a black layer. This last fragment was studied to determine if it was a painting or a weathering product from the rock. In parallel, fragments of rocks were collected close to the paints in order to characterize the rock support and weathering crusts surrounding the paintings. These supply a background for pigment characterization.

Weathering crusts are defined as layers composed of alteration products from the rock and paints, of weathering products, and of eolian deposits. As fragments stayed for an undetermined period of time in water, these weathering crusts include products resulting from the life in the lake water such as bacteria, fish eggs, water salts, etc.

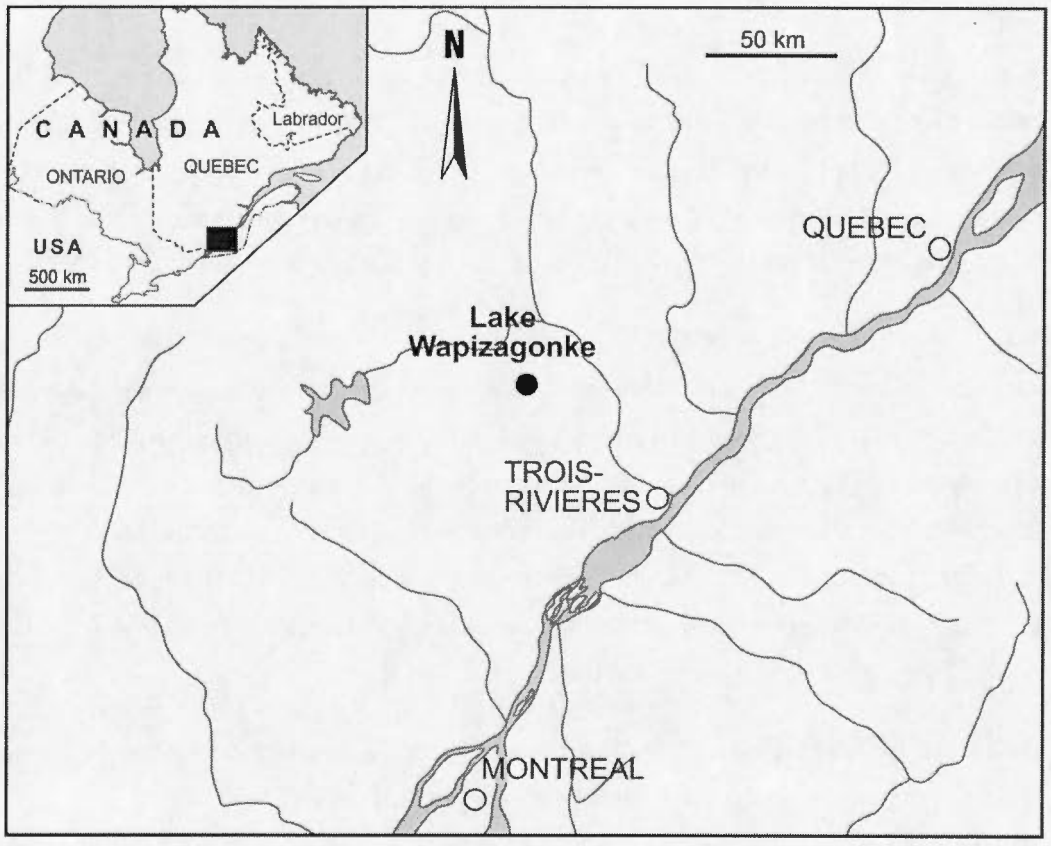


**Figure 6.1** Location of *Mikinak* Site, Lake Wapizagonke, Canada

## 6.3 Methodology

### 6.3.1 Dating methods

Studies of the *Mikinak* site (Lemaitre, 1996, Tassé and Dewdney, 1977, Arsenault and Gagnon, 2001) proposed different dating methods such as lichenometry, water level marks, and typology. However, none of them were attempted. In 2012, the amorphous silica layers surrounding the paint layer were analysed by LA-ICP-MS by Dr Maxime Aubert at the Australian National University. Uranium and thorium-232 concentrations indicated that the silica layers were highly contaminated by detrital materials and as a consequence uranium-series dating was not attempted to date the site. In this study, radiocarbon and optically stimulated luminescence were experimented.

6.3.1.1 Radiocarbon dating

Radiocarbon dating has been widely used to date rock art around the world (e.g. Valladas, 2003, Valladas *et al.*, 2001, Bednarik, 2002, Bednarik, 1996). In the Canadian Shield, two dates were obtained on diatoms sealed in the amorphous silica crusts underneath paintings by Aubert et al. (2004) at the Nisula site. Dates were obtained on very small samples resulting in large errors: 2500 ± 275 $y^{14}C$ BP ($\delta^{13}C$ assumed = –25‰), and 2440 ± 610 $y^{14}C$ BP ($\delta^{13}C$ assumed= –25‰).

Radiocarbon dating was here investigated as a black layer is present on one fragment sampled, which if composed of carbon, and reveals to be a paint layer may provide an absolute date for the site. Investigations were also conducted on fragments from the rock face which exhibited a 200 to 500µm thick weathering crust in order to assess the possibility of radiocarbon dating diatoms, calcium carbonates or calcium oxalates. However, the dates resulting from these components are difficult to interpret as the origin of the carbon dated is not well understood (Bednarik, 2002, Bonneau *et al.*, 2016).

Because of the long exposure of the fragments to water, no investigation was conducted on potential organic matters from any binders surviving in the paintings.

6.3.1.2 Optically stimulated luminescence (OSL)

The principle of OSL dating is based on the emission of light, or luminescence, by some minerals, such as quartz and feldspars. These act as natural dosimeters, recording the surrounding radioactivity to which they are exposed. In most luminescence studies, the samples (e.g. sediments, rocks, ceramics) were buried after heating or exposure to sunlight, protecting them from daylight exposure.

In this project, the paintings studied have existed on cliffs which are exposed to daylight for several hours per day. Thus one can assume that the rock surface is bleached and does not have a remnant OSL signal. However, when a painting is made on the surface, it can protect the rock face from the sun and an OSL signal will emerge. This hypothesis has not been tested in any previous work.

In order to be able to apply OSL dating, quartz and feldspars, especially K-feldspars, need to have specific defects in their matrix such that they emit a luminescence signal. The rock support at the *Mikinak* site is pyroxene-rich gneiss, composed mainly of pyroxene, plagioclases, alkaline-feldspars, quartz, amphiboles and magnetite (Desrochers, 2011). Therefore, only quartz was investigated. Two pieces of rock were collected on the bank of the lake about 50 m to the right of the site to test the suitability for OSL dating of the quartz constituting the rock support (preparation details are given in supplementary online information).

### 6.3.2 Characterization protocol

A multi-instrumentation protocol was selected to acquire all the information needed to characterize the pigment and its alterations. Following preliminary researches on San rock art, a first protocol was published (Bonneau *et al.*, 2012), and subsequently formed the basis of the protocol used in this project.

Painting analyses were carried out on unprepared samples whereas rock and rock face fragments were analysed unprepared and in cross-section with epoxy resin (Epofix from Struers) and polished. Samples were first observed with light microscopy, and then under scanning electron microscopy (SEM). Elemental analyses were carried out with SEM-EDS (Scanning Electron Microscopy coupled with Energy-Dispersive X-ray Spectrometry), and molecular analyses with Raman spectroscopy and FTIR (Fourier Transform Infrared) spectroscopy. Unless otherwise stated, all analyses were carried out in the conservation science laboratory of Parks Canada, Ottawa, Canada.

Microscopic observations are of crucial interest. They are used to assess the homogeneity of the sample: whether it is a mixture or one material, whether crystals are on top of or under the paint layer. Observations were carried out using a LEICA binocular glass equipped with a LEICA camera.

SEM-EDS analyses have two objectives: observation of the shape of the particles and analysis of the chemical elements comprising the sample. The instrument was a VEGA equipped with an Oxford Instruments EDS. An electron beam of 15 kV was used.

Observations were conducted on samples mounted on carbon-stubs with a carbon coating, using secondary electrons. EDS analyses were done with a 180 second acquisition time. Rock and rock fragments were analysed on a Hitachi TM-3000 SEM equipped with a Quantax 70 Bruker EDS, cooled with Peltier effect, at the Laboratoire de luminescence LUX, Geotop, Université du Québec à Montréal, Canada. Analyses were carried out on variable pressure with a 15 kV electron beam. Observations were made with backscattered electrons.

Raman and FTIR spectroscopic analyses allow investigation of the molecular composition of the sample. Raman spectroscopy was carried out at the Laboratoire de caractérisation des matériaux, Université de Montréal, Canada with an InVia microspectrometer Raman equipped with green (514 nm) and near-infrared (near-IR, 785 nm) lasers, and a x50 long-focal objective. For FTIR analysis, samples were crushed in two diamond cells and analysed with a Bruker micro-FTIR over a spectral range of 4000 - 400 $cm^{-1}$, with 128 scans at 2 $cm^{-1}$ resolution. Interpretations of spectra were conducted using Grams and CrystalSleuth as softwares, the RRUFF database, the IRUG database and available literature.

## 6.4 Results

The analyses reported here were carried out on seventeen fragments with red paints, one fragment with a black layer from the Parks Canada collection, on three fragments of rock face collected close to the paintings, and one rock collected on the bank of the lake. Painted fragments are numbered according to the following sequence: 25M (site number), 1 (place of the underwater excavation), A1 (square A, strata 1), a/1 (number given to each fragment found in a single strata).

### 6.4.1 Paintings

Observations of the fragments with the naked eye show that at least two presented darker red hues than the others. This was subsequently confirmed by microscope observations and two more samples showed a dark red colour.

Two textures were recorded: a coarse-grained texture (n=1; 25M1A1-1) and a fine-grained texture (n=15). The red paint layers are homogeneous in colour: no orange or black grains are visible. However, the layer is often very sparse and thin (ca.20-50µm). A transparent to white

layer is observed on top of all the samples and is doubtless a weathering crust. The red paint layer is found on a white to grey layer, with a smooth texture.

Two fragments exhibit very thin paint layers (less than 10μm); thus they were not characterized. Fragments with two or more stripes of paint were split into two or three samples (Table 6.1). Thus, nineteen samples were analysed with SEM-EDS, Raman spectroscopy and FTIR spectroscopy.

**Table 6.1** Summary of samples studied (S = Stripe)

| Sample Name | Excavation | Nb of samples | Characterization Group |
|---|---|---|---|
| **25M99A1-2-a** | 1985 | 1 | Group 3 |
| **25M99A1-2-b** | 1985 | 1 | Group 1 |
| **25M99A1-2-c** | 1985 | 1 | Group 2 |
| **25M99A1-2-d** | 1985 | 3 | S1: Group 1, S2: Group 1, S3: Group2 |
| **25M99A1-2-e** | 1985 | 2 | S1: Group 1, S2: Group 1 |
| **25M99A1-2-f** | 1985 | 2 | S1: Group 2, S2: Group 1 |
| **25M99A1-1-g** | 1985 | 2 | S1: Group 1, S2: Group 2 |
| **25M99A1-2-h** | 1985 | 1 | Group 1 |
| **25M99A1-2-i** | 1985 | | Not characterized |
| **25M99A1-2-j** | 1985 | 1 | Non anthropic black layer |
| **25M99A1-2-k** | 1985 | 1 | Group 2 |
| **25M1A1-1** | 2010 | 1 | Group 1 |
| **25M1A1-2** | 2010 | 1 | Group 2 |
| **25M1A1-3** | 2010 | 1 | Group 2 |
| **25M1A1-4** | 2010 | 1 | Group 1 |
| **25M1A1-5** | 2010 | 1 | Group 2 |
| **25M1A1-6** | 2010 | | Not characterized |
| **25M1A1-7** | 2010 | 1 | Group 3 |

Observations under secondary electrons with SEM show iron oxides crystals with two different shapes: small flakes 0.5 to 2µm in diameter (n=10), flakes of mixed sizes (2 to 4 µm in diameter and sometimes slightly larger) (n=9) (Figure 6.2).

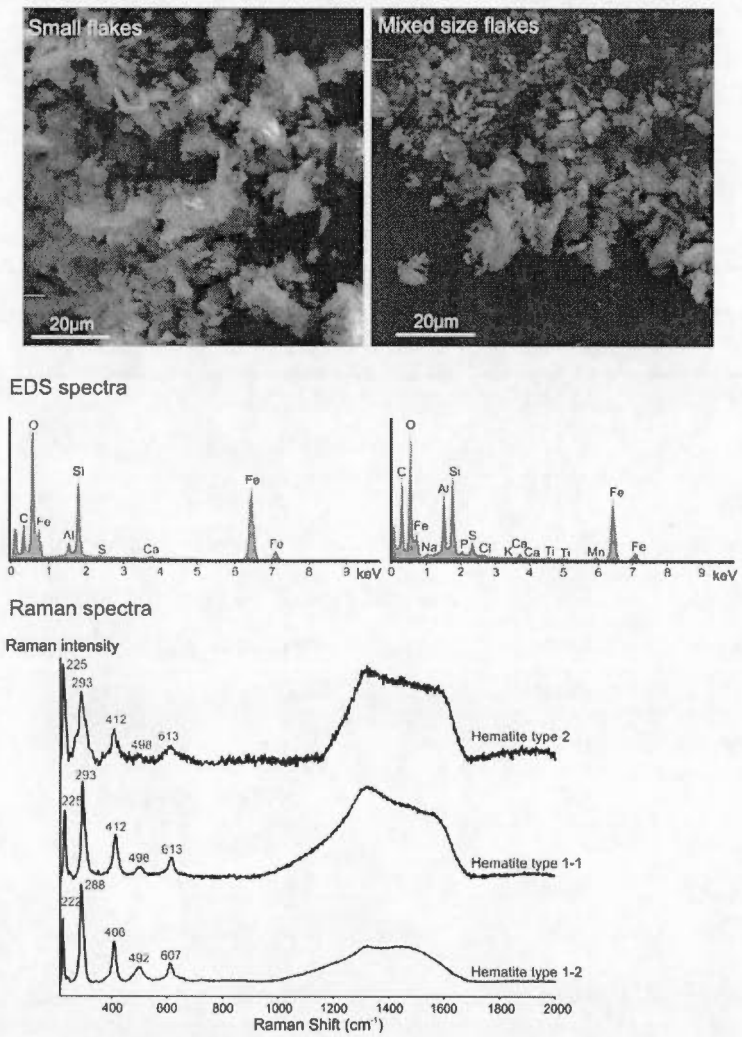


**Figure 6.2** SEM images (secondary electrons), EDS spectra, and Raman spectra recorded on red paintings

On sample 25M1A1-1, small balls, about 1 µm in diameter, were observed. They are composed of iron and sulphur, and are interpreted as bacteria or fish eggs.

The spectra acquired with EDS show the presence of iron, which seems to be under the form of iron oxides, in all the red samples. In few samples, iron is associated with titanium, manganese, copper and/or zinc (Figure 6.2). If compared to the iron oxides morphology:

- The tiny flakes contain titanium and manganese in one sample, zinc in one sample, titanium and copper in one sample, and manganese in one sample.

- The mixed size flakes contain manganese in two samples, and manganese and titanium in one sample.

Interestingly the stripes present on the same fragment do not have the same morphology and/or composition. These morphologies and compositions tend to show that iron oxides from different geological sources were used to make the paints (Garate *et al.*, 2004).

For all samples, peaks of hematite were recorded with Raman spectroscopy. Peaks commonly assigned to hematite are 225 (Fe-O stretching), 247, 293, 412 (Fe-O bending), 498 (Fe-O stretching), and 613 $cm^{-1}$ (Fe-O bending) (de Faria and Lopes, 2007). However, depending on samples, different intensities and shifts in peak positions were observed. One can argue that these differences are due to physical interferences due to the ruggedness of the sample unprepared surface. However, they were constant in each sample studied, and on the 5 to 10 spectra recorded on each of them.

These differences served to categorize hematite in types (Figure 6.2):

- Type 1-1: Peak at 293 $cm^{-1}$ is the most intense

- Type 1-2: Peak at 293 $cm^{-1}$ is the most intense and peak positions shift to 222, 239, 288, 406, 492, and 607 $cm^{-1}$

- Type 2: Peak at 225 $cm^{-1}$ is the most intense

Hematite type 2 (Figure 6.2) was observed on two samples. For both samples, a peak at 270 $cm^{-1}$ appears along with the conventional peaks of hematite. Associated with the Fe-O bending mode, this is due to hydration of the iron oxides. This has been previously recorded

in the process of heated goethite to turn it into hematite (Coentro *et al.*, 2012). However, the long exposure of the fragments to water may have introduced similar hydration by turning hematite into goethite (process previously reported by Cornell and Schwertmann (2003)).

Hematite type 1-1 was found on ten samples, whereas hematite type 1-2 was recorded on seven samples (Figure 6.2). The shifts observed in hematite peaks can be introduced by impurities due to its geological history, by the presence of aluminosilicates or by the immersion of the painted fragments in water. *In-situ* samples would be required to determine which of these hypotheses is correct.

A peak at 1330cm$^{-1}$ (shifting from 1310 to 1335cm$^{-1}$) is attributed to hematite too (de Faria and Lopes, 2007). It is associated with the Fe-OH asymmetric stretching mode and is linked to the presence of water in the iron oxides matrix which may be due to the presence of iron hydroxides and/or clayish minerals.

Under FTIR spectroscopy, all samples show the presence of amorphous alumino-silica and amorphous silica with peaks at 790, 920, 1070, 1190 and 1630cm$^{-1}$. The denomination "amorphous alumino-silica and silica" has been retained here as these crusts are composed of silicon and aluminium in variable proportions. It follows the terminology used in Chen *et al.* (2000). The frequency of each of these peaks varies from sample to sample with a shift up to 10cm$^{-1}$. Moreover, the intensities of peaks composing the main massif centred on 1070cm$^{-1}$ vary too, resulting in two different shapes. "Shape 1" shows a thin massif. "Shape 2" shows a larger massif with a 1190cm$^{-1}$ peak of greater intensity. Only three samples have been identified as "Shape 2" (Figure 6.3).

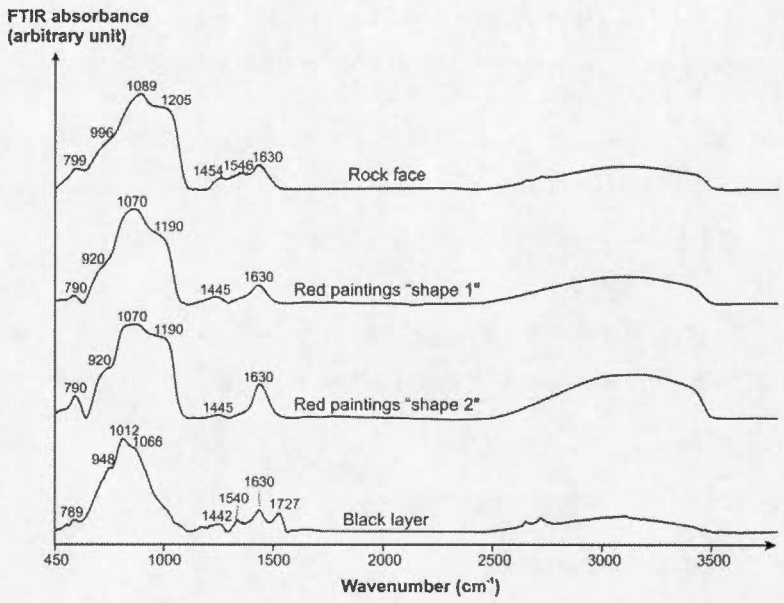


**Figure 6.3** FTIR spectra recorded on the rock face, red paints, and black layer

The shift and shapes of the main peak can be explained by the amorphous nature of the alumino-silica and silica matrix recorded. Indeed, amorphous alumino-silica and silica crusts have been recorded for a long time on Canadian rock art but their formation mechanisms are still unclear (Taylor *et al.*, 1974, Wainwright, 1985, Wainwright, 1990, Aubert *et al.*, 2004). The matrix formed may be seen as a glass with silicon atoms bonded to 0 to 4 oxygen atoms, with more or less aluminium and metallic ions as impurities in it. Thus depending on the kinds of bonds present, the peaks may shift and have different intensities as FTIR spectroscopy reflects the proportion of a specific chemical bond present in the sample. On the other hand, these peaks are at the same place as the ones of clay minerals which are present in the red paints. Indeed, aluminium and silicon were recorded in samples of red paints which may indicate that the pigment used is red "ochre" with clay minerals inside. Their peaks may have influenced the shape of the FTIR spectra too.

Calcium carbonates were recorded on eight samples with peaks at 720 and 1445cm$^{-1}$. These could be a weathering product or an intentional addition of the artist. Peaks of water at 1635

and 3330cm$^{-1}$ (broad peak) were found on all the samples with more or less intensity. This sometimes interferes with amorphous alumino-silica and silica peaks.

Sample 25M1A1-1 presents a different FTIR spectrum compared to the other samples. Peaks of amorphous silica (578, 636, 1034, 1081, and 1205cm$^{-1}$) with the "Shape 1" were recorded. Peaks at 829 and 1034cm$^{-1}$ are attributed to pyroxenes, doubtless coming from the rock support. Peaks at 578, 636 and 1034cm$^{-1}$ can be linked to amphiboles and quartz. These minerals are present in the rock too. Despite its different peaks, this sample shows components which are in agreement with the nature of the pigment and of the rock (Figure 6.3).

### 6.4.2 Rock supports and non-anthropic deposits

#### 6.4.2.1 Rock and weathering crusts

On site, white and red layers were found on top of the rock as weathering crusts. The white layer is composed of fine white grains in a transparent matrix, showing iridescence under the microscope. The red layer is thinner than the white one and composed of fine red grains.

Observations on samples, on rock and on rock face flakes collected close to paint, show the presence of a transparent to white layer on top of them. It is smooth and seems to have made undulating marks. Under the paint, a white to grey layer with a fine-grained texture is observed. The same layer is found under the smooth layer on the rock support.

In cross-section, the rock is composed of black, white, transparent and brown crystals of variable sizes. No matrix was observed. This agrees with the study by Desrochers (2011).

The rock face exhibits a white 70µm-thick layer at its surface. It comprises black grains in some places which may be attributed to lichens.

SEM-EDS analyses show that the white layer at the surface of the rock face is composed of silicon, aluminium and calcium. It is consistent with alumino-silica and silica crusts and calcium carbonates recorded from the paintings. The rock itself is composed of silicon, aluminium, calcium and iron with titanium and manganese as minor elements.

Under SEM observations, a smooth and thin layer was found on top of the paints and the rock. It is composed mainly of silicon but aluminium and calcium are present too.

Elemental analysis recorded calcium, sulphur, phosphorus, chlorine and magnesium in paintings. They are all attributed to weathering products but their mineralogical form is sometimes unclear. Long crystals composed of sulphur and calcium are interpreted as calcium sulphates. Chlorine and magnesium may have come from salts dissolved in water.

In the rock weathering crusts (from samples of rock face collected on site), diatoms were observed such as previously reported at the Nisula site by Aubert *et al.* (2004). These organisms live in water and may have been introduced through the rise of water levels during the year, by water percolating or by visitors who throw water on the paintings to make them more visible.

Raman analysis on the rock reveals peaks at 325, 355, 389, 665, and 1012$cm^{-1}$ attributed to high-Ca pyroxenes (Acosta-Maeda *et al.*, 2013) and were previously reported by Desrochers (2011). Peaks of amorphous silica were recorded at 281, 481, 510, 1138, 1218, 1295, 1393, 1483, 1629, and 1898$cm^{-1}$ on both samples and rock face fragments. Magnetite with peaks at 233, 286, 658$cm^{-1}$ was found too but is attributed to the rock support and not to weathering products (Desrochers, 2011).

The FTIR spectra recorded on the rock support present a large massif with peaks at 747, 786, 911, 972, 1001, 1032, and 1196$cm^{-1}$. This comprises peaks related to Si-O and Al-O bonds which can be attributed to a large number of minerals including quartz, feldspars, pyroxenes, etc. Moreover, the presence of amorphous alumino-silica and silica with the peak at 1649$cm^{-1}$ has been confirmed. Thus their other peaks around 1000 and 1100$cm^{-1}$ are included in the previously mentioned massif.

Two series of peaks of amorphous alumino-silica and silica were recorded on both paintings and the rock face fragments: 799, 996, 1089, 1205, 1454, 1546, 1630$cm^{-1}$, and 753, 777, 795, 996, 1103, 1154, 1434, 1674$cm^{-1}$. The second group of peaks can be attributed to a mixture of quartz and alkali feldspars too. However, these two series of peaks reveal the heterogeneity of the amorphous alumino-silica and silica crust on the surface of the rock and

paintings. Indeed, in previous studies of this site and of other Canadian sites (Taylor *et al.*, 1974, Wainwright, 1985, Aubert *et al.*, 2004, Helwig, 2011), this crust was found to be composed mainly of silicon and aluminium with a high variation in their proportions and presence of other elements such as sodium, potassium and calcium. This difference is visible even for samples taken at few centimetres of distance. Thus the peaks recorded with FTIR are expected to move and vary depending on the composition of this crust.

Peaks at 1430-1450cm$^{-1}$ are attributed to calcium carbonates. They have been recorded on paints and on the rock itself. They are interpreted as weathering products.

6.4.2.2 Black layer

The black layer has a smooth texture and is found on top of a grey layer also exhibiting a smooth texture. The black layer is thick (about 100µm), sparse and homogeneous in colour. A thin transparent to white layer was observed on top of it. It is unclear here if this layer is a paint or a weathering crust.

Observations with secondary electrons show a flaky texture composed of flakes of different sizes: from 1 to 6-7 µm (Figure 6.4). A thin smooth layer is visible on top of the black layer at some points. Composed mainly of silicon, it is attributed to amorphous alumino-silica and silica crust.

The black layer is composed of iron with manganese, titanium and zinc. Sodium, aluminium, silicon and potassium can be attributed to both black layer and rock. Finally magnesium, potassium, sulphur and calcium are linked to weathering products. The presence of carbon is due to the carbon coating made for SEM observations but is part of the weathering products too.

Two series of peaks were recorded with Raman spectroscopy on the black sample: 287, 400, 485, 603, and 665cm$^{-1}$; 233, 279, 390, 483, and 589cm$^{-1}$ (Figure 6.4). They are both attributed to hematite. In the case of the first set of peaks, the peak at 665cm$^{-1}$ is associated with magnetite and to the decrease in the crystallinity of the sample. This might have been introduced by heating but other causes such as weathering, grinding, or biological actions are

possible (de Faria and Lopes, 2007). This broad peak attached to that at 603cm$^{-1}$ may hide another at 659cm$^{-1}$, linked to $Mn_2O$.

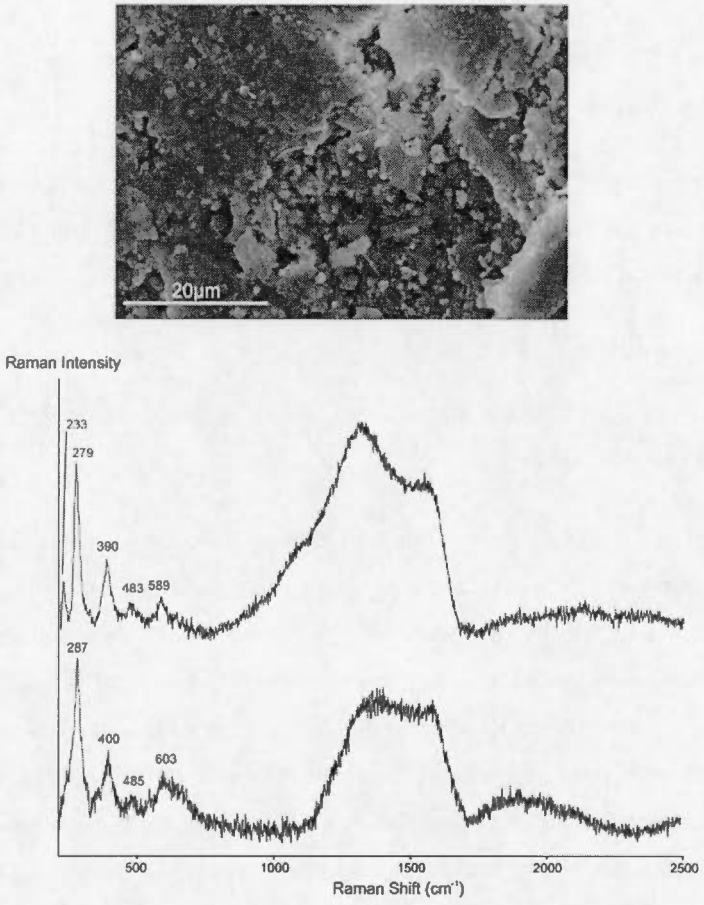


**Figure 6.4** SEM image (secondary electrons) and Raman spectra recorded on the black weathering crust

The second set of peaks represents a disordered hematite too but due here to impurities and possible heating. The same set of peaks was identified as a heated goethite in Coentro *et al.* (2012), for a brownish coloured glaze where manganese was present. On the other hand, a study of iron corrosion with addition of zinc and manganese reveals a similar set of peaks on the resulting corrosion product (Colomban *et al.*, 2008). The shift in peak positions is here the result of zinc and manganese bonded to Fe-O. The peak at 1325cm$^{-1}$ is associated with a

Fe-OH asymmetric stretching mode and is linked to the presence of water in the iron oxide matrix which may be due to the presence of iron hydroxides and/or clayish minerals (de Faria and Lopes, 2007).

These results point to a black hematite rich in zinc and manganese which might have been heated or developed as the result of a weathering process.

With FTIR spectroscopy, peaks of amorphous alumino-silica and silica coupled to quartz and feldspars were recorded at 576, 789, 948, 1012, 1066, 1540, 1630, and 1727cm$^{-1}$. Calcium carbonates were found with peak at 1442cm$^{-1}$.

### 6.4.3 Radiocarbon dating

Characterization conducted on the black layer shows that it is composed of hematite and is thus not datable using radiocarbon.

Analysis of the rock fragments from the rock face reveals the presence of diatoms in the amorphous alumino-silica and silica crusts, along with calcium carbonates. Both of these compounds can be dated by radiocarbon but the origin of their carbon needs to be investigated first. Diatoms present in weathering crusts may represent natural life on the rock. However, these organisms live in water and may have been deposited by the rise of water levels during the year, by water dripping or by visitors who throw water on the paintings to make them brighter. In that case, the carbon metabolized by these algae would be different from the carbon in the air, resulting in a reservoir effect. It means that in obtaining a radiocarbon date, it would be generated by diatoms from different ages, resulting in a determination that would be difficult to interpret. Abstracting these problems, at the *Mikinak* site, the layer of weathering products on top of the paint is thin, 20 to 70 µm in thickness, which would require large samplings in order to obtain a proper date. This is not feasible since it would damage the paintings and may accelerate degradation processes.

As regards calcium carbonates, they are present in very small quantities, as indicated by the weak peaks recorded by FTIR spectroscopy. Even though these weathering products yielded dates in similar projects (Taçon *et al.*, 2013), they are too few and a date would require a large sample, which is not feasible for the same reasons as detailed for the diatoms.

### 6.4.4 OSL dating

Quartz sensitivity for OSL was tested but no OSL signal was recorded. New discs were made and a dose of 2000Gy was given to assess the suitability of quartz for OSL dating. Once again, no OSL signal was recorded. Quartz in the rock at Lake Wapizagonke was not suitable for OSL dating. This can be explained by the nature and geological history of the rocks. Canadian rocks are metamorphic, and as such did not experience exposure and burial cycles. Since, quartz sensitivity may be a function of these burial/exposure cycles, as a result, primary rocks such as those in the Canadian Shield are not expected to have any OSL signal for quartz (Tsukamoto *et al.*, 2011). In the study conducted by Sohbati *et al.* (2011), no exploitable OSL signal was recorded on quartz from metamorphic rocks either. Further work will focus on plagioclases and other possible luminescent dosimeters such as pyroxenes (Jain *et al.*, 2006).

In conclusion, the attempts to apply radiocarbon and OSL were not successful. On the other hand, the precise characterization conducted to assess the possibility of applying them gives detailed information which can be used to help in site interpretation.

## 6.5 Discussion

### 6.5.1 Paintings and their environment

Characterization identified three different red pigments (Table 6.1):

- The first group has a fine flaky texture with SEM observations and is a type 1 hematite (n = 10).

- The second group has a flaky texture with SEM observations and is a type 1 hematite (n = 7).

- The third group has a flaky texture with SEM observations and is a type 2 hematite (n = 2).

These groups were established using only data which were undoubtedly linked to the original pigment. Indeed, since samples were exposed to water for an undetermined period of time,

peaks of amorphous alumino-silica and silica crusts recorded with FTIR spectroscopy may have been influenced by hydration and by the presence of clay minerals from the paints, hence their shape. Moreover, as SEM-EDS analysis was carried out on unprepared samples, minor elements which may be linked to the geological history of hematite such as titanium, manganese, zinc or copper but which are present in the rock support too were not considered in the group as their origin is imperfectly established. Finally, the sub-groups of type 1 hematite, recorded with Raman spectroscopy, were not used either.

Regarding FTIR spectra, it is interesting to note that the shape 2 is present only on samples composed of hematite type 1-1. Peaks in this massif are comprised of clayish minerals, and as a result the shape of the 1000 $cm^{-1}$ massif will be influenced. The presence of clay minerals reveals that either red ochre or a mixture of clay and hematite has been used. A known source of red ochre is mentioned by Béland (1959) about 30 miles south-east of the Lake Wapizagonke. This might have been one of the sources of pigment used.

One specific sample, 25M1A1-1, attributed to the first group, needs to be detailed on its own, as its characterization shows differences from the other pigments. This dark red paint is composed of coarse grains under the microscope and its hematite appears as fine flakes, about 1 µm in diameter. It is covered with balls (about 1µm in diameter) and mounds of balls which are composed of iron and sulphur. They are thought to be bacteria or fish eggs. As fragments were found in the lake, aquatic life prospered on them. However, they were observed only on this sample. This may be a bias due to the necessity of sampling paint for analysis, or it could be a difference in the binder used which provides a good environment (food) for bacterial life. Nevertheless, because of their stay in water and posterior manipulations, it was impossible to conduct proper binder analysis on these fragments. Such analysis may be conducted on the original panel, but weather conditions and the numerous human visits would make such analysis challenging.

If examined for colour at macroscopic scale, the third group is composed only of light red paints, and dark red colours are found in the first group. These colours may be due to the thickness of the layer of paint applied or to the nature of the pigment used. However, as no cross-section was authorized, it was impossible to distinguish between the two options.

The two samples of hematite type 2 show a peak at 270cm$^{-1}$ which has been previously reported as a peak from heated goethite. The fact that the SEM texture shows flakes of mixed sizes and that the resulting colour was light red, argues more in favour of heating. However, it may have been introduced through the exposure of fragments to water as previously detailed. These results are not enough to conclude to the heating of goethite to turn it into hematite and thus to make red paint out of orange/yellow ochre. Further analysis with X-ray diffraction and transmitted electron microscopy as conducted by Salomon *et al.* (2012) is necessary.

Fragments of this site were previously characterized (Helwig, 2011, Taylor *et al.*, 1974, Wainwright, 1985) and the hematite was found to be the source of the red colour of the paints. However, their studies were limited to two or three samples which precludes wider interpretation of the site. On the other hand, SEM-EDS analysis carried out by Helwig (2011) shows two different kinds of red paints layers on two different fragments (not identified in the report), which is consistent with our results.

Weathering products surrounding paintings and present on the surface of the rock face have been identified as amorphous alumino-silica and silica and calcium carbonates. These are common in the Canadian Shield. The formation of amorphous alumino-silica and silica crusts is still not well understood and two possibilities are discussed in the literature. The first possibility (Aubert *et al.*, 2004) assigns its formation to dissolution of silicon, aluminium and other chemical elements composing the rock due to acid rain percolating on cliffs. When it evaporates, chemical elements, as ions, crystallize and form a thin crust on top of the rock and paintings. The second possibility is the action of lichens on the rock. Chen *et al.* (2000) discuss the potential of oxalic acids, produced by lichens, to mobilize and recrystallize silicon, aluminium, and metallic ions from the rock to product alumino-silica gels. These gels have been found on various rock types but seem to be limited to volcanic and metamorphic rocks. Amorphous silica gels are seen by Chen *et al.* (2000) as the result of posterior degradation of the alumino-silica gels. This may explains the presence of signatures of both alumino-silica and silica on the Lake Wapizagonke rock and paints as the process of formation and degradation is still in progress.

Results obtained on the black layer point to the presence of hematite rich in manganese and zinc. As with the red pigments studied, an amorphous alumino-silica and silica crust is present on top of it and calcium carbonates were also recorded as weathering products.

Is this black layer paint? This is difficult to determine for a number of reasons. Firstly, no black paint was ever mentioned in the records of this site. However, it can be postulated that the fragment fell into water before any observations were made. Analytical results seem to point to a possible pigment but the shape of the layer, which is very sparse, tip the scale in favour of weathering products from the rock. Moreover, magnetite has been identified in this study and by Desrochers (2011) as a component of the rock support and is known to turn into hematite through a maghemite form in air and acidic environment (Cornell and Schwertmann, 2003). It was thus concluded that this black layer is due to weathering and is not paint.

### 6.5.2 Interpretation of the site

Characterization of the pigments from Lake Wapizagonke would suggest the use of three different paints. Interestingly, the red paints from the same fragments were not made with the same pigments. This suggests that even representations which were closely associated in the panel were not made with the same paint recipe. Here arise more questions: were these paintings made at the same time but by different artists who did not prepare their paint in the same way or were they made at different periods but the artists decided to paint close to the previous paintings to complement the panel?

In his study of rock art in the Canadian Shield, Lemaitre (2013) points out a uniformity of the representations, of the organisation of the panels, and in the choice of rock supports in Canadian rock art. Can this uniformity be applied to the preparation of paintings? Possibly. Even if the act of painting is not in the hands of specific people, it is tinted of sacredness. The raw material used to make the painting, called the "Indian red" (term used by French and British colonists to refer to the red paint used by Amerindians to create rock art (Lemaitre, 2013), is sacred too. It points in favour of a particular recipe transmitted in each group/large family. This hypothesis of a single paint recipe shared by a group has been previously stated by Chalmin (2003) for European Palaeolithic cave paintings.

The three recipes found can be interpreted in two ways:

- They reveal that the site was used at three different independent periods when artists added their own representations to the panel

- They reveal that three artists from up to three different groups painted this panel in as many as, three different periods, suggesting then that it was a gathering site for different families, clans or groups.

It would be interesting to know which parts of the panel are different from others in order to propose a better understanding of the panel. However, flakes were collected from the lake and no information is available about their place on the site. Following the photos and surveys made by Béland, Dewdney and Tassé, the part on the left side of the site, identified as a quadruped, a human figure and an anthropomorphic figure with a bird head (Lemaitre, 1996), disappeared between Béland and Dewdney records, that is to say between 1952 and 1966. This has been attributed to intentional degradation by visitors who wanted to bring back a souvenir (Lemaitre, 1996). But what if these fragments detached from the rock and fell into the lake? Comparing photos of fragments with photos of the site, it was possible to propose that fragment 25M1A1-1 may be a part of the quadruped and fragment 25M99A1-2-d may be placed under the glyph of three stripes, called number 4 in Lemaitre (1996) (Figure 6.5). Interestingly, the two stripes on the left are made of the same paint but not the third stripe on the right.

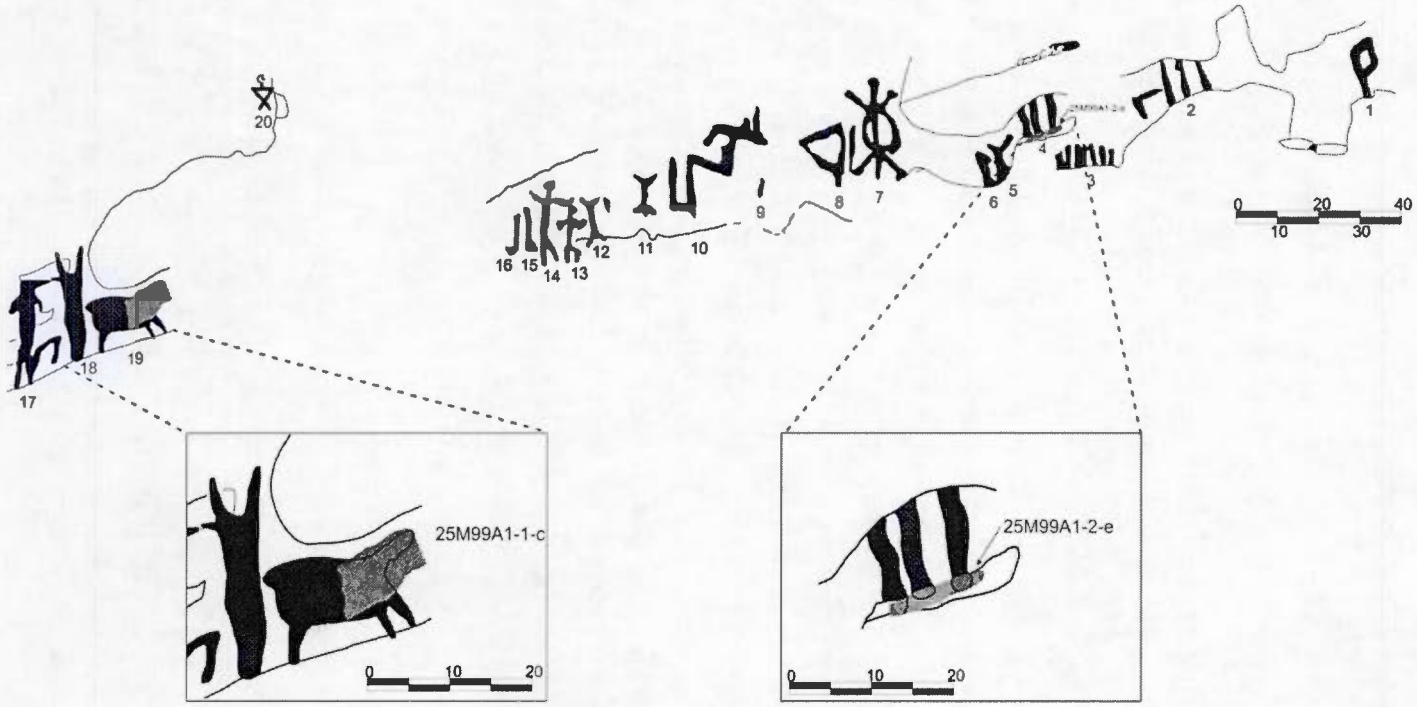


**Figure 6.5** Reconstitution proposal of two fragments on the panel

## 6.6 Conclusion

The choice of a multi-instrumental and detailed characterization protocol to assess the possibility of applying either radiocarbon or OSL dating methods proves to be successful at distinguishing different paint recipes and as a result provides new keys to interpret the *Mikinak* site.

The present study has put the interpretation a step forward and proves the importance of characterization in this process. The possibility of making cross-sections and sampling of paintings *in-situ* would help in the future to further reconstruct the steps of the panel's creation. This would form part of the *chaîne opératoire* process which details each step of the "life" of a rock art site, from the choice of the site and raw materials to the abandonment of the site.

No absolute date is provided for paintings at the site, but relative dating is now possible which gives an alternatives given the lack of superpositioning of rock art in the Canadian Shield. However, this is unlikely to be the final attempt to date the site.

## 6.7 Acknowledgments

This project has been conducted as a collaboration between the University of Quebec in Montreal and Parks Canada. Albert Van Dijk, Resource Conservation Manager of La Mauricie and Western Québec Field Unit, Parks Canada, is thanked for his assistance in accessing the site. We thank Prof. Thomas Higham, University of Oxford, United Kingdom, for his assistance on attempts of radiocarbon dating. Dr. Maxime Aubert is acknowledged for Uranium-series analysis and attempts of dating. This project has been funded by Parks Canada and the Social Sciences and Humanities Research Council of Canada.

Supplementary online materials are given in appendix E.

Bibliography

Acosta-Maeda, T.E., Scott, E.R.D., Sharma, S.K. and Misra, A.K. (2013). The pressures and temperatures of meteorite impact: Evidence from micro-Raman mapping of mineral phases in the strongly shocked Taiban ordinary chondrite. *American Mineralogist*, 98(5-6), 859-869.

Arias, P., Laval, E., Menu, M., Sainz, C.G. and Ontañón, R. (2011). Les colorants dans l'art pariétal et mobilier paléolithique de La Garma (Cantabrie, Espagne). *L'Anthropologie, 115*(3–4), 425-445.

Arsenault, D. and Gagnon, L. (2001). *Site rupestre à tracés digitaux du lac Wapizagonke 2000-2001 : réexamen du site rupestre CdFg-5 et évaluation de ses conditions hivernales de conservation, lac Wapizagonke, parc national de la Mauricie, rapport final*. Université Laval, Projet PETRARQ. Sainte-Foy, Québec.

Aubert, M., Watchman, A., Arsenault, D. and Gagnon, L. (2004). L'archéologie rupestre du Bouclier canadien: Potentiel archéométrique. *Canadian Journal of Archaeology*, 28(1), 51-74.

Bednarik, R.G. (1996). Only time will tell: a review of the methodology of direct rock art dating. *Archaeometry*, 38(1), 1-13.

Bednarik, R.G. (2002). The dating of rock art: A critique. *Journal of Archaeological Science*, 29(11), 1213-1233.

Béland, J. (1959). Peintures et outils en pierre indiens au lac Wapizagonké. *Le Naturaliste Canadien*, 86(22), 46-52.

Bonneau, A., Pearce, D.G. and Pollard, A.M. (2012). A multi-technique characterization and provenance study of the pigments used in San rock art, South Africa. *Journal of Archaeological Science*, 39(2), 287-294.

Bonneau, A., Staff, R.A., Higham, T., Brock, F., Pearce, D.G. and Mitchell, P.J. (2016). Dating rock art in southern Africa by improvement of sampling and success of dating using new characterization and pretreatment protocols. *Radiocarbon, In press.*

Chen, J., Blume, H.-P. and Beyer, L. (2000). Weathering of rocks induced by lichen colonization — a review. *CATENA*, 39(2), 121-146.

Clottes, J., Menu, M. and Walter, P. (1990). La préparation des peintures magdaléniennes des cavernes ariégeoises. *Bulletin de la Société préhistorique française, 87*(6), 170-192.

Coentro, S., Mimoso, J.M., Lima, A.M., Silva, A.S., Pais, A.N. and Muralha, V.S.F. (2012). Multi-analytical identification of pigments and pigment mixtures used in 17th century Portuguese azulejos. *Journal of the European Ceramic Society*, 32(1), 37-48.

Colomban, P., Cherifi, S. and Despert, G. (2008). Raman identification of corrosion products on automotive galvanized steel sheets. *Journal of Raman Spectroscopy*, 39(7), 881-886.

Cornell, R.M. and Schwertmann, U. (2003). *The iron oxides structure, properties, reactions, occurrences, and uses*. Weinheim : Wiley-VCH.

Dagneau, C. (2010). *Expertise archéologique subaquatique du site rupestre du lac Wapizagonke (CdFg-5), 2010*. Parks Canada.

de Faria, D.L.A. and Lopes, F.N. (2007). Heated goethite and natural hematite: Can Raman spectroscopy be used to differentiate them? *Vibrational Spectroscopy*, 45(2), 117-121.

Desrochers, A. (2011). *Minéralogie de la paroi rocheuse au site rupestre du Lac Wapizagonke, Parc national du Canada de la Mauricie, Québec*. Parks Canada.

Ford, B., MacLeod, I. and Haydock, P. (1994). Rock Art Pigments from Kimberley Region of Western Australia: Identification of the Minerals and Conversion Mechanisms. *Studies in Conservation, 39*(I), 57-69.

Helwig, K. (2011). *Analyse d'échantillons du site rupestre du lac Wipizagonke* (CdFg-5). Canadian Conservation Institute.

Huntley, J., Aubert, M., Ross, J., Brand, H.E.A. and Morwood, M.J. (2015). One Colour, (at Least) Two Minerals: A Study of Mulberry Rock Art Pigment and a Mulberry Pigment 'Quarry' from the Kimberley, Northern Australia. *Archaeometry, 57*(1), 77-99.

Jain, M., Andersen, C.E., Bøtter-Jensen, L., Murray, A.S., Haack, H. and Bridges, J.C. (2006). Luminescence dating on Mars: OSL characteristics of Martian analogue materials and GCR dosimetry. *Radiation Measurements, 41*(7–8), 755-761.

Lemaitre, S. (1996). Les peintures rupestres amérindiennes du Lac Wapizagonke (Québec) : une vision chamanique? Dans Bonenfant, P. (dir.), *La préhistoire au quotidien : mélanges offerts à Pierre Bonenfant* (p. 99-117). Grenoble : J. Millon.

Lemaitre, S. (2013). *Kekeewin ou Kekeenowin : les peintures rupestres de l'est du bouclier canadien.* Mascouche : Recherches amérindiennes au Québec.

Menu, M. and Walter, P. (1992). Prehistoric cave painting PIXE analysis for the identification of paint pots. *Nuclear Instruments & Methods in Physics Research Section B-Beam Interactions with Materials and Atoms, 64*(1-4), 547-552.

Menu, M., Walter, P., Vigears, D. and Clottes, J. (1993). Façons de peindre au Magdalénien. *Bulletin de la Société préhistorique française*, 426-432.

Prinsloo, L.C., Barnard, W., Meiklejohn, I. and Hall, K. (2008). The first Raman spectroscopic study of San rock art in the Ukhahlamba Drakensberg Park, South Africa. *Journal of Raman Spectroscopy, 39*(5), 646-654.

Salomon, H., Vignaud, C., Coquinot, Y., Beck, L., Stringer, C., Strivay, D. and D'Errico, F. (2012). Selection and heating of colouring materials in the Mousterian level of Es-Skhul (c. 100 000 years BP, Mount Carmel, Israel). *Archaeometry, 54*(4), 698-722.

Sohbati, R., Murray, A., Jain, M., Buylaert, J.-P. and Thomsen, K. (2011). Investigating the resetting of OSL signals in rock surfaces. *Geochronometria*, 38(3), 249-258.

Taçon, P.S.C., Boivin, N., Petraglia, M., Blinkhorn, J., Chivas, A., Roberts, R.G., Fink, D., Higham, T., Ditchfield, P., Korisettar, R. and Zhao, J.-x. (2013). Mid-Holocene age obtained for nested diamond pattern petroglyph in the Billasurgam Cave complex, Kurnool District, southern India. *Journal of Archaeological Science*, 40(4), 1787-1796.

Tassé, G. and Dewdney, S.H. (1977). *Relevés et travaux récents sur l'art rupestre amérindien.* Montreal : Montreal Université du Québec a Montréal, Laboratoire d'archéologie.

Taylor, J.M., Myers, R.M. and Wainwright, I.N.M. (1974). Scientific Studies of Indian Rock Paintings in Canada. *Bulletin of the American Institute for Conservation of Historic and Artistic Works*, 14(2), 28-43.

Tournié, A., Prinsloo, L.C., Paris, C., Colomban, P. and Smith, B. (2011). The first in situ Raman spectroscopic study of San rock art in South Africa: procedures and preliminary results. *Journal of Raman Spectroscopy, 42*(3), 399-406.

Tsukamoto, S., Nagashima, K., Murray, A.S. and Tada, R. (2011). Variations in OSL components from quartz from Japan sea sediments and the possibility of reconstructing provenance. *Quaternary International*, 234(1–2), 182-189.

Valladas, H. (2003). Direct radiocarbon dating of prehistoric cave paintings by accelerator mass spectrometry. *Measurement Science and Technology*, 14(9), 1487-1492.

Valladas, H., Tisnerat-Laborde, N., Cachier, H., Arnold, M., de Quiros, F.B., Cabrera-Valdes, V., Clottes, J., Courtin, J., Fortea-Perez, J.J., Gonzalez-Sainz, C. and Moure-Romanillo, A. (2001). Radiocarbon AMS dates for paleolithic cave paintings. *Radiocarbon*, 43(2B), 977-986.

Wainwright, I.N.M. (1985). Rock art conservation research in Canada. *Bolletino del Centro Camuno di Studi Preistorici*, 22, 15-46.

Wainwright, I.N.M. (1990). Rock painting and petroglyph recording projects in Canada. *Association for Preservation Technology Bulletin*, 22(1/2), 55-84.

# CONCLUSION

In this PhD, rock paintings from two world areas, southern Africa and the Canadian Shield, were studied with two main objectives: i) providing an absolute and direct date, that is to say the date of the event of painting, ii) without damaging the integrity of the sites. A third objective arose during the project, following preliminary results, as a possibility to obtained dates matching the two first objectives, on specific figures present in the Maclear District (Eldritch figures and LH-SDFs), which are thought to be linked to changes in the San society and to contacts with other communities.

Following estimated periods of paint provided by the archaeologists in charge of the sites (8000 to 100 BP in southern Africa, and 5000 to 100 BP in the Canadian Shield), and according to previous researches conducted in these areas and around the globe, radiocarbon and OSL were selected. However, to apply one or both of these methods, a sample should be composed of suitable compounds and thus should be characterized.

A multi-instrumental characterization protocol was developed to finely characterize the different components of the sample from the rock support to weathering products through paint and its degradations. Using a sample as small as 0.5 to 1 $mm^2$, almost non-invasive for rock paintings, this protocol provides detailed information to select the dating methods, to adjust them to the specificities of each sample, leading in obtaining a reliable and reproducible date, with as less sample as possible.

If carbon is present in the sample, radiocarbon can be applied. However, carbon may be under various forms. The multi-instrumentation protocol was efficient at characterizing these forms and at estimating their proportion and location in the sample. Hence, carbon related to the event of painting was found in the black paints under the form of carbon-blacks and soot, charcoal paints have been identified but provide a maximum age. The other compounds containing carbon as calcium oxalates, calcium carbonates and humic acids, which are considered as radiocarbon contaminants, were tracked in the sample and their proportion

estimated. Following these results, the chemical pre-treatment was adjusted to remove radiocarbon contaminants previously identified, and to keep as much as possible of the sample to be dated. FTIR analysis is carried out at the end of the chemical pre-treatment to check the absence of radiocarbon contaminants. The chemical pre-treatment being precisely adapted, it has become less invasive and smaller samples were needed (2 $cm^2$). Moreover, combined to the results of the characterization protocol, samples which are the most likely to provide a date and the quantity of sample needed to achieve it are proposed to archaeologists for collection discussion in the aim to obtain a date and at the same time to conserve the integrity of the figures.

If quartz and feldspars are present in the rock support and if the paint layer is thick enough to have protected the rock from daylight, OSL may be applied. The ubiquity of quartz and feldspars on Earth makes OSL a good alternative to provide absolute dating in archaeology when radiocarbon or other techniques are not applicable. However, quartz from rocks studied in this project were either not suitable for OSL dating, or were too few in the rocks. On the other hand, K-feldspars exhibit thermal transfer of about 1 Gy which prevents any dating of samples less than 1000 years old, a constraint in the case of sites studied as they were mostly from 100 to 3000 years old. Using a modified SAR sequence by the addition of a bleaching/thermal wash step after each Ln-Lx and Tn-Tx measurements, they proved to be suitable for OSL dating. A novel working hypothesis has been applied by postulating that the rock face of a rock shelter was bleached before application of the paint layer, which provides a protection against daylight. If K-feldspars at the surface of the rock were indeed bleached, the paint layer provides only an incomplete protection against daylight, keeping only about 5% of the signal. It is few but on the other hand, only red soils as a paint layer of 20 µm thick, corresponding to the recipe encountered on studied sites, were tested. Further tests with different colouring material and thickness should be realized to give a final conclusion to the possibility of dating rock art using this technique.

If neither radiocarbon, nor OSL can be applied, information about the realization of the site can be obtained by using the detailed characterization provided by the multi-instrumentation protocol. Indeed, it has been proved comparing paint recipes and their age, that within the same panel or superposition layer, the same paint recipes were used. Hence, if different paint

recipes were used on a site for the same colour, it can be deduced that they were not realized together. Moreover, following details provided by the archaeologists, an assumption can be made: one recipe is linked to one population. Thus, keys about the realization of rock art sites can be provided, helping at some points their interpretation.

This protocol makes it possible to know that southern African hunter-gatherers were creating images on rock-shelter walls as long ago as 5723–4420 cal. BP in southeastern Botswana, 2326-965 cal. BP in western Lesotho, and 2998–2381 cal. BP in the Maclear District of South Africa. These dates are the first obtained on San rock art in Botswana and Lesotho, and the 46 dates obtained in this project constitute the largest chronological project so far conducted on San rock art. Along with dates, a large pallet of paint recipes was identified. Amongst them, cremated bones for white paints and soot for black paints were for the first time identified, and confirm assumptions formulated by Rudner (1982). Moreover, intentional admixtures were identified. These results coupled to analysis and processing of locally found soils make it possible to reconstitute parts of the *chaîne opératoire* of the site which was found to be particularly constant through time and southern African areas. In the Canadian Shield, dates could not be obtained, but the precise characterization conducted at the *Mikinak* site provides for the first time a new light on this site which was initially thought to have been made as a single scene but which was in fact produced with three paint recipes, possibly corresponding to three phases of paintings.

The two main objectives of this PhD were achieved using a multi-instrumentation characterization protocol efficient at selecting samples for either radiocarbon or OSL, and at providing an alternative by giving keys about the realization of sites using the detailed characterization of paintings. The third objective was not achieved as no datable material was found on the specific figures, Eldritch figures and LH-SDFs. However, by characterizing all paints from these figures and by dating figures from the same panel or superposition layer, it may be possible to extend the dates obtained and provide an absolute date.

The dates and characterization results obtained in this PhD open up space for developing a chronometrically grounded approach to diversity and change within San rock art. Because the meaning of San rock art is so well understood, these chronological changes should be

understood in social terms. Moreover, it makes it possible for archaeologists to start developing a dialogue between the record of hunter-gatherer activity preserved in paint and that preserved in excavatable deposits.

# CONCLUSION

Dans cette thèse de doctorat, les peintures rupestres de deux principales régions du monde, l'Afrique australe et le Bouclier canadien, ont été étudiées avec deux objectifs principaux: i) fournir une date directe et absolue, à savoir la date de la réalisation de la peinture, ii) sans endommager l'intégrité des sites. Un troisième objectif a été ajouté au cours du projet, à la suite de résultats préliminaires en datation et caractérisation, à savoir essayer d'obtenir des âges correspondant aux deux premiers objectifs, sur des représentations spécifiques présentes dans le district de Maclear (figures d'Eldritch et LH-SDF), qui sont interprétées comme étant liées à des changements dans la société San et à des contacts avec d'autres communautés.

D'après les estimations des périodes de réalisation des peintures fournies par les archéologues en charge des sites (de 8000 à 100 BP en Afrique australe, et de 5000 à 100 BP dans le Bouclier canadien), et d'après les recherches antérieures menées dans ces zones géographiques et dans le monde entier, les méthodes de datation par le radiocarbone et par luminescence stimulée optiquement (OSL) ont été sélectionnées. Cependant, pour appliquer l'une ou l'autre de ces méthodes, un échantillon doit être composé d'éléments spécifiques, et doit donc être caractérisé.

Un protocole de caractérisation multi-instrumental a été développé afin de caractériser de façon détaillée les différents composants de l'échantillon depuis la roche support de la peinture jusqu'aux altérations dues aux intempéries en passant par la peinture et ses dégradations. En utilisant un échantillon aussi petit que 0.5 à 1 $mm^2$, échantillon presque non-invasif pour les peintures rupestres, ce protocole fournit des informations détaillées afin de sélectionner la méthode de datation à utiliser, de l'adapter aux spécificités de chaque échantillon, et d'obtenir une date fiable et reproductible, avec le plus petit échantillon possible.

Si du carbone est présent dans l'échantillon, la datation par le radiocarbone peut être appliquée. Cependant, le carbone peut être sous diverses formes. Le protocole multi-instrumental permet la caractérisation de ces formes et l'estimation de leur place et de leur

proportion dans l'échantillon. Ainsi, le carbone lié à l'événement de réalisation de la peinture a été trouvé dans les peintures noires sous la forme de noirs de carbone et de suie. Des peintures faites de charbon de bois ont été identifiées, mais seul un âge maximum peut être obtenu pour ces peintures. Les autres composés contenant du carbone comme les oxalates de calcium, les carbonates de calcium et les acides humiques, qui sont considérés comme des contaminants pour la datation par le radiocarbone, ont été localisés dans l'échantillon et leur proportion estimée. Suite à ces résultats, le prétraitement chimique a été ajusté pour éliminer ces contaminants pour la datation par le radiocarbone, et pour conserver autant d'échantillon que possible pour la datation. Une analyse FTIR est effectuée à la fin du prétraitement chimique pour vérifier l'absence de ces contaminants. Le prétraitement chimique étant précisément ajusté, il est devenu moins invasive et de plus petits échantillons peuvent être utilisés (2 $cm^2$). Ainsi, en combinant les résultats du protocole de caractérisation, les échantillons qui sont les plus susceptibles de fournir une date et la quantité d'échantillon nécessaire pour y parvenir sont proposés aux archéologues. Une discussion autour de la collecte de ces échantillons est ainsi possible dans le but d'obtenir d'une date et de préserver l'intégrité des peintures rupestres.

Si des quartz et des feldspaths sont présents dans la roche support des peintures et si la couche de peinture est assez épaisse pour avoir protégé la roche de la lumière du jour, la datation par OSL pourrait être appliquée. L'omniprésence de quartz et de feldspaths sur Terre fait de l'OSL, une bonne alternative pour fournir une datation absolue en archéologie quand la datation par le radiocarbone ou d'autres techniques ne sont pas applicables. Toutefois, le quartz des roches étudiées dans ce projet soit ne convenait pas pour la datation OSL (pas de signal), soit étaient trop peu nombreux dans la roche support. D'autre part, les feldspaths potassiques (K-feldspaths) présentent un transfert thermique d'environ 1 Gy, ce qui compromet toute datation d'échantillons jeunes, une contrainte dans le cas des sites étudiés car ils datent pour la plupart de 100 à 3000 cal. BP (d'après les âges obtenus par le radiocarbone). L'utilisation d'une séquence SAR modifiée par l'ajout d'une étape de mise à zéro, soit par exposition à une lumière artificielle, soit par *thermal wash*, après chaque mesure de Ln-Lx et de Tn-Tx, s'est avérée appropriée pour permettre une datation par OSL malgré les contraintes imposées par le transfert thermique. Une hypothèse de travail originale

a été utilisée : en postulant que la paroi rocheuse d'un abri-sous-roche ait été remise à zéro avant l'application de la couche de peinture, cette dernière lui fournit une protection contre la lumière du jour et le signal OSL commence à s'accumuler. Si les K-feldspaths à la surface de la roche ont été en effet remis à zéro, la couche de peinture ne fournit qu'une protection partielle contre la lumière du jour, gardant seulement 5 à 10 % du signal. Ce qui est peu. Néanmoins, seuls les sols rouges, sous la forme de couches de peinture de 20 à 100 µm d'épaisseur, correspondant à la recette rencontrée sur les sites étudiés, ont été testés. D'autres essais avec différentes peintures et épaisseurs devraient être réalisées pour donner une conclusion définitive sur la possibilité de dater l'art rupestre en utilisant cette technique.

Enfin quand ni la datation par le radiocarbone, ni la datation par OSL ne peuvent être appliquées, des informations sur la réalisation du site peuvent être obtenues en utilisant la caractérisation détaillée fournie par le protocole multi-instrumental. En effet, il a été prouvé en comparant les recettes de peinture et leur âge, que, sur un même panneau ou couche de superposition, des recettes de peinture identiques ont été utilisées. Par conséquent, si des recettes de peinture différentes ont été utilisées sur un même panneau/couche de superposition pour réaliser la même couleur, on peut en déduire que les figures n'ont pas été réalisées en même temps. En outre, suivants les détails fournis par les archéologues, une hypothèse peut être faite: chaque recette pourrait être liée à une population. Ainsi, des informations clés au sujet de la réalisation des sites rupestres peuvent être fournies, contribuant à leur interprétation.

Ce protocole a permis de découvrir que les chasseurs-cueilleurs d'Afrique australe créaient des peintures sur les murs des abris-sous-roche il y a aussi longtemps que 5723 à 4420 cal. BP dans le sud du Botswana, 2326 à 965 cal. BP dans l'ouest du Lesotho, et 2998 à 2381 cal. BP dans le district de Maclear, en Afrique du Sud. Ces dates sont les premières obtenues sur l'art rupestre San au Botswana et au Lesotho, et les 46 dates obtenues dans le cadre de ce doctorat constituent le plus grand projet de chronologie jusqu'ici réalisé sur l'art rupestre San. A côté de ces dates, une large palette de recettes de peinture a été identifiée. Parmi elles, des os calcinés pour les peintures blanches et de la suie pour les peintures noires ont été pour la première fois identifiées, et confirment les hypothèses formulées par Rudner (1982). De plus, des mélanges intentionnels ont été identifiés. Ces résultats, couplés à l'analyse et à des essais

de préparation des sols trouvés à proximité des sites rupestres, ont permis de reconstituer des parties de la chaîne opératoire des sites, qui est particulièrement constante à travers le temps et les régions d'Afrique australe étudiées. Dans le Bouclier canadien, des dates n'ont pas pu être obtenues, mais la caractérisation précise des peintures menée sur le site *Mikinak* fournit pour la première fois une lumière nouvelle sur ce site. Initialement, il était vu comme ayant été réalisé en une seule fois sous la forme d'un seul panneau. Mais la présence de trois recettes de peinture différentes, pouvant correspondre à trois phases de peinture, remet en question cette hypothèse.

Les deux principaux objectifs de cette thèse de doctorat ont été réalisés en utilisant un protocole de caractérisation multi-instrumental permettant de sélectionner des échantillons soit pour la datation par le radiocarbone, soit pour la datation par OSL. De plus, ce protocole fournit une alternative à la datation absolue en fournissant des informations clés à propos de la réalisation des sites, en utilisant une caractérisation détaillée des peintures. Le troisième objectif n'a pas été atteint car aucun matériel datable n'a été trouvé sur les figures spécifiques que sont les figures d'Eldritch et les LH-SDF. Cependant, en caractérisant toutes les peintures de ces figures et en datant les figures du même panneau ou de la même couche de superposition, il peut être possible d'étendre les dates obtenues et ainsi de fournir une date absolue.

Les dates et les résultats de caractérisation obtenus dans cette thèse ouvrent la possibilité de développer une approche chronologique bien établie pour appréhender la diversité et le changement au sein de l'art rupestre San. Le sens de l'art rupestre San étant bien connu et compris, ces changements au cours du temps pourraient être interprétés en termes sociaux. En outre, cette approche chronologique permet aux archéologues de commencer à développer des liens entre les activités des chasseurs-cueilleurs préservées dans la peinture et celles conservées dans des dépôts archéologiques.

# APPENDIX A

## INSTRUMENT PRINCIPLES

In this appendix, a brief description of the principles of the instruments used for characterization is given.

### A.1 Scanning electron microscopy coupled with Energy-dispersive X-ray Spectrometry (SEM-EDS)

The SEM uses an electron beam generated by a filament, usually made from tungsten. This beam is focused by electromagnetic lenses, and interacts with a microscopic part of the sample placed in the analysis chamber.

When the electron beam arrives on the sample, it interacts with atoms and electrons at the surface of the sample. Various forms of radiation and particles are then emitted by the sample (Figure A.1): secondary electrons which show the topography of the sample, backscattered electrons which give an image with chemical contrast, the X-rays which are used for the qualitative and quantitative analyses. Cathodoluminescence and Auger electrons are also emitted but were not used for this project.

The analysis chamber in a conventional SEM, is under vacuum, approximately $10^{-6}$ mbar (High Vacuum). This can cause charge effects which prevent formation and recording of a good image. To limit these effects, it is possible to coat the sample with a layer of carbon, gold or other conductive metal.

In some SEMs, it is possible to vary vacuum (SEM with variable pressure) in the analysis chamber and thus limit the charging of the sample, without the need for carbon or gold coating.

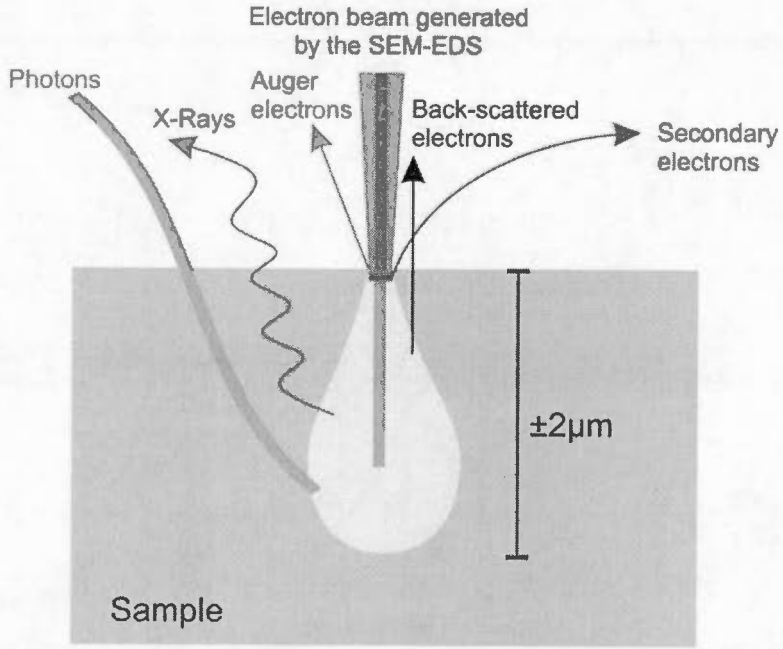


**Figure A.1** Interaction between electron beam and sample in SEM-EDS

## A.2 Raman spectroscopy

Raman spectroscopy works using monochromatic lasers as excitation rays. When monochromatic radiation is focussed on an object, several phenomena are observed: reflected light, transmitted light and diffused light. This last phenomenon contains two parts: one radiation, called Rayleigh diffusion, having the same wavelength as primary radiation ($v_0$) and a second radiation, called Raman diffusion, having a different wavelength ($v_{vib}$) than the primary one (Figure A.2).

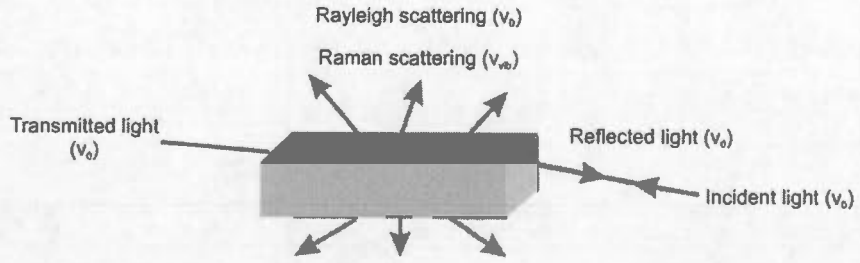


**Figure A.2** Phenomena observed under a primary monochromic radiation

When energy is focussed on a sample, the electrons adopt an excited state. They need then to come back to their stable state. There are several scenarios for this (Figure A.3):

- The electron returns to its original energy state. This is Rayleigh scattering. In this case, no information is obtained ($v_0$).

- The electron releases less energy than it absorbed, giving rise to a Stokes scattering effect ($v_0$-$v_{vib}$).

- The electron releases more energy than it absorbed. This is an anti-Stokes Raman diffusion ($v_0$+$v_{vib}$).

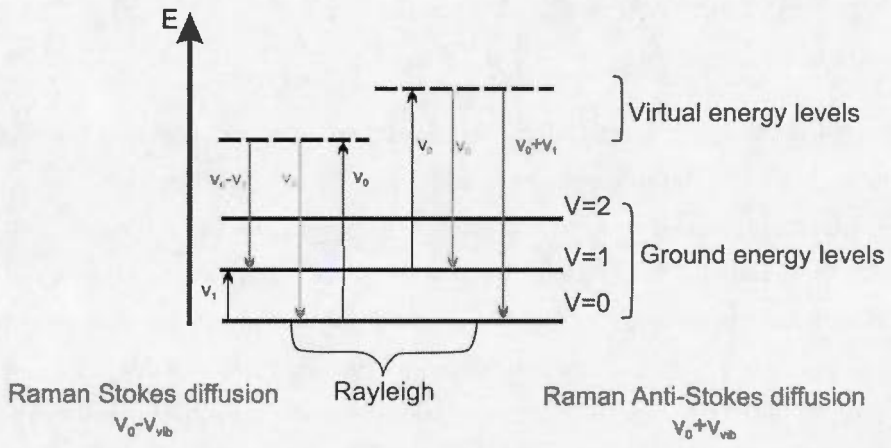


**Figure A.3** Rayleigh and Raman diffusions

Therefore, the diffusion which the instrument detects has three components: the Rayleigh diffusion accounting for 99% of the signal, the anti-Stokes Raman diffusion and the Stokes Raman diffusion, the former having intensity lower the latter than. The Stokes Raman diffusion is used for Raman spectroscopy analysis, although its intensity is ten million times weaker than that of incidental radiation.

## A.3 Fourier Transform InfraRed (FTIR) spectroscopy

FTIR spectroscopy is based on the absorption by molecular bonds of infrared wavelengths. They extend from 12 800 $cm^{-1}$ to 10 $cm^{-1}$ and are divided into three groups: near infrared,

middle infrared and far infrared. Conventional FTIR spectrometers use middle infrared wavelengths which extend from 4 000 $cm^{-1}$ to 400 $cm^{-1}$ (that is to say 2.5 µm to 25 µm).

When an infrared ray is focused on a molecule, the latter absorbs a part of it which corresponds to the types of bonds present. The absorption of the infra-red radiation can take place only if the wavelength corresponds to the energy associated with a particular mode of vibration of the molecule. Middle infrared wavelengths are the area in which the majority of the organic compounds produce a single absorption spectrum (Stuart, 2007).

In the FTIR spectrometer, infrared rays follow two paths. One part goes to the sample and the other to a space with no sample to act as reference. Combining the two, it is possible to know which wavelengths were absorbed by the sample and with what intensity. This gives a quantitative feature to the analysis.

Samples can be analysed in several modes: transmission, reflectance or Attenuated Total Reflectance (ATR). Transmission and ATR are the most commonly used modes. Transmission analysis requires a preparation of the sample as a pellet. It is reduced to powder and mixed with salts transparent to infrared such as KBr, NaCl or $CIF_2$. Samples can be sliced with a microtome to form films of about 10µm thickness which can thus be used directly in transmission. This preparation is more often used when analyses are carried out with a micro-FTIR. In the case of ATR, samples are put on a diamond window and crushed with a "screw". Micro-ATRs exist as well, made with diamond or germanium and offer the possibility to point on an area of about 100 $µm^2$ without destruction. It is often used to analyse paintings and manuscripts.

# APPENDIX B

## ROCK SUPPORT CHARACTERIZATION: SOUTH AFRICA, LESOTHO AND BOTSWANA

In this appendix, characterization conducted on rock faces on which paintings were created is detailed step by step, following the same protocol as for paint characterization. To avoid unnecessary repetitions of peaks observed during Raman spectroscopy and FTIR spectroscopy analyses, only the name of the compounds identified are given. Peaks associated can be found in Table 3.1 and 3.2 in Chapter III. Where unconventional peaks are found or where a detailed explanation of the position of peaks is required, further developments will be provided.

### B.1 Rock support characterization, Maclear District, South Africa

#### B.1.1 Microscope

At its surface, the rock face exhibits a white layer which covers a rock composed of white, transparent, and yellow grains (Figure B.1a). Few darker grains (red or black) are visible at the surface, mixed in the white layer. They may be part of the weathering of the rock, or aerosol particles.

The observations of the rock in cross-section show the presence of grains of almost the same size (about 100 µm) comprised in a yellow matrix (Figure B.1b). Under direct reflected light, a few grains are very bright.

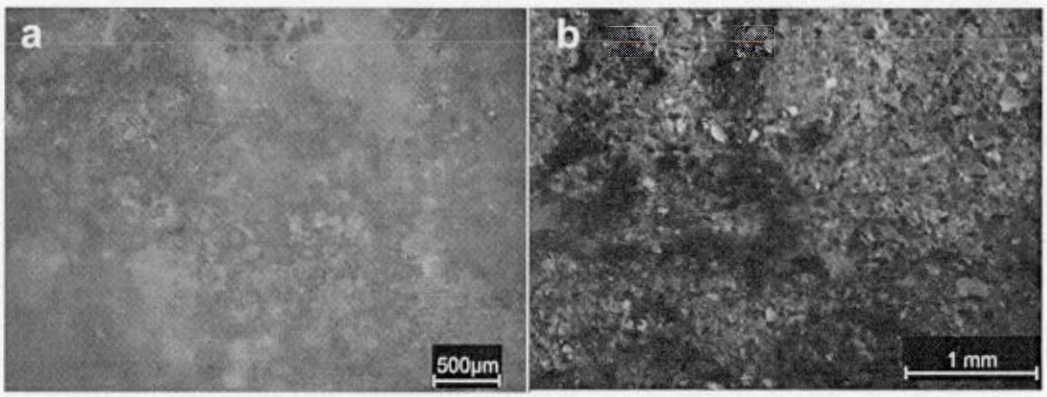


**Figure B.1** Microscope observation on Maclear rock: a) surface, b) cross-section

B.1.2 SEM-EDS

At its surface, the rock contains grains of different sizes (from 1 to 20 µm diameter) and of different shapes: round, long, polygon. Most of these grains are composed of silicon and aluminium. The smallest are composed of calcium and may be calcium oxalates or calcium carbonates. Sodium, magnesium, potassium and iron were recorded as minor elements.

In cross-section, the rock is composed of small grains about 100 µm diameter such as previously observed under microscope. They are composed of silicon for about 50% of them, and silicon, aluminium, potassium or sodium for the other 50%. The former are identified as quartz, whereas the latter are potassium and alkali-feldspars. The matrix is composed of calcium.

B.1.3 Raman spectroscopy

At its surface, the rock is composed of calcite. They are doubtless correlated with the fine round grains composed of calcium recorded with SEM-EDS.

In cross-section, quartz and albite were recorded. K-feldspars appear with albite on some spectra indicating the possible presence of perthites.

B.1.4 FTIR spectroscopy

Peaks of quartz mixed with feldspars were recorded at 782, 799, 992 and 1060 $cm^{-1}$. If the doublet 782, 799 $cm^{-1}$ is characteristic of quartz, the other peaks can be attributed to both quartz and feldspars, thus no more detailed interpretation is proposed.

Peaks at 1113, 1162, 1645 and 3629 $cm^{-1}$ are attributed to alumino-silicates. The same peaks were found in amorphous alumino-silica and silica crusts from Canadian rock art sites. They are common peaks found in clay minerals too, the two first being attributed to Si-O stretching, the third to OH deformation of water, and the last one to OH stretching of hydroxyl groups (Madejova and Komadel, 2001). The attribution to clay minerals is the most likely as clay is a common degradation of the Clarens formation sandstone (Johnson *et al.*, 2006).

Finally, calcium oxalates were recorded (Figure B.2).

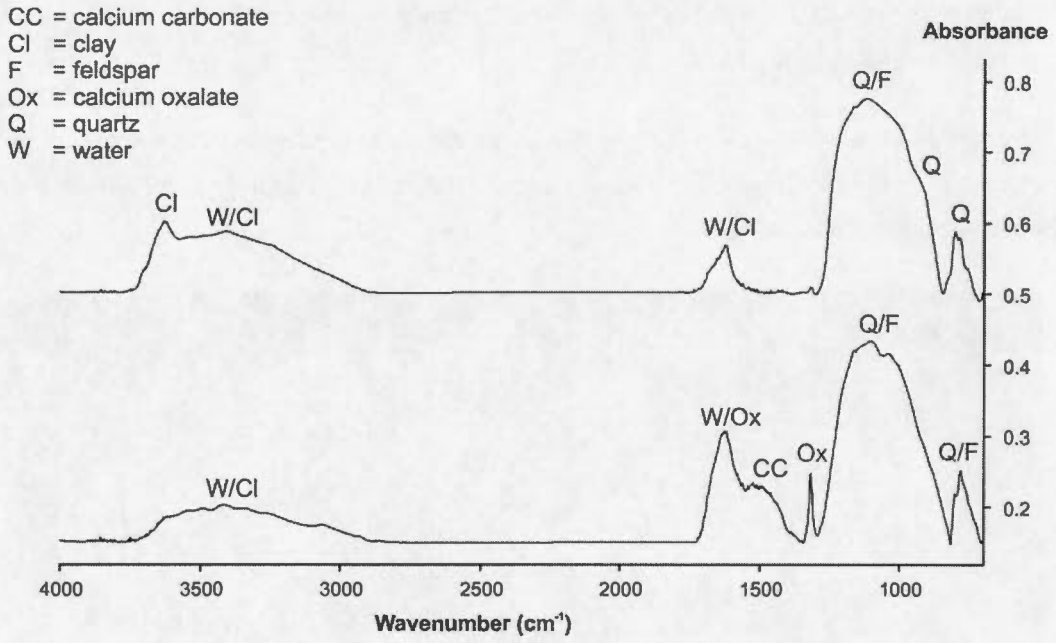


**Figure B.2** FTIR spectra of Maclear rock

### B.1.5 Conclusion

Results are in agreement with the known composition of Clarens formation sandstone. At its surface, weathering products and eolian deposits consist of calcium oxalates, calcite, quartz and feldspars grains, and clay minerals. Minor elements as sodium, magnesium, potassium and iron were recorded without finding their exact mineralogy. They may be part of the feldspars grains and clay minerals, or occur as salts.

No preparation of the rock surface is visible. However, all the paintings were realized on the white weathering crust visible at the surface of the rock and which may act as a preparation layer for the artists.

## B.2 Rock support characterization, Phuthiatsana Valley, Lesotho

### B.2.1 Microscope

At the surface, the rock exhibits a white layer, punctuated of dark red grains (Figure B.3). Underneath, the rock is composed of transparent, white and yellow grains in a white/yellow matrix. The rock is highly friable.

The observations of the rock in cross-section show the presence of grains of almost the same size (about 100 µm) comprised in a yellow matrix. The matrix seems to be more present than in the rock from South Africa.

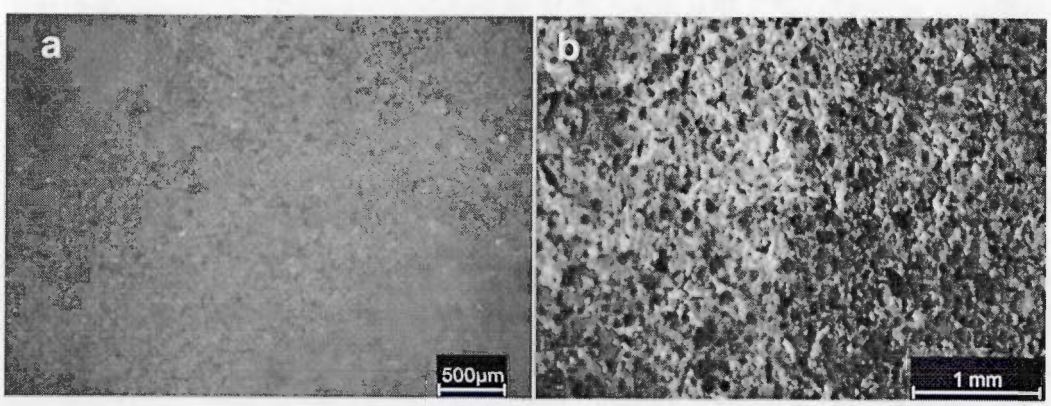


**Figure B.3** Microscopic images of Lesotho rock: a) surface, b) cross-section

### B.2.2 SEM-EDS

At its surface, the rock exhibits a smooth texture with grains from 1 to 50 μm on top. They are of different shapes: round, long, polygons. They are composed of silicon, aluminium, sodium and potassium, for the largest, whereas the smallest are composed of calcium sometimes accompanied of sulphur. Minor elements recorded are magnesium, chlorine, titanium, manganese and iron.

Observations under SEM confirm the ones made with microscope: small grains, about 100 μm, in a matrix composed of calcium. The grains are mostly quartz, potassium feldspars and sodium feldspars. The presence of grains composed of iron and titanium has been recorded.

### B.2.3 Raman spectroscopy

Quartz was the only mineral recorded on both surface and cross-section of the rock. At its surface, the rock exhibits a high fluorescence.

Broad peaks at 1301 and 1601 $cm^{-1}$ found at the surface of the rock may be interpreted as clay minerals.

### B.2.4 FTIR spectroscopy

Quartz and anorthoclase were recorded along with possible peaks of clay. Calcium carbonates were found too (Figure B.4).

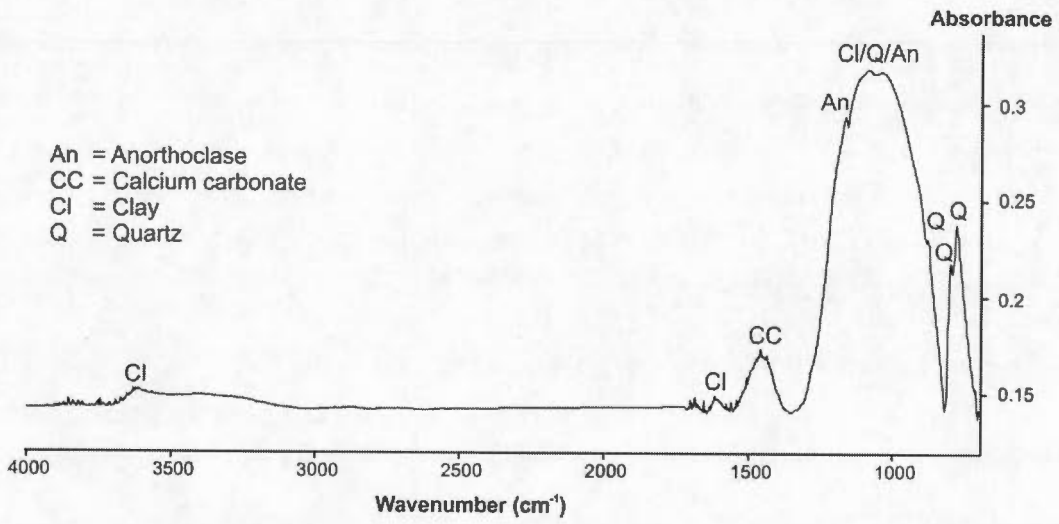


**Figure B.4** FTIR spectrum on Lesotho rock

B.2.5 Conclusion

The rock is composed of quartz, potassium feldspars and sodium feldspars in a calcitic matrix. The presence of calcium sulphates and clay was found at its surface. Minor elements as magnesium, chlorine, titanium, manganese and iron were found mainly at the surface of the rock and are attributed to weathering products.

It is in agreement with the known composition of Clarens formation sandstone and with the composition of the rock from Maclear sites.

B.3 Rock support characterization, Thune Valley, Botswana

B.3.1 Microscope

At the surface, the rock exhibits a black to grey layer at some places. White and orange crusts were observed too. Underneath them, large transparent and white grains are comprised into a red matrix. It is possible that the red matrix turned black because of fires made close to the rock face.

The observations of the rock in cross-section show the presence of grains of almost the same size (about 200 μm) comprised in an orange-red matrix (Figure B.5). The grains are much larger than in the rocks from South Africa and from Lesotho.

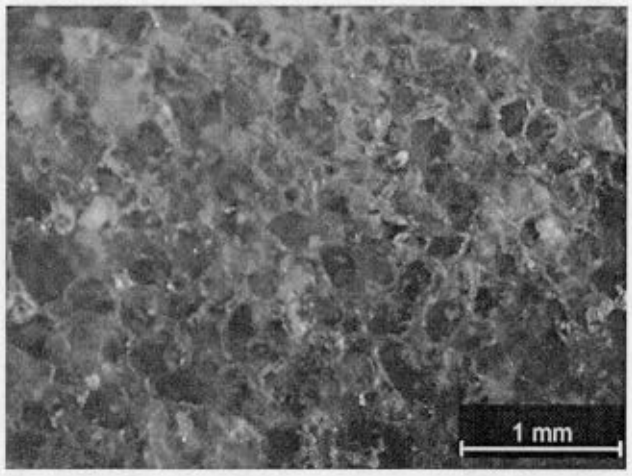


**Figure B.5** Botswana rock in cross-section (microscope with incident light)

B.3.2 SEM-EDS

At its surface, the rock presents a smooth layer with round grains and flakes from 10 to 200 μm diameter. It is composed of magnesium, aluminium, silicon and calcium, with minor elements as phosphorus, sulphur, chlorine, potassium and iron.

In cross-section, the rock is composed of grains from 50 μm to 200 μm diam. They are mostly with a round shape and composed of silicon. The smallest grains are composed of aluminium, silicon and potassium and are identified as K-feldspars whereas the other grains are quartz. No matrix has been identified.

### B.3.3 Raman spectroscopy

At its surface, clay, anhydrite and feroxyhyte were found (Figure B.6).

In cross-section, only peaks of quartz were recorded.

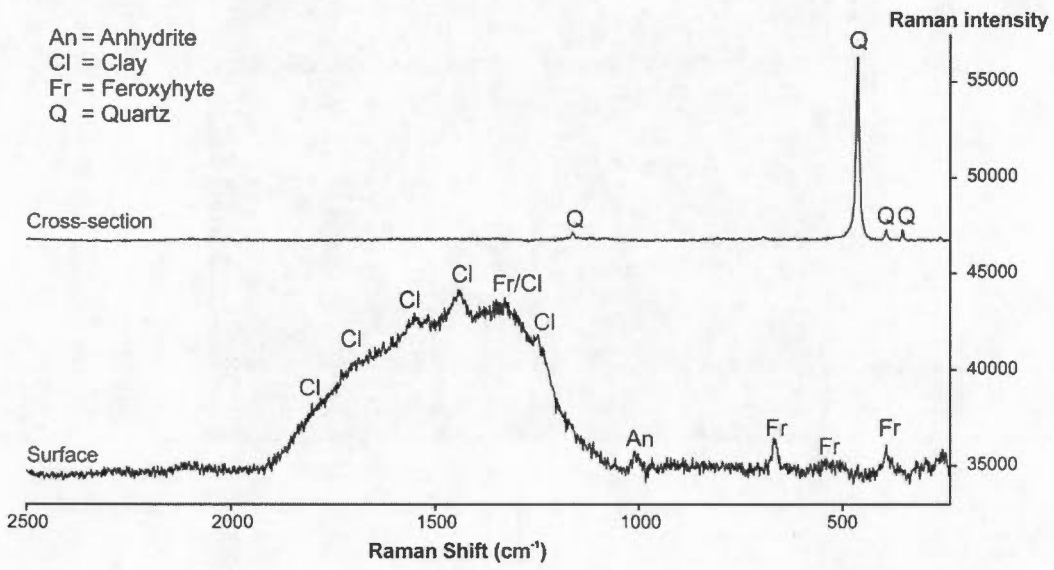


**Figure B.6** Raman spectra recorded on Botswana rock

### B.3.4 FTIR spectroscopy

K-feldspars and quartz were recorded on FTIR spectra from the rock. Peaks at 913, 3621, 3699 $cm^{-1}$ can be attributed to clay which can be found in this sandstone as weathering products (Johnson *et al.*, 2006). Calcite was identified too (Figure B.7).

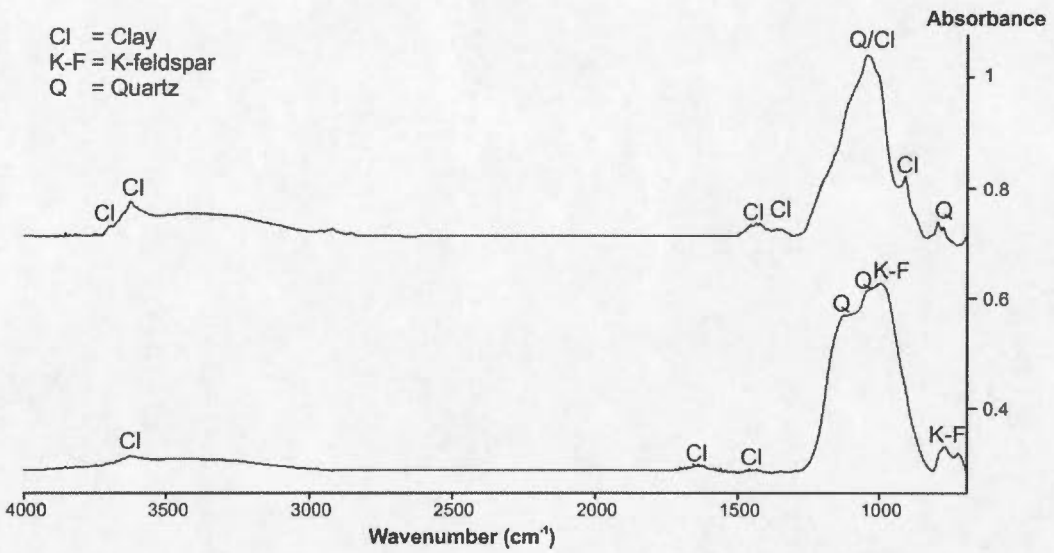


**Figure B.7** FTIR spectrum recorded on Botswana rock

### B.3.5 Conclusion

The rock support of the paints is sandstone composed mostly of quartz and K-feldspars. Calcite and clay were recorded in and on the rock and they can be both weathering products and the matrix of the rock. At its surface, it exhibits a thick white to black layer composed of calcium sulphates and clay, and feroxyhyte (that is to say iron oxide hydroxide under the form $\delta$-$Fe^{3+}O(OH)$).

# APPENDIX C

## TRANSFER FROM LEXSYG TO RISØ: TESTS AND NEW SETTINGS

Due to a break in the Lexsyg instrument which requires long-term fixing at the end of the PhD project, final OSL analyses were transferred to the Risø instrument (details of the instrument are given in chapter II).

The transfer needed to take into account the differences between the two instruments. First, the Lexsyg was running under helium atmosphere whereas the Risø was using nitrogen atmosphere. These two gases have different heat conduction properties, the helium being more conductive than nitrogen. As my protocol was highly dependent of pre-heat temperature, pre-heat tests were first conducted to determine the corresponding temperature to be used. The rock Aral 175 has been selected for these tests. Second, the Risø is equipped with a lamp reproducing sunlight but being about 10 times less powerful than the Lexsyg one. The protocol established with the Lexsyg requires a 15min-bleach after each Ln-Lx and Tn-Tx. Due to the weak power of the lamp, such bleaching could not be done as it requires too much instrument time. Hence, a test was conducted with thermal wash to replace the bleaching step. Results are detailed in the following sections beginning by thermal transfer determination, then dose recovery tests using given doses of 2 and 20 Gy and finally, the adjusted protocol was tested on a core taken from the rock from RSA MEL8, on which painting tests were conducted.

### C.1 Thermal transfer determination

During experimentations detailed in chapter V, the presence of a thermal transfer due to the necessity of pre-heating the sample prior to IRSL recording was found and estimated depending on the pre-heat temperature used. To estimate more precisely its influence and to reduce it, a bleaching step was introduced after each Ln-Lx and Tn-Tx.

However, this step cannot be done with the Risø. To replace this step, a thermal wash was tested. It consisted of an IRSL record at 225°C for 100s. Details of sequences are given in table C.1.

**Table C.1** Thermal transfer sequences (a: without thermal wash, b: with thermal wash)

a

| Step | Treatment |
|---|---|
| 1 | Preheat at 0/50/100/150/200/250°C for 60s |
| 2 | IRSL at 50°C for 100s |
| 3 | Test dose, 1Gy |
| 4 | Preheat at 0/50/100/150/200/250°C for 60s |
| 5 | IRSL at 50°C for 100s |
| 6 | Regenerative dose: 1Gy, 5Gy, 10Gy, 0Gy, 1Gy |
| 7 | Return to step 1 |

b

| Step | Treatment |
|---|---|
| 1 | Preheat at 0/50/100/150/200/250°C for 60s |
| 2 | IRSL at 50°C for 100s |
| 3 | IRSL at 225°C for 100s |
| 4 | Test dose, 1Gy |
| 5 | Preheat at 0/50/100/150/200/250°C for 60s |
| 6 | IRSL at 50°C for 100s |
| 7 | IRSL at 225°C for 100s |
| 8 | Regenerative dose: 1Gy, 5Gy, 10Gy, 0Gy, 1Gy |
| 9 | Return to step 1 |

Results were plotted in figure C.1 with results obtained with the Lexsyg instrument. Comparing thermal transfer with the bleach step on Lexsyg and the one with the thermal wash step on Risø shows similar results for both the intensity and the shape of the curves. A slight shift on pre-heat temperatures is observed and is due to the difference of conductivity

properties of helium and nitrogen. It is estimated to about 10% of the pre-heat temperature set in the sequence. Hence, with a pre-heat of 100°C, the shift is 10°C, whereas it is 20°C with a 200°C pre-heat.

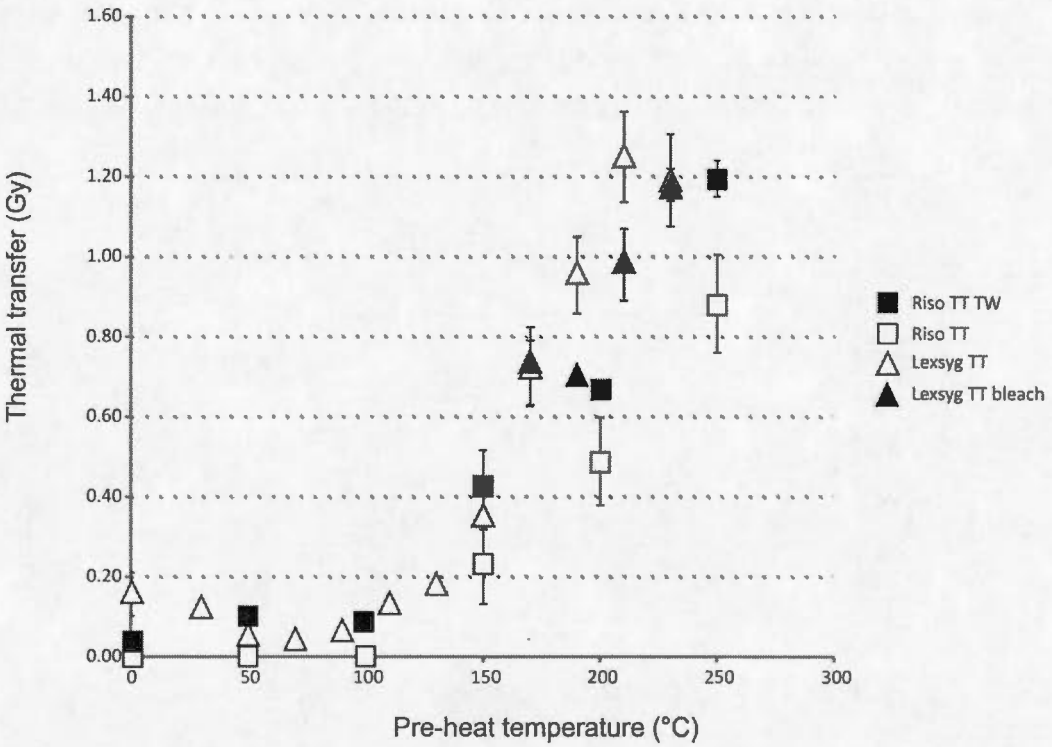


**Figure C.1** Thermal transfer depending on pre-heat temperatures (Lexsyg and Risø)

Results show that a better estimation of the thermal transfer is achieved when using the thermal wash step after each Ln-Lx and Tn-Tx. They are similar to those obtained with Lexsyg using the bleach step.

To confirm that the use of a thermal wash step produces similar results as the bleach step, dose recovery tests at 2 Gy and 20 Gy were then carried out.

## C.2 Dose recovery tests

### C.2.1 Dose recovery: 2 Gy

Dose recovery tests were carried out at different pre-heat temperatures following the same sequences as detailed in Table B.1, but adding a preliminary given dose of 2 Gy. Then ratios between the recovered dose and the given dose were calculated (Figure C.2). Then thermal transfer was subtracted to the recovered dose and the ratio was again calculated (Figure C.3).

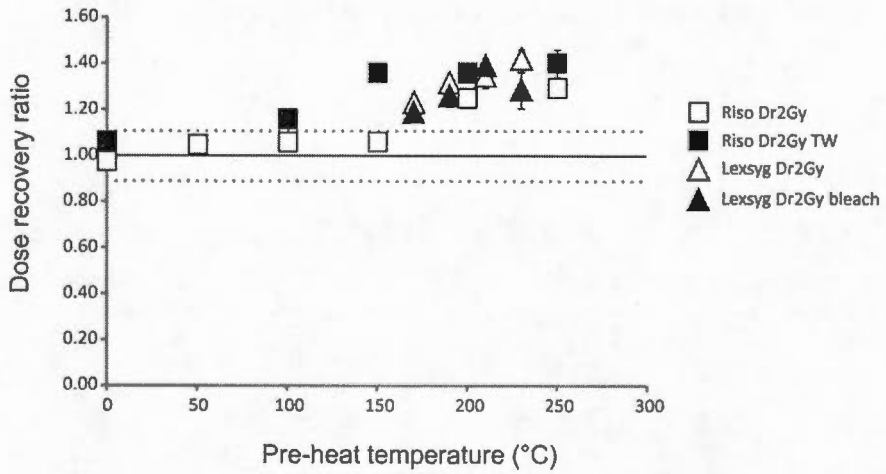


**Figure C.2** Dose recovery ratios (2 Gy, Lexsyg and Risø)

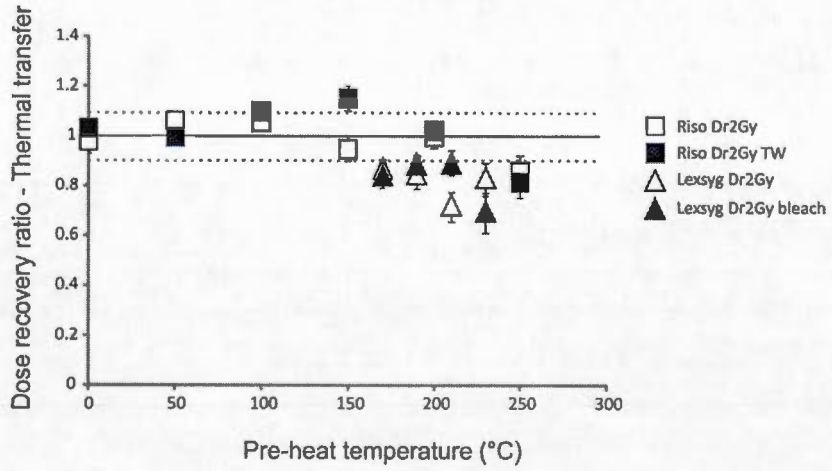


**Figure C.3** Dose recovery ratios (2 Gy, thermal transfer subtracted, Lexsyg and Risø)

Once thermal transfer is subtracted, using the Risø instrument, dose recovery ratios are within the 0.9 to 1.1 range recommended by Murray and Wintle (2000) with a pre-heat temperature of 200°C. Results using the thermal wash step or not are in the same range. However, using thermal wash, the dispersion of results is less.

According to these results, the thermal wash step and a pre-heat temperature of 200°C are thought to be the best parameters to set the Risø. Further tests were conducted on higher given doses.

### C.2.6 Dose recovery: 20 Gy

As demonstrated in chapter V, dose recovery tests using a given dose of 20 Gy were always successful whatever pre-heat temperatures and using or not a bleach step. Hence, they were conducted to confirm that the thermal wash step does not influence the dose determination, whatever high or weak is the initial dose. Sequence used is given in Table C.2.

**Table C.2** Dose recovery test (20 Gy) sequence

| Step | Treatment |
|---|---|
| 1 | Preheat at 0 - 250°C for 60s |
| 2 | IRSL at 50°C for 100s |
| 3 | IRSL at 225°C for 100s |
| 4 | Test dose, 3Gy |
| 5 | Preheat at 0 - 250°C for 60s |
| 6 | IRSL at 50°C for 100s |
| 7 | IRSL at 225°C for 100s |
| 8 | Regenerative dose: 10Gy, 50Gy, 30Gy, 0Gy, 10Gy |
| 9 | Return to step 1 |

Results are presented in Figure C.4. It shows that the dose recovery ratios are within 10% whatever pre-heat temperatures and subtracting or not thermal transfer. Thermal transfer has been estimated to about 0.6 to 1.2 Gy depending on pre-heat temperatures. It represents about

5% of the given dose; hence it does not have a real impact in the dose determination at 20 Gy.

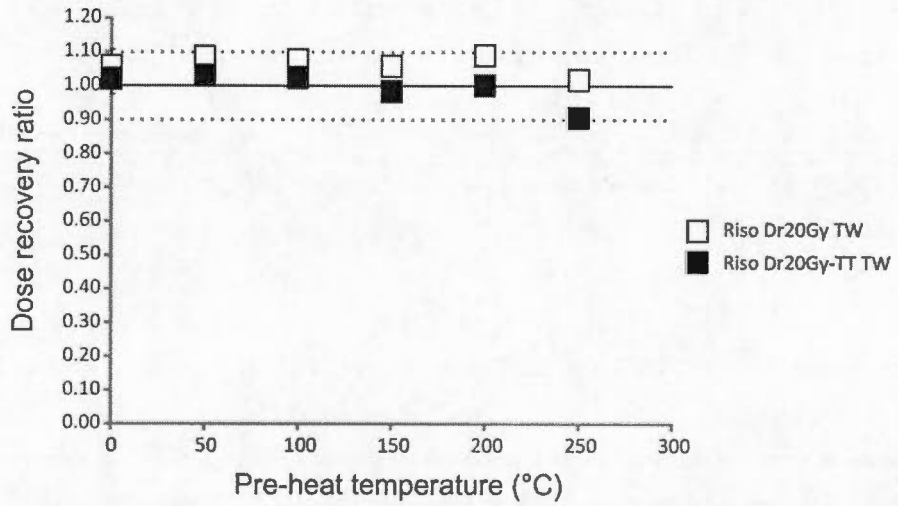


**Figure C.4** Dose recovery ratios (20 Gy) using thermal wash on Risø

These results confirm parameters selected previously: the thermal wash step and a pre-heat temperature of 200°C are thought to be the best parameters to set the Risø. They were then tested on core 3 of rock from RSA MEL8, rock being artificially painted at its surface and exposed to SOLE Lamp.

## C.3 Tests on core 3 of rock from RSA MEL8

Ln-Tn determinations were first conducted on the entire core using the same sequence as previously used with Lexsyg (§5.3.2.1) but replacing the bleach step by the thermal wash step and using a pre-heat temperature of 200°C (Figure C.5). Then, sequences to calculate equivalent doses were conducted once again using the Lexsyg sequences but replacing bleaching step and pre-heat temperatures (Figure C.6).

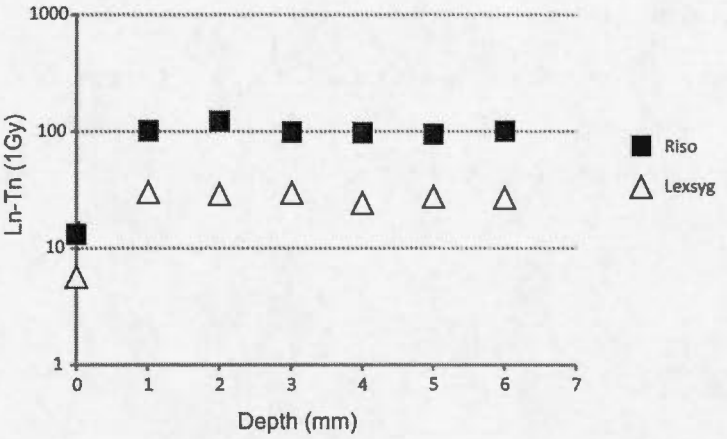


**Figure C.5** Ln-Tn determination of core 3 of rock form RSA MEL8 with Lexsyg and Risø

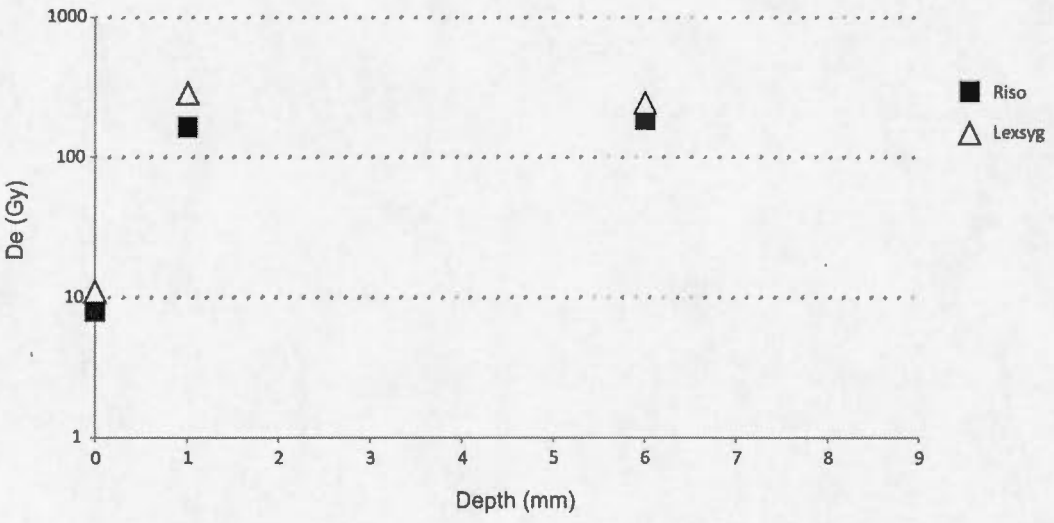


**Figure C.6** Equivalent dose determination of three slices of core 3 of rock from RSA MEL8 (Lexsyg and Risø)

Ln-Tn profile results show a slightly higher ratio for the entire core but the shape of the profile stays the same. When comparing equivalent doses determinations, they all fall in the same range. Moreover, the recovered dose underneath the paint layer is again about 5% of the initial dose.

## C.4 Conclusion on the transfer

Using these results, it is possible to conclude that a transfer can be done from Lexsyg to Risø adjusting the sequence used: pre-heat temperature is set at 200°C and the bleach step after each Ln-Lx and Tn-Tx is replaced by a thermal wash step consisting of an IRSL recording at 225°C for 100s.

# APPENDIX D

## BAYESIAN MODELLING DETAILS AND SETTINGS

In this section, details and settings are given for the Bayesian models presented in this thesis.

### D.1 Software settings

Bayesian modelling was conducted using OxCal online (https://c14.arch.ox.ac.uk/oxcal/OxCal.html ). Models were constructed as a sequence in which continuous phases were added. In each of these phases, radiocarbon dates were included.

Outlier constraints were added to the entire sequence and to each date. For the sequence, an outlier model was used with a distribution of T(5), i.e. "this assumes that the outliers are in the time dimension (for example samples deposited at a time other than that of their formation), and are assumed to be distributed according to a student T distribution with 5 degrees of freedom (a long tailed distribution more suitable than a Normal distribution for outliers" (Bronk Ramsey, 2009), and a magnitude distribution of U(0,4), i.e. "the scale is allowed to lie anywhere between $10^0$ to $10^4$ years" (Bronk Ramsey, 2009). For each date, an outlier command has been added to "flag a measurement as a definite outlier and remove it from the model" (Bronk Ramsey, 2009). It has been set at 0.05 or 5%.

The calibration curve selected in ShCal13, as dates were obtained on sites from the South Hemisphere.

It results in the model code presented in Figure D.1. It is then run in the OxCal software online.

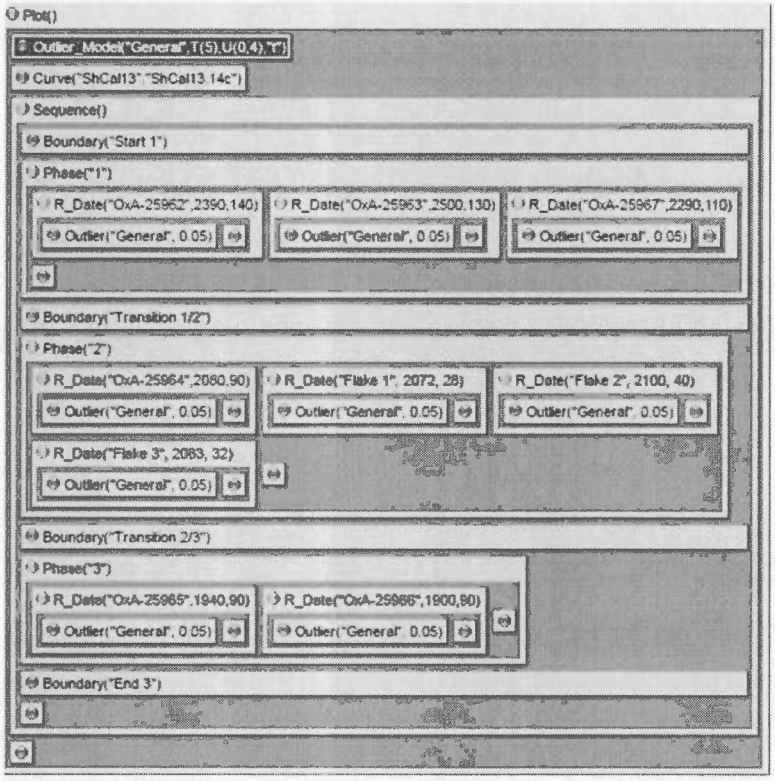


**Figure D.1** Example of the construction of a Bayesian model used in this thesis

## D.2 Archaeological constraints given to the models

Firstly, constraints were given according to the dates obtained. They can be roughly arranged to make a preliminary chronology of a site or a region. Then they are confronted to superpositions of paintings observed by the archaeologists. Hence a painting on top of another will be assumed to have been created after the one underneath it. Phases result of these observations.

However, superpositions are not present on all the sites and they may be confused. Bayesian models were used to estimate the probability that one representation would be younger than another and thus corroborate or not archaeological interpretations. For this step, the outlier commands on each date offered the possibility to track dates which do not fit with the model

and rearrange them. However, different models have the same probability and it results in different possible scenarios.

Finally, models were constrained by archaeological evidence of the presence of San groups in the area. It was especially the case for the Metolong catchment since San hunter-gatherers were absent from it after the end of the 1830's (Vinnicombe, 1976; Arthur and Mitchell, 2010).

### D.3 Interpretations of the results

Results from the models are firstly evaluated using the two diagnostic measures given by OxCal:

- The agreement indices: a measure of the agreement between the model (prior) and the observational data (likelihood). They should be over 60%
- The convergence integral: a test of the effectiveness of the Monte-Carlo-Monte-Carlo algorithm. It should be over 95%.

Then, outlier models and commands give flag on potential outliers in the model. It makes it possible to correct the model and then run it again to adjust the sequence of phases. If all flags are green, the model is used for the interpretation of the site.

# APPENDIX E

## SUPPLEMENTARY ONLINE INFORMATION FOR "PIGMENT CHARACTERIZATION AS AN ALTERNATIVE TO INTERPRET ROCK ART SITES WHEN DATING METHODS FAIL: THE CASE OF THE MIKINAK SITE, LAKE WAPIZAGONKE, QUEBEC, CANADA"

### E.1 OSL preparation and experimental details

As the OSL signal is light sensitive, all the preparation process has to be carried out under red light.

Two rocks collected on the banks of the Lake Wapizagonke were prepared to test the suitability for OSL dating of quartz composing the rock support of the paintings. About 1 cm of the surface of the rocks was retrieved, and the rest was ground in an agate mortar. The samples were acidified with hydrochloric acid (HCl) at 10% for 1 hour in order to dissolve calcium carbonates and other weathering products, followed by three distilled water cleanings and one methanol cleaning. Samples were left to dry at room temperature overnight. Sieving was subsequently undertaken and the fraction between 150-250 μm was selected. Samples were then acidified with hydrofluoric acid (HF) at 10% for 15 minutes, cleaned three times with distilled water, acidified again with HF 45% for 45 minutes, cleaned three times with distilled water, acidified with HCl 10% for 30 minutes to remove calcium and fluorine ions liberated by the HF acidification, cleaned three times with distilled water and finally cleaned once with methanol.

Once dried, they were mounted on aluminium discs for OSL recording. Samples were analysed using a Lexsyg system (Richter et al., 2013), with blue LED stimulation, under helium atmosphere. The luminescence was filtered with a combination of two filters and detected with a photomultiplier. Data were treated using Analyst and Excel.

To test the suitability of quartz, an Ln-Tn sequence was applied (Table E.1).

**Table E.1** Ln-Tn sequence used for quartz sensitivity

| Step | Treatment |
|---|---|
| 1 | Preheat 240°C for 10s |
| 2 | IRSL at 50°C for 100s |
| 3 | OSL at 110°C for 40s |
| 4 | Test dose, 20Gy |
| 5 | Preheat 160°C for 10s |
| 6 | IRSL at 50°C for 100s |
| 7 | OSL at 110°C for 40s |

No OSL signal was recorded (Figure E.1). A second test was carried out by giving to the natural quartz sample an added dose of 2000Gy. No OSL signal was recorded either.

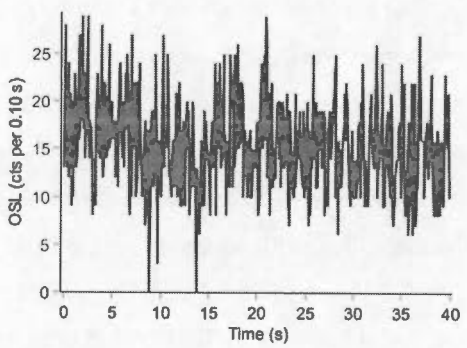


**Figure E.1** Example of OSL signal recorded for Lake Wapizagonke quartz

E.2 Supplementary figures and photos

We would like to include the following figures and photos to complete our article.


**Figure E.2** Painting panel at *Mikinak* Site


**Figure E.3** Painted fragments collected in 1985 (Parks Canada)

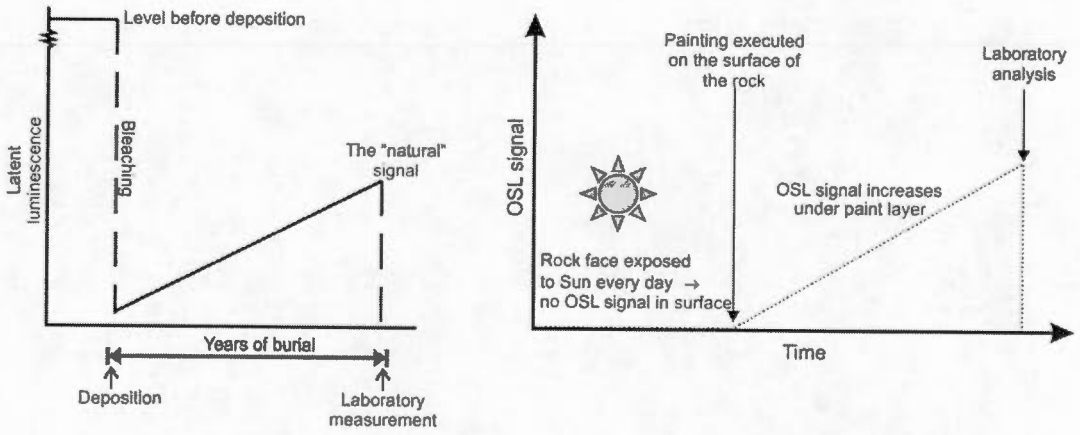


**Figure E.4** Common OSL hypothesis (left) and OSL hypothesis of this study (right)

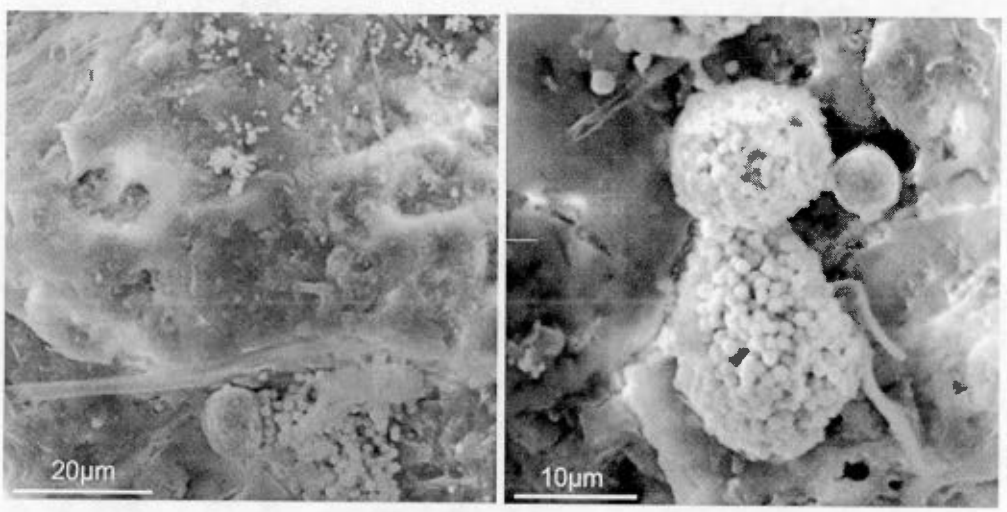


**Figure E.5** Small balls observed on 25M1A1-1 (SEM secondary electron image)

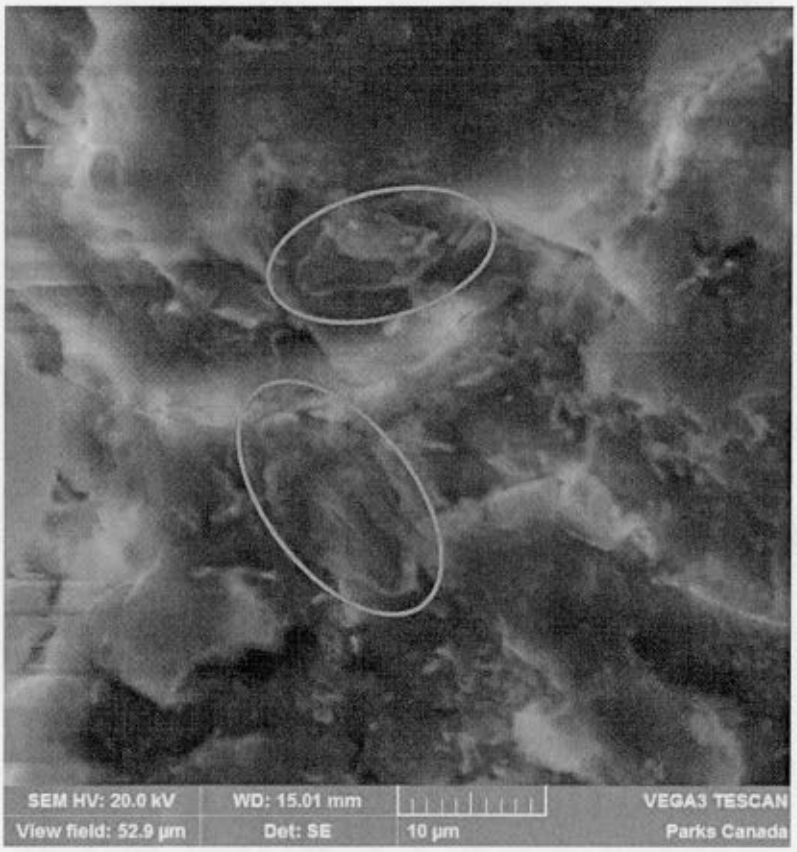


**Figure E.6** Diatoms in the silica crusts

## E.3 Bibliography

Richter, D., Richter, A. et Dornich, K. (2013). Lexsyg — A new system for luminescence research. *Geochronometria, 40*(4), 220-228.

# APPENDIX F

## A NOTE ON THE SAN NAME ORTHOGRAPHY

Many of the San words used in this thesis are spelled with symbols. They represent the clicks that are a distinctive feature of the Khoisan languages. The descriptions of these sounds are taken from Lewis-Williams and Pearce (2004).

/ (*Dental click*). The tip of the tongue is placed against the back of the upper front teeth; in the release, it is pulled away with a fricative sound.

! (*Alveolar-palatal click*). The tip of the tongue is pressed firmly against the back of the alveolar ridge where it meets the hard palate and is snapped down very sharply on release. A loud pop results.

≠ (*Alveolar click*). The front part of the tongue, more than the tip, is pressed against the alveolar ridge and drawn sharply downward when released.

/ / (*Lateral click*). The tongue is placed as for the alveolar click. It is released at the sides by being drawn in from the teeth. Drivers of horses sometimes use lateral clicks to encourage their steeds to start or go faster.

ʘ (*Labial click*). The frontal closure is made with pursed lips; when the lips are released, the sound is like a kiss. This click is found only in southern San languages.

X is a guttural sound as in the Scottish *loch*.

# APPENDIX G

## GENERAL MAP

The following map is given to localise the different sites and places mentioned in this PhD. Points which locate two or three sites are accordingly larger.

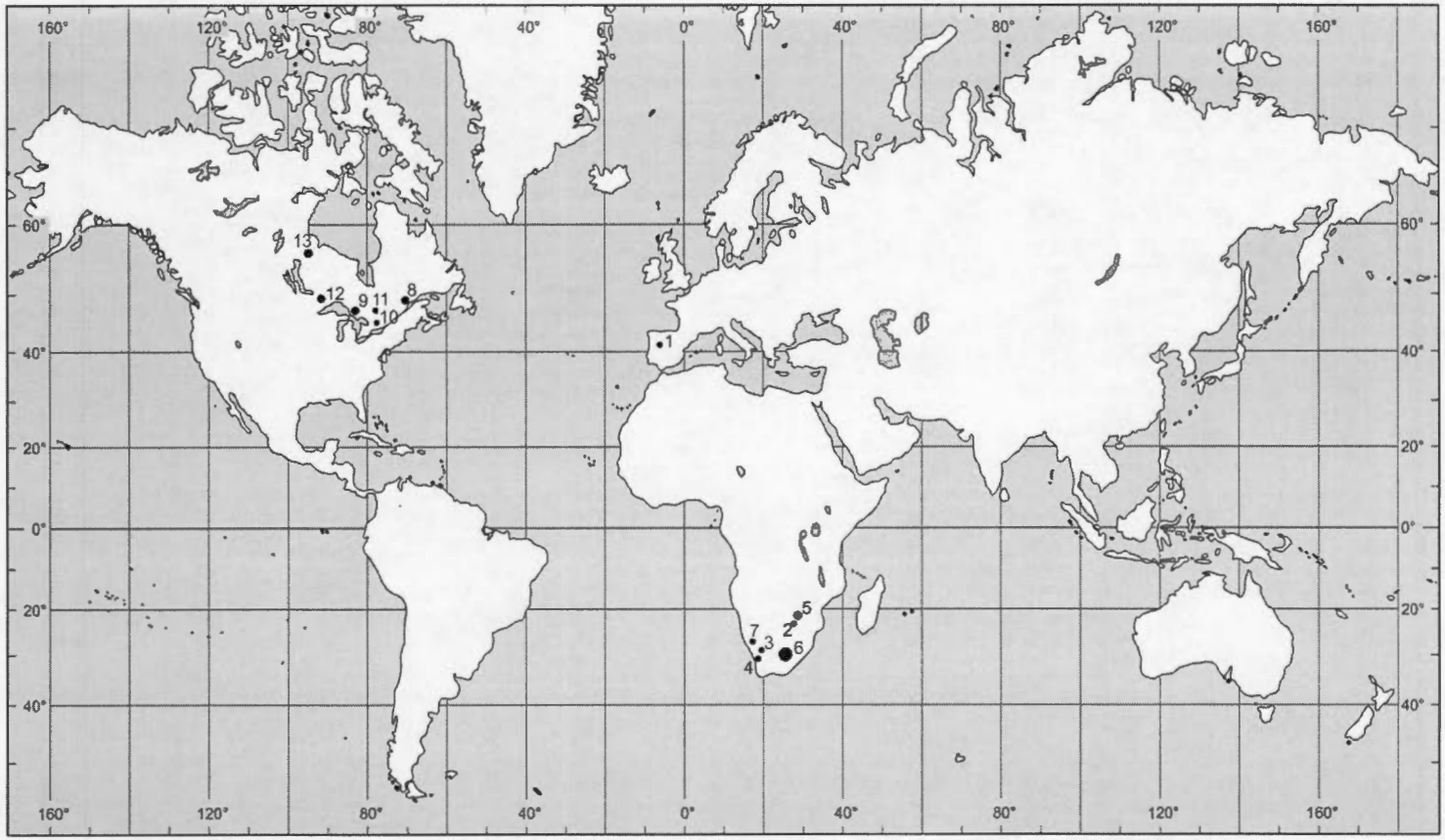


1 : Côa Valley, Portugal
2 : Wonderkrater, South Africa
3 : Sonia's Cave Upper, South Africa
4 : Steenbokfontein Cave, South Africa
5 : Limpopo River, South Africa
: Makgabeng, South Africa
6 : Phuthi, South Africa
: Lundean's Nek Area, Nqabayo, SA
: Mdwebo, South Africa
7 : Apollo 11 Shelter, Namibia
8 : Cassette Lake, Qc, Canada
: Nisula site, Qc, Canada
9 : Sault Ste Marie, On, Canada
: Agawa Rock, On, Canada
10 : Peterborough, On, Canada
11 : Hell's door, On, Canada
12 : Cuttle Lake, On, Canada
: Lake of the Painted Cave, On, Canada
13 : Oxford House Area, MB, Canada
: Moose Pictograph Site, MB, Canada

# APPENDIX H

## ANALYSIS CATALOG

The analysis catalog is given as a numeric file, to be found in the CD attached to this manuscript.

# BIBLIOGRAPHY


Acosta-Maeda, T.E., Scott, E.R.D., Sharma, S.K. and Misra, A.K. (2013). The pressures and temperatures of meteorite impact: Evidence from micro-Raman mapping of mineral phases in the strongly shocked Taiban ordinary chondrite. *American Mineralogist*, 98(5-6), 859-869.

Adamiec, G. and Aitken, M.J. (1998). Dose-rate conversion factors: update. Ancient *Thermoluminescence*, 16(2), 37-50.

Aitken, M.J. (1985). *Thermoluminescence dating*. London : London Academic Press.

Aitken, M.J. (1998). *An introduction to optical dating : the dating of quaternary sediments by the use of photon-stimulated luminescence*. Oxford : Oxford Oxford University Press.

Arias, P., Laval, E., Menu, M., Sainz, C.G. and Ontañón, R. (2011). Les colorants dans l'art pariétal et mobilier paléolithique de La Garma (Cantabrie, Espagne). *L'Anthropologie*, 115(3–4), 425-445.

Armitage, R.A., Brady, J.E., Cobb, A., Southon, J.R. and Rowe, M.W. (2001). Mass Spectrometric Radiocarbon Dates from Three Rock Paintings of Known Age. American *Antiquity*, 66(3), 471-480.

Arocena, J.M., Hall, K. and Meiklejohn, I. (2008). Minerals provide tints and possible binder/extender in pigments in san rock paintings (South Africa). *Geoarchaeology*, 23(2), 293-304.

Arsenault, D. and Gagnon, L. (2001). *Site rupestre à tracés digitaux du lac Wapizagonke 2000-2001 : réexamen du site rupestre CdFg-5 et évaluation de ses conditions hivernales de conservation, lac Wapizagonke, parc national de la Mauricie*, rapport final. Université Laval, Projet PETRARQ. Sainte-Foy, Québec.

Arsenault, D. (2004). From natural settings to spiritual places in the Algonquian sacred landscape. An archaeological, ethnohistorical, and ethnographic analysis of Canadian Shield

rock-art sites. In Chippindale, C. and Nash, G. (dir.), *The Figured Landscapes of Rock Art. Looking at Pictures in Place* (p. 289-317), Cambridge and New York: Cambridge University Press.

Arsenault, D. and Zawadzka, D. (2013). Canadian rock art specificities. In Gillette, D. L., Greer, M., Hayward, M. H. and Murray, W. B. (dir.), *Rock art and sacred landscapes* (p. 117-137). London and New York : Springer.

Arthur, C. and Mitchell, P.J. (2010). *Metolong Cultural Resource Management Phase 2 Report*. Oxford : St Hugh's College, University of Oxford.

Arthur, C., Mitchell, P.J. and Mallen, L. (2010). *Metolong Cultural Resource Management, Phase 2, Rock Art Recording and Interpretation*. Oxford : School of Archaeology, University of Oxford.

Aubert, M., Watchman, A., Arsenault, D. and Gagnon, L. (2004). L'archéologie rupestre du Bouclier canadien: Potentiel archéométrique. *Canadian Journal of Archaeology*, 28(1), 51-74.

Baes, A.U. and Bloom, P.R. (1989). Diffuse Reflectance and Transmission Fourier Transform Infrared (DRIFT) Spectroscopy of Humic and Fulvic Acids. *Soil Science Society of America Journal*, 53(3), 695-700.

Barham, L. (2002). Systematic Pigment Use in the Middle Pleistocene of South-Central Africa. *Current Anthropology*, 43(1), 181-190.

Barré, M., Lamothe, M., Backwell, L. et McCarthy, T. (2012). Optical dating of quartz and feldspars: A comparative study from Wonderkrater, a Middle Stone Age site of South Africa. *Quaternary Geochronology, 10*, 374-379.

Basedow, H. (1914). Aboriginal Rock Carvings of Great Antiquity in South Australia. *The Journal of the Royal Anthropological Institute of Great Britain and Ireland*, 44, 195-211.

Beck, L., Rousselière, H., Castaing, J., Duran, A., Lebon, M., Moignard, B. and Plassard, F. (2014). First use of portable system coupling X-ray diffraction and X-ray fluorescence for in-situ analysis of prehistoric rock art. *Talanta*, 129(0), 459-464.

Bednarik, R.G. (1995). The Coa petroglyphs: An obituary to the stylistic dating of Palaeolithic rock-art. *Antiquity*, 69(266), 877-883.

Bednarik, R.G. (1996). Only time will tell: a review of the methodology of direct rock art dating. *Archaeometry*, 38(1), 1-13.

Bednarik, R.G. (2002). The dating of rock art: A critique. *Journal of Archaeological Science*, 29(11), 1213-1233.

Béland, J. (1959). Peintures et outils en pierre indiens au lac Wapizagonké. *Le Naturaliste Canadien*, 86(22), 46-52.

Blundell, G. (2004). *Nqabayo's Nomansland: San Rock Art and the Somatic Past*. PhD Thesis, African and Comparative Archaeology, Department of Archaeology and Ancient History, Uppsala University.

Blundell, G. and Lewis-Williams, J.D. (2001). Storm Shelter: a rock art discovery in South Africa. *South African Journal of Science*, 97, 1-4.

Bonneau, A., Brock, F., Higham, T., Pearce, D.G. and Pollard, A.M. (2011). An improved pretreatment protocol for radiocarbon dating black pigments in San rock art. *Radiocarbon*, 53(3), 419-428.

Bonneau, A., Pearce, D.G., Mitchell, P.J., Arthur, C., Higham, T., Lamothe, M. and Arsenault, D. (2014). Comparing painting pigments and subjects: the case of white paints at the Metolong Dam (Lesotho). In *Proceedings of the 39th International Symposium for Archaeometry, Leuven (2012)*. Centre for Archaeological Sciences, Catholic University of Leuven, Leuven, 319-323.

Bonneau, A., Pearce, D.G. and Pollard, A.M. (2012). A multi-technique characterization and provenance study of the pigments used in San rock art, South Africa. *Journal of Archaeological Science*, 39(2), 287-294.

Bourgeois, G. and Marquet, J.-C. (1992). Des traces de graisses animales sur le site néolithique final du Petit Paulmy à Abilly (Indre-et-Loire). *Bulletin de la Société préhistorique française*, 89(2), 47-49.

Brock, F., Higham, T., Ditchfield, P. and Bronk Ramsey, C. (2010). Current pretreatment methods for AMS radiocarbon dating at the Oxford radiocarbon Accelerator Unit (ORAU). *Radiocarbon*, 52(1), 103-112.

Bronk Ramsey, C., Higham, T. and Leach, P. (2004). Towards high-precision AMS: progress and limitations. *Radiocarbon*, 46(1), 17-24.

Bronk Ramsey, C. (2009). Bayesian analysis of radiocarbon dates. *Radiocarbon, 51*(1), 337-360.

Chaffee, S.D., Hyman, M., Rowe, M.W., Coulam, N.J., Schroedl, A. and Hogue, K. (1994). Radiocarbon Dates on the All American Man Pictograph. *American Antiquity*, 59(4), 769-781.

Chapot, M.S., Sohbati, R., Murray, A.S., Pederson, J.L. and Rittenour, T.M. (2012). Constraining the age of rock art by dating a rockfall event using sediment and rock-surface luminescence dating techniques. *Quaternary Geochronology*, 13, 18-25.

Chen, J., Blume, H.-P. and Beyer, L. (2000). Weathering of rocks induced by lichen colonization — a review. *Catena*, 39(2), 121-146.

Clottes, J., Menu, M. and Walter, P. (1990). La préparation des peintures magdaléniennes des cavernes ariégeoises. *Bulletin de la Société préhistorique française*, 87(6), 170-192.

Coccato, A., Jehlicka, J., Moens, L. and Vandenabeele, P. (2015). Raman spectroscopy for the investigation of carbon-based black pigments. *Journal of Raman Spectroscopy*, in press.

Coentro, S., Mimoso, J.M., Lima, A.M., Silva, A.S., Pais, A.N. and Muralha, V.S.F. (2012). Multi-analytical identification of pigments and pigment mixtures used in 17th century Portuguese azulejos. *Journal of the European Ceramic Society*, 32(1), 37-48.

Colomban, P., Cherifi, S. and Despert, G. (2008). Raman identification of corrosion products on automotive galvanized steel sheets. *Journal of Raman Spectroscopy*, 39(7), 881-886.

Cornell, R.M. and Schwertmann, U. (2003). *The iron oxides structure, properties, reactions, occurrences, and uses*. Weinheim : Wiley-VCH.

Corrado, G., Sanchez-Cortes, S., Francioso, O. and Garcia-Ramos, J.V. (2008). Surface-enhanced Raman and fluorescence joint analysis of soil humic acids. *Analytica Chimica Acta*, 616(1), 69-77.

Dagneau, C. (2010). *Expertise archéologique subaquatique du site rupestre du lac Wapizagonke (CdFg-5), 2010*. Parks Canada.

Dayet, L. (2012). *Matériaux, transformations et fonctions de l'ocre au Middle Stone Age le cas de Diepkloof Rock Shelter dans le contexte de l'Afrique australe*. (PhD Thesis). Université Bordeaux III.

de Faria, D.L.A. and Lopes, F.N. (2007). Heated goethite and natural hematite: Can Raman spectroscopy be used to differentiate them?, *Vibrational Spectroscopy*, 45(2), 117-121.

Dee, M. and Bronk Ramsey, C. (2000). Refinement of graphite target production at ORAU. *Nuclear Instruments and Methods in Physics Research Section B: Beam Interactions with Materials and Atoms*, 172(1–4), 449-453.

Denninger, E. (1971). The use of paper chromatography to determine the age of albuminous binders and its applications to rock paintings. *South African Journal of Science*, Supplement to the Special Issue 2, 80-84.

Desrochers, A. (2011). *Minéralogie de la paroi rocheuse au site rupestre du Lac Wapizagonke, Parc national du Canada de la Mauricie, Québec*. Parks Canada.

Dewdney, S. and Kidd, K.E. (1967). *Indian rock paintings of the Great Lakes*. (Second ed.). Toronto: published for the Quetico Foundation by University of Toronto Press.

Directorate of Overseas Surveys (1982), Geological map of Lesotho, North sheet: Department of Mines and Geology, Scale 1:250 000.

Dowson, T.A. (2007). Debating Shamanism in Southern African Rock Art: Time to Move on. *The South African Archaeological Bulletin*, 62(185), 49-61.

Du Toit, A.L. (1939). *The Geology of South Afric*a. Edinburg : Oliver and Boyd.

Duller, G.A.T. (1997). Behavioural studies of stimulated luminescence from feldspars. *Radiation Measurements*, 27(5–6), 663-694.

Duller, G.A.T. (2008). *Luminescence dating guidelines on using luminescence dating in archaeology*. Swindow : English Heritage.

Eastaugh, N. (2008). *Pigment compendium : a dictionary and optical microscopy of historical pigments*. Oxford : Butterworth-Heinemann.

Eriksson, P.G. (1979). *A Paleoenvironmental Study of the Clarens Formation in the Natal Drakensberg Escarpment*. University of Natal, Pietermaritzburg. Master thesis.

Evershed, R.P., Heron, C. and Goad, L.J. (1990). Analysis of Organic Residues of Archaeological Origin by High-temperature Gas Chromatography and Gas Chromatography Mass Spectrometry. *Analyst*, 115(10), 1339-1342.

Fensome, R., Williams, G., Achab, A., Clague, J., Corrigan, D., Monger, J. et Nowlan, G. (2014). *Four billion years and counting: Canada's geological heritage*. Halifax, Nova Scotia: Canadian Federation of Earth Sciences and Nimbus Publishing.

FM Associates and Southern Waters (2008). *Metolong Dam Environmental and Social Impact Assessment*. World Bank.

Ford, B., MacLeod, I. and Haydock, P. (1994). Rock Art Pigments from Kimberley Region of Western Australia: Identification of the Minerals and Conversion Mechanisms. *Studies in Conservation*, 39(1), 57-69.

Forget Brisson, L., Lamothe, M., Huot, S., Hardy, F. and Chapdelaine, C. (2015). Optical dating of St. Lawrence Iroquoian ceramics from the Mailhot-Curran site, southern Québec. *Quaternary Geochronology*, 1-6.

Freiesleben, T. (2014). *Developing a mathematical model to describe multiple daylight exposure and burial events for rocks and developing a preparation method for rock samples for Optically Stimulated Luminescence Dating*. Roskilde University & The Nordic Centre for Luminescence Reseach. Master thesis.

Freiesleben, T., Sohbati, R., Murray, A., Jain, M., al Khasawneh, S., Hvidt, S. and Jakobsen, B. (2015). Mathematical model quantifies multiple daylight exposure and burial events for rock surfaces using luminescence dating. *Radiation Measurements*, In press.

Galli, A., Martini, M., Maspero, F., Panzeri, L. and Sibilia, E. (2014). Surface dating of bricks, an application of luminescence techniques. *The European Physical Journal Plus*, 129(5), 1-9.

Garate, D., Laval, É. and Menu, M. (2004). Étude de la matière colorante de la grotte d'Arenaza (Galdames, Pays Basque, Espagne). *L'Anthropologie*, 108(2), 251-289.

Geological Survey Department (1966). *Annual report of the Geological Survey Department*. Lobatse : Ministry of Commerce, Industry and Water Affairs.

Geological Survey and Mines Department (1973), Geological map of Botswana: Director of Geological Survey and Mines, Scale 1:1 000 000.

Gillespie, R. (1997). On human blood, rock art and calcium oxalate: Further studies on organic carbon content and radiocarbon age of materials relating to Australian rock art. *Antiquity*, 71(272), 430-437.

Godfrey-Smith, D.I., Huntley, D.J. and Chen, W.H. (1988). Optical dating studies of quartz and feldspar sediment extracts. *Quaternary Science Reviews*, 7(3–4), 373-380.

Gosse, J.C. and Phillips, F.M. (2001). Terrestrial in situ cosmogenic nuclides: theory and application. *Quaternary Science Reviews*, 20(14), 1475-1560.

Grant, C. (1984). *L'art rupestre des indiens de l'Amérique du Nord.* (Dutard, D., Trad.). Milan : Jaca Book Milan.

Guo, Y. and Bustin, R.M. (1998). FTIR spectroscopy and reflectance of modern charcoals and fungal decayed woods: implications for studies of inertinite in coals. *International Journal of Coal Geology*, 37(1–2), 29-53.

Hall, K., Meiklejohn, I. and Arocena, J. (2007). The thermal responses of rock art pigments: Implications for rock art weathering in southern Africa. *Geomorphology*, 91(1–2), 132-145.

Hall, K., Meiklejohn, I., Sumner, P. and Arocena, J. (2010). Light penetration into Clarens sandstone and implications for deterioration of San rock art. *Geoarchaeology*, 25(1), 122-136.

Hamayon, R.N. (2006). L'idée de « contact direct avec des esprits » et ses contraintes d'après l'exemple de sociétés sibériennes. *Afrique & histoire*, 6(2), 13-39.

Harris, E.C. (1975). The Stratigraphic Sequence: A Question of Time. *World Archaeology*, 7(1), 109-121.

Hedges, R.E.M., Ramsey, C.B., Van Klinken, G.J., Pettitt, P.B., Nielsen-Marsh, C., Etchegoyen, A., Niello, J.O.F., Boschin, M.T. and Llamazares, A.M. (1998). Methodological issues in the C-14 dating of rock paintings. *Radiocarbon*, 40(1), 35-44.

Helwig, K. (2011). *Analyse d'échantillons du site rupestre du lac Wipizagonke* (CdFg-5). Canadian Conservation Institute.

Henshilwood, C.S., d'Errico, F. and Watts, I. (2009). Engraved ochres from the Middle Stone Age levels at Blombos Cave, South Africa. *Journal of Human Evolution*, 57(1), 27-47.

Hoerlé, S. (2005). A preliminary study of the weathering activity at the rock art site of Game Pass Shelter (KwaZulu-Natal, South Africa) in relation to its conservation. *South African Journal of Geology*, 108(2), 297-308.

Hoerlé, S., Pearce, D., Bertrand, L., Sandt, Ch. and Menu, M. (2016). Imaging the layered fabric of paints from Nomansland rock art (South Africa). *Archaeometry*, in press.

Hogg, A.G., Hua, Q., Blackwell, P.G., Niu, M., Buck, C.E., Guilderson, T.P., Heaton, T.J., Palmer, J.G., Reimer, P.J. and Reimer, R.W. (2013). SHCal13 Southern Hemisphere calibration, 0–50,000 cal yr BP. *Radiocarbon*, 55(4), 1889–1903.

Hughes, J.C. and Solomon, A. (2000). A preliminary study of ochres and pigmentaceous materials from KwaZulu-Natal, South Africa : towards an understanding of San pigment and paint use. *Southern African Humanities*, 12, 15-31.

Huntley, D.J., Godfrey-Smith, D.I. and Thewalt, M.L.W. (1985). Optical dating of sediments. *Nature*, 313(5998), 105-107.

Huntley, D.J. and Lamothe, M. (2001). Ubiquity of anomalous fading in K-feldspars and the measurement and correction for it in optical dating. *Canadian Journal of Earth Sciences*, 38(7), 1093-1106.

Huntley, J., Aubert, M., Ross, J., Brand, H.E.A. and Morwood, M.J. (2015). One Colour, (at Least) Two Minerals: A Study of Mulberry Rock Art Pigment and a Mulberry Pigment 'Quarry' from the Kimberley, Northern Australia. *Archaeometry*, 57(1), 77-99.

Huwiler, K. (1972). More light on rock paintings. *Rhodesian Prehistory*, 8, 3-6.

Huyge, D., Aubert, M., Barnard, H., Claes, W., Darnell, J.C., De Dapper, M., Figari, E., Ikram, S., Lebrun-Nélis, A. and Therasse, I. (2007). Lascaux along the Nile': Late Pleistocene rock art in Egypt. *Antiquity*, 81(313), 1-4.

Jerardino, A. and Swanepoel, N. (1999). Painted slabs from Steenbokfontein Cave: The oldest known parietal art in Southern Africa. *Current Anthropology*, 40(4), 542-548.

Johnson, M.R., Van Vuuren, C.J., Hegenberger, W.F., Key, R. and Show, U. (1996). Stratigraphy of the Karoo Supergroup in southern Africa: an overview. *Journal of African Earth Sciences*, 23(1), 3-15.

Johnson, M.R., van Vuuren, C.J., Visser, J.N.J., Cole, D.I., Wickens, H.d.V., Christie, A.D.M., Roberts, D.L. and Brandl, G. (2006). Sedimentary rocks of the Karoo Supergroup. In Anhaeusser, C. R., Johnson, M. R. and Thomas, R. J. (dir.), *The Geology of South Africa* (p. 461-499). Johannesburg/Pretoria : Geological Society of South Africa and Council for Geoscience.

Koenig, C.W., Castañeda, A.M., Boyd, C.E., Rowe, M.W. and Steelman, K.L. (2014). Portable X-Ray Fluorescence Spectroscopy of Pictographs: A Case Study From the Lower Pecos Canyonlands, Texas. *Archaeometry*, 56, 168-186.

Košařová, V., Hradil, D., Němec, I., Bezdička, P. and Kanický, V. (2013). Microanalysis of clay-based pigments in painted artworks by the means of Raman spectroscopy. *Journal of Raman Spectroscopy*, 44(11), 1570-1577.

Lahlil, S., Lebon, M., Beck, L., Rousseliere, H., Vignaud, C., Reiche, I., Menu, M., Paillet, P. and Plassard, F. (2012). The first in situ micro-Raman spectroscopic analysis of prehistoric cave art of Rouffignac St-Cernin, France. *Journal of Raman Spectroscopy*, 43(11), 1637-1643.

Le Quellec, J.-L. (2008). Rock art research in southern Africa, 2000–2004. In Bahn, P. et Fossati, A. (dir.), *Rock Art Studies : News of the World I* (Vol. 1, p. 97-111) : Oxbow Books, Limited.

Lemaitre, S. (1996). Les peintures rupestres amérindiennes du Lac Wapizagonke (Québec) : une vision chamanique? In Bonenfant, P. (dir.), *La préhistoire au quotidien : mélanges offerts à Pierre Bonenfant* (p. 99-117). Grenoble : J. Millon.

Lemaitre, S. (2013). *Kekeewin ou Kekeenowin : les peintures rupestres de l'est du bouclier canadien*. Mascouche : Recherches amérindiennes au Québec.

Lemaitre, S. and Arsenault, D. (2011). L'art rupestre du Bouclier Canadien. In Vialou, D. (dir.), *Peuplements et préhistoire en Amérique* (p. 467-482). Paris : Éditions du Comité des travaux historiques et scientifiques.

Lewis-Williams, J.D. (1995). *Modelling the Production and Consumption of Rock Art*. The South African Archaeological Bulletin, 50(162), 143-154.

Lewis-Williams, J.D. (2003). *Images of Mystery: Rock Art of the Drakensberg*. Double Storey Books.

Lewis-Williams, J.D. and Pearce, D.G. (2004). *San Spirituality: Roots, Expression, and Social Consequences*. AltaMira Press.

Livingston, A., Robinson, E. and Armitage, R.A. (2009). Characterizing the binders in rock paintings by THM-GC–MS: La Casa de Las Golondrinas, Guatemala, a cautionary tale for radiocarbon dating. *International Journal of Mass Spectrometry*, 284(1–3), 142-151.

Madejova, J. and Komadel, P. (2001). Baseline studies of the clay minerals society source clays: infrared methods. *Clays and clay minerals*, 49(5), 410-432.

Mallen, L. (2008). *Rock art and identity in the North Eastern Cape Province*. Master thesis. University of the Witwatersrand.

Marcet, S., Verhaegen, M., Blais-Ouellette, S. and Martel, R. (2012). Raman spectroscopy hyperspectral imager based on Bragg tunable filters. *Proceedings of SPIE*, 8231, 84121J-84121 to 84121J-84127.

Marean, C.W., Bar-Matthews, M., Bernatchez, J., Fisher, E., Goldberg, P., Herries, A.I.R., Jacobs, Z., Jerardino, A., Karkanas, P., Minichillo, T., Nilssen, P.J., Thompson, E., Watts, I. and Williams, H.M. (2007). Early human use of marine resources and pigment in South Africa during the Middle Pleistocene. *Nature*, 449(7164), 905-908.

Matheson, C.D. and Veall, M.-A. (2014). Presumptive blood test using Hemastix® with EDTA in archaeology. *Journal of Archaeological Science*, 41, 230-241.

Maud, R.R. (2008). The Macro-Geomorphology of the Eastern Cape. In Lewis, C. A. (dir.), *Geomorphology of the Eastern Cape, South Africa* (Second ed., p. 1-20). Grahamstown : NISC.

Mazel, A.D. (2009a). Images in time: Advances in the dating of Maloti-Drakensberg rock art since the 1970s. In Mitchell, P. J. and Smith, B. (dir.), *The Eland's People: New Perspectives on the Rock Art of the Maloti-Drakensberg Bushmen.* Essays in Memory of Patricia Vinnicombe (p. 81-97). Johannesburg : Wits University Press.

Mazel, A.D. (2009b). Unsettled times: shaded polychrome paintings and hunter-gatherer history in the southeastern mountains of southern Africa. *Southern African Humanities*, 21, 85-115.

Mazel, A.D. and Watchman, A.L. (1997). Accelerator radiocarbon dating of Natal Drakensberg paintings: Results and implications. *Antiquity*, 71(272), 445-449.

Mazel, A.D. and Watchman, A.L. (2003). Dating rock paintings in the uKhahlamba-Drakensberg and the Biggarsberg, KwaZulu-Natal, South Africa. *Southern African Humanities*, 15, 59-73.

McCarty, D., Payen, L. and Ennis, P. (1994). Use of amino acid racemization methods on rock paintings at Motte Rimrock Reserve. *American Indian Rock Art*(13), 17-22.

Menu, M. and Walter, P. (1992). Prehistoric cave painting PIXEanalysis for the identification of paint pots. *Nuclear Instruments & Methods in Physics Research Section B-Beam Interactions with Materials and Atoms*, 64(1-4), 547-552.

Menu, M., Walter, P., Vigears, D. and Clottes, J. (1993). Façons de peindre au Magdalénien. *Bulletin de la Société préhistorique française*, 426-432.

Mitchell, P. (1994). The archaeology of the Phuthiatsana-ea-Thaba Bosiu Basin, Lesotho, southern Africa: changes in Later Stone Age regional demography. *Antiquity*, 68(258), 83-96.

Mitchell, P. and Arthur, C. (2014). Ha Makotoko: Later Stone Age occupation across the Pleistocene/Holocene transition in western Lesotho. *Journal of African Archaeology*, 12(2), 205-232.

Mitchell, P. and Whitelaw, G. (2005). The archaeology of southernmost Africa from c. 2000 BP to the early 1800s: a review of recent research. *The Journal of African History*, 46(02), 209-241.

Mori, F., Ponti, R., Messina, A., Flieger, M., Havlicek, V. and Sinibaldi, M. (2006). Chemical characterization and AMS radiocarbon dating of the binder of a prehistoric rock pictograph at Tadrart Acacus, southern west Libya. *Journal of Cultural Heritage*, 7(4), 344-349.

Motuzaite-Matuzeviciute, G., Staff, R.A., Hunt, H.V., Liu, X. and Jones, M.K. (2013). The early chronology of broomcorn millet (Panicum miliaceum) in Europe. *Antiquity*, 87(338), 1073-1085.

Murray, A.S. and Mejdahl, V. (1999). Comparison of regenerative-dose single-aliquot and multiple-aliquot (SARA) protocols using heated quartz from archaeological sites. *Quaternary Science Reviews*, 18(2), 223-229.

Murray, A.S. and Wintle, A.G. (2000). Luminescence dating of quartz using an improved single-aliquot regenerative-dose protocol. *Radiation Measurements*, 32(1), 57-73.

Nathan, Y. and Lucas, J. (1972). Synthèse de l'apatite à partir du gypse; application au problème de la formation des apatites carbonatées par précipitation directe. *Chemical Geology*, 9(1–4), 99-112.

Nelson, D.E., Chaloupka, G., Chippindale, C., Alderson, M.S. and Southon, J.R. (1995). Radiocarbon dates for beeswax figures in the prehistoric rock art of northern Australia. *Archaeometry*, 37(1), 151-156.

Nic Eoin, L. (2015). *The Gatherer and the Grindstone: Functional analysis of grindstones from Southern Africa*. University of Oxford, Oxford. Ph.D thesis.

Ontario Geological Survey (1991), Bedrock Geology of Ontario, west-central sheet: Ontario Geological Survey, Map 2542, Scale 1:1 000 000

Opperman, H. and Heydenrych, B. (1990). A 22 000 Year-Old Middle Stone Age Camp Site with Plant Food Remains from the North-Eastern Cape. *The South African Archaeological Bulletin*, 45(152), 93-99.

Pager, H.L., Mason, R.J. and Welbourne, R.G. (1971). *Ndedema: A documentation of the rock paintings of the Ndedema Gorge*. Graz : Akademische Druck.

Pearce, D.G. (2010a). Conservation and management of collapsing rock paintings: three sites in Maclear District, Eastern Cape Province, South Africa. *The South African Archaeological Bulletin*, 65(191), 96-103.

Pearce, D.G. (2010b). The Harris matrix technique in the construction of relative chronologies of rock paintings in South Africa. *The South African Archaeological Bulletin*, 65(192), 148-153.

Peisach, M., Pineda, C. and Jacobson, L. (1991). Nuclear analytical study of rock paintings. *Journal of Radioanalytical and Nuclear Chemistry*, 151(1), 221-227.

Pettitt, P. and Pike, A. (2007). Dating European Palaeolithic cave art: Progress, prospects, problems. *Journal of Archaeological Method and Theory*, 14(1), 27-47.

Percival, J.A. and Easton, R.M. 2007. *Geology of the Canadian Shield in Ontario: an update*; Ontario Geological Survey, Open File Report 6196, Geological Survey of Canada, Open File 5511, Ontario Power Generation, Report 06819-REP-01200-10158-R00, 65p.

Phillips, F.M., Montgomery, E.D. and Sharma, P. (1997). Maximum ages of the Coa valley (Portugal) engravings measured with chlorine-36. *Antiquity*, 71, 100-104.

Pike, A.W.G., Hoffmann, D.L., Garcia-Diez, M., Pettitt, P.B., Alcolea, J., De Balbin, R., Gonzalez-Sainz, C., de las Heras, C., Lasheras, J.A., Montes, R. and Zilhao, J. (2012). U-Series Dating of Paleolithic Art in 11 Caves in Spain. *Science*, 336(6087), 1409-1413.

Pillans, B. and Fifield, L.K. (2013). Erosion rates and weathering history of rock surfaces associated with Aboriginal rock art engravings (petroglyphs) on Burrup Peninsula, Western Australia, from cosmogenic nuclide measurements. *Quaternary Science Reviews*, 69, 98-106.

Pollard, A.M. (2007). *Analytical chemistry in archaeology*. Cambridge : Cambridge University Press.

Pollard, A.M. and Heron, C. (1996). *Archaeological chemistry*. Cambridge : Royal Society of Chemistry.

Pomies, M.P., Menu, M. and Vignaud, C. (1999). Red Palaeolithic pigments: natural hematite or heated goethite?. *Archaeometry*, 41(2), 275-285.

Prasad, P.S.R., Chaitanya, V.K., Prasad, K.S. and Rao, D.N. (2005). Direct formation of the γ-CaSO4 phase in dehydration process of gypsum: In situ FTIR study. *American Mineralogist*, 90(4), 672-678.

Prescott, J.R. and Hutton, J.T. (1988). Cosmic ray and gamma ray dosimetry for TL and ESR. International Journal of Radiation Applications and Instrumentation. Part D. *Nuclear Tracks and Radiation Measurements*, 14(1–2), 223-227.

Prescott, J.R. and Hutton, J.T. (1994). Cosmic ray contributions to dose rates for luminescence and ESR dating: Large depths and long-term time variations. *Radiation Measurements*, 23(2–3), 497-500.

Prinsloo, L.C., Barnard, W., Meiklejohn, I. and Hall, K. (2008). The first Raman spectroscopic study of San rock art in the Ukhahlamba Drakensberg Park, South Africa. *Journal of Raman Spectroscopy*, 39(5), 646-654.

Prinsloo, L.C., Tournié, A., Colomban, P., Paris, C. and Bassett, S.T. (2013). In search of the optimum Raman/IR signatures of potential ingredients used in San/Bushman rock art paint. *Journal of Archaeological Science*, 40(7), 2981-2990.

Rajnovich, G. (1994). *Reading rock art : interpreting the Indian rock paintings of the Canadian Shield.* Toronto : Toronto : Dundurn.

Regert, M., Garnier, N., Decavallas, O., Cren-Olivé, C. and Rolando, C. (2003). Structural characterization of lipid constituents from natural substances preserved in archaeological environments. *Measurement Science and Technology*, 14(9), 1620-1630.

Resano, M., García-Ruiz, E., Alloza, R., Marzo, M.P., Vandenabeele, P. and Vanhaecke, F. (2007). Laser Ablation-Inductively Coupled Plasma Mass Spectrometry for the Characterization of Pigments in Prehistoric Rock Art. *Analytical Chemistry*, 79(23), 8947-8955.

Rhodes, E.J. and Bailey, R.M. (1997). The effect of thermal transfer on the zeroing of the luminescence of quartz from recent glaciofluvial sediments. *Quaternary Science Reviews*, 16(3–5), 291-298.

Rhodius, C., Kadereit, A., Siegel, U., Schmidt, K., Eichmann, R. and Khalil, L. (2015). Constraining the time of construction of the irrigation system of Tell Hujayrat al-Ghuzlan near Aqaba, Jordan, using high-resolution optically stimulated luminescence (HR-OSL) dating. *Archaeological and Anthropological Sciences*, 1-26.

Richter, D., Richter, A. and Dornich, K. (2013). Lexsyg — A new system for luminescence research. *Geochronometria*, 40(4), 220-228.

Roberts, P., Lee-Thorp, J.A., Mitchell, P.J. and Arthur, C. (2013). Stable carbon isotopic evidence for climate change across the late Pleistocene to early Holocene from Lesotho, southern Africa. *Journal of Quaternary Science*, 28(4), 360-369.

Roberts, R., Walsh, G., Murray, A., Olley, J., Jones, R., Morwood, M., Tuniz, C., Lawson, E., Macphall, M., Bowdery, D. and Naumann, I. (1997). Luminescence dating of rock art and past environments using mud-wasp nests in northern Australia. *Nature*, 387(6634), 696-699.

Rudner, I. (1982). Khoisan Pigments and Paints and Their Relationship to Rock Paintings. *Annals of the South African Museum*, 87, 1-281.

Rudner, I. (1983). *Paints of the Khoisan Rock Artists*. Goodwin Series, 4, 14-20.

Russ, J., Hyman, M., Shafer, H.J. and Rowe, M.W. (1990). Radiocarbon dating of prehistoric rock-paintings by selective oxidation of organic-carbon. *Nature*, 348(6303), 710-711.

Russ, J., Hyman, M., Shafer, H.J. and Rowe, M.W. (1991). 14C dating of ancient rock art: A new application of plasma chemistry. *Plasma Chemistry and Plasma Processing*, 11(4), 515-527.

Russell, T. (2000). The Application of the Harris Matrix to San Rock Art at Main Caves North, Kwazulu-Natal. *The South African Archaeological Bulletin*, 55(171), 60-70.

Smith, B.W. (2010). Envisioning San History: Problems in the Reading of History in the Rock Art of the Maloti-Drakensberg Mountains of South Africa. *African Studies*, 69(2), 345-359.

Smith, B.W. and van Schalkwyk, J.A. (2002). The White Camel of the Makgabeng. *The Journal of African History*, 43(2), 235-254.

Smits, L.G.A. (1983). Rock Paintings in Lesotho: Site Characteristics. *The South African Archaeological Bulletin*, 38(138), 62-76.

Sohbati, R., Murray, A., Jain, M., Buylaert, J.-P. and Thomsen, K. (2011). Investigating the resetting of OSL signals in rock surfaces. *Geochronometria*, 38(3), 249-258.

Sohbati, R., Murray, A.S., Chapot, M.S., Jain, M. and Pederson, J. (2012). Optically stimulated luminescence (OSL) as a chronometer for surface exposure dating. *Journal of Geophysical Research: Solid Earth*, 117(B9), B09202.

Sohbati, R., Murray, A.S., Porat, N., Jain, M. and Avner, U. (2015). Age of a prehistoric "Rodedian" cult site constrained by sediment and rock surface luminescence dating techniques. *Quaternary Geochronology*, 30(A), 90-99.

Solomon, A. (2006). Roots and revolutions: a critical overview of early and late San rock art research. *Afrique & histoire*, 6(2), 77-110.

Spades, S. et Russ, J. (2005). GC–MS analysis of lipids in prehistoric rock paints and associated oxalate coatings from the lower Pecos region, Texas. *Archaeometry*, 47(1), 115-126.

Staff, R.A., Reynard, L., Brock, F. and Ramsey, C.B. (2014). Wood pretreatment protocols and meassurement of tree-ring strandards at the Oxford Radiocarbon Accelerator Unit (ORAU). *Radiocarbon*, 56(2), 709-715.

Stuart, B.H. (2007). *Analytical techniques in materials conservation*. Chichester : John Wiley & Sons.

Stuiver, M. and Polach, H.A. (1977). Discussion; reporting of C-14 data. *Radiocarbon*, 19(3), 355-363.

Swart, J. (2004). Rock art sequences in uKhahlamba-Drakensberg Park, South Africa. *Southern African Humanities*, 16, 13-35.

Taçon, P.S.C., Boivin, N., Petraglia, M., Blinkhorn, J., Chivas, A., Roberts, R.G., Fink, D., Higham, T., Ditchfield, P., Korisettar, R. and Zhao, J.-x. (2013). Mid-Holocene age obtained for nested diamond pattern petroglyph in the Billasurgam Cave complex, Kurnool District, southern India. *Journal of Archaeological Science*, 40(4), 1787-1796.

Tassé, G. and Dewdney, S.H. (1977). *Relevés et travaux récents sur l'art rupestre amérindien*. Montréal : Montréal Université du Québec a Montréal, Laboratoire d'archéologie.

Taylor, J.M., Myers, R.M. and Wainwright, I.N.M. (1974). Scientific Studies of Indian Rock Paintings in Canada. *Bulletin of the American Institute for Conservation of Historic and Artistic Works*, 14(2), 28-43.

Thebe, P.C. (2009). *Report on Mitigation of Stone Age Sites in the Thune Dam Inundation Area*. Botswana. Gaborone : Water Resources Consultants for the Republic of Botswana, Ministry of Minerals, Energy and Water Resources.

Thomas, C. (2002), Kokstad, Geological series, Council for Geoscience, Map 3028, Scale 1:250 000.

Tomasini, E., Siracusano, G. and Maier, M.S. (2012). Spectroscopic, morphological and chemical characterization of historic pigments based on carbon. Paths for the identification of an artistic pigment. *Microchemical Journal*, 102(0), 28-37.

Tournié, A., Prinsloo, L.C., Paris, C., Colomban, P. and Smith, B. (2011). The first in situ Raman spectroscopic study of San rock art in South Africa: procedures and preliminary results. *Journal of Raman Spectroscopy*, 42(3), 399-406.

Trompowsky, P.M., Benites, V.d.M., Madari, B.E., Pimenta, A.S., Hockaday, W.C. and Hatcher, P.G. (2005). Characterization of humic like substances obtained by chemical oxidation of eucalyptus charcoal. *Organic Geochemistry*, 36(11), 1480-1489.

Tsukamoto, S., Nagashima, K., Murray, A.S. and Tada, R. (2011). Variations in OSL components from quartz from Japan sea sediments and the possibility of reconstructing provenance. *Quaternary International*, 234(1–2), 182-189.

Valladas, H. (2003). Direct radiocarbon dating of prehistoric cave paintings by accelerator mass spectrometry. *Measurement Science and Technology*, 14(9), 1487-1492.

Valladas, H., Tisnerat-Laborde, N., Cachier, H., Arnold, M., de Quiros, F.B., Cabrera-Valdes, V., Clottes, J., Courtin, J., Fortea-Perez, J.J., Gonzalez-Sainz, C. and Moure-Romanillo, A. (2001). Radiocarbon AMS dates for paleolithic cave paintings. *Radiocarbon*, 43(2B), 977-986.

Van der Merwe, N.J., Sealy, J. and Yates, R. (1987). First accelerator carbon-14 date for pigment from a rock painting. *South African Journal of Science*, 83(1), 56-57.

Van Rijssen, W.J. (1990). Analysis of South African rock art pigments by X-ray fluorescence spectroscopy (EDS). *The South African Archaeological Bulletin*, 58-59.

Vázquez, C., Maier, M., Parera, S., Yacobaccio, H. and Solá, P. (2008). Combining TXRF, FT-IR and GC–MS information for identification of inorganic and organic components in black pigments of rock art from Alero Hornillos 2 (Jujuy, Argentina). *Analytical and Bioanalytical Chemistry*, 391(4), 1381-1387.

Vergnoux, A., Guiliano, M., Di Rocco, R., Domeizel, M., Théraulaz, F. and Doumenq, P. (2011). Quantitative and mid-infrared changes of humic substances from burned soils. *Environmental Research*, 111(2), 205-214.

Vignaud, C., Salomon, H., Chalmin, E., Geneste, J.-M. and Menu, M. (2006). Le groupe des « bisons adossés » de Lascaux. Étude de la technique de l'artiste par analyse des pigments. *L'Anthropologie*, 110(4), 482-499.

Vinnicombe, P. (1976). *People of the Eland: Rock Paintings of the Drakensberg Bushmen as a Reflection of Their Life and Thought*. Pietermaritzburg : University of Natal Press.

Visser, D.J.L. (1937). *Ochre Deposits of the Riversdale District, Cape Province*. Pretoria : Government Printer.

Wadley, L. (1995). Review of dated Stone Age sites recently excavated in the eastern Free State, South Africa. *South African Journal of Science*, 91(11-12), 574-579.

Wainwright, I.N.M. (1985). Rock art conservation research in Canada. *Bolletino del Centro Camuno di Studi Preistorici*, 22, 15-46.

Wainwright, I.N.M. (1990). Rock painting and petroglyph recording projects in Canada. *Association for Preservation Technology Bulletin*, 22(1/2), 55-84.

Walker, M.J.C. (2005). *Quaternary Dating Methods*. Chichester : Wiley.

Walker, N.J. (2009). *Archaeological Mitigation Measures for the Thune Dam Construction and Associated Works*. Gaborone : Water Resources Consultants for the Republic of Botswana, Ministry of Minerals, Energy and Water Resources.

Waller, S.J., and Arsenault, D. (2008). Echo Spirits Who Paint Rocks: Memegwashio Dwell Within Echoing Rock Art Site EiGf-2. *American Indian Rock Art*, 35, 191-201.

Watchman, A. (1990). A summary of occurrences of oxalate- rich crusts in Australia. *Rock Art Research*, 7(1), 44-50.

Watts, I. (2002). Ochre in the Middle Stone Age of Southern Africa: Ritualised Display or Hide Preservative?. *The South African Archaeological Bulletin*, 57(175), 1-14.

Wendt, W.E. (1976). 'Art Mobilier' from the Apollo 11 Cave, South West Africa: Africa's Oldest Dated Works of Art. *The South African Archaeological Bulletin*, 31(121/122), 5-11.

Wheeler, J.O., Hoffman, P.F., Card, K.D., Davidson, A., Sanford, B.V., Okulitch, A.V. and Roest, W.R. (comp.) (1996). Geological Map of Canada; Geological Survey of Canada, Map 1860A, scale 1:5 000 000.

White, R., Mensan, R., Bourrillon, R., Cretin, C., Higham, T.F.G., Clark, A.E., Sisk, M.L., Tartar, E., Gardere, P., Goldberg, P., Pelegrin, J., Valladas, H., Tisnerat-Laborde, N., de Sanoit, J., Chambellan, D. and Chiotti, L. (2012). Context and dating of Aurignacian vulvar representations from Abri Castanet, France. *Proceedings of the National Academy of Sciences of the United States of America*, 109(22), 8450-8455.

Williamson, B.S. (2000). Direct Testing of Rock Painting Pigments for Traces of Haemoglobin at Rose Cottage Cave, South Africa. *Journal of Archaeological Science*, 27(9), 755-762.

Wilson, M.L., Van Rijssen, W.J.J. et Gerneke, D.A. (1990). An Investigation of the" Coldstream Stone". *Annals of the South African Museum*.

Winter, J. (1983). The Characterization of Pigments Based on Carbon. *Studies in Conservation*, 28(2), 49-66.

Wintle, A.G. (2008). Luminescence dating: where it has been and where it is going. *Boreas*, 37(4), 471-482.

Wright, J.V. (1995). *A history of the Native people of Canada.* Hull : Canadian Museum of Civilization.

Zazzo, A., Saliège, J., Person, A. and Boucher, H. (2009). Radiocarbon dating of calcined bones: where does the carbon come from? *Radiocarbon*, 51(2), 601-611.

Zipkin, A.M., Hanchar, J.M., Brooks, A.S., Grabowski, M.W., Thompson, J.C. and Gomani-Chindebvu, E. (2014). Ochre fingerprints: Distinguishing among Malawian mineral pigment sources with Homogenized Ochre Chip LA–ICPMS. *Archaeometry*, 57(2), 297-317.